INVESTIGATION OF A COUNTERFLOW WATER-STEAM COOLED NUCLEAR REACTOR FOR MARINE STEAM CYCLE APPLICATION

by

WARREN CARLTON DIETZ

B.S. in Physics, University of Washington

(1955)

SUBMITTED IN PARTIAL FULFILLMENT
OF THE REQUIREMENTS FOR THE
DEGREE OF DOCTOR OF
SCIENCE
at the
MASSACHUSETTS INSTITUTE OF TECHNOLOGY
September, 1965

H. FENECH
Associate Professor of Nuclear Engineering
Thesis Supervisor

S. C. POWELL
Associate Professor of Marine Engineering
Chairman, Interdepartmental Thesis Committee

INVESTIGATION OF A COUNTERFLOW WATER-STEAM COOLED NUCLEAR REACTOR FOR MARINE STEAM CYCLE APPLICATION

by

WARREN CARLTON DIETZ

B.S. in Physics, University of Washington

(1955)

SUBMITTED IN PARTIAL FULFILLMENT

OF THE REQUIREMENTS FOR THE

DEGREE OF DOCTOR OF

SCIENCE

at the

MASSACHUSETTS INSTITUTE OF TECHNOLOGY

September, 1965

Signature of Author ....
Department of Naval Architecture and Marine
Engineering, 20 September 1965

Certified by ....
Thesis Supervisor

Accepted by ....
Chairman, Departmental Committee
on Graduate Students

INVESTIGATION OF A COUNTERFLOW WATER-STEAM COOLED NUCLEAR REACTOR FOR MARINE STEAM CYCLE APPLICATION by WARREN CARLTON DIETZ, USN. Submitted to the Department of Naval Architecture and Marine Engineering on 20 September 1965 in partial fulfillment of the requirements for the degree of Doctor of Science.

ABSTRACT

Reactor development is primarily oriented toward the utilization of nuclear heat sources of high power ratings in central station application. There is a relative void in the development of reactors of intermediate power for shipboard application. This study presents the results of an engineering evaluation of a new concept for reactor cooling, which yields superheated steam at thermodynamic conditions and flow rates appropriate to generating 25,000 SHP.

The reactor core is arranged as a shell-and-tube heat exchanger, in which the tube wall separating the two counterflowing coolant streams contains the nuclear fuel. The first pass coolant, comprised of the returning feedwater and recirculating saturated water, flows upwards through the core, boiling in an annular channel and exhausting into a common plenum at the top of the core. At the design condition for full load, the ten percent saturated steam produced on first pass heating passes through steam separators, located above the plenum, and then enters circular flow tubes, defined by the inner radius of the annular fuel tubes, to flow back down through the core for the second pass and superheating. The moderator region of the core is in the space between first pass flow channels.

The steam cycle used has been based on a direct cycle plant. The design power for the reactor at full load is 57.4 MW_t. Entering feedwater at 404 °F mixes with saturated water at 530 °F to make up the first pass flow. Second pass exit conditions were set at 177,500 lb/hr at a temperature of 955 °F and a pressure of 865 psia. The cycle efficiency was determined to be 32.6%.

The nuclear fuel is 50% enriched UO_2 and the cladding regions are made of Inconel-X. Two moderators were studied - H_2O (the returning feedwater) and BeO. The H_2O moderator was separated from the first pass coolant in order to reduce the coupling between the axial power distribution in the fuel tubes and the steam voids generated during first pass boiling. Constraints on the design were taken to be a maximum fuel temperature of 4500 °F and a maximum cladding temperature of 1350 °F. The latter was found to be controlling.

The advantage of this design is that the maximum second pass exit temperature occurs at the bottom of the core where the relatively cold first pass coolant enters the core. Based on heat transfer considerations, a certain fraction of the heat produced in the annular fuel tube will flow inwards to the second pass flow, the remainder flowing outwards to the first pass flow. Because of the temperature differential between the two counterflowing coolant streams, a heat flow also exists across the fuel tube from the second to the first pass coolant. This secondary heat flow plus the low first pass coolant temperature reduce the second pass cladding temperature at a given second pass steam temperature. More heat is transferred to the first pass coolant than the second pass coolant. The intermediate mixing plenum at the top of the core averages out the effects of radial power peaking across the core on the first pass coolant flow. Thus, the thermodynamic state of the second pass coolant for all channels is identical as it enters the core for the second pass and superheating.

ABSTRACT (Continued)

The neutron spectrum for both the H_2O and BeO moderated cores was found to be above thermal. The cores are undermoderated and there is an axial skewing of the power distribution toward the bottom of the core. Because of this, control rods must enter the core from the bottom if full power is to be achieved without exceeding the metallurgical constraints. The power level in the reactor can be partially controlled by varying the flow rate of feedwater or recirculating water through the core.

The analysis of this core configuration becomes quite involved, it being necessary to solve the coupled effects of flux and power distributions, thermodynamic state of the coolant and hydraulic flow patterns across the core. To achieve this end, a mathematical model was developed and then programmed, using numerical analysis techniques. In order to achieve this result, the steady state nuclear calculations have used a modified one-dimensional, two-group model which "marches" from the consideration of small segments of an individual fuel cell to the whole reactor, generating correction factors to account for the two-dimensional nature of the idealized problem. The power distribution determined is used to calculate the thermodynamic state parameters of the coolant and the flow rates and pressure drops involved. This information is fed back into the nuclear calculations and the solution between successive iterations is compared until specified convergence limits are achieved.

Thesis Supervisor: H. Fenech
Title: Associate Professor of Nuclear Engineering

TABLE OF CONTENTS

Page

Page

LIST OF FIGURES

Figure	Title	Page

LIST OF TABLES

ACKNOWLEDGMENTS

I wish to express my appreciation to the many persons who have contributed to this thesis. As Thesis Supervisor, Professor H. Fenech is due most of the credit for its successful culmination. The other members of my interdepartmental thesis committee, Professor S. C. Powell, Chairman, and Professors M. Benedict and E. G. Frankel, also contributed of their time and talent to enhance the scope and depth of the study.

My thanks are also extended to the U. S. Navy, which funded the expense of this study program. On an individual basis, I am appreciative of the time and assistance that I received from Captain E. S. Arentzen, USN (Ret.), Commander J. R. Baylis, USN, Captain W. M. Nicholson, USN, and Commander W. R. Porter, USN. I am especially grateful to Commander Porter, whose many acts of assistance were "above and beyond the call of duty".

I wish to acknowledge the facilities and services of the MIT Computation Center, which were used to bring this study to fruition.

Last but not least, I wish to permanently and publicly acknowledge my wife, Irene, without whose help this thesis could not have been written. Her patience, understanding and optimism enabled the work to always go forward.

Chapter 1

INTRODUCTION

1.1 Background

Reactor development throughout the world is primarily oriented toward the application of nuclear power to central station electrical generation plants. Economic considerations normally dictate that the power ratings of such plants be large to be feasible. Consequently, there is what may be termed a "relative void" in the development of small reactors for application to propulsion systems or as portable power plants.

Over the complete spectrum of reactor development, many different types have been studied or built. In general, the cycles involved are of two different types - indirect or direct. The plant which utilizes the indirect cycle can be schematically divided into two distinct parts on the basis of flow loops, one loop for the reactor coolant, the other for the working fluid flowing through the turbomachinery, with coupling between the two loops provided by a heat exchanger. Another means of classifying a particular reactor is on the basis of the type or thermodynamic state of the reactor coolant and the moderator used. For instance, the common reactor types are pressurized water, boiling water, organic moderated and cooled, liquid metal cooled and gas cooled. From a purely nuclear point of view, the reactor can be described in terms of the characteristic neutron spectrum, i.e., thermal, intermediate or fast. In all of the types used today, heat is removed by single pass coolant flow along the fuel element.

Design constraints limit the power that may be removed from a reactor. These constraints are normally stated in terms of a maximum fuel temperature, a maximum cladding temperature or a maximum heat flux (applicable to a water cooled reactor). One of these is found to be controlling and the design is limited by this particular constraint.

Power reactors using steam cycles have been generally limited to small or modest superheat conditions at the turbine [1]. The pressurized water reactors, in general, produce secondary steam at temperatures below 500 °F and pressures ranging up to 675 psig. Boiling water reactors, depending upon whether the cycle is direct or indirect, have yielded turbine steam up to 550 °F.. The attainment of high superheat has been gained with the BONUS (Boiling Nuclear Superheat) reactor, which is direct cycle and produces steam at 875 psig, 900 °F. The BONUS reactor design incorporates an integral nuclear superheater region surrounded by a boiling water region. The continuing drive for higher steam conditions results from the fact that as the temperature increases the maximum achievable cycle efficiency increases.

1.2 CFR Power Source and Plant Concept

The concept which forms the basis of this study utilizes a water cooled nuclear reactor as the power source. The reactor produces superheated steam which goes directly to the turbine. The plant is thus described as being direct cycle. The primary investigation of the study has been centered upon the design facets of the reactor. The concept was originally motivated in an attempt to develop a reactor design which would be suitable for a marine installation. As such, the design variables considered throughout the study are pertinent to a power plant of about 25,000 SHP. At reasonable cycle efficiencies, this places the thermal power of the core in the vicinity of 60 MW_t. Where specific values are mentioned, they will be appropriate only to reactors in this region of power. The concept for the reactor configuration is not limited to only these powers or for the specific application to a marine plant; investigation of design variables peculiar to higher power ratings can be easily undertaken. Likewise, the cycle investigated could be either direct or indirect.

The nuclear reactor is arranged internally as a counterflow shell and

tube heat exchanger. From the internal description the reactor will be subsequently referred to as the CFR (Counter Flow Reactor). The annular tube separating the two counterflowing coolant streams contains the nuclear fuel. Horizontal and vertical cross sections of this arrangement are shown in Figure 1.1.

Subcooled first pass coolant enters the core from an inlet plenum immediately below the core and flows upward in the region exterior to the fuel material. As indicated, the first pass flow path is bounded on the exterior by a moderator region. During its upward passage through the core, it begins to boil and a two-phase saturated mixture exits into the upper mixing plenum, which is common to all first pass coolant flow.

Dry saturated steam is taken from the upper mixing plenum and flows back down through the core for second pass heating within the annular fuel elements. During this second pass, the steam is superheated. It should be noted that this concept makes each individual fuel element into a pseudo counterflow heat exchanger. In this reactor application, the separating tube provides a source of power to the two coolant streams; the system, in this sense, is an active rather than a passive one.

With the counterflow arrangement, the temperature profile of the two coolant streams can be used to work against each other. The wall temperature of a solid fuel pin producing heat is controlled by the temperature of the coolant. In the counterflow arrangement, there are two coolant temperatures which regulate both the inside and outside fuel element temperatures. At the bottom of the reactor core, superheated steam is leaving which raises the inner fuel element wall temperature. On the outside of the fuel tube, the relatively cold feedwater is entering which depresses the outer wall temperature. Based upon the radial power distribution across the fuel material and the heat transfer parameters, a certain fraction of the power generated will go to the

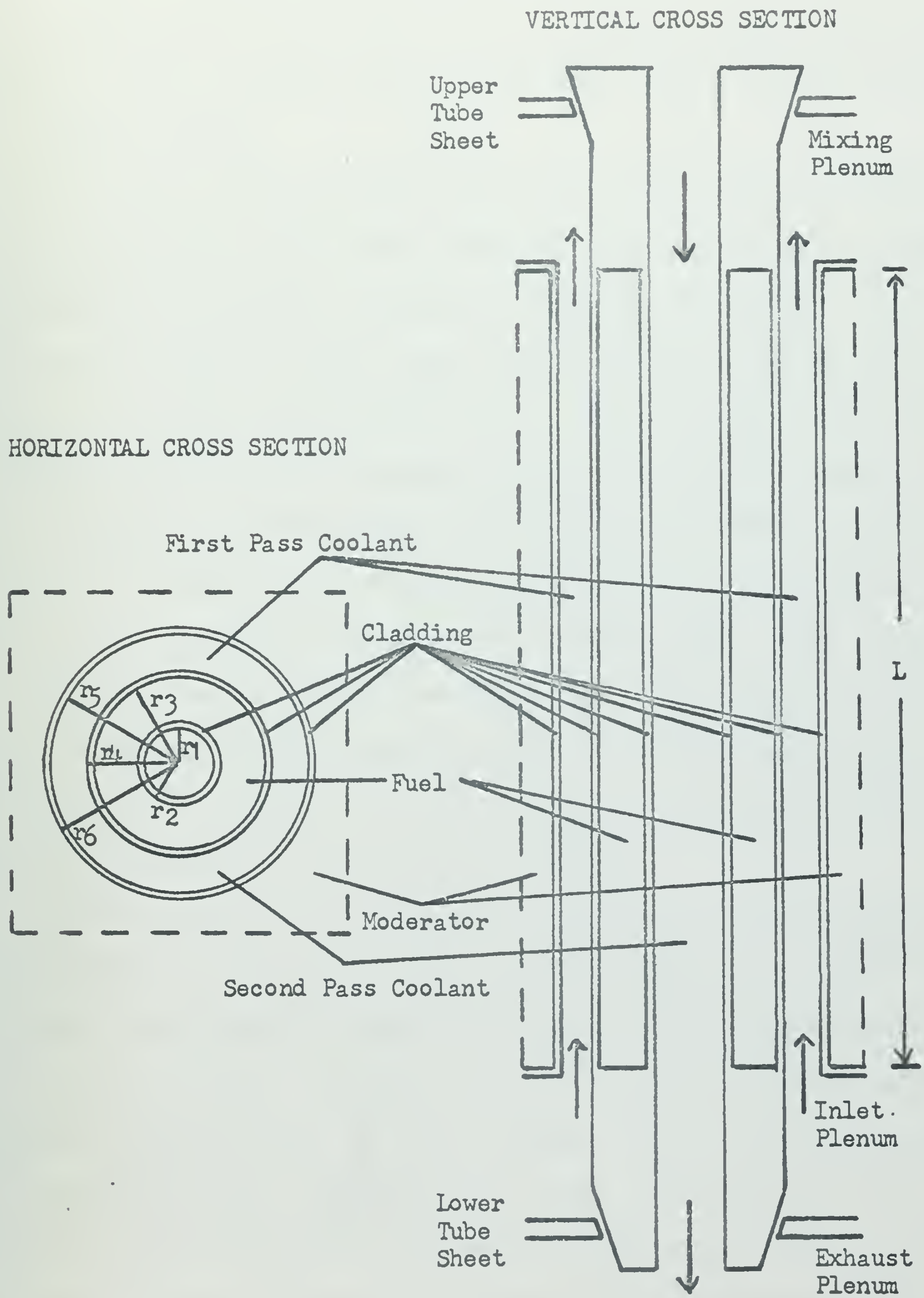

SCHEMATIC ARRANGEMENT OF CFR FUEL ELEMENT

Figure 1.1

exiting steam. However, the temperature rise from the tube wall to the steam is decreased because of the counter heat flux caused by the temperature difference of the two coolant streams on opposite sides of the fuel element (a heat exchanger effect).

What appears to be the greatest advanage of this system is the presence of the upper mixing plenum, which brings all first pass flow to a common state before the individual second pass entrances are reached. This then damps out the effect of radial power peaking across the reactor and its influence on the second pass entrance state. Thus, the dry saturated steam entering a channel, which is producing power above the core average, leaves with a temperature which is higher than that from the other channels, but not as high as the temperature which would result from a once-through arrangement when the fuel is producing power at the same high level. Also, as mentioned, the increased steam temperature resulting from this situation is lessened because the counter heat flux from the second to the first pass coolant, is increased, thus decreasing the total heat flux to the second pass coolant and the wall temperature of the second pass cladding.

The fact that the first pass flow is exterior to the fuel tube can significantly reduce the final variation of steam temperature from the CFR core, since more heat will flow outwards from the fuel to the first pass than to the second pass region. To illustrate this, consider the idealized situation in which a constant 65% of the power produced in the fuel material goes to the first pass coolant. Neglecting the effect of the heat flux due to the temperature difference between the coolant streams, and considering that only two cells are present which have the same coolant flow rates but that one is producing twice as much power as the other, the enthalpy rise of the second pass coolant in the peaked channel will be twice that from the other channel. Considering the total enthalpy rise from first pass inlet to second pass

outlet, the average enthalpy rise is 1.5 units with that from the peaked channel being 1.675 and that from the second channel 1.325. With the intermediate mixing stage, the ratio of maximum to minimum enthalpy rise is reduced to 1.264 (= 1.675/1.325) instead of two.

A certain measure of safety is provided in this design against the adverse effects of scale deposition, manufacturing tolerances or other phenomena which would cause an increase in the thermal resistance between the fuel and coolant. When an increased thermal resistance is present on one side of the annular fuel element, more of the generated heat flows to the other side. Such an occurrence results in raising both wall temperatures and the maximum fuel temperature in the region of the obstruction. Cooling the annular fuel element on both the inside and outside lessens the danger of exceeding a temperature constraint when this situation occurs. A solid fuel element cooled on the exterior surface only does not possess this feature.

One other advantageous feature of this design can be seen in Figure 1.1. A separate moderator region is provided for each fuel element which is entirely distinct from the coolant regions. In the boiling water reactor, the axial variation of power generation is dependent on the local condition of the coolant with a definite skewing of the power distribution toward the bottom of the core because of the increased coolant density and, hence, moderation present at the bottom of the core. The presence of the moderator in the CFR core reduces the dependence of the local power generation rate in the fuel to the local thermodynamic state of the coolant.

1.3 Steam Cycle

The plant power for this study has been arbitrarily set at 25,000 SHP. Although higher than the plant power installed in the SAVANNAH,[2] it is representative of the requirements of a large number of current conventional marine power plants. On the other hand, it is much lower than the ratings

of the majority of shore-based electrical power generating stations. Thus, the assigned rating of 25,000 SHP (approximately equivalent to 18.6 MW_e) results in a relatively small plant. In this sense, the study then becomes appropriate to portable power plants, be they for electrical power generation and heat or for propulsion. Since the context for the CFR plant concept has been in the marine field, only that area will be considered in selecting the plant steam cycle.

A considerable number of conventional oil-fired plants now operate with throttle inlet conditions of 600 psig, 850 °F. Naval units have been built which produce steam at 1200 psig, 1050 °F. The selection of the higher conditions for naval ships is influenced by the effect of plant weight on the ship's military characteristics and mission and is not as greatly dependent on the "dollar" economics which govern the selection of a merchant marine plant cycle.

In the search for an optimum conventional steam cycle, numerous studies have been made. These studies considered such variables as fuel price, operating expense, return-on-investment, and capital cost, among others. Their conclusions reflect the then current fuel oil price and plant ratings and include some comments on the effects of variations of these factors.

In 1948 MacMillan and Ireland[3] concluded that the optimum throttle conditions were 450 psig, 750 °F for installations producing 6000 SHP. For plants of higher ratings, they suggested that conditions at 615 psig, 850 °F be selected.

Ten years later Cheng and Dart[4] published the results of an economic study on a 25,000 SHP single screw tanker. Their conclusions substantially reflect those of the previous study, namely that 600 psig, 850 °F represent near optimum conditions when referred to round trip distances of 3000 and 25,000 miles. In their opinion, raising the steam conditions to 850 psig,

900 °F could only be justified on the basis of longer distances and higher fuel prices.

Later Nichols, Rubin and Davidson[5] discussed the selection of machinery for 30,000 SHP tankers. Throttle steam at 600 psig, 850 °F is a common design point for current tankers of 25,000 to 160,000 deadweight tons. The advancement of these conditions to 600 psig, 920 °F is, in their opinion, a step which can be reasonably taken to yield a higher cycle efficiency.

MacMillan and Rhode[6] have reviewed the selection of cycle conditions for plants in the 12,000 to 25,000 SHP range. Compared with a plant of 600 psig, 850 °F, they concluded that an improved conventionally fired plant at 850 psig, 950 °F will result in a plant weight savings of 155 tons and a reduction in fuel costs of about 13%.

The conditions of 850 psig, 950 °F have also been recommended for the throttle design conditions for the "630A Nuclear Steam Generator", the proposed adaptation of the reactor studied for the nuclear powered aircraft to a marine propulsion plant[7].

Based on these considerations, the design point for the throttle steam conditions in the CFR plant has been selected as 850 psig, 950 °F. These points then represent the current state of the art as regards the components of a marine steam plant.

The salient features of the steam cycle into which the CFR is to be integrated are shown in Figure 1.2. The calculational method used follows that recommended for generating comparative marine heat balances[8]. Data for main turbines, turbogenerator and main feed pump turbine steam rates were taken from reference 9. The summary of plant load requirements is given in Table 1.1.

Considering that all plant load requirements other than those of the main propulsion turbines are parasitic, the cycle efficiency is calculated

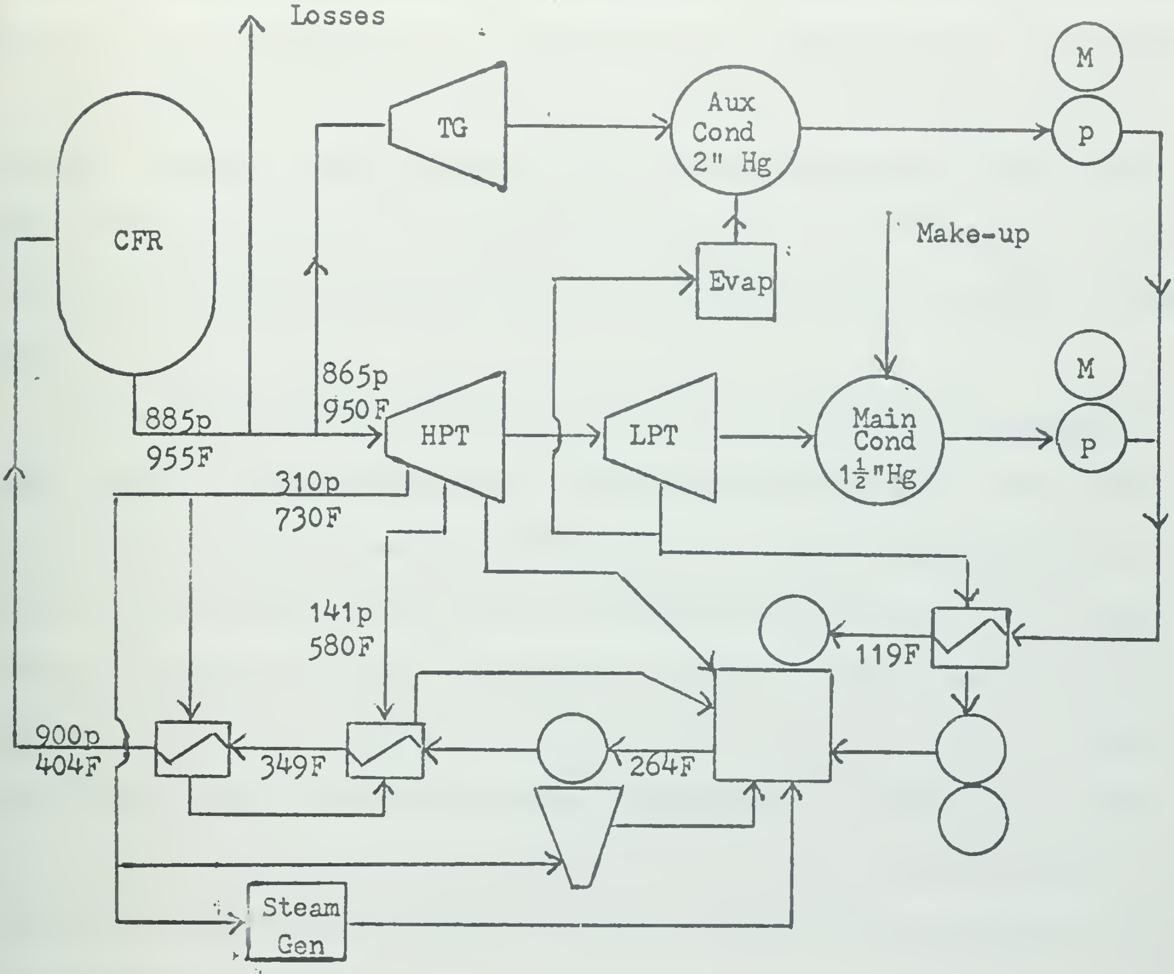

CFR STEAM CYCLE WITH FOUR STAGES OF FEEDWATER HEATING

Figure 1.2

Table 1.1

PLANT LOAD REQUIREMENTS

Item	Requirement
Main Propulsion Turbine	25,000 SHP
Counterflow Reactor	57.4 MW_t
Reactor Coolant	177,500 LB/HR
Turbogenerator	600 KW
Distillation Plant	2500 GPD
Low Pressure Steam Generator	100 LB/HR

as 32.6%. Utilizing the results of reference 9, a reactor inlet temperature of 404 °F is in the region of a relatively flat optimum for cycle efficiency.

The turbogenerator load includes the effect of circulating pumps for condenser cooling. Scoop injection alone (using the velocity head of the ship to force cooling water through the condenser) is not feasible. The system must provide adequate cooling water to the condenser when the ship is backing down.

The selection of this cycle does not include considerations based on plant weight. An independent and detailed optimization of a cycle with respect to plant weight or cycle efficiency and plant weight is beyond the scope of this study. References in the technical literature[10,11] to correlations of equipment weight as a function of flow or performance characteristics are no longer current and the effort necessary to perform an optimization using these correlations is not considered to be justified. Suffice it to say that the steam cycle chosen parallels current marine practice and should not cause the plant weight to deviate sharply from its minimum value.

1.4 Scope of the Study

The primary aim of this study was to investigate the engineering feasibility of the reactor concept. Because of the relatively complicated geometry most of the effort expended has been in the development of an analytical and computational tool which will simultaneously solve the coupled nuclear, thermodynamic, heat transfer and hydraulic behavior of the two coolant passes through the fuel elements across the reactor. A detailed description of the approach used is set forth in Appendices A through E. To facilitate the investigation of power ratings and inlet conditions other than those chosen for the plant under discussion, the mathematical model used has been programmed in FORTRAN languate for the IBM 7090 digital computer. A listing of the program is given in Appendix G.

After the development of the necessary mathematical tools, the study has investigated those reactor configurations suitable to the power rating of the 25,000 SHP marine plant discussed in the preceding section. The work "suitable" can be intrepreted to mean many things. For the purpose of this study, it will refer to an engineering optimization of the core size such that the maximum power density will result, subject to the limitations of a design constraint. Before the application of any new concept, an economic investigation is normally conducted. This type of investigation is beyond the scope of this study. Minimum core size has been chosen as the variable to be optimized. For the marine application, reactor size is one of the primary factors that must be considered.

The consequences of using a direct cycle arrangement with this reactor concept are briefly investigated. Emphasis here is placed upon the necessary machinery space shielding weights that must be provided as protection against the effects of a distributed radioactive coolant. Necessarily, the exact shielding configuration and weight is determined by the specific arrangement of the machinery space and cycle under consideration. Some generalized results of the requirements for a particular reactor power and overall machinery compartment size are derived from a simplified mathematical model.

All investigations in this study have been conducted for the steady state condition. A complete transient study of a marine power plant using the reactor power source described is beyond the scope of this study. Using numerical analysis techniques to define a mathematical model to study the transient behavior can be shown to lead to completely impractical solution times. The maximum time increments that can be used for such an analysis to ensure stability of the time-dependent difference equations for either nuclear or temperature transients is limited by the physical dimensions of the fuel tube. These time increments necessarily have to be of the order of a

microsecond. When the total number of space points within the reactor is considered, the solution time for a one-minute transient study requires a computer running time expressed in tens of hours.

Because of the spatial distributions of power and temperature within the reactor, a method for formulating and solving the coupled transients by means of analog techniques and a lumped parameter model is not sufficiently accurate. The spatial temperature distribution in the fuel tube is crucial in determining the heat flow to the first or second pass coolant stream. This temperature distribution is functionally dependent on the state variables of the coolants, which show large variations over the height of the core and cannot be represented by any simple mathematical correlation.

As a starting point for conditions perturbed within the core, the study presents the results of calculating the maximum temperatures achieved when flow is blocked to one of the coolant channels. The validity of such calculations, as to whether they represent the final steady state thermodynamic and power profiles for such perturbations, can be only determined from a complete transient analysis or by experimental verification.

Chapter 2

OPTIMIZATION OF CFR FUEL ELEMENT PARAMETERS

2.1 Scope

An optimization of the reactor parameters could be based on any one of several different economic philosophies. For example, the optimization could be conducted on maximum return on initial investment or on minimum operating expense. Regardless of which criterion is selected, one of the sources of economic data that is not available is fuel cycle costs. There are several computer programs available to calculate reactivity as a function of core operating life but the deficiency with the present programs, as applied to the CFR core, centers around the fact that the provision for considering the shift in power distribution across the fuel tube as the fuel is expended is missing.

In the typical nuclear reactor, in which individual fuel elements are cooled by a one-pass coolant stream, the change in power distribution across the core affects the "macroscopic" or "gross" limitations on available power generation rate. In the CFR reactor, the "macroscopic" or "gross" shift in power distribution is also present but additionally "microscopic" or "fine" shifts of power generation within each fuel element cause a variation in time of the heat produced that goes to either the first or second pass counter-flowing coolant. Presently available computational tools cannot describe this "fine" shift of power distribution which is necessary to determine the maximum power that can be achieved at any point in the core life.

In lieu of selecting the reactor parameters on the basis of economic considerations, the optimization subsequently described is based on achieving a core with maximum power density. This optimization is a static one, since only the effect of the "gross" and "fine" power distributions within the core and fuel element, respectively, are considered during the hot clean condition

of the core. The optimization is set up to determine the core of minimum volume that produces the requisite amount of power subject to the condition that none of the design constraints are violated but that one of the constraints is achieved.

As a first step in defining the core of minimum volume, the investigation described in the subsequent sections of this chapter is directed toward determining the m inimum channel height for various other parameter combinations that cause one of the limiting variables to approach its constrained value. During the presentation of the model used during the optimization study, it will become apparent that the primary variables defining the minimum fuel element length depend primarily on the second pass flow rate and the fuel element radial dimensions. This first approach neglects the influence of nuclear parameters on the design and concentrates only on heat transfer and thermodynamic variables. The optimization thus finds only the minimum channel height, i.e., the core height, which satisfies the constraint. Nuclear aspects of the problem are uncoupled and are considered separately in the next chapter.

2.2 Fuel Element Materials and Design Constraints

At first glance, either of two oxide fuels appears suitable. The first is UO_2, using U^{235} as the fissionable material and U^{238} as the fertile material. Uranium dioxide has a melting point of roughly 5000 °F, but this high temperature is offset by its low thermal conductivity of 1 Btu/hr/ft/°F. For the counterflow arrangement of the annular fuel element cooling, the low value of the thermal conductivity masks the variation in the heat transfer coefficients to the first and second pass coolant streams.

An oxide mixture in which thorium dioxide forms the basic structure with uranium dioxide ($U^{233}O_2$) interspersed is also a possibility. Like the all uranium oxide fuel, the melting point is high and the thermal conductivity is low. The advantage of this fuel revolves around the absorption characteristics

of thorium, which because of its resonance absorption cross section is more easily converted to a fissionable material. The technological experience with this type of fuel is small and because of this it has not been considered further in this study. Its heat transfer properties are not significantly different from the all uranium oxide fuel. This is not to say that fuel cycle studies would not vindicate its use but only that present knowledge of its characteristics is not considered to be broad enough to extrapolate its use to this study.

An alternative to the use of a ceramic fuel is to consider the use of a fuel dispersion in a metallic lattice. Although the heat transfer coefficient of this type of fuel is significantly higher and the temperature gradient between the two counterflowing coolant streams is consequently reduced, the nuclear properties of such an element are undesirable. Present technology indicates that the only dispersed fuel elements of this type which would be compatible with high temperature steam are iron or nickel base alloys. Both of these elements have high absorption cross sections, which would raise fuel cycle costs because of the increased parasitic neutron absorption within the core.

Of these three possible fuel materials, the one selected for this study is uranium dioxide. No extrapolation is required to justify its use in the CFR core. With the exception of a small amount of absorption by oxygen, all absorptions in the fuel material take place in the U^{235} or U^{238} (disregarding fission products). The crystal structure of the oxide is cubic, which has an interstial space for retention of fission products. The material is compatible with high temperature steam or water so that the effect of a cladding rupture is minimized. The constraint which will be used during the course of the optimization is that the maximum fuel temperature is limited to 4500 °F and that the average thermal conductivity is 1 Btu/hr/ft/°F; these values

have been applied in the past by the U.S. Atomic Energy Commission as constraints for other reactor feasibility studies.

The cladding material chosen for the fuel element is Inconel-X. Under current USAEC design restrictions, the maximum allowable temperature at an interface between steam and Inconel is 1350 °F. Inconel is also compatible with the high temperature fuel oxide which it encloses. It is possible to conceive of Zircaloy, for instance, as being the cladding on the first pass side. The use of Inconel on both sides of the fuel is based on the premise that easier manufacturing and assembly of the fuel element will result. Although not directly related to the heat transfer optimization of the channel length,, this material will also be considered to be the boundary material between the first pass coolant and moderator.

As will become evident later, the controlling design constraint is the maximum cladding temperature on the second pass coolant side. The subsequent discussion is directed toward demonstrating a technique of satisfying this constraint. The final result, optimized on the assumption that the cladding temperature is controlling, shows from the calculation of the maximum fuel temperature that this assumption is indeed correct.

2.3 Design Variables

The geometry of each cell is relatively complicated. On the basis of geometrical considerations, seven variables representing the various radial dimensions are introduced into the core optimization. Of these, three can be neglected for heat transfer and thermodynamic calculations, the three being the radial dimensions defining interfaces at the first pass coolant-moderator cladding, moderator cladding-moderator, and the equivalent moderator exterior radius. The remaining variables define the radial dimensions of the annular fuel element and its associated cladding. One additional dimension must be considered , that of the fuel element length (height of the active core).

The nomenclature which will be used throughout the remainder of this chapter is shown in Table 2.1.

Table 2.1

NOMENCLATURE FOR FUEL ELEMENT OPTIMIZATION

Symbol	Description
r_1	Second pass coolant and internal fuel tube cladding interface radial distance measured from the center of the second pass flow channel
r_2	Internal fuel tube cladding and fuel interface distance
r_3	Fuel and exterior fuel tube cladding interface distance
r_4	Exterior fuel tube cladding and first pass coolant interface distance
R	Ratio of r_3 to r_2
V_2	Second pass coolant exit velocity
v_2	Specific volume of second pass coolant at exit
T_2	Temperature of second pass coolant
T_{2e}	T_2 at exit
H_2	Enthalpy of second pass coolant
H_{2e}	H_2 at exit
c_2	Average specific heat of second pass coolant
k_c	Thermal conductivity of cladding material
k_f	Thermal conductivity of fuel material
h_1	Heat transfer coefficient at r_1
h_4	Heat transfer coefficient at r_4
h_i	Heat transfer coefficient at r_2 and r_3 between conducting regions
H_1	Enthalpy of returning feedwater
H_g	Enthalpy of saturated vapor at first pass exit
T_1	Temperature of first pass coolant
W_2	Mass flow rate out of second pass coolant channel
k_e	Effective thermal conductivity between the two counter-flowing coolant streams
Q	Total power produced in the fuel element
L	Length of the active fuel element
h_3	Effective heat transfer coefficient from fuel to first pass coolant
h_2	Effective heat transfer coefficient from fuel to second pass coolant
f_2	Fraction of heat produced in the fuel material that goes to the second pass coolant, disregarding the heat flux due to the temperature differential between the two coolant streams
z	Distance variable measured from second pass exit point up along the fuel element
α	Derived parameter dependent on heat transfer and fluid flow
ΔT	Temperature differential between the cladding and second pass coolant
T_c	Cladding temperature at r_1

2.4 Simplified Mathematical Model

The variation of power generation rate within a fuel tube is dependent on the nuclear flux shape. If, as a first approximation, it is assumed that the power generation rate, both radially and axially is constant, the nuclear aspects of the problem are completely uncoupled from the non-nuclear heat transfer and thermodynamic aspects of the problem. The determination of a set of fuel element parameters, which will satisfy the design constraints and lead to an element of minimum length can be achieved using only those parameters which involve heat transfer and thermodynamics.

This assumption permits the development and utilization of a simplified model to determine the approximate set of values for an element of minimum height. If the second pass exit velocity V_2 and the thermodynamic inlet and exit conditions for the first and second pass coolant are stated for a typical cell in the core, the geometrical values r_1 through r_4 can be varied and the corresponding value of the maximum cladding temperature determined, once the length L of the cell has been found. Knowing the second pass flow through a channel within a cell, the total number of fuel elements in the core is fixed.

Certain heat transfer quantities are necessary to solve the transcendental equation which defined the channel (core) length. These can be defined as follows:

$$\frac{1}{r_2 h_2} = \frac{1}{r_1 h_1} + \frac{\ln(r_2/r_1)}{K_c} + \frac{1}{r_2 h_i}$$

$$\frac{1}{r_3 h_3} = \frac{1}{r_3 h_i} + \frac{\ln(r_4/r_3)}{K_c} + \frac{1}{r_4 h_4}$$

$$\frac{1}{K_e} = \frac{1}{r_2 h_2} + \frac{\ln(R)}{K_f} + \frac{1}{r_3 h_3}$$

On the basis of the thermal barriers which are present and are represented by the terms just defined, it can be shown (Appendix B) that the fraction f_2 of the total heat produced in an incremental length of fuel that would go to the second pass coolant (inside the fuel tube) is defined by:

$$f_2 = \frac{\frac{1}{r_5 h_3} - \left[\frac{\ln(R)}{K_f} + \frac{1}{r_3 h_3}\right] + \frac{1}{2K_f}\left[R^2 - 1\right]}{\frac{1}{K_c}\left[R^2 - 1\right]}$$

An approximate thermodynamic balance can be written for an incremental length of second pass coolant channel as follows

$$-W_2 \frac{dH_2}{dz} = f_2 \frac{Q}{L} + 2\pi K_e (T_2 - T_1)$$

As a further simplification to the problem, it can be assumed that the temperature T_1 of the first pass coolant is constant. The first pass coolant undergoes boiling, so that in the boiling region of the channel the only influence on the bulk coolant temperature is caused by the pressure loss as the coolant travels up the channel. Between entrance and the point where boiling occurs, the bulk coolant temperature rises. For the desired condition of second pass exit temperature T_{2e} at 955 °F when the pressure is 885 psia, the temperature differential, assuming no subcooling of the first pass coolant at inlet pressure of 900 psia, between the two coolant streams is 423 F°. For the case when the returning feedwater is at 404 °F and the recirculation through the first pass channel is adjusted such that 10% steam exits into the upper plenum, the first pass inlet temperature is 520 °F and the temperature differential between the streams at the bottom of the core is 435 F°. This introduces an error of approximately 3% in the heat flow from the second to first pass stream, which is within the limitations of the model. With this assumption, the temperature T_1 is not a function of position.

The rate of change of second pass enthalpy H_2 can also be expressed in terms of the rate of change of temperature T_2 and the average specific heat capacity of the second pass coolant. The second pass coolant enters as dry saturated steam at the temperature T_1, if the pressure loss in going from first pass exit to second pass inlet is neglected. If the desired second pass exit temperature and enthalpy are specified, the average specific heat

c_2 of the second pass coolant is

$$c_2 = \frac{H_{2e} - H_g}{T_{2e} - T_1}$$

The final approximation in this model is to neglect the axial variation of the derived heat transfer properties f_2 and k_e. When this is done, the equation for second pass temperature variation is

$$-W_2 c_2 \frac{dT_2}{dz} = f_2 \frac{Q}{L} - 2\pi k_e (T_2 - T_1)$$

The boundary conditions for integrating this equation are that at z = 0, $T_2 = T_{2e}$, and at z = L, $T_2 = T_1$. Evaluating the integration constant at z = L and then writing the transcendental equation at z = 0 yields

$$\frac{W_2 c_2 (T_{2e} - T_1)}{Q} = \frac{f_2 (1 - e^{-\alpha L})}{\alpha L}$$

where

$$\alpha = \frac{2\pi k_e}{W_2 c_2}$$

The total heat Q produced in a fuel tube is simply

$$Q = W_2 (H_{2e} - H_1)$$

where H_1 is the enthalpy of the returning feedwater. Using the definition of the average second pass coolant specific heat c_2, the transcendental equation reduces to

$$\frac{H_{2e} - H_g}{H_{2e} - H_1} = \frac{f_2 (1 - e^{-\alpha L})}{\alpha L}$$

The left hand side of this equation is fixed by the inlet and outlet coolant conditions and operating pressure in the core. All terms in the RHS are known except L, the length of the channel. A trial-and-error solution to this equation fixes the channel length L.

Once the channel length L has been determined, the maximum temperature differential at the interface between second pass coolant and cladding can be determined. It is defined by

$$\Delta T = \frac{1}{2\pi r_1 h_1}\left[f_2 \frac{Q}{L} - 2\pi k_e (T_{2e} - T_1)\right]$$

since it must occur at the bottom of the core under the assumption that the power generation rate along the fuel and first pass coolant temperature are constants. The calculation of ΔT is the first indication as to the acceptability of the particular parameter set to meet the design constraint on maximum allowable cladding temperature. The maximum cladding temperature is simply the sum of T_{2e} and ΔT.

The second pass flow rate W_2 through an individual channel is determined from the specified second pass exit velocity V_2, second pass channel radius r_1, and the specific volume of steam at the desired exit conditions of temperature and pressure.

2.5 Influence of Design Variables on the Cladding Temperature Constraint

The two variables r_1, the second pass channel radius, and V_2, the second pass coolant exit velocity, jointly play a major role in the determination of the maximum cladding temperature. In conjunction with the stated coolant inlet and exit thermodynamic states, they fix the following derived quantities:

a. Second pass mass flow rate through a channel

b. Power produced in a fuel element

c. Number of cells in the core

d. Heat transfer coefficient at the second pass coolant-cladding interface, which determines temperature rise from the coolant to the cladding and is a controlling term in the definition of the effective thermal conductivity k_e and hence the heat flow fraction f_2.

The two dimensions, which specify the fuel material thickness, r_2 and r_3, jointly fix one of the more controlling terms in the definition of k_e and f_2, namely the term $\ln(R)/k_f$. For an application in which a metallic fuel material could be used, the relative importance of the ratio R would be reduced, since the thermal conductivity of the fuel is the divisor in the term. The ceramic

fuel UO_2 has a relatively low thermal conductivity, as specified in the ground rules for the optimization, and the direct effect of a large ratio of R is not reduced in the expression entering the definition of effective thermal conductivity k_e. It should be noted that the fuel material dimensions are described in terms of the non-dimensional ratio R in both the expressions for k_e and f_2. This ratio then is a controlling design variable rather than the dimensional values for r_2 and r_3.

The cladding thicknesses, which are determined by the variables r_1, r_2 and r_3, r_4 must be fixed by strength and safety considerations. For the case of the cladding surrounding the fuel, the maximum thermal stresses will occur at the bottom of the core because of the steeper temperature gradients present there. For the selection of parameters resulting in a fuel element of minimum height, these other considerations rule out the possibility of independently varying these dimensions. The effect of the inner cladding thickness on the determination of the channel length L is small compared to the other inputs to the expression for effective heat transfer coefficient h_2 and its influence on the expressions for k_e and f_2. The outer cladding thickness provides an input to the effective heat transfer coefficient h_3, but this term does not significantly affect the values of k_e and f_2.

2.6 Optimization Technique

With the definition of an analytical model, the determination of the fuel element of minimum length L becomes relatively straightforward. The primary variables for investigation are V_2, r_1 and R. For each combination of these variables, a value for the fuel element length L and maximum temperature differential between cladding and second pass coolant is fixed.

The manner in which these calculated values are used is optional. The method used in this study proceeded by fixing V_2 and R and generating a curve of ΔT vs r_1 and a curve of L vs r_1. Holding the velocity V_2 constant, families

of curves were generated for different values of R. When the curve of ΔT vs r_1 reached the constrained value of ΔT (the difference of the limiting cladding temperature and second pass steam exit temperature), the value of r_1 at which this took place was used to enter the second set of curves of L vs r_1 at constant V_2 and R to pick off the corresponding length L.

The resulting set of values of L, r_1, R and V_2 defined a family of curves which had one thing in common - the curves were valid for a constant value of ΔT, the variable used to represent the design constraint. Plotting curves at constant values of V_2 for L vs R and r_1 vs R permitted the determination of the channel of minimum length L for a given R and the value of r_1 on the curve of r_1 vs R uniquely fixed the combination that satisfied the constraint. Subsequent plots of minimum L vs V_2 and r_1 and R at minimum L vs V_2 then completely fixed the dimensions.

The search for values, at which the constrained cladding temperature was achieved, used the cladding-coolant temperature differential as the initial variable upon which the optimization was performed. It should be noted that this choice is only valid for the situation assumed in the model, that is, that the power generation rate along the fuel element is constant. In a more realistic situation, the maximum cladding temperature would not necessarily occur at the exit point of the second pass coolant but would depend on the local heat flux and coolant temperature at some arbitrary point up the fuel element. If the effect of a variable axial power generation rate had been introduced into the model used, the maximum cladding temperature and the exiting steam temperature could be used to define a new dummy variable (the temperature differential) which would vary with position along the channel; nevertheless, a maximum differential would exist.

The temperature differential is a function of the power produced in the fuel element. The resultant calculated data is better presented using this

quantity as a measure of a given combination of values to meet the constraint temperature than the actual maximum cladding temperature. A log-log plot of ΔT vs r_1 at fixed values of V_2 and R results in a gently sloping line. Presentation of the calculated terms using the maximum cladding temperature directly vs r_1 yields a much more sharply curving line and hence requires additional points to more accurately describe the loci of points on the curve.

2.7 Optimization Results

The range of the three controlling parameters V_2, r_1 and R used in performing the optimization were as follows:

Variable	Range	Increment
V_2	100 - 300 ft/sec	100 ft/sec
r_1	0.25 - 2.0 cm	Various
R	1.1 - 5.0	Various

Those values needed to conduct the analysis, other than those specified by the thermodynamic state of the coolants, are given. The thickness of the interior and exterior cladding around the annular fuel region was set at 20 mils; this value thus determined r_2 when r_1 was given and r^4 when r_2 and R were specified. The interface heat transfer coefficient h_i between the cladding and fuel regions was assigned the value of 1000 Btu/hr/ft^2/^{o}F. The thermal conductivity of the Inconel cladding k_c was taken at 8.4 Btu/hr/ft/^{o}F. Lastly, the average value of the heat transfer coefficient between cladding and first pass coolant h_4 was taken as 5000 Btu/hr/ft/^{2}/^{o}F. With these values and those determined by the thermodynamic state of the coolant, the results were calculated.

The results of plotting the maximum cladding-coolant temperature differentials are shown in Figures 2.1 - 2.3. The calculated channel lengths L are shown in Figures 2.4 - 2.6. After those points are established on Figures 2.1 - 2.3 for a given temperature differential, the corresponding channel lengths

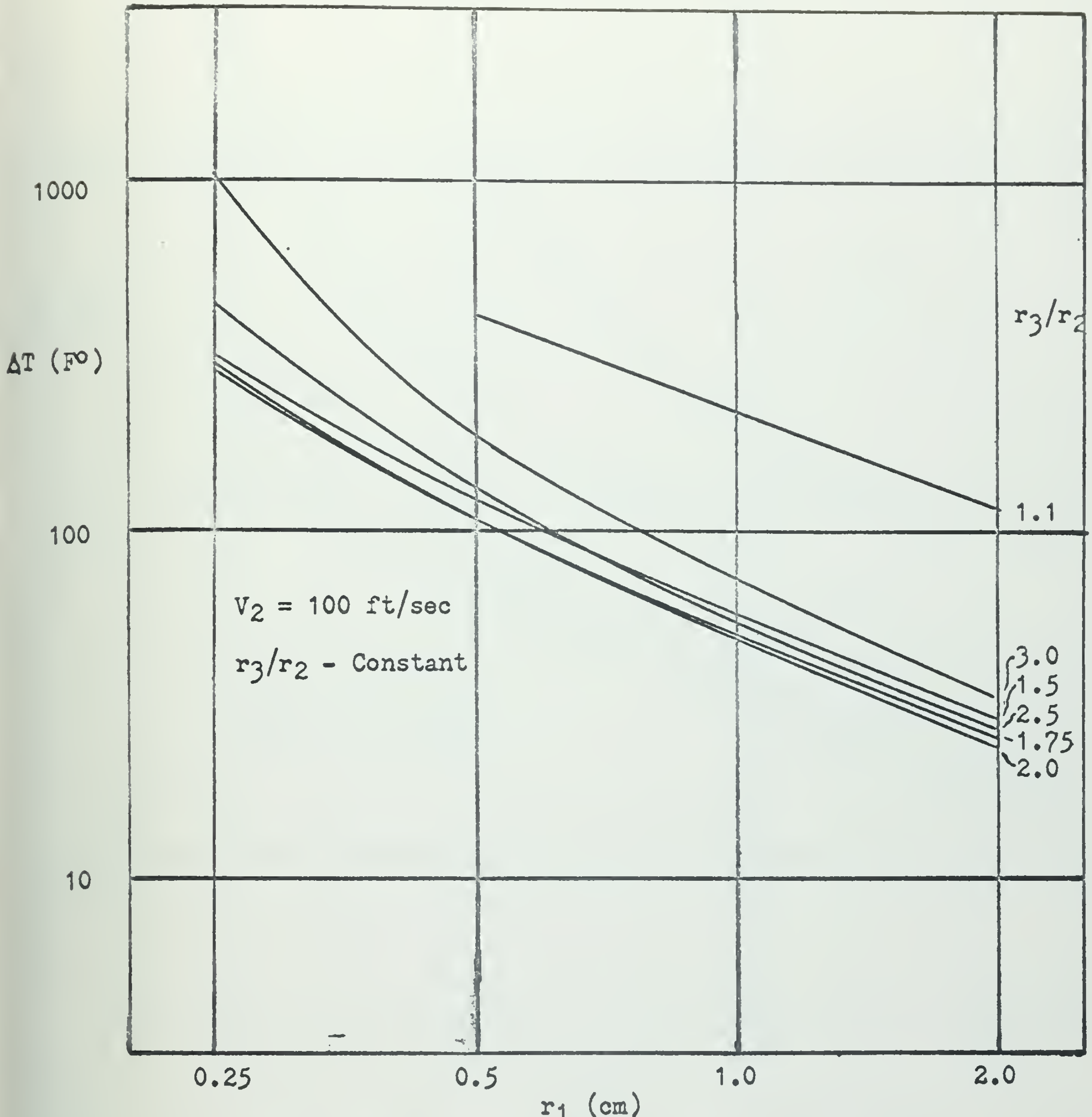

MAXIMUM SECOND PASS CLADDING-COOLANT TEMPERATURE DIFFERENTIAL ΔT VS SECOND PASS CHANNEL RADIUS r_1 FOR CONSTANT VALUES OF FUEL MATERIAL RADII RATIOS (r_3/r_2) AT A SECOND PASS EXIT VELOCITY V_2 OF 100 FT/SEC

Figure 2.1

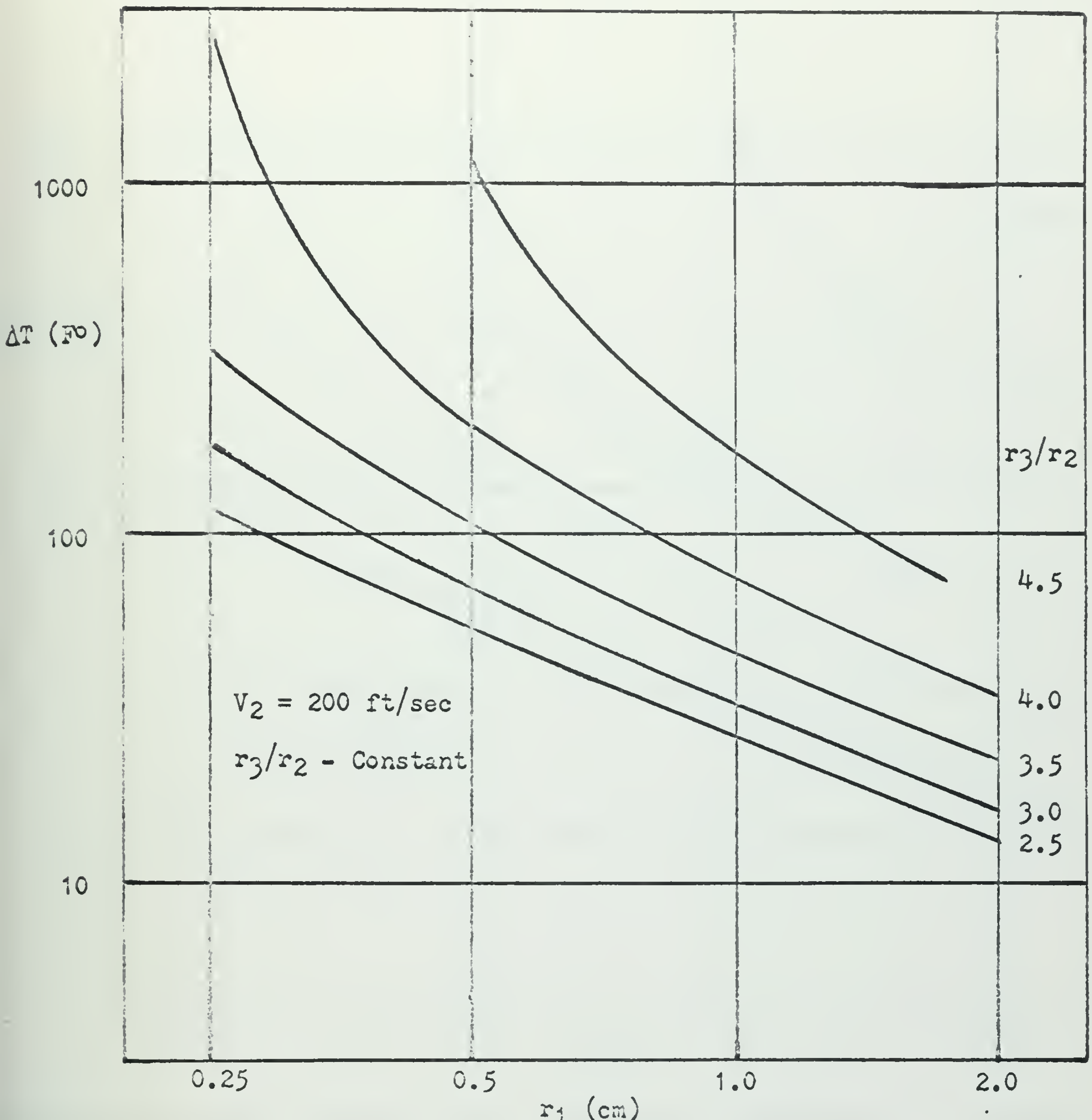

MAXIMUM SECOND PASS CLADDING-COOLANT TEMPERATURE DIFFERENTIAL ΔT VS SECOND PASS CHANNEL RADIUS r_1 FOR CONSTANT VALUES OF FUEL MATERIAL RADII RATIOS (r_3/r_2) AT A SECOND PASS EXIT VELOCITY V_2 OF 200 FT/SEC

Figure 2.2

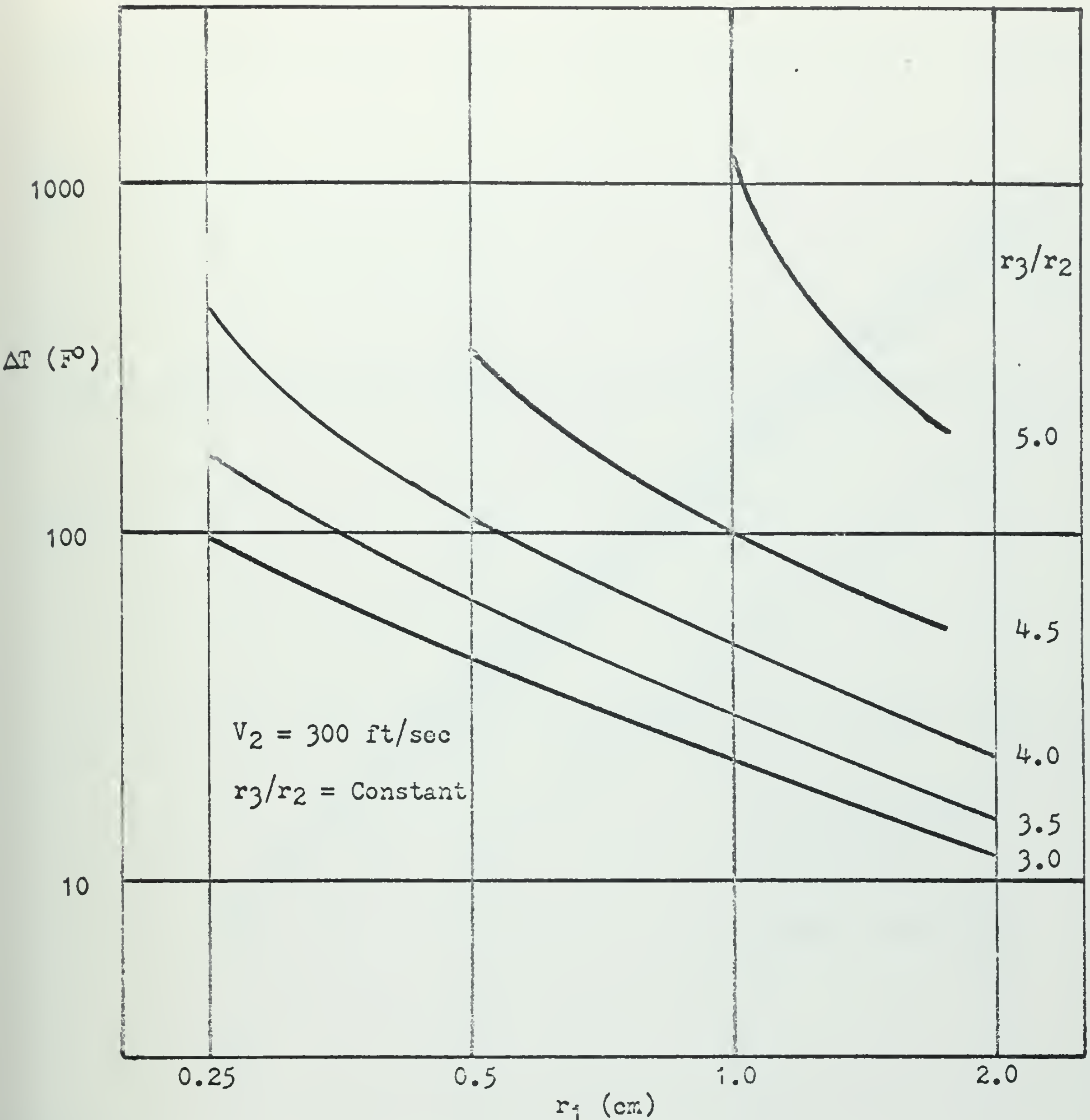

MAXIMUM SECOND PASS CLADDING-COOLANT TEMPERATURE DIFFERENTIAL ΔT VS SECOND PASS CHANNEL RADIUS r_1 FOR CONSTANT VALUES OF FUEL MATERIAL RADII RATIOS (r_3/r_2) AT A SECOND PASS EXIT VELOCITY V_2 OF 300 FT/SEC

Figure 2.3

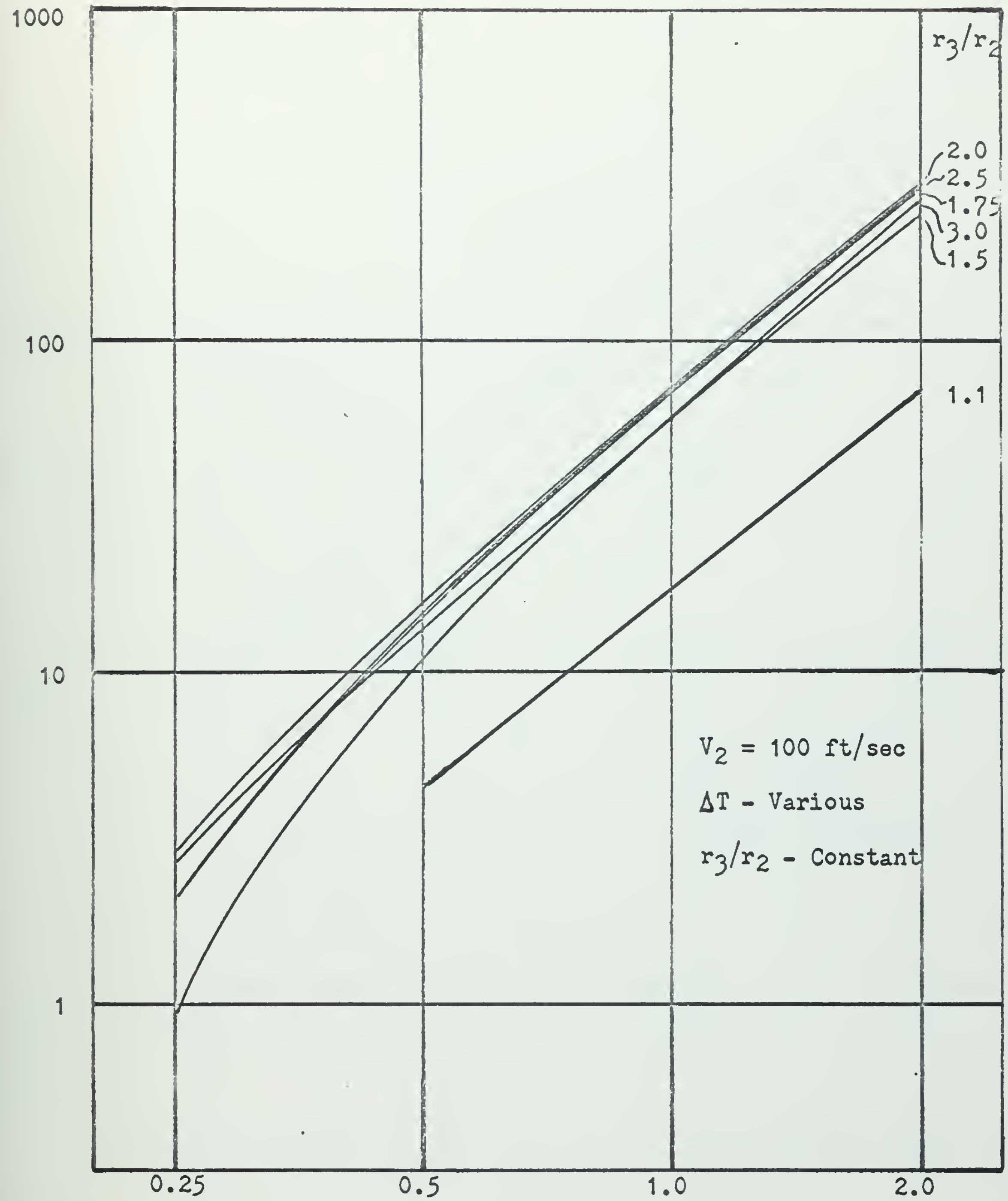

FUEL TUBE LENGTH L VS SECOND PASS CHANNEL RADIUS r_1 FOR VARIOUS VALUES OF FUEL MATERIAL RADII RATIOS (r_3/r_2) AT A SECOND PASS EXIT VELOCITY OF 100 FT/SEC

Figure 2.4

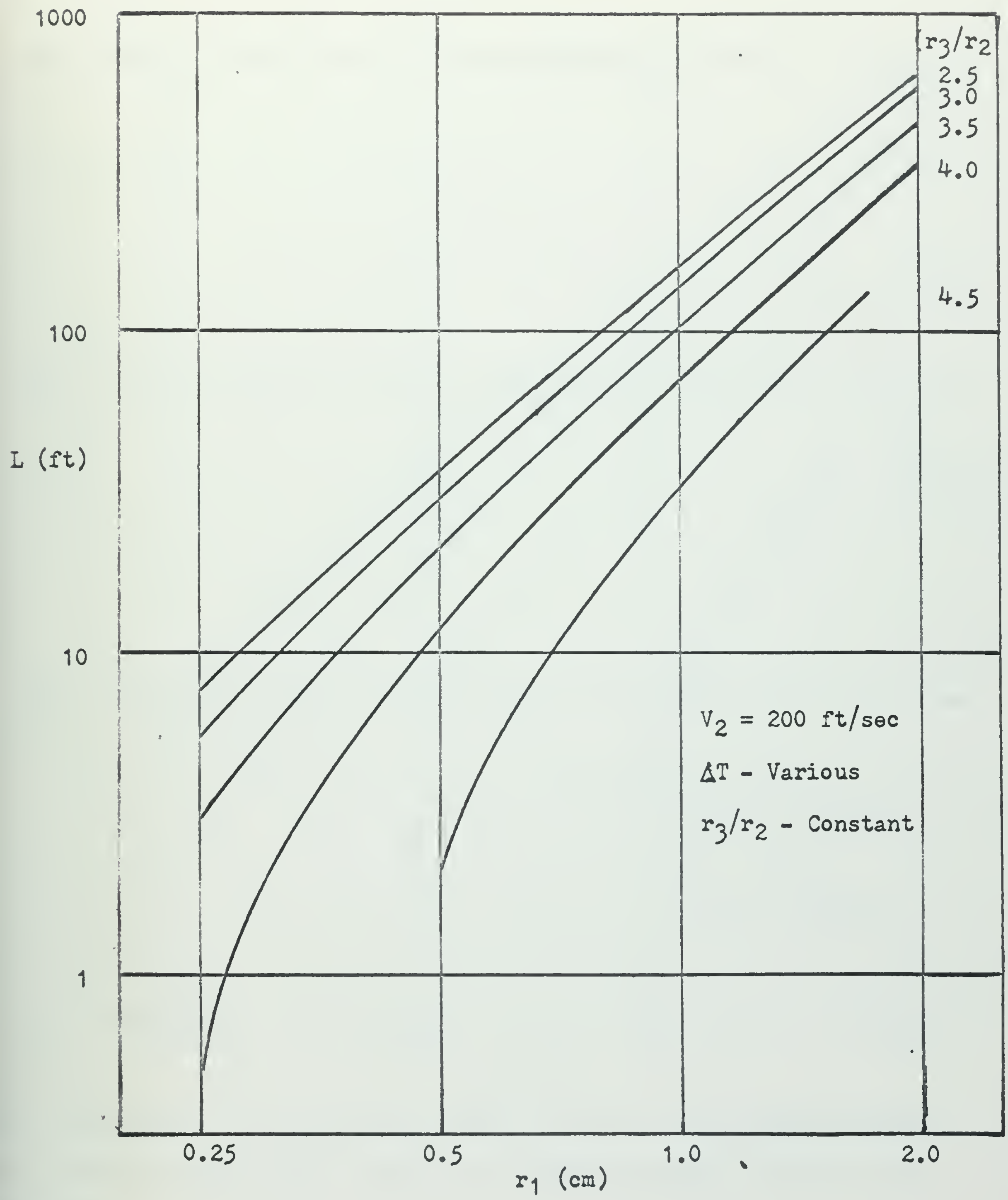

FUEL TUBE LENGTH L VS SECOND PASS CHANNEL RADIUS r_1 FOR VARIOUS VALUES OF FUEL MATERIAL RADII RATIOS (r_3/r_2) AT A SECOND PASS EXIT VELOCITY V_2 OF 200 FT/SEC

Figure 2.5

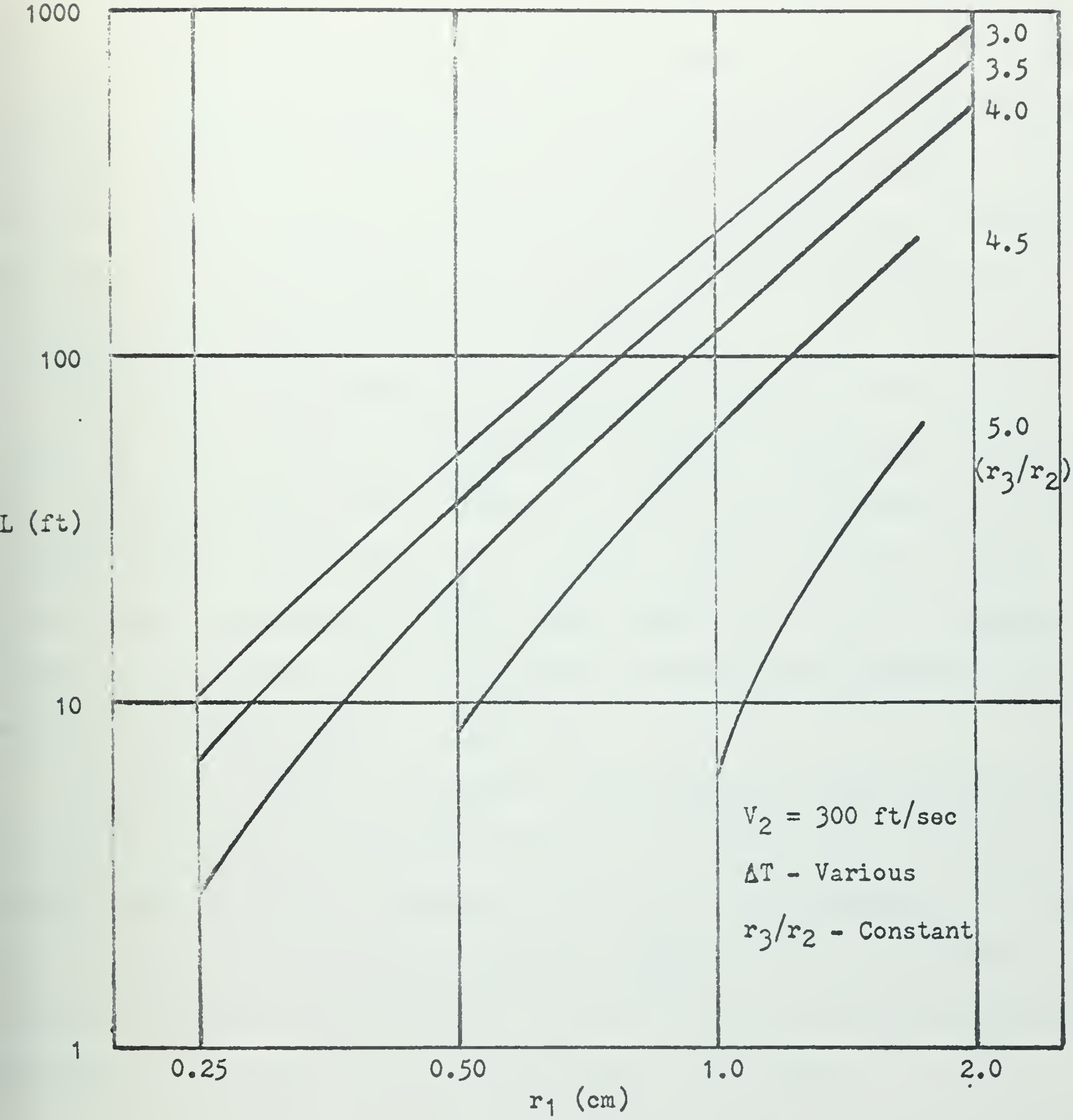

FUEL TUBE LENGTH L VS SECOND PASS CHANNEL RADIUS r_1 FOR VARIOUS VALUES OF FUEL MATERIAL RADII RATIOS (r_3/r_2) AT A SECOND PASS EXIT VELOCITY V_2 OF 300 FT/SEC

Figure 2.6

can be read from the second set of figures.

The desired second pass steam exit temperature is 955 °F. From Section 2.2, the maximum allowed Inconel cladding temperature is 1350 °F. The maximum allowable temperature differential is thus fixed at 395 F°. It must be remembered that this value is only valid for the ideal situation in which the power generation rate is constant throughout the core. The model used to generate Figures 2.1 - 2.6 had no provisions for including the effects of spatial variation of power generation, i.e., power peaking.

The values of the cladding-steam interface temperature differential chosen for further detailed investigation are 295 F°, 245 F°, 195 F° and 145 F°. These correspond then to margins of safety for not exceeding the constrained maximum cladding temperature of 100 F°, 150 F°, 200 F° and 250 F°, respectively, under the assumption of flat power generation. As a first approximation, this presupposes that the maximum-to-average power generation rate will fall someplace between 1.35 and 2.6.

When one of the chosen temperature differentials is used to enter Figures 2.1 - 2.3, the value of the inner radius r_1 for a given ratio of annular fuel element radii (r_3/r_2) is determined. Entering the corresponding set of Figures 2.4 - 2.6 with these values then fixes the length L of the fuel element. The results of plotting these points for a given value of ΔT and second pass exit velocity V_2 are shown in Table 2.2 and Figures 2.7 - 2.12.

In the discussion of design constraints in Section 2.2, it was pointed out that the maximum allowable temperature for the UO_2 fuel is 4500°F. Taking the case of the minimum channel length for $\Delta T = 295$ F° at $V_2 = 100$ ft/sec, the maximum temperature in the fuel is calculated to be 1570 °F. Thus, the cladding temperature constraint is controlling in the optimization.

Inspection of Figure 2.9 and Figure 2.11 shows that the curves of length L for V_2 at 200 and 300 ft/sec are still decreasing as the value of R decreases.

Table 2.2

FUEL ELEMENT PARAMETERS SATISFYING CLADDING TEMPERATURE CONSTRAINTS

V_2 (ft/sec)	r_3/r_2	ΔT = 295 F°		ΔT = 245 F°	
		r_1 (cm)	L (ft)	r_1 (cm)	L (ft)
100	1.1	0.735	9.76	0.886	14.30
	1.5	0.256	2.82	0.290	3.87
	1.75	0.244	2.66	0.278	3.67
	2.0	0.254	2.87	0.282	3.89
	2.5	0.301	3.88	0.332	5.14
	3.0	0.391	5.52	0.425	7.05
200	3.29			0.250	4.25
	3.42	0.250	3.60		
	3.5	0.272	3.92	0.302	5.35
	4.0	0.425	7.40	0.459	9.19
	4.5	0.743	14.61	0.809	18.10
300	3.78			0.250	4.57
	3.87	0.250	3.82		
	4.0	0.286	4.51	0.310	5.95
	4.5	0.723	9.79	0.753	12.89
	5.0	1.427	31.0	1.552	42.8

V_2 (ft/sec)	r_3/r_2	ΔT = 195 F°		ΔT = 145 F°	
		r_1 (cm)	L (ft)	r_1 (cm)	L (ft)
100	1.1	1.048	22.45	1.519	41.1
	1.5	0.339	5.65	0.428	9.76
	1.75	0.326	5.30	0.401	9.15
	2.0	0.326	5.62	0.400	9.59
	2.5	0.381	7.27	0.460	11.8
	3.0	0.481	9.76	0.578	15.58
200	2.77			0.250	6.62
	3.0			0.290	8.21
	3.10	0.250	5.13		
	3.5	0.343	7.76	0.407	12.71
	4.0	0.514	12.90	0.611	21.45
	4.5	0.925	25.98	1.108	42.7
300	3.39			0.250	7.43
	3.5			0.274	8.40
	3.63	0.250	5.64		
	4.0	0.353	8.65	0.422	11.98
	4.5	1.732	61.5		

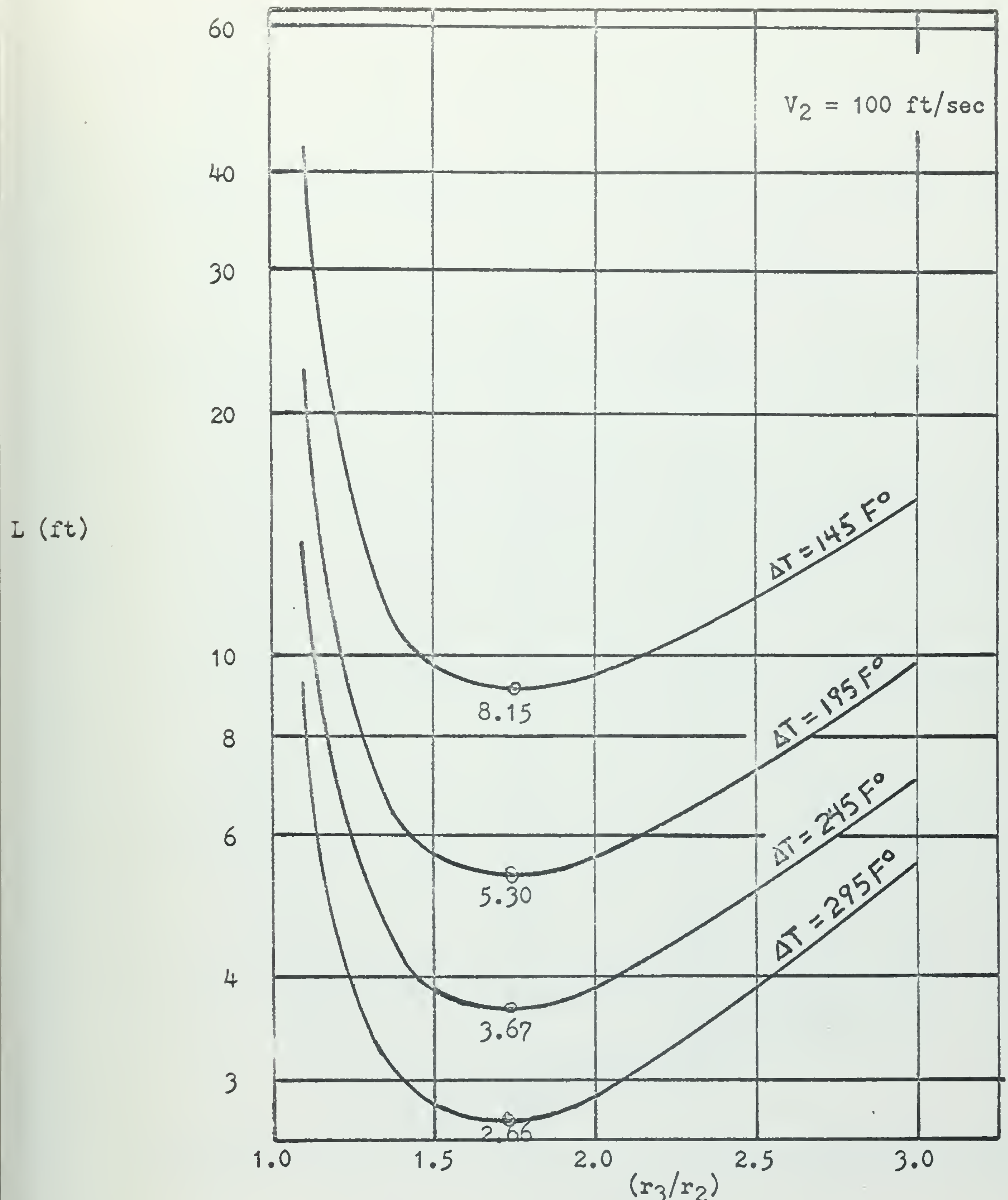

FUEL TUBE LENGTH L VS FUEL MATERIAL RADII RATIO (r_3/r_2) FOR CONSTANT VALUES OF MAXIMUM SECOND PASS CLADDING-COOLANT TEMPERATURE DIFFERENTIAL ΔT AT A SECOND PASS EXIT VELOCITY OF 100 FT/SEC

Figure 2.7

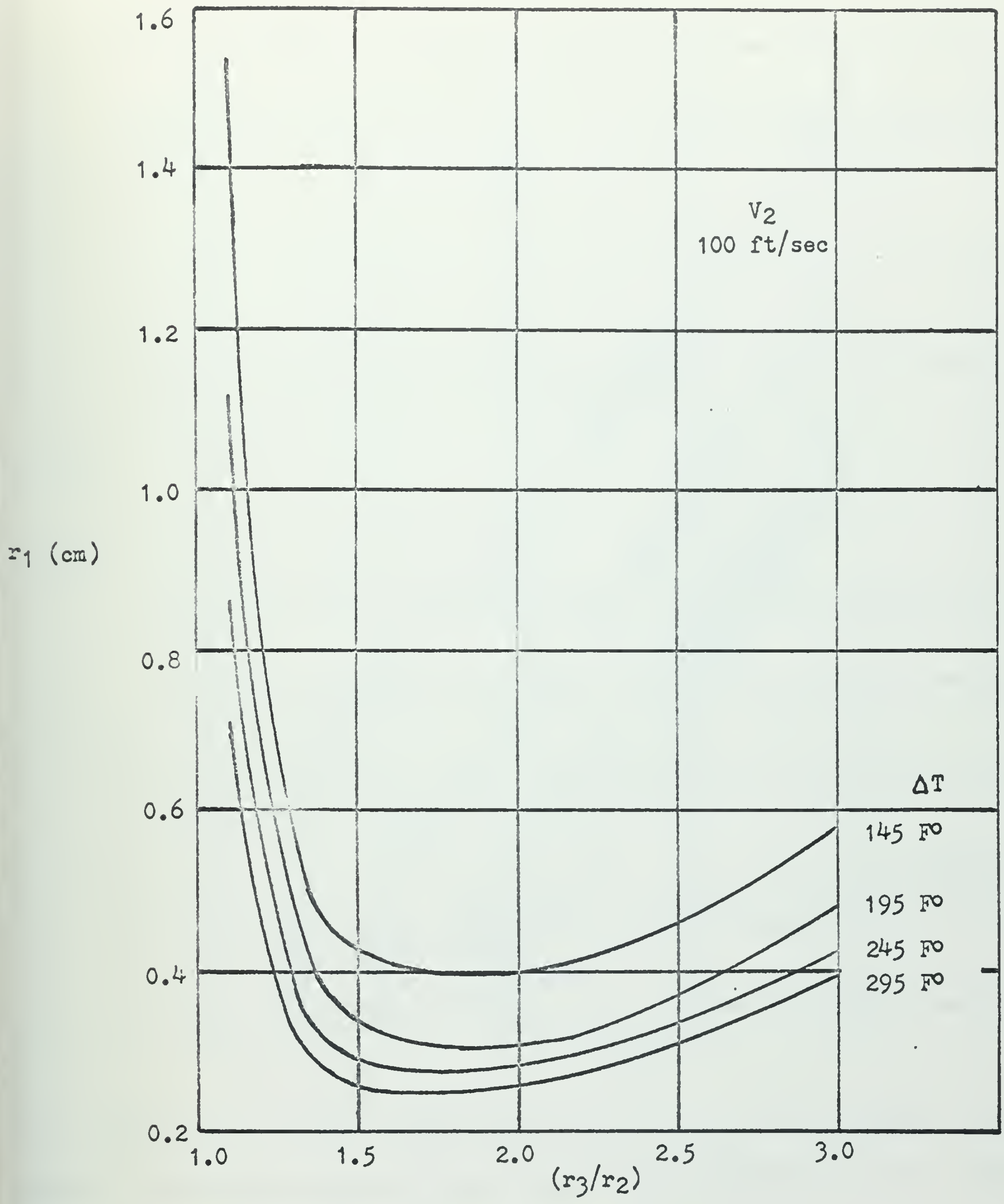

SECOND PASS CHANNEL RADIUS r_1 VS FUEL MATERIAL RADII RATIO (r_3/r_2) FOR CONSTANT VALUES OF MAXIMUM SECOND PASS CLADDING-COOLANT TEMPERATURE DIFFERENTIAL ΔT AT A SECOND PASS EXIT VELOCITY V_2 OF 100 FT/SEC

Figure 2.8

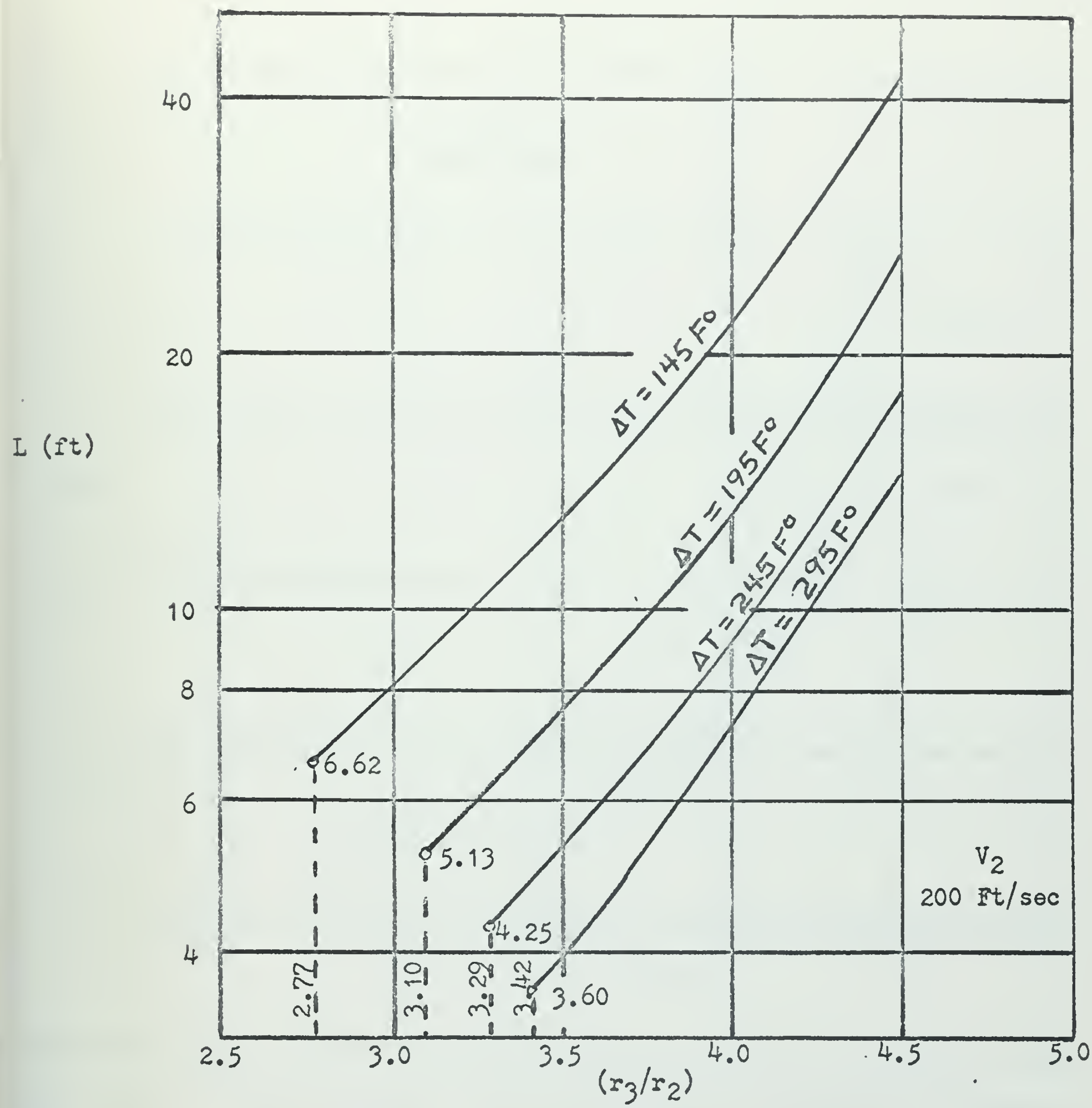

FUEL TUBE LENGTH L VS FUEL MATERIAL RADII RATIO (r_3/r_2) FOR CONSTANT VALUES OF MAXIMUM SECOND PASS CLADDING-COOLANT TEMPERATURE DIFFERENTIAL ΔT AT A SECOND PASS EXIT VELOCITY OF 200 FT/SEC

Figure 2.9

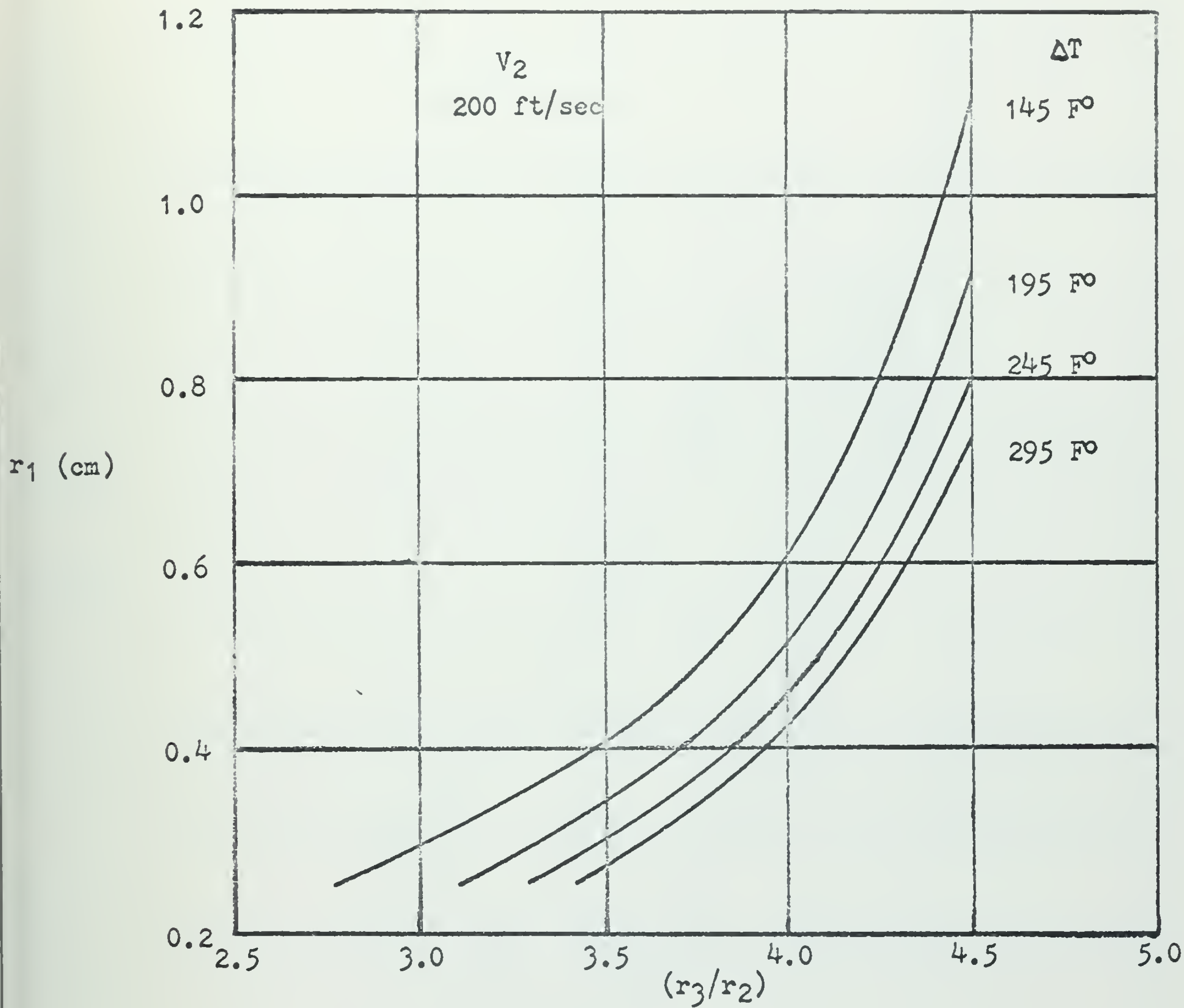

SECOND PASS CHANNEL RADIUS r_1 VS FUEL MATERIAL RADII RATIO (r_3/r_2) FOR CONSTANT VALUES OF MAXIMUM SECOND PASS CLADDING-COOLANT TEMPERATURE DIFFERENTIAL ΔT AT A SECOND PASS EXIT VELOCITY V_2 OF 200 FT/SEC

Figure 2.10

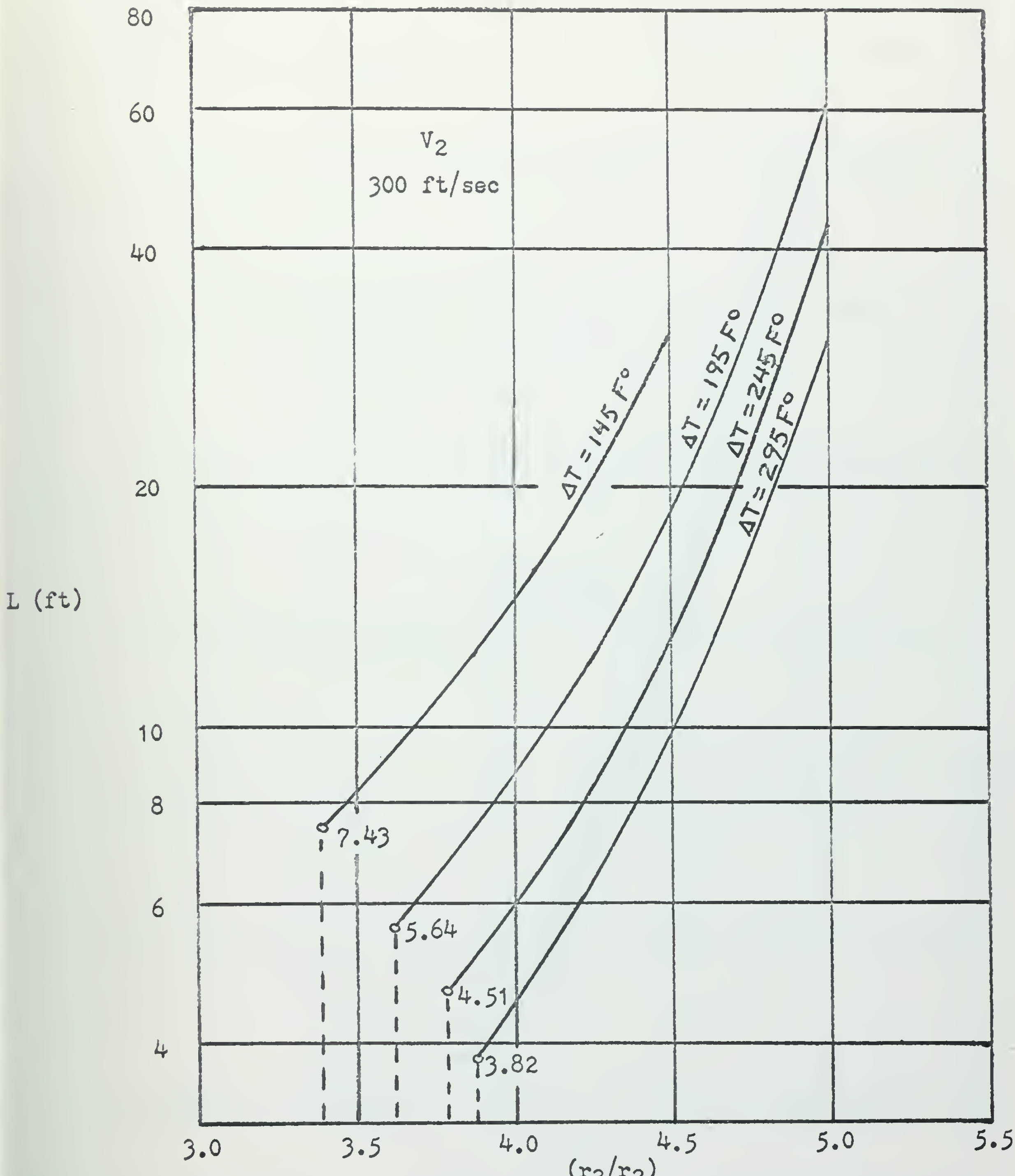

FUEL TUBE LENGTH L VS FUEL MATERIAL RADII RATIO (r_3/r_2) FOR CONSTANT VALUES OF MAXIMUM SECOND PASS CLADDING-COOLANT TEMPERATURE DIFFERENTIAL ΔT AT A SECOND PASS EXIT VELOCITY OF 300 FT/SEC

Figure 2.11

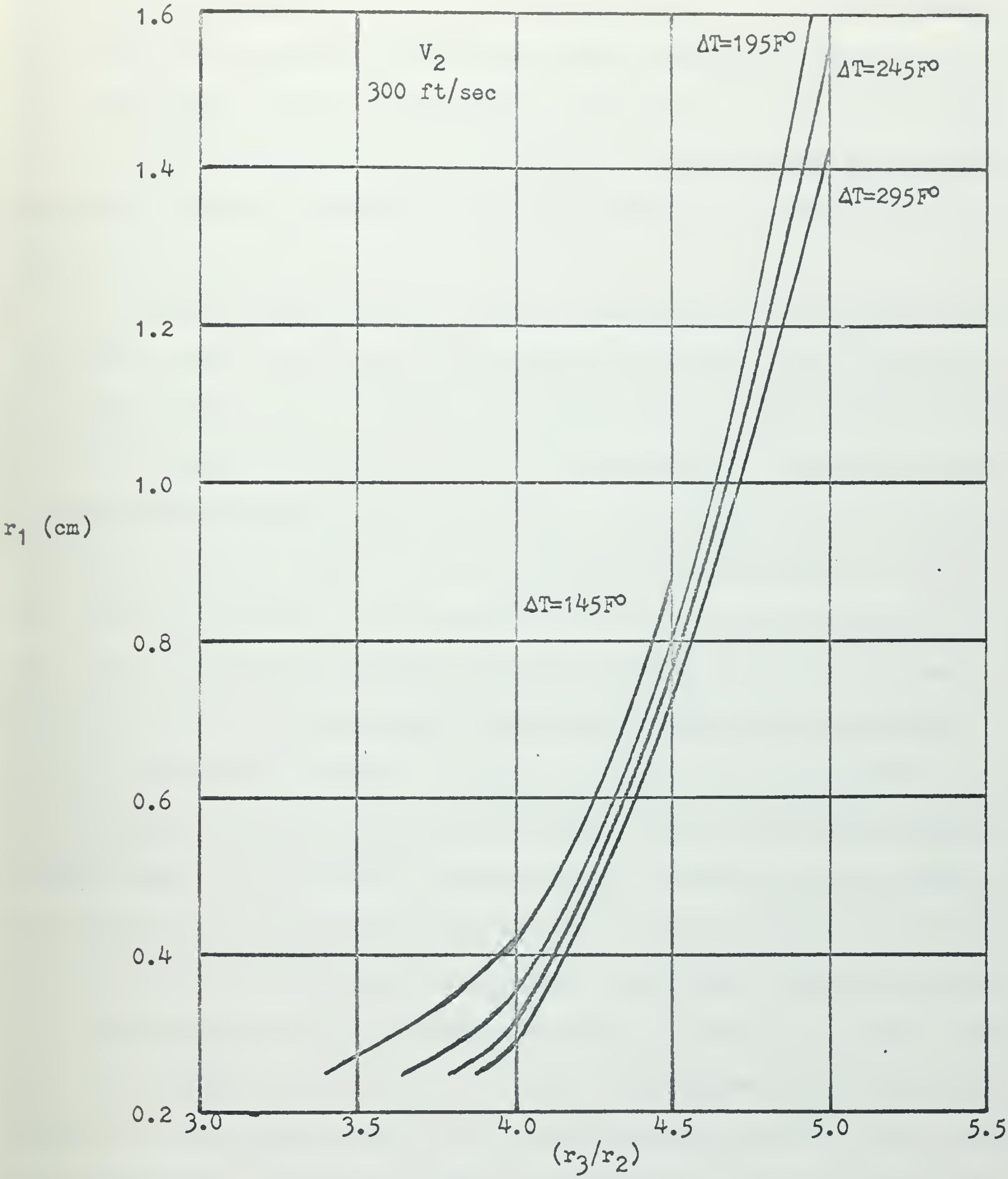

SECOND PASS CHANNEL RADIUS r_1 VS FUEL MATERIAL RADII RATIO (r_3/r_2) FOR CONSTANT VALUES OF MAXIMUM SECOND PASS CLADDING-COOLANT TEMPERATURE DIFFERENTIAL ΔT AT A SECOND PASS EXIT VELOCITY V_2 OF 300 FT/SEC

Figure 2.12

The lowest point of these curves was calculated when r_1 was equal to 0.25 cm. The curves were terminated at this value since continuation beyond is considered to be unrealistic from the manufacturing standpoint. The graphical minimum for V_2 at 100 ft/sec and ΔT at 295 F° occurs at slightly under this cut-off dimension. Only for the case of V_2 at 100 ft/sec does a minimum exist in the plot of length L.

As shown in Figure 2.8, the radius r_1 decreases above 0.25 cm as (r_3/r_2) approaches unity. For values of V_2 at 200 and 300 ft/sec, one would expect that the radius r_1 would increase as (r_3/r_2) decreases for any given temperature differential ΔT. For $r_1 = 0.25$ cm and $(r_3/r_2) = 1.5$, the calculated temperature differential is 90.7 F° for $V_2 = 200$ ft/sec and 43.3 F° for $V_2 =$ 300 ft/sec. In both cases, the minimum temperature differential T had not been reached when (r_3/r_2) was reduced to 1.5 and r_1 was held constant at 0.25 cm. Thus, even though values of r_1 might be found above 0.25 cm for small values of (r_3/r_2), no calculations were actually carried out to determine them. At these small values of (r_3/r_2), the volume percentage of fuel that can be loaded into the core becomes very small and, hence, that of the cladding becomes larger. The fact that a higher rate of parasitic neutron capture in the cladding would result for parameters in this region obviated the requirement to perform the calculations necessary to demonstrate a graphical minimum.

The optimum set of fuel element dimensions for maximum core power density can be determined from the curves of length L for a given steam velocity and temperature differential based on the assumed power distribution, heat transfer and thermodynamic conditions. Nuclear considerations, not included in this model, must also be weighed when choosing the optimum set. The dimensional sets generated here provide a starting point for determining the complete set of core dimensions.

Chapter 3

MATHEMATICAL MODEL TO ANALYZE THE COUNTERFLOW REACTOR

3.1 Introduction

The results presented in Chapter 2 dealt specifically with the fuel element parameters under several simplifying assumptions. Briefly recapping, the assumptions made were (1) power generation within individual fuel elements and across the core had not spatial dependence, (2) the temperature of the first pass coolant throughout the height of the core was constant, and (3) the heat transfer properties of the coolant streams did not change within their respective channels. With these assumptions, it was possible to define optimum fuel element dimensions by not considering the nuclear aspects of the power source.

The above noted model does not present the power and coolant property variations in sufficient detail. In addition, there is no means of telling if, for a given fuel enrichment, that the reactor will even achieve criticality. Because of the coolant density changes, there is no means of determining whether the flow pattern across the core is stable or unstable. In summary, finer details are necessary to determine whether or not the concept is feasible.

3.2 Scope

The reactor is an assemblage of the cells shown in Figure 1.1. As such, a rigorous analysis of the reactor would involve the solution of a three-dimensional problem. Making the assumption that the parameter variation is rotationally symmetric about the center line of the right circular cylinder which is the core, the problem can be reduced to one of a two-dimensional nature.

The variation of the different parameters (flux, power, temperature, etc.) could be represented in terms of analytical functions. Unfortunately

the problem is so complex that a trial-and-error type of solution is required. The reiterative approach, which is required to solve the coupled nuclear, heat transfer, fluid flow, and thermodynamics problem, suggests that the problem be formulated in sets of difference equations. This approach has been used here, particularly because of the relative ease to which this type of problem lends itself to programming on a digital computer. The majority of the effort expended in this study has been devoted to the development of the analytical model which described parameter variation and the subsequent programming of the model. As such, the program which has resulted can be applied to any reactor which follows the concept of the CFR and is not limited to reactors of the power rating, total flow or inlet conditions discussed here.

Programming the model imposes some limitations on the scope of the problem, although it almost completely eliminates the computational effort involved, once the program has been written, to study a particular parameter set. The computer storage size and the time available to run the program are the primary limitations on the detail to which the coupled problems can be solved. With the facilities available at the MIT Computation Center, the model had to be formulated in terms of a one-dimensional problem. To make the results more realistic, correctional factors are generated internally during the course of running the program to re-insert the two-dimensional nature of the problem into the various nuclear calculations. The computer storage size not only reduced the problem statement to one-dimension but limited the number of nuclear groups that could be studied to two.

Since the problem has to be formulated in one dimension, a detailed analysis of the effect of control rods on the flux and power distribution is not readily achieved. The height to which control rods are inserted into the core causes a variation of the axial power distribution. Likewise

the presence of control rods introduces local variations into the radial power distribution which cannot be considered in terms of rotational symmetry. To determine whether the particular reactor configuration and constituent make-up lead to a critical system, the assumption has been to load the core homogeneously with a poison. If the poison concentration required to give the reactor a reactivity of zero or more is positive, the reactor will attain criticality.

These opening remarks have dealt primarily with the nuclear aspect of the problem, since their solution most severely limits the scope of the computational model which can be used. The remaining sections of this chapter will present the concepts used in solving the coupled problems. The details of their implementation are left to the appendices for presentation.

3.3 Nuclear Model and Reactor Subdivision

The model chosen to describe the steady state flux and power distribution is that of two-group diffusion theory, because of the relative simplicity with which it can be applied and a solution obtained, in contrast to the greater complexity which results when a higher order transport theory approximation is used. It does suffer from a lack of precision, particularly in the fuel regions. The basic equations which apply to this model for the j^{th} group ($j = 1$, fast; $j = 2$, thermal) are

a. Conservation Equation

$$0 = D^j \nabla^2 \phi^j - \Sigma_p^j \phi^j - \Sigma_a^j \phi^j - \delta(j,1)\Sigma_s^{1\to 2}\phi^1 + \chi^j \sum_{K=1}^{2}\left[\nu^K \Sigma_f^K \phi^K\right] + \delta(j,2)\Sigma_s^{1\to 2}\phi^1$$

b. Flux Boundary Condition at an Interface

$$\phi^j\big|_{left} = \phi^j\big|_{right}$$

c. Current Boundary Condition at an Interface

$$-D^j \nabla\phi^j\big|_{left} = -D^j \nabla\phi^j\big|_{right}$$

d. Power Generation at a Spatial Point

$$P \propto \sum_{K=1}^{2} \left[\Sigma_f^K \, \phi^K \right]$$

All these terms are assumed to be constant within a given region except the flux ϕ^j and the local power generation rate P. One assumption made here has been that the power generation rate P arises only from direct fission particle heating; the model thus neglects the effect of gamma heating in regions other than the fuel. The conservation equation is formulated in terms of central differences.

The equations, describing the flux distribution, have been applied to a reactor which is subdivided as shown in Figure 3.1. The reactor can be broken into a total of 49 different subdivision (in the present computer program) of which 30 are peculiar to the core. The exterior subdivisions define either the radial or axial reflector regions. The nuclear properties within each of the 49 regions are assumed to be constant and are determined from homogenization of a cell producing power at a rate which is characteristic of that given radial region of the core. Rotational symmetry about the reactor centerline is assumed.

<u>3.3.1 Cell Homogenization</u>

The fact that the coolant, particularly in its boiling first pass through a cell, can undergo large volumetric changes requires that the nuclear calculations include a provision for this effect. Based upon the power generation rate within a given region of the core, the first and second pass coolants within that region are assigned average density values. This assignment then fixes all the properties within the thirty core subdivisions. The properties of this average cell region are homogenized and made applicable to the whole region.

Cross sections for this composite region are homogenized by flux and [illegible] weighting the individual properties to gain an average representative

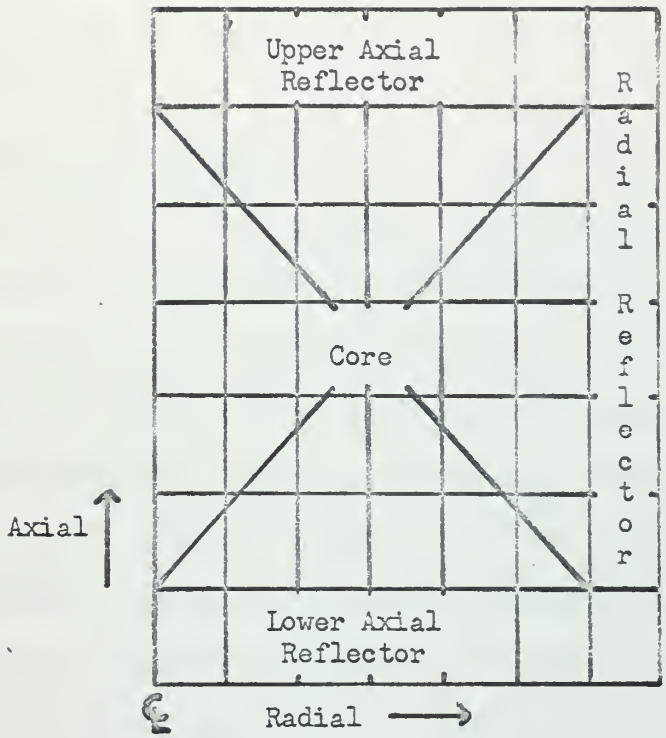

REACTOR SUBDIVISION

Figure 3.1

value. In the calculations, the flux shape within the cell is assumed to be rotationally symmetric about the center of the cell. The fact that the cells are set on a square pitch, as shown in Figure 1.1, is circumvented when applying the rotational geometry by assuming that an equivalent exterior cell radius can be defined such that the area enclosed by it is equal to the area enclosed by the square perimeter. The diffusion coefficient homogenization is accomplished by converting the diffusion coefficient back to its equivalent transport cross section, homogenizing the transport cross section by flux and volume weighting, and converting this homogenized transport cross section back to an equivalent diffusion coefficient.

The cell region homogenization is performed on a strictly one-dimensional basis at the position in the cell where the average coolant density was

defined. The boundary conditions imposed are that the neutron current is zero at the origin and at the equivalent cell radius. Additionally, the assumption is made that the leakage cross section for neutron loss in the axial direction is zero.

3.3.2 Axial Nuclear Calculations

With the generation of the homogenized subdivision properties at some given radial position in the reactor, it is possible to calculate the flux and power shape along an axial line in this region. For this calculation the boundary conditions are zero flux at the top and bottom of the reactor (which includes the axial reflector regions). The leakage cross section, which refers to neutron flow in a radial direction, can now be either positive or negative, respectively, depending upon whether the net number of neutrons flowing into the axial region is negative or positive. The details of the way in which the leakage cross section is generated are presented in Section A.12; equations (A-71) through (A-74), which summarize the results, are quite lengthy and will not be repeated here.

One of the results, which is obtained from the axial calculations, is the axial power distribution in a typical cell within that radial region of the core.

3.3.3 Radial Nuclear Calculations

The power distribution radially across the core is calculated after boundary conditions of zero current at the reactor centerline and zero flux at the edge have been assigned. The properties used in this calculation are the same as those used in the axial calculation except that only the subdivision properties at mid-height in the core are used. The leakage cross section for this type of calculation now refers to loss out through the top and bottom axial reflector regions. The leakage cross section is defined in terms of the system "buckling" and the technique used to generate it is

described in Section A.13.

The radial calculation is used to determine the flux and power distribution across the core. The total power produced in each radial region of the core is assigned to the cells in that radial region on the basis that they are producing at the same rate. From the axial calculations, which determined the axial power distribution, the power produced in a given length of fuel rod is fixed; with the completion of a radial reactor calculation, the power generation map for the core is fixed.

After a radial calculation has been completed, the criticality of the system is calculated. Based upon the results of this calculation, the homogenous poison cross section is varied such that the reactor meets the specified value of criticality. If the poison concentration does in fact have to be changed, the new concentration is inserted and another radial calculation is performed. The procedure is repeated until the desired criticality is achieved.

3.3.4 Sequence of Performing Nuclear Calculations

The nuclear properties of all materials within the core are assumed to be constant. In the generation of macroscopic cross sections and diffusion coefficients for each of the reactor subdivisions, only the coolant regions show variation in density. Thus, specifying the macroscopic properties of all cell regions other than those for the coolant and the microscopic properties of the coolant fixes the external nuclear inputs to the problem.

Before a series of nuclear calculations is started, the coolant densities at the different locations within the core are assumed to be known. For a given radial region, the properties of the different axial subdivisions are homogenized starting at the lowest subdivision in the core and working to the top subdivision. After the axial calculations are performed on this radial region, the sequence advances to the next outward radial subdivision and is

repeated. When the axial calculation in the outermost radial core subdivision has been completed, the radial calculation is performed.

This approach can be characterized as being a "marching" type of solution. The major step is outwards, the minor steps are upwards. With the inclusion of the leakage across sections, it provides a satisfactory solution to the two-dimensional nuclear problem using a one-dimensional model.

3.4 Heat Transfer and Thermodynamics

These two problems are considered together because of their close relationship. Actually, heat transfer is dependent upon fluid flow, but the technique used to determine the fluid flow profiles require slightly more than the "broad brush" treatment of this section.

The solution to the nuclear problem, previously discussed, determines the power generation rates of a typical cell in each of the radial regions of the core. The axial nuclear calculations determine how much power is produced in a given axial slice of the different typical cells. Within two adjacent axial slices of the same cell, the variation of heat transfer and thermodynamic properties can be calculated by utilizing the technique indicated in Figure 3.2. All the heat transfer properties and thermodynamic properties within a given core subdivision are assumed to be constant.

3.4.1 Selection Basis for Average Coolant Properties

The axial position within an axial slice at which the average coolant properties are defined is made to coincide with that position in the subdivision at which half the power produced has been generated. This point may or may not occur at the median position of that subdivision. This assumption neglects the curvature of the power generation rate within the subdivision.

3.4.2 Calculation of the Heat Flow Fraction

During the course of the cell homogenization calculations, a radial flux plot is made across the cell at the position where the average coolant

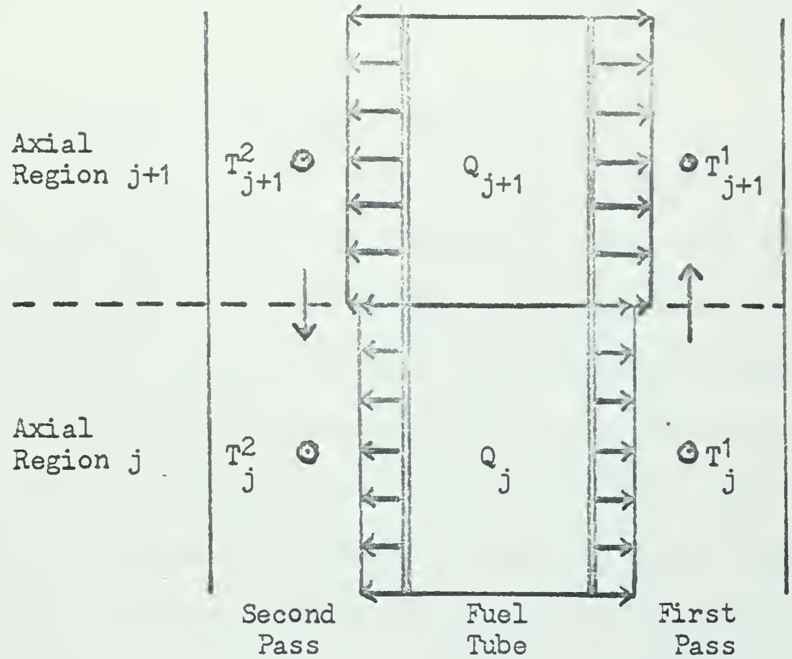

SCHEMATIC FOR THERMODYNAMIC CALCULATIONS

Figure 3.2

properties occur. Within the fuel material, the "fine" radial variation of the power generation rate is calculated. The shape of this curve is a factor in determining what fraction of the heat produced in that segment of the cell will flow either inwards or outwards, based on the thermal resistances that are present.

The heat flow fraction can be described in terms of an analytical function. In the discussion of Chapter 2, the power distribution across the fuel in a cell was assumed to be constant. Using the discrete values of power generation in the fuel, as determined by the nuclear calculations, an analytical function is generated which defines the local power curve. The function used is a fourth order polynomial, which is found by making a least squares fit.

Using the local calculated value of the first and second pass heat

transfer coefficients, the heat flow fraction to the first or second pass can be calculated. Appendix B demonstrates in detail the procedure which is used.

3.4.3 Calculation of the Average Coolant Properties

The fact that power can be transferred from the second coolant pass to the first across the fuel tube makes the direct solution for the average coolant properties impossible. The solution is obtained by trial-and-error, the question being which approach will most expeditiously produce the solution. The technique which has been used is to first uncouple the interactions between the two coolant streams, work through the core, first upwards along the first pass channels and then back down along the second pass channels. Using the heat flow fractions and temperature differentials between the two coolant streams, as determined by the preceding iteration, it then is possible to generate a new set of heat flow fractions and coolant properties. At the end of this subsequent iteration, the values generated are checked against those from the previous iteration; if the two values agree within specified convergence limits, the iterations cease and the problem is assumed to be solved for the given core power generation map.

3.5 Fluid Flow

All flow of coolant through the core is bounded on the bottom and top of the core by common plenums. The different first or second pass flow channels thus are equivalent to a set of parallel circuits. Because the flow originates and exits into common plenums, the pressure drop across the core for all first pass flow channels must be the same and the pressure drop for all second pass flow chan nels must be the same.

As noted in the preceding section, the calculation of the coolant properties at each of the different core subdivisions is obtained by uncoupling the counterflow effect. That this method of solution was used is caused by

the requirements for determining the fluid flow profiles across the core. The sequence of operations described in the preceding section involved sweeping out across the core, first for the first pass channels and then for the second pass channels.

After a sweep has been completed, the pressure drop across the core for the individual coolant channels is calculated. If the pressure drops do not agree within specified convergence limits, the flow through the channel is either increased or decreased, depending upon whether the pressure drop is too small or too large. When the individual flow rates have been calculated to yield the same pressure drop for all the channels, the total flow through the core is calculated. If this total agrees with that specified in the problem statement, the calculation proceeds to either the second pass sweep or to the verification of no significant change between average coolant properties between two complete radial sweeps. The problem is terminated if the pressure drop vs flow rate curve has a negative slope, i.e., that the flow conditions are not stable.

The total flow through the first pass channels is specified by the input to the problem. Either of two options are employed for the second pass flow. If the average enthalpy of the upper mixing plenum is below the enthalpy of saturated liquid at the plenum pressure, all the first pass flow will be assumed to go to the second pass. If, on the other hand, the average enthalpy of this plenum is above that for saturated liquid, only that fraction of the first pass flow, calculated as the net steam quality, will go to the second pass channels. This second option corresponds to the concept of the CFR.

3.6 Sequence for Solving the Coupled Problem

The idealsituation which could be encountered would require that the power generation rates within the core were constant. Using this as a starting point, the average subdivision coolant properties are calculated. The

problem then shifts to nuclear calculations and generates the power distribution which would result if the assumed coolant properties did exist. The calculated power distribution will not agree with the assumed, until a sufficient number of iterations have been performed for convergence to take place.

The power generation map is averaged out between the two nuclear iterations, subject to the condition that the total power produced within the core is equal to its stated input value. This averaging process is based on weighting the calculated value by 0.75 and the value of the previous iteration by 0.25. These weighting factors were chosen to eliminate the possibility of oscillations as the iterations progressed toward convergence.

Once the new power map has been established, the problem shifts back to generating a new set of average coolant properties. For a given power mapping, the resultant average coolant properties have already achieved convergence before the generation of a new map starts. The coupled problem is assumed to have achieved convergence when subsequent power mappings agree.

Chapter 4

CHARACTERISTICS OF THE CFR

4.1 Description

The concept of the CFR arrangement is the same as that of the conventional counterflow tube-and-shell heat exchanger. The difference between the CFR and the passive heat exchanger is that the tube material itself contains nuclear fuel and generates heat which is transferred to the two counterflowing fluids which surround the tube. On the detailed scale, Figure 1.1 presented schematically the concept as it exists for a single cell or fuel element. Section 1.2 discussed some of the advantages of this concept.

Two alternatives are available for this concept as regards the method in which moderation of the neutron spectrum can be achieved. One is to employ the returning feedwater as the moderator. The other is to consider the use of a solid material. For both these concepts, the presence of a third cladding region is required, this region separating the first pass coolant from the moderator. In the case of feedwater moderation, separation of the first pass coolant and moderator prevents mixing of the two fluids and uncouples the effects of the moderator density variation on the power distribution. The returning feedwater at a temperature of 404°F (Figure 1.2) mixes with saturated water recirculated down from the top of the core to give a first pass entrance temperature of approximately 520°F. Boiling occurs in the first pass channel but the temperature rise from entrance to exit is small since only 10% steam is produced (Section 2.4), the saturation temperature for steam at 900 psia being 532°F. Thus, there is a variation of the temperature driving force between coolant and moderator which varies only from 128°F to 116°F along the height of the coolant-moderator cladding region.

As a first choice for a solid moderator, beryllium oxide has been chosen. This material is compatible with water and provides the best moderating

properties of a solid material. The utilization of a solid moderator frees the power distribution in the fuel element from the effects of density variation of the moderator.

As stated earlier in this section and also in Section 2.4, the core has been designed to produce first pass coolant at the saturated state with 10% steam. This choice is arbitrary. It was chosen since the resultant "DNB ratio" or "critical heat flux ratio" is not approached and the effect of coolant density change does not severely restrict the design due to flow instability problems. For the range of conditions studied, the maximum calculated "critical heat flux ratio" was found to be of the order of 0.20. Using the Tong model to describe either the maximum enthalpy rise or maximum heat flux (Appendix, Section C.6), the value of the "critical heat flux ratio" was determined to be the larger of either the ratio of local to burn-out heat flux or the actual to burn-out enthalpy rise of the coolant.

Figure 4.1 and Figure 4.2 schematically depict the flow of the coolant and recirculating water in the H_2O and BeO moderated CFR's, respectively. The solid lines in both figures extending from the upper to the lower tube sheets represent the fuel element tube. Within the region defined by the core, these tubes contain nuclear fuel. First pass coolant flows up along each of these tubes in a small annular region defined by the outer fuel cladding and the moderator cladding and exits from the core region into the liquid layer above the core, which serves as both an axial reflector and the upper mixing plenum. Wet steam rises from the liquid layer and must pass through steam separators before it can reach the dry steam plenum located in the upper hemispherical region of the pressure vessel; the separated liquid fraction falls back into the liquid layer on top of the core. The dry saturated steam is then drawn back downward through the core for the second pass and is superheated, exiting into the second pass core exhaust plenum where it mixes before being directed

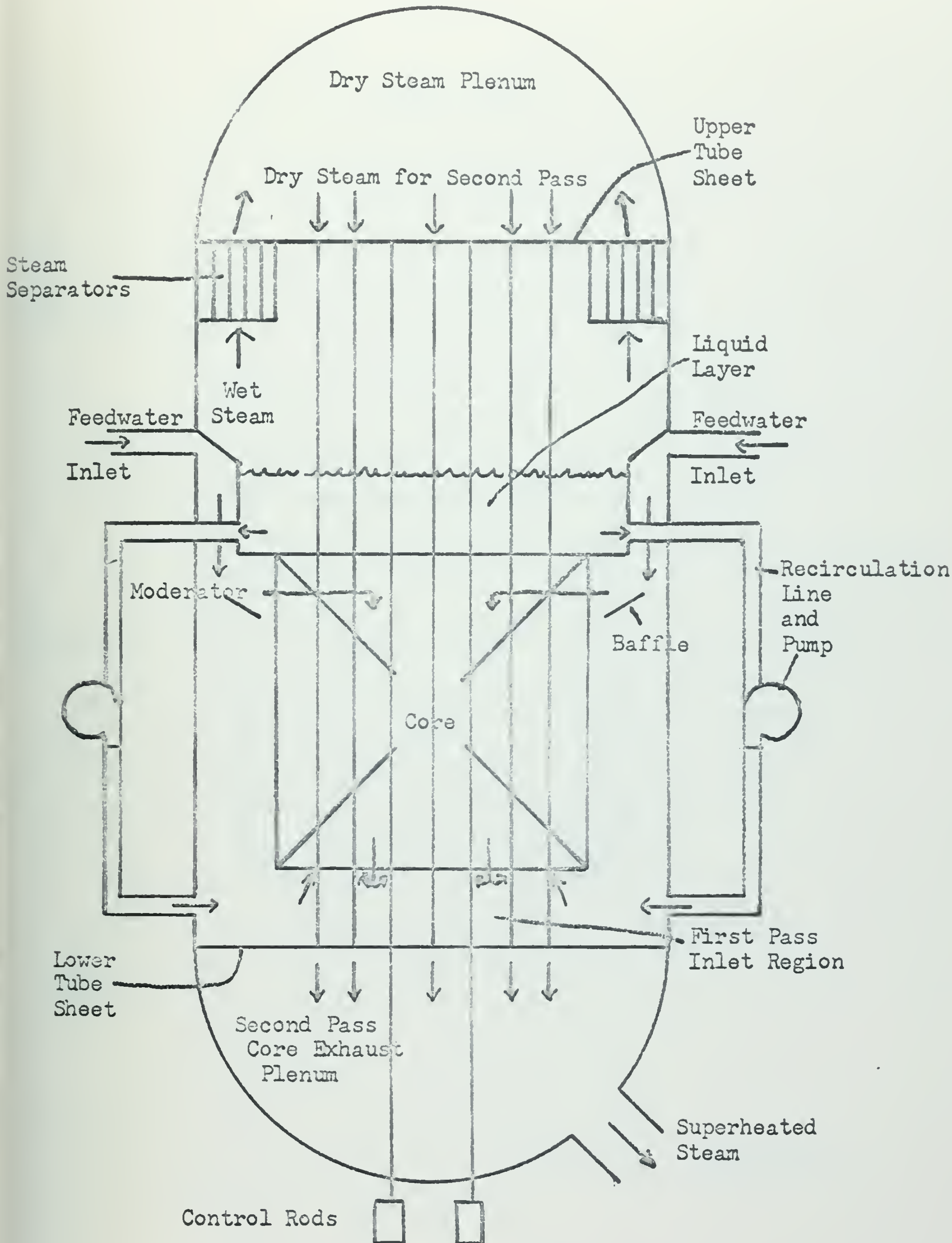

SCHEMATIC REPRESENTATION OF AN H_2O MODERATED CFR

Figure 4.1

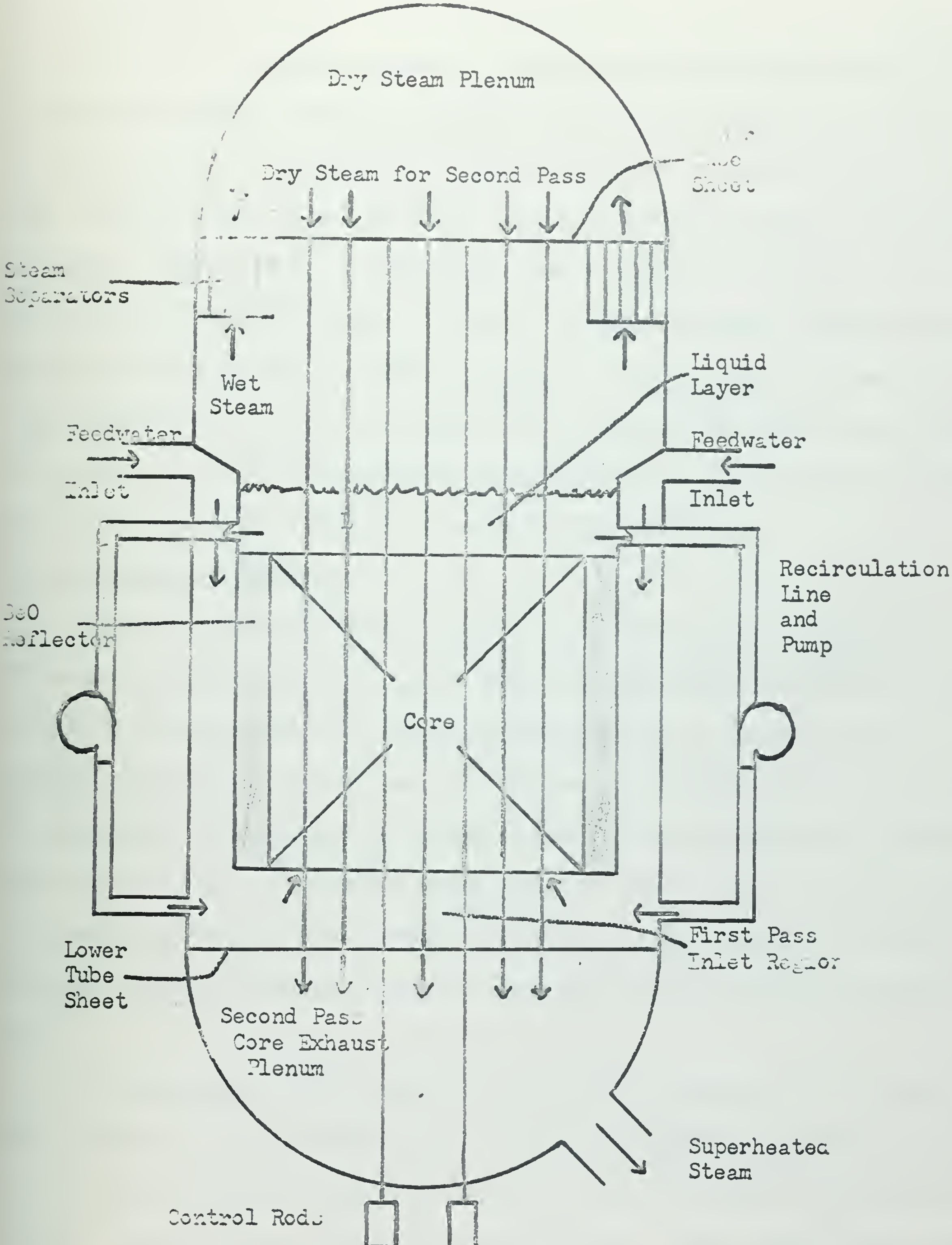

SCHEMATIC REPRESENTATION OF A BEO MODERATED CFR

Figure 4.2

out of the pressure vessel to the turbomachinery.

Within the core itself, there is a significant difference between the H_2O and BeO moderated concepts. For the H_2O moderated CFR shown in Figure 4.1, part of the returning feedwater is diverted into the moderator region of the core. This is accomplished by baffle plates at the upper region of the radial reflector. This portion of the feedwater-moderator flows down the core in the region of the individual cells, defined by r_6 and the dashed line indicating the outer cell boundary, as shown in Figure 1.1, mixing with the recirculating saturated water below the core and then entering the first pass channel for heating. For the BeO moderated CFR in Figure 4.2, all returning feedwater flows down around the exterior of the BeO radial reflector.

4.2 Selection of Parameters

Chapter 1, Optimization of CFR Fuel Element Parameters, described some of the arbitrary decisions that were made for determining the initial round of values for optimized fuel element parameters based on minimum core size or maximum power density within the core, subject to certain material constraints. The discussion of Chapter 2 was oriented solely to the selection of parameters that would lead to an optimized design based on heat transfer considerations for completely uniform power generation within the fuel material. In this respect, fuel and cladding materials were chosen and the cladding thickness fixed.

The nominal inlet first pass flow velocity has been set at 7.5 ft/sec. This selection is somewhat arbitrary. One of the problems inherent in this concept is that first pass flow is through an annular column outside the fuel element. The entering coolant is pressurized water with a much higher density than the exiting second pass steam. The required area for first pass flow per channel can be easily determined by the selected second pass exit steam thermodynamic conditions, flow rate and channel area as a function of first pass

inlet velocity. To make the selected first pass radial dimensions realistic, the width of the resultant annulus cannot be beyond manufacturing tolerances. The smaller radius of the annulus will be several times larger than the channel radius for the second pass flow. Because of the ratio of densities between the two coolants, the resultant width of the annulus can become quite small. The lower the inlet velocity of the first pass coolant is made, the greater the width of the annulus must be.

The parameter combinations displayed in Table 2.2 were used in determining the reactor characteristics set forth in this chapter. With the earlier specification of first pass inlet velocity and first pass exit steam quality, all radial physical dimensions of a cell assembly are fixed except the equivalent cell radius for a given second pass exit velocity. What the value of the equivalent cell radius would be was determined by fixing the cell moderator-to-fuel volume ratio. In the case of the H_2O moderator, the moderator-to-fuel volume ratio was fixed at 2, for the BeO moderator at 10.

Investigation of the parameters for an H_2O moderated reactor with a second pass exit steam velocity of 100 ft/sec yielded the following results. For the smaller values of (r_3/r_2), the ratio of outer-to-inner fuel material radii, the core could not be made critical. The cladding thicknesses had been fixed and for the small values of (r_3/r_2) the cladding acted as a poison to prevent criticality, regardless of the fuel enrichment, occupying a large relative percentage of the total core volume. At the value of (r_3/r_2) equal to 2.5, the core would not go critical with fuel enrichments of 15% but would go critical at fuel enrichments of 50%. When the value of (r_3/r_2) was increased to 2.75, the core would go critical at 15% with the thermal flux accounting for approximately 75% of the power produced. The fuel enrichment of 50% was used to continue scoping the design with (r_3/r_2) fixed at 2.5.

During the course of earlier investigation, the values of calculated

Table 4.1

CALCULATED PROPERTIES OF A 50% ENRICHED, H_2O MODERATED CFR WITH MODERATOR-TO-FUEL VOLUME RATIO = 2. GEOMETRICAL PROPERTIES SPECIFIED BY TABLE 2.2 WITH V_2 = 100 FT/SEC AND $(r_3/r_2) = 2.5$.

Assumed Max Clad-Coolant Temp Diff (F°)	245	195	145
Maximum/Average Power (Radial)	1.260	1.216	1.157
Fast Flux Power/Total Power	0.72	0.73	0.74
Thermal Poison Cross Section (cm^{-1})	0.1460	0.1443	0.1417
Total Second Pass Flow (10^5 lb/hr)	1.966	1.983	2.016
Temperatures (°F)			
Average Second Pass Exit	863.4	853.7	834.1
Maximum Second Pass Exit	893.0	886.3	870.5
Maximum Cladding	1164.	1087.	998.
Maximum Fuel	1321.	1212.	1090.
Core Length (cm)	156.8	221.9	360.0
Core Radius (cm)	60.2	58.9	57.3
Power Density (kw/liter)	32.1	23.7	15.5

maximum cladding temperature exceeded the design constraint of 1350 °F when the equivalent ΔT lay in the region of 145 F° to 245 F° (corresponding to maximum cladding temperatures between 1100 °F and 1200 °F for the uniform power assumption). Thus, the next iteration of calculations worked in this region of (r_3/r_2) at 2.5. The results obtained indicated that the maximum calculated cladding temperature was 1164 °F for the combination of parameters specified for a T of 245 F°, 50% enrichment and 100 ft/sec steam exit velocity. The principal properties for this set of calculations are shown in Table 4.1.

The results shown in Table 4.1 do not approach the temperature constraint placed on either the cladding or fuel. In order to achieve a set of parameters that would exceed the constrained maximum cladding temperature, all dimensions

and properties of the previous calculation were held constant except the core length. Two additional parameter combinations were solved, one with the core length reduced by 25 cm, the second by 50 cm, of the calculated length for the assumed cladding-coolant temperature differential of 245 F°. The results of these calculations are shown in Table 4.2. By graphical interpolation of these results, it was determined that the cladding temperature constraint would be achieved if the core length was 111.0 cm or 45.8 cm less than the length determined for the clad-coolant temperature differential of 245 F°.

Parameters for the BeO moderated core were also taken from Table 2.2. For the case of the BeO core, those dimensional properties peculiar to an assumed exit velocity of 300 ft/sec were investigated. As shown in the graphical presentation in Chapter 2 and evident from Table 2.2, the lowest value of (r_3/r_2) for which results are available for the four temperature differential variables investigated is 4.0. This parameter was selected as the control parameter. The principal data figures arising from this calculation are shown in Table 4.3. By graphical interpolation, the set corresponding to an assumed temperature differential of 165 F° was found to yield a maximum cladding temperature of 1350 °F.

Using the interpolated results of Tables 4.2 and 4.3, a complete set of the properties pertinent to H_2O and BeO moderated cores that yield the constrained maximum cladding temperature are shown in Table 4.4. The fuel temperature was not found to be the limiting constraint in either case.

For the results shown it is immediately apparent that the desired average steam exit temperature of 955 °F has not been achieved. The mean outlet temperatures are 886.7 °F for the H_2O moderated core and 916.6 °F for the BeO moderated core. On the other hand, the calculated outlet flow rate has exceeded the assumed design point of 1.776×10^5 lb/hr; for the H_2O moderated core it is 1.969×10^5 lb/hr, for the BeO moderated core 1.902×10^5 lb/hr.

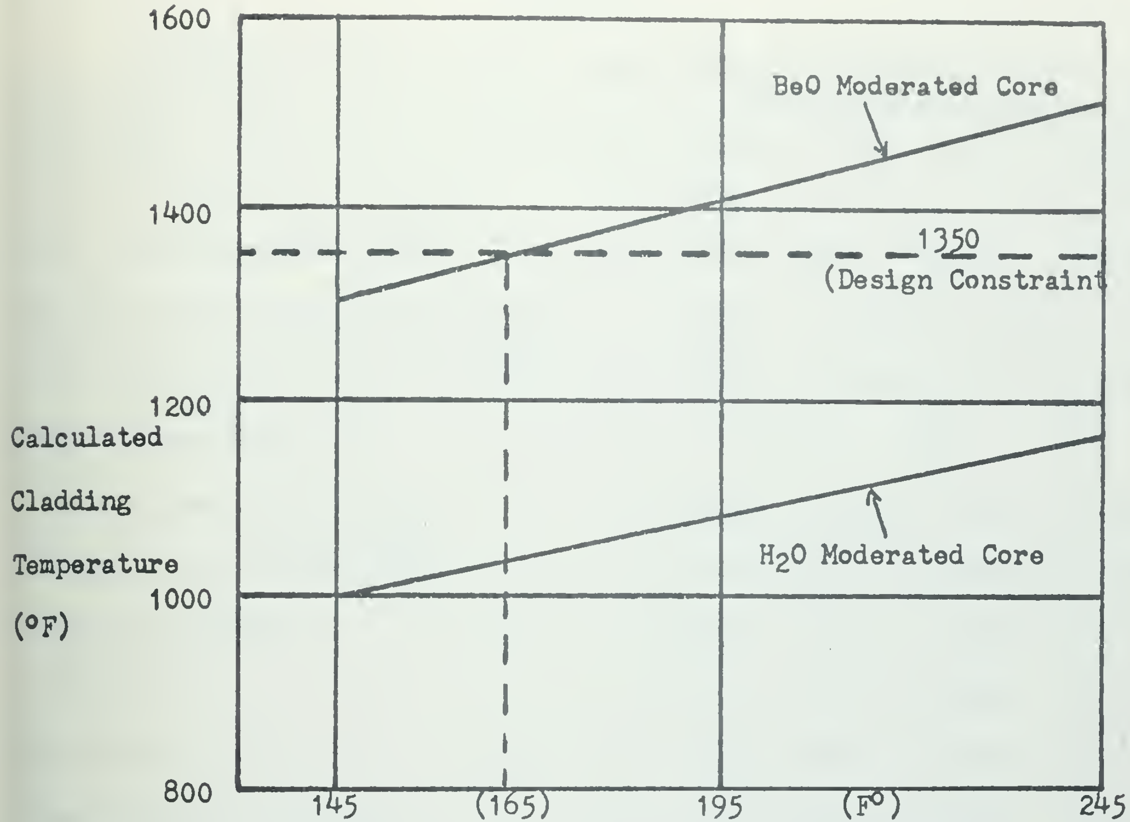

Assumed Maximum Clad-Coolant Temperature Difference ΔT for Second Pass Exit Coolant at 955 F°

CALCULATED VS ASSUMED CLADDING-COOLANT TEMPERATURE DIFFERENCE FOR H_2O AND BEO MODERATED CORES

Figure 4.3

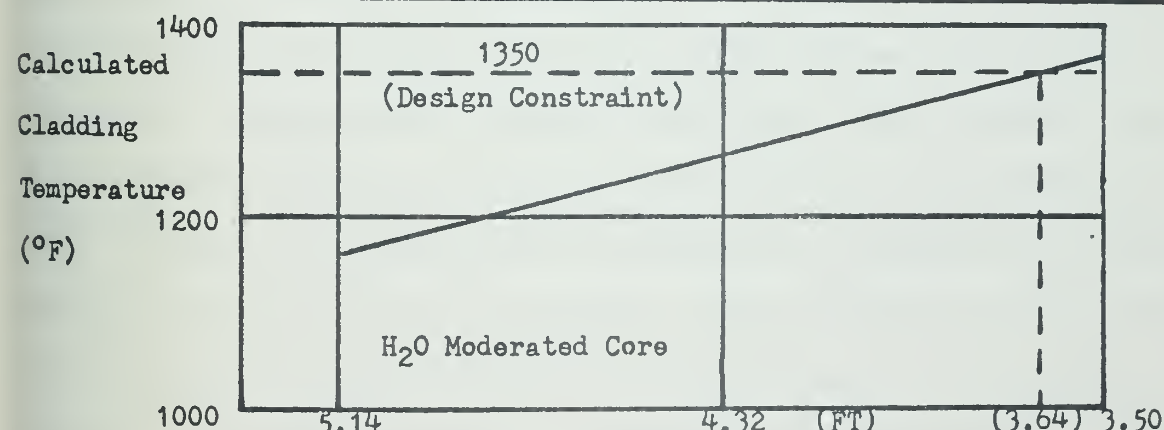

Fuel Tube Length

CLADDING TEMPERATURE OBTAINED BY VARYING FUEL TUBE LENGTH OF H_2O MODERATED CORE WITH ALL OTHER PARAMETERS CONSTANT FROM CORE WITH ΔT(CLAD-COOLANT)=245F°

Figure 4.4

Table 4.2

INTERPOLATION TABLE SHOWING PARAMETERS OF H_2O MODERATED CFR

Core Length (cm)	106.8	(111.0)	131.8	156.8
Maximum/Average Power (Radial)	1.254	1.259	1.269	1.260
Fast Flux Power/Total Power	0.72	0.72	0.72	0.72
Thermal Poison Cross Section (cm^{-1})	0.1435	0.1435	0.1435	0.146
Total Second Pass Flow (10^5 lb/hr)	1.962	1.969	1.978	1.966
Temperatures (°F)				
Average Second Pass Exit	888.8	886.7	876.6	863.4
Maximum Second Pass Exit	917.9	901.8	891.8	893.0
Maximum Cladding	1371.2	1350.	1263.4	1163.8
Maximum Fuel	1614.	1590.	1471.	1321.
Core Radius (cm)	60.2	60.2	60.2	60.2
Power Density (kw/liter)	47.1	45.3	38.2	32.1

This variance from the assumed design point has been caused by more heat flowing to the first pass coolant and thus causing a higher exit steam quality. The actual heat transfer coefficients were calculated to be higher than the assumed value used to generate Table 2.2, thus reducing the resistance for heat flow to the first pass coolant. Also, Table 2.2 was generated under the assumption of flat power radially across the fuel in the annular fuel tube; in fact, the volumetric power generation rate decreases as the inner radius of the fuel material is approached. Even though the results shown do not agree exactly with the initially assumed temperature design point, they illustrate the salient features of either an H_2O or BeO moderated CFR which lies in the region of maximum power density.

In concluding the remarks on the selection of parameters, additional comment is warranted on the choice of assumed exit velocity and moderator-

Table 4.3

INTERPOLATION TABLE SHOWING PARAMETERS OF BEO MODERATED CFR

Assumed Max Clad-Coolant Temp Diff (F°)	145	(165)	195	245
Maximum/Average Power (Radial)	1.433	1.435	1.437	1.442
Fast Flux Power/Total Power	0.97	0.97	0.97	0.97
Thermal Poison Cross Section (cm^{-1})	0.345	0.339	0.332	0.320
Total Second Pass Flow (10^5 lb/hr)	1.903	1.902	1.899	1.896
Temperatures (°F)				
Average Second Pass Exit	916.7	916.6	916.4	916.2
Maximum Second Pass Exit	1081.2	1081.0	1080.8	1080.3
Maximum Cladding	1310.	1350.	1410.	1513.
Maximum Fuel	1592.	1682.	1797.	2015.
Core Length (cm)	365.9	318.9	263.9	181.4
Core Radius (cm)	97.4	97.7	98.2	101.6
Power Density (kw/liter)	5.3	6.0	7.2	9.9

to-fuel volume ratio for the two moderators studied. Neutron economy studies show that a core has minimum leakage for a given volume when the length-to-diameter ratio is in the vicinity of unity. Inspection of Table 2.2 shows that the calculated core lengths generally increase as the second pass exit velocity increases. Small core height is peculiar to low velocities. In order to make the core L/D ratio approach unity for low velocities, the H_2O moderator was used. At the higher velocity, the BeO moderator was used. In the case of the H_2O moderated reactor, the calculated L/D ratio for the core is 0.918 with the moderator/fuel volume ratio of 2. For the BeO moderated reactor, the calculated L/D ratio is 1.63; to make the L/D ratio equal unity, the moderator/fuel volume ratio would have to be increased to 29.5 vice 10 which would consequently require new cross section data to account for the change in neutron spectrum.

Table 4.4

CHARACTERISTICS OF A 57.4 MW_t COUNTER FLOW REACTOR

	MODERATOR	
	H_2O	BeO
Core Dimensional Parameters		
Diameter D (inches)	47.5	76.9
Length L (inches)	43.6	125.6
Composition (Volume %)		
Moderator	51.9	85.4
Fuel	25.6	8.82
Cladding	8.5	1.08
First Pass Coolant	11.0	4.11
Second Pass Coolant	3.6	0.45
Cell Dimensional Parameters (cm)		
Radius of Second Pass Flow Channel r_1	0.332	0.388
Outer Radius of Inner Fuel Cladding Annulus r_2	0.383	0.439
Outer Radius of Fuel Annulus r_3	0.958	1.756
Outer Radius of Outer Fuel Cladding Annulus r_4	1.008	1.807
Outer Radius of First Pass Coolant Annulus r_5	1.165	2.158
Outer Radius of Moderator Cladding Annulus r_6	1.216	2.209
Equivalent Radius of Cell Assembly r_7	1.736	5.810
Lattice Pitch	3.080	10.31
Fuel Element Parameters		
Fuel	UO_2	UO_2
Enrichment (%)	50	50
Cladding (All Regions)	Inconel	Inconel
Number of Fuel Elements	1198	282

Table 4.4 (Continued)

	MODERATOR	
	H_2O	BeO
Temperature (°F)		
Fuel Maximum	1590	1682
Cladding Maximum	1350	1350
Heat Transfer Data - First Pass Flow		
Coolant	H_2O	H_2O
Flow (10^6 lb/hr)	1.776	1.776
Inlet Temperature (°F)	520	520
Inlet Enthalpy (Btu/lb)	511.9	511.9
Outlet Temperature (°F)	527.8	527.7
Outlet Enthalpy (Btu/lb)	595.7	593.6
Outlet Steam Quality (%)	11.09	10.71
Inlet Pressure (psia)	880.0	880.0
Channel Pressure Drop (psi)	10.6	11.7
Restrictor Pressure Drop (psi)	5.7	5.7
Restrictor Area Ratio	0.25	0.25
Inlet Velocity (ft/sec)	7.5	7.5
Heat Transfer Surface (ft^2)	901	1097
Average Heat Flux (Btu/hr/ft^2)	165000	132200
Heat Transfer Data - Second Pass Flow		
Coolant	H_2O	H_2O
Flow (10^5 lb/hr)	1.969	1.902
Inlet Temperature (°F)	527.8	527.7
Inlet Enthalpy (Btu/lb)	1196.4	1196.4
Outlet Temperature (°F)	886.7	916.6
Outlet Enthalpy (Btu/lb)	1445.9	1466.4

Table 4.4 (Continued)

	MODERATOR	
	H_2O	BeO
Outlet Degree Superheat (F^o)	360.1	405.9
Inlet Pressure (psia)	869.4	868.3
Channel Pressure Drop (psi)	9.4	119.2
Restrictor Area Ratio	1.0	1.0
Outlet Velocity (ft/sec)	109	389
Heat Transfer Surface (ft^2)	297	236
Average Heat Flux ($Btu/hr/ft^2$)	165000	218000

4.3 Graphical Presentation of Property Variation

Figures 4.5 through 4.13 show the variation of different properties with an H_2O or BeO moderated core. The set of parameters defined in Table 4.4 arose from interpolation of the properties shown in Tables 4.2 and 4.3. The data given in Figures 4.5 through 4.13 is not that of Table 4.4 but results from performing the following calculations on the core configuration headed by a core length of 131.8 cm in Table 4.2 for the H_2O moderated core and by 195 F^o in Table 4.3 for the BeO moderated core.

Figure 4.5 shows the variation of power radially across the reactors. Both curves have been plotted through a plane running at mid-height through the reactor (one-dimensional) with a buckling calculated for leakage in the axial direction. The amount of power peaking at the edge of the BeO moderated reactor is indiscernible - the reactor produces 97% of its power with neutrons having an energy above 1.85 ev; the radial reflector is a 15 cm thickness of BeO.

Figures 4.6 through 4.13 show the linear power, cladding temperature, coolant temperature and coolant enthalpy distributions for the H_2O and BeO moderated cores. The abcissa for these plots has been normalized to the

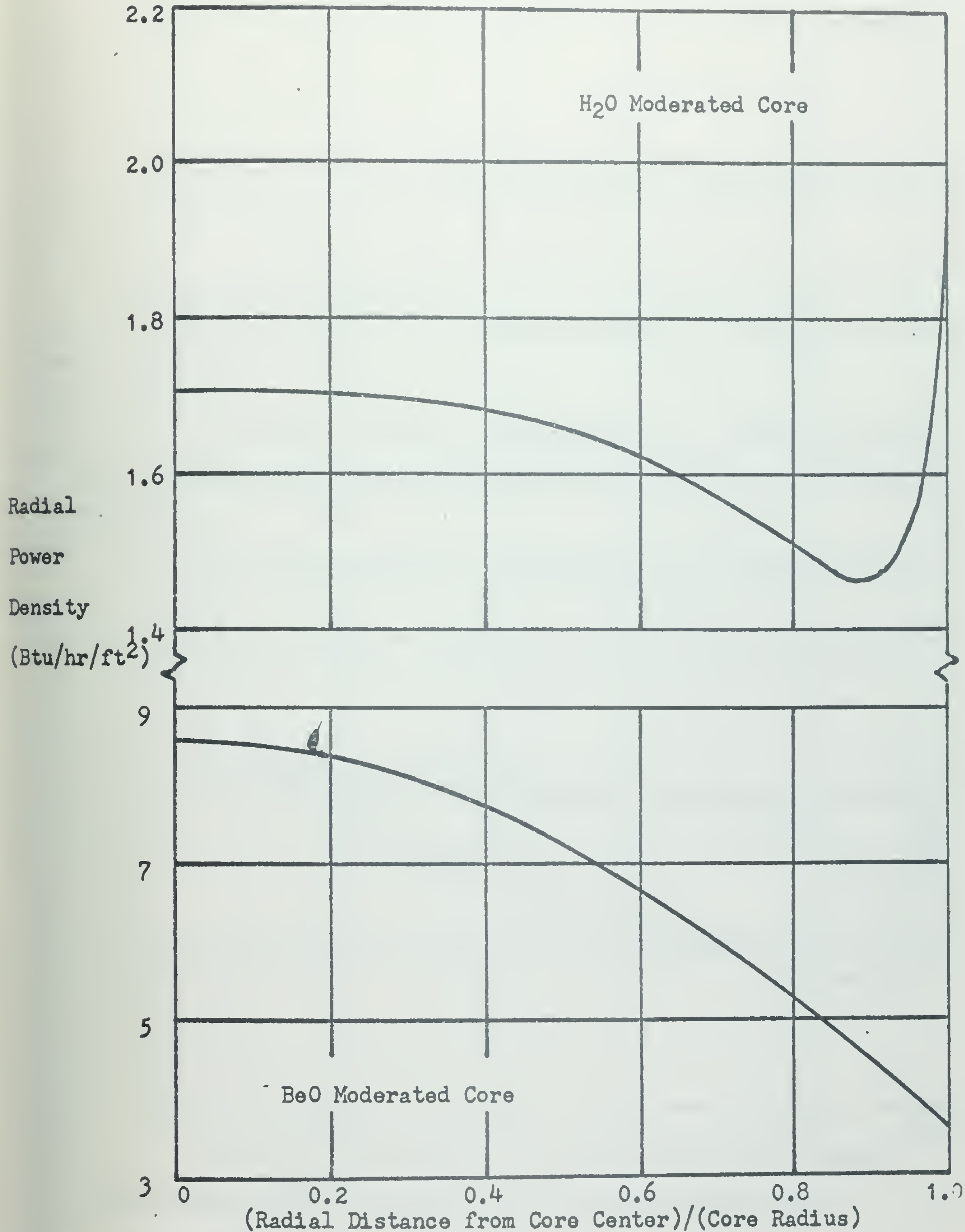

RADIAL POWER DISTRIBUTION FOR AN H_2O AND A BEO MODERATED CORE

Figure 4.5

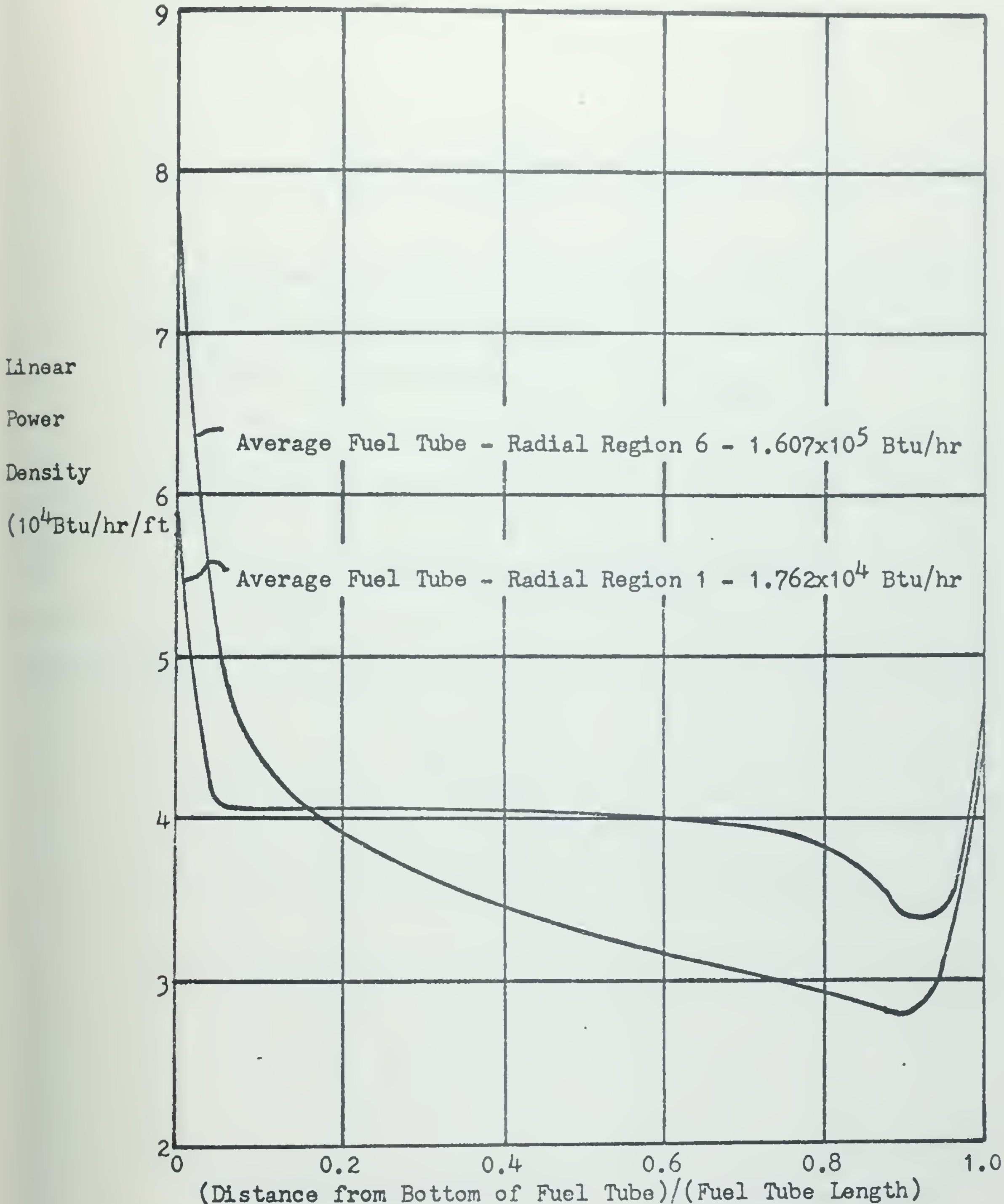

LINEAR POWER DENSITY DISTRIBUTION FOR AN H_2O MODERATED CFR

Figure 4.6

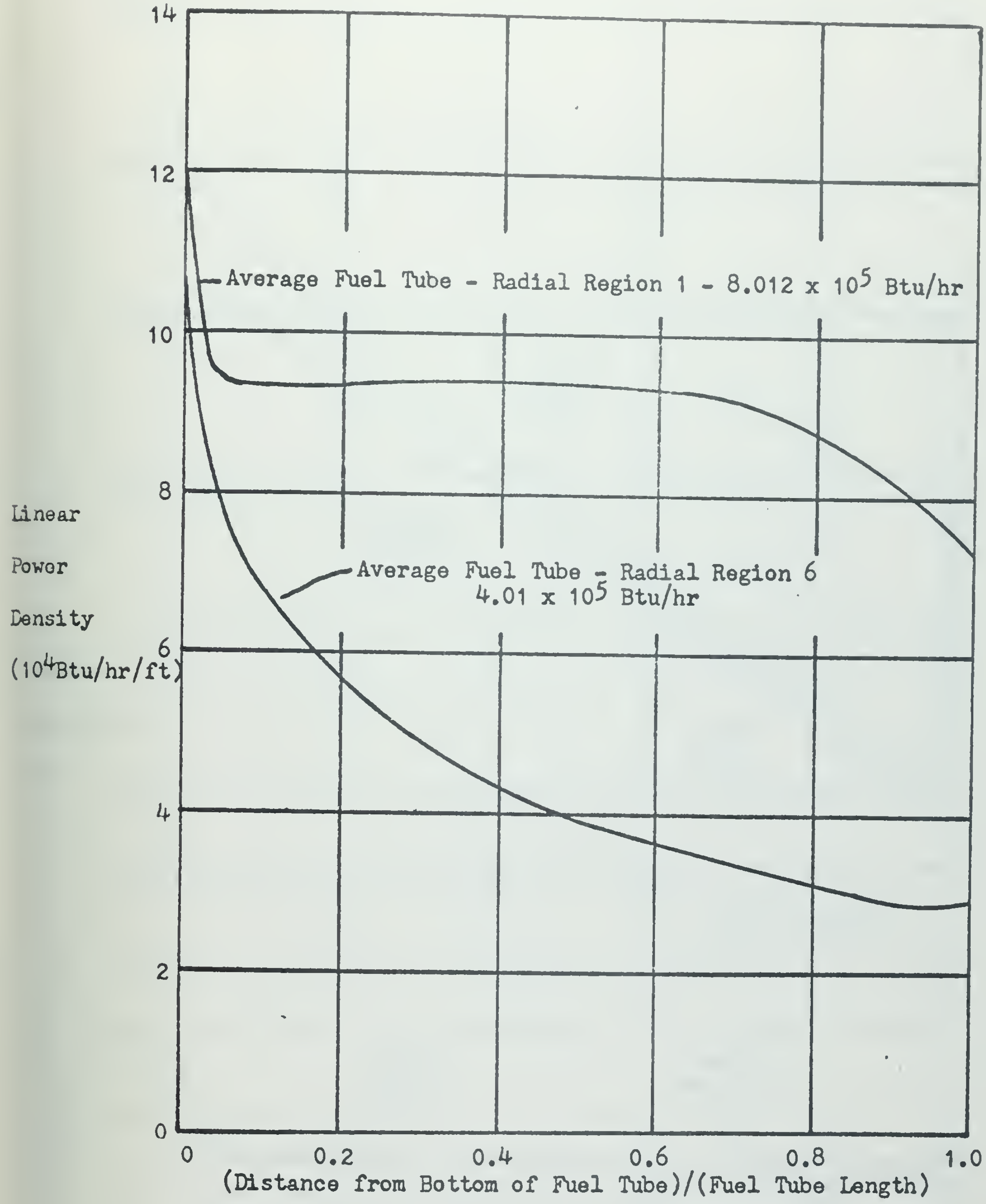

LINEAR POWER DENSITY DISTRIBUTION FOR A BEO MODERATED CFR

Figure 4.7

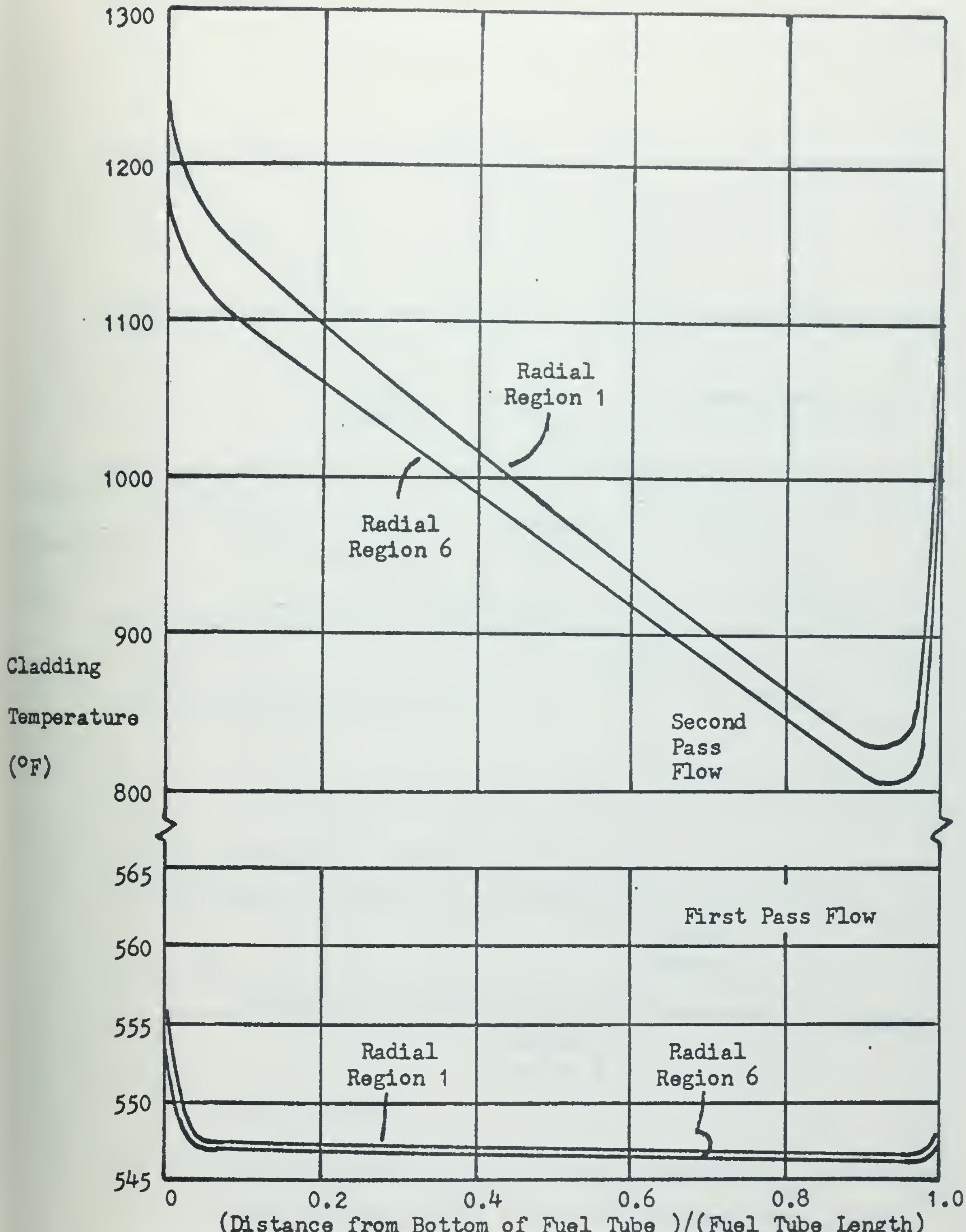

CLADDING TEMPERATURE DISTRIBUTION FOR AN H_2O MODERATED CFR

Figure 4.8

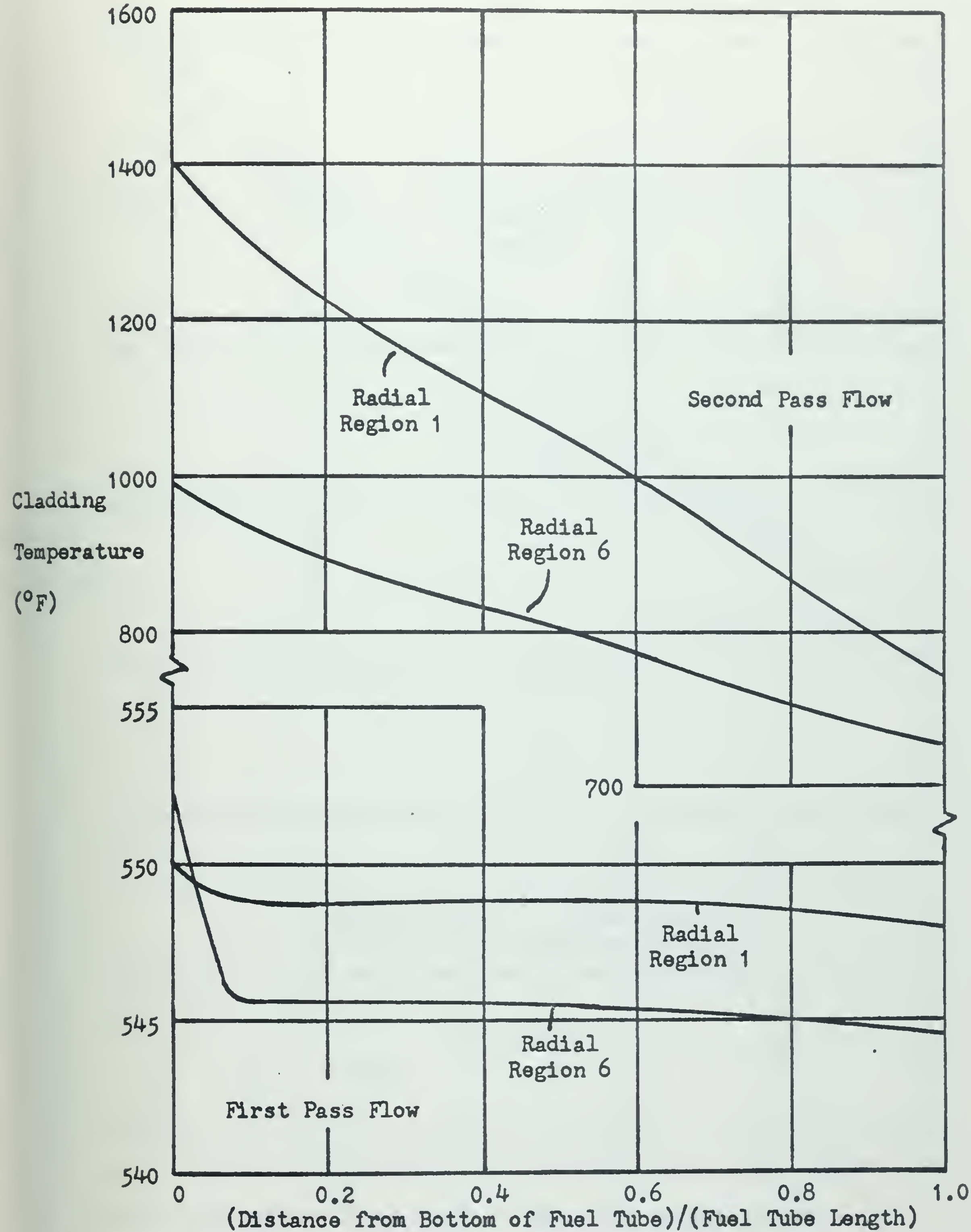

CLADDING TEMPERATURE DISTRIBUTION FOR A BEO MODERATED CFR

Figure 4.9

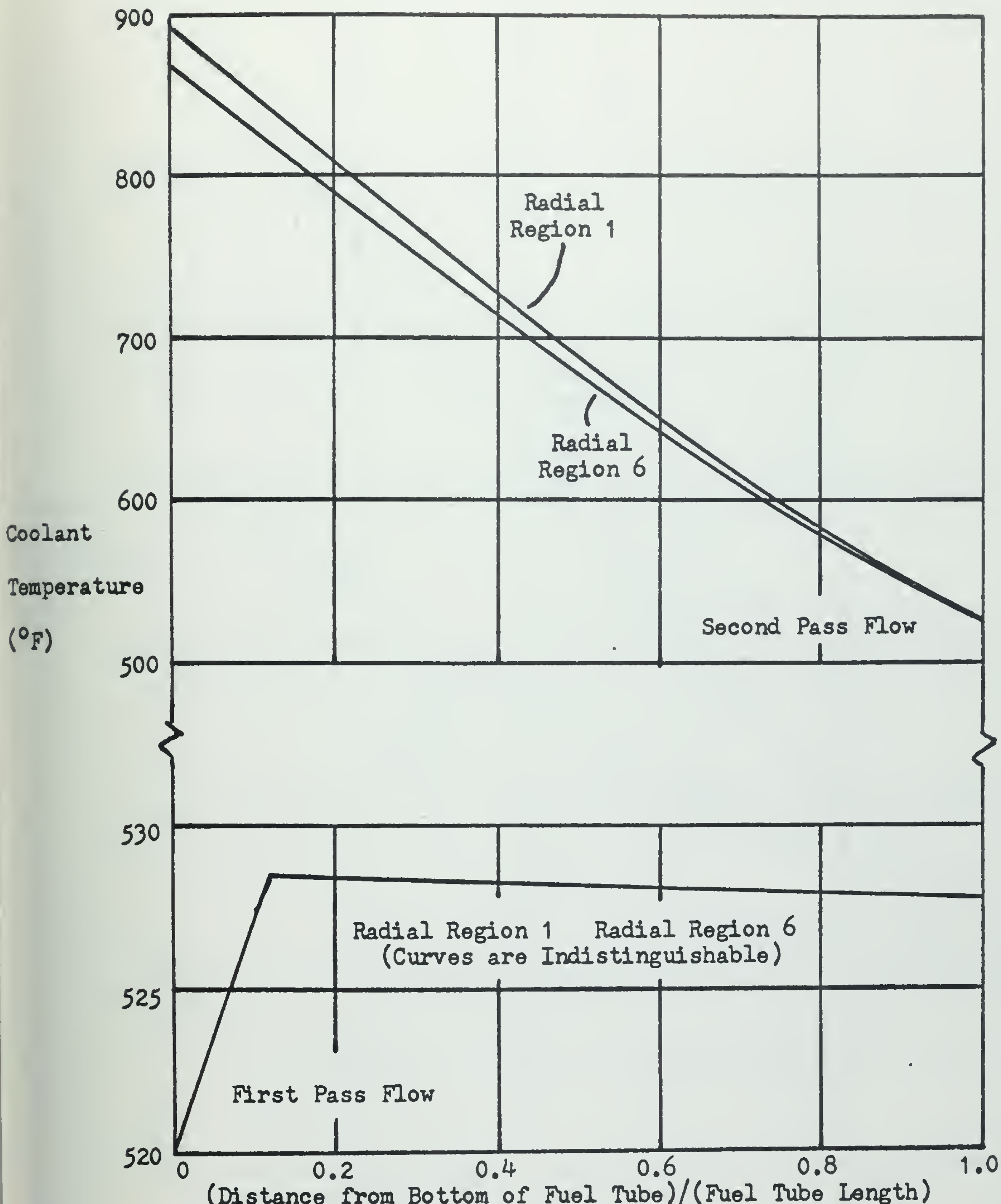

COOLANT TEMPERATURE DISTRIBUTION FOR AN H_2O MODERATED CFR

Figure 4.10

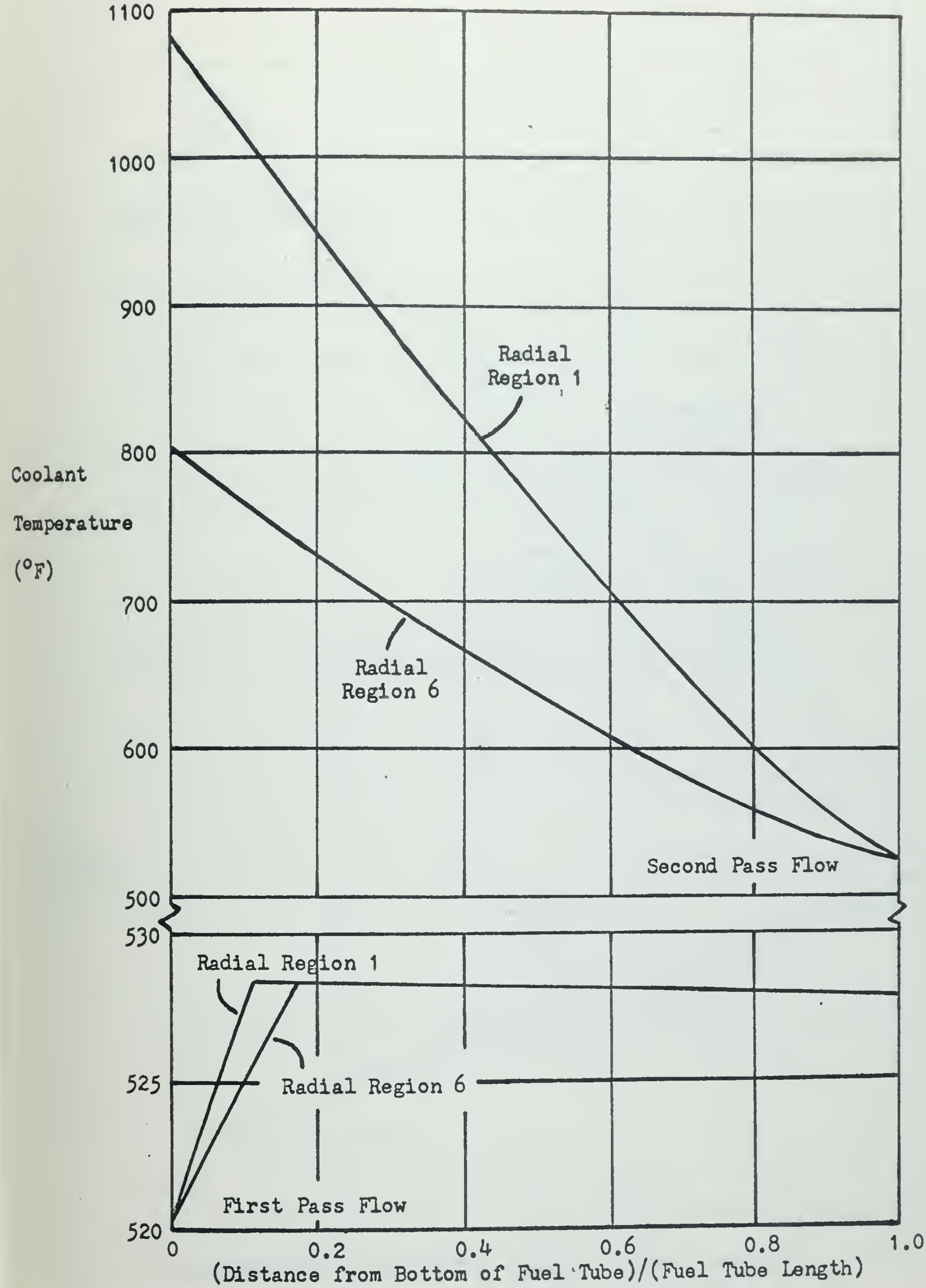

COOLANT TEMPERATURE DISTRIBUTION FOR A BEO MODERATED CFR

Figure 4.11

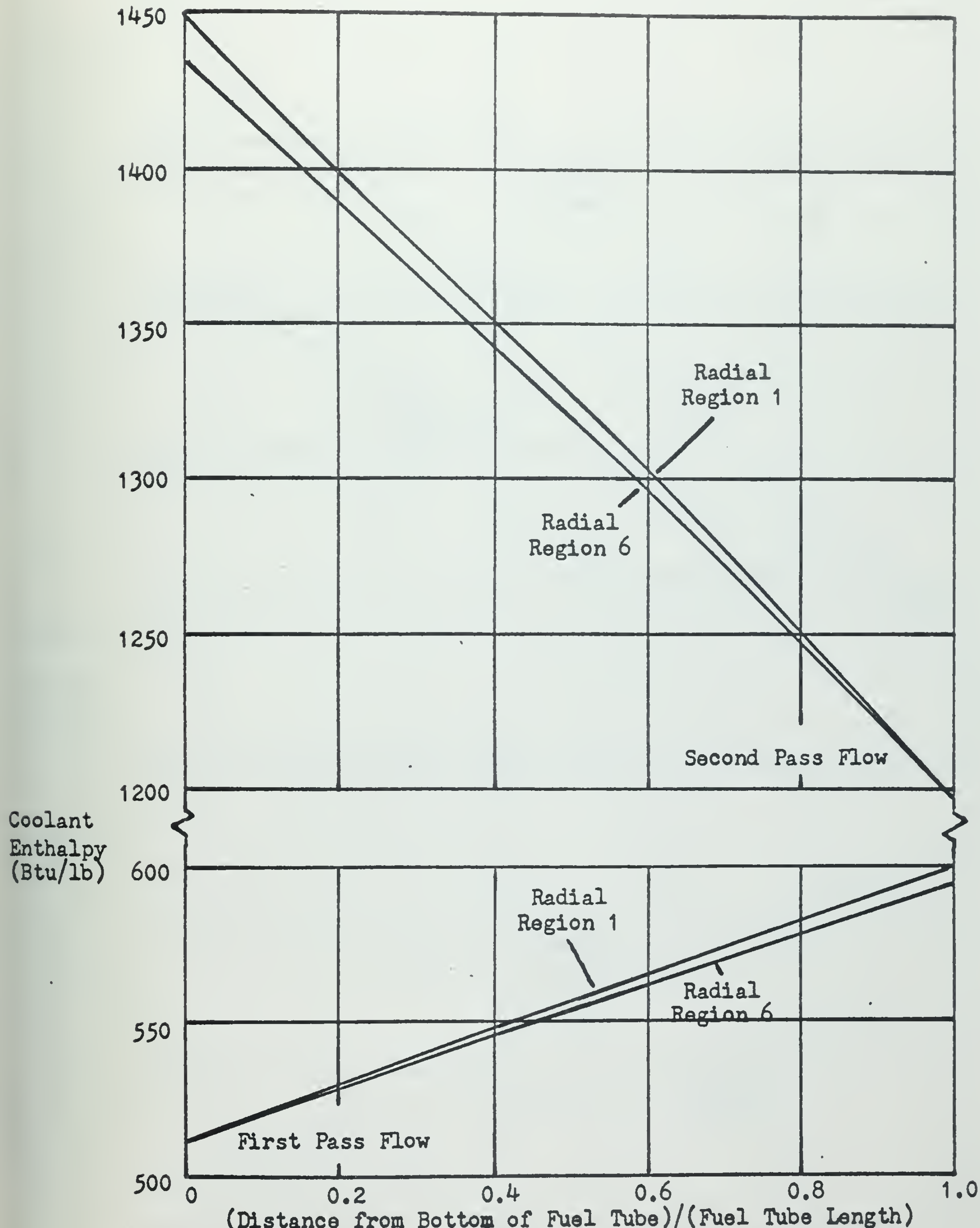

COOLANT ENTHALPY DISTRIBUTION FOR AN H_2O MODERATED CFR

Figure 4.12

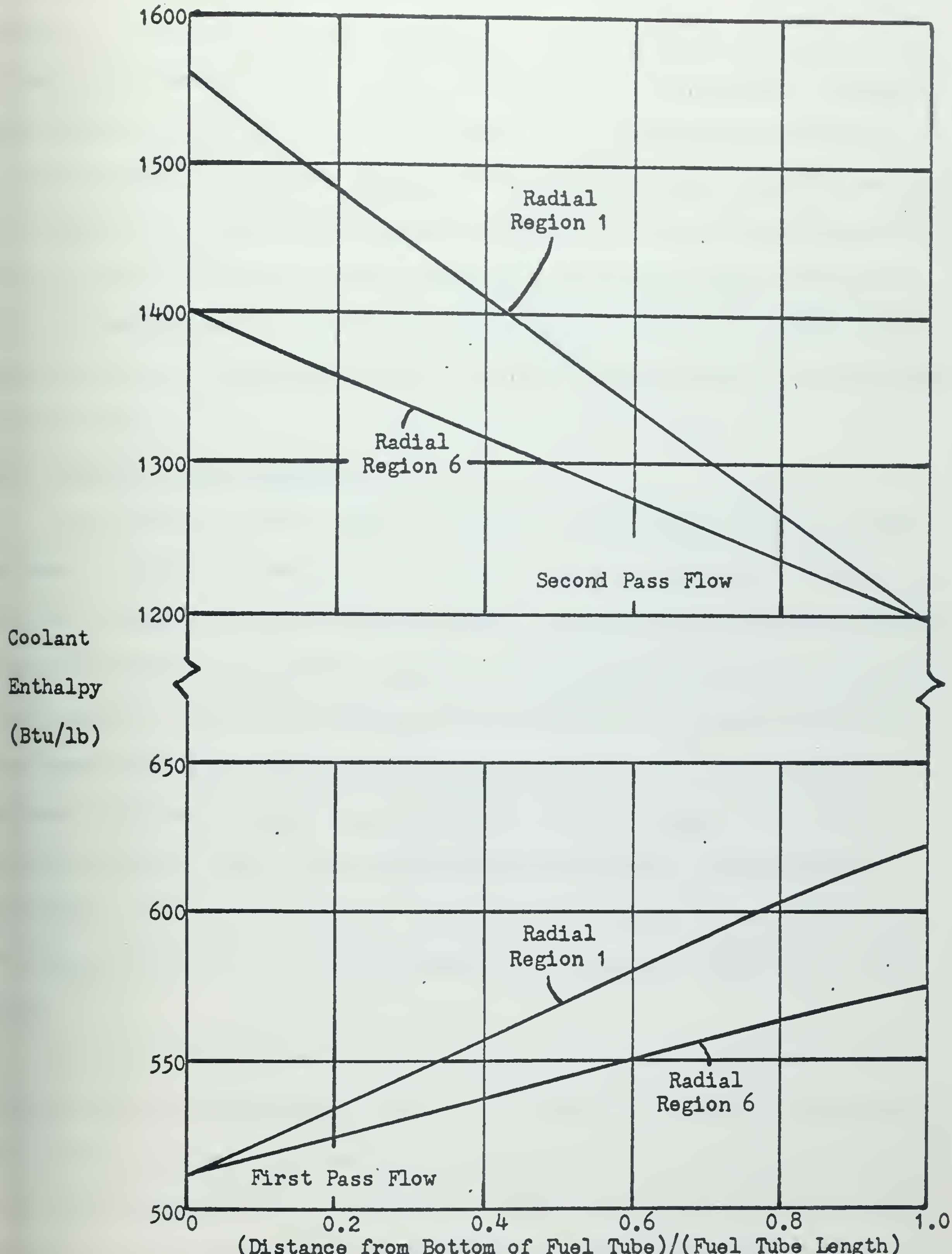

COOLANT ENTHALPY DISTRIBUTION FOR A BEO MODERATED CFR

Figure 4.13

core length. For each of the figures, two curves are shown - one for "Radial Region 1", the other for "Radial Region 6". "Radial Region 1" is the right circular cylinder at the center of the core extending the height of the core and defined by radii of 10.1 cm and 16.4 cm for the H_2O and BeO moderated cores, respectively. "Radial Region 6" is the right annular cylinder extending the height of the core, being defined by radii of (50.5 cm, 60.2 cm) and (82.0 cm, 98.2 cm) for the H_2O and BeO moderated cores, respectively. The properties defined for the two curves are the properties related to a fuel element producing heat at the average rate of all fuel elements within that particular radial region.

4.4 Remarks on Flow Stability

Flow through the core, either for first or second pass flow, is through a group of channels connecting two plenums. Since the channels all begin at the same point and end at the same point, the pressure drop between plenums must be the same, regardless of which individual flow channel is followed between plenums. Since heat is added to the coolant as it transits the core, the density change of the coolant influences the pressure drop along the channel, the density change being a function of the coolant flow rate and the heat input. Radial flow stability across the core is the subject of Appendix E, but a brief summary of the points made there and comments on the calculated values for the two configurations presented in Table 4.4 will be made.

As a first step in the discussion, consider the values determined for the two reactors for first pass flow. In the case of the H_2O moderated core, the total calculated first pass drop was 10.6 psi with 5.7 psi (or 53.8% of the total drop) occurring at the inlet. For the BeO reactor, the total drop was 11.7 psi with 5.7 psi (or 48.8% of the total drop) occurring at the inlet. For both reactors, the inlet velocity was 7.5 ft/sec and the throat area

ratio was 0.25, giving a nominal 30 ft/sec velocity through the throat.

Since boiling takes place in the first pass flow channels, flow instability would be present if no means were used to add a pressure drop independent of the friction and momentum change within the channel causing the intrinsic channel pressure drop. Because of the momentum change within the boiling channel, the curve of pressure drop vs flow rate (at constant total heat input) has a negative slope. Thus, if due to some circumstance, the flow in a boiling channel was reduced, the pressure drop across the channel would rise and the flow would be further reduced. Similarly, if the pressure drop across the channel was increased, the flow would decrease.

To avoid this possibility, a nozzle or restrictor has been installed at the entrance to each flow channel. The characteristics of such a device are that the slope of a curve of pressure drop vs flow rate through it is always positive. When the curve of pressure drop vs flow rate for this external device is added to the curve of pressure drop vs flow rate for the heated channel, the desired result is a cruve that has a positive slope over the anticipated operating conditions (flow rate and heat input) of the channel.

The data presented in Table 4.3 was derived by graphical interpolation or results calculated for reactors of different physical configuration. The calculated results in all cases showed a maximum variance of 0.1 psi for total pressure drop between inlet and mixing plenum for first pass flow channels across the core when the total first pass flow was equally divided among the different channels. Within the convergence limits specified during numerical solution of the problem, this variance was considered to be acceptable (0.1 in 10.6 psi for the H_2O moderated reactor, 0.1 in 11.7 psi for the BeO moderated reactor, in both cases less than 1% variance). During the course of scoping the design, larger variances were encountered for some parameter combinations and the flow rate through individual channels had to be varied

to achieve the same pressure drop between plenums, regardless of which flow channel was selected for performing the calculations.

4.5 Reactor Control and Criticality

The schematic representations of Figures 4.1 and 4.2 indicate control rods entering the core from the bottom. In the case of the boiling water reactor design, coolant rods normally enter from the bottom of the core since the power distribution is skewed toward the bottom of the core because of the coolant moderator density distribution and its coupling to the power distribution through axial variation in moderating properties.

The preferred direction of control rod insertion would be downward. If the mechanical, electrical or hydraulic mechanisms for inserting control rods fail, the force of gravity would seat the rods inside the core providing that the rods are not bound by the failed mechanism. If insertion is in an upwards direction, as required for the CFR application, compressed springs or some other form of safety device must be relied upon to store sufficient potential mechanical energy to seat and hold the rods against gravity in the event of a power failure to the control rod drive mechanism.

Aside from the advantage of using rather than overcoming gravity for the insertion of control rods, a shipboard reactor installation should be designed for minimum distance above the hull base line. This is due to the decrease in metacentric radius that occurs as the center of gravity of the ship is raised. The controlling criterion in this case would be athwartship stability.

Power peaking occurs at the bottom of the core of both the H_2O and BeO moderated reactors, as shown in Figures 4.6 and 4.7. For the H_2O moderated reactor, the ratio of maximum-to-average axial power is 1.48 and 2.18 for radial regions 1 and 6, respectively. For the BeO moderated reactor of Figure 4.7, the ratio of maximum-to-average axial power is 1.37 and 2.26 for

radial regions 1 and 6, respectively.

Insertion of the control rods from the top would tend to additionally skew the power distribution toward the bottom. The metallurgical constraint limiting the design of the reactor is at the bottom of the core, where the highest second pass coolant temperatures are reached. Thus, with control rods partially inserted from the top during full power operation, the additional skewing of the power distribution would cause the metallurgical constraint to be exceeded and the reactor could not in fact be operated at full power. Because of this, it is necessary to design for control rod entry from the bottom, thus reducing the axial power peaking but with the attendant problems associated with rod drive mechanisms, foundations to elevate the reactor assembly and the subsequent reduction in metacentric radius.

Both of the reactor configurations discussed in Section 4.2 are described as "fast", since over half of the power is produced in the "fast" group of the two-group calculation. At the time that the cross-sectional data was determined for these two configurations (Table 4.5), the cut-off energy of the fast group was set at 1.85 ev, the lower limit of the data for the GAM-1 program. (Note that the "fast" cross sections in Table 4.5 do not reflect the N-2N reaction for beryllium; no provision is made for this in the GAM-1 program data.) The lower energy limit of the "fast" group is only 75 times that of a "thermal" neutron at 20 °C, so to avoid misinterpretation it should be remembered that "fast" as used here refers to the spectrum extending down to 1.85 ev, possibly more appropriately described as the "faster" group as opposed to the "slower" group.

As mentioned in Section 4.2, the enrichment required to just reach criticality with no poison in the H_2O moderated core lies between 15% and 50%; for the core with $(r_3/r_2) = 2.75$, an enrichment of 15% yielded criticality and also a fast/total flux power ratio of 25%. No analysis was made to

Table 4.5

INPUT NUCLEAR PROPERTIES OF CELL REGIONS BEFORE HOMOGENIZATION

CFR Moderator	H_2O		BeO	
Spectrum Group	Fast	Thermal	Fast	Thermal
Cladding				
Absorption Cross Section (cm^{-1})	0.003449	0.1853	0.00266	0.0714
Diffusion Coefficient (cm)	0.452	0.265	0.373	0.2782
Transfer Cross Section (cm^{-1})	0.001161		0.0001778	
Fuel				
Nu x Fission Cross Section (cm^{-1})	0.236	8.21	0.199	2.405
Nu	2.46	2.47	2.447	2.47
Absorption Cross Section (cm^{-1})	0.1768	3.98	0.1338	1.15
Diffusion Coefficient (cm)	0.564	0.275	0.5782	0.524
Transfer Cross Section (cm^{-1})	0.000604		0.0000979	
Moderator				
Absorption Cross Section (cm^{-1})	0.0003104	0.00812	0.00001438	0.0005215
Diffusion Coefficient (cm)	0.518	0.438	0.5734	0.491
Transfer Coefficient (cm^{-1})	0.02881		0.000491	
Coolant				
Absorption Cross Section (barns)	0.008224	0.3173	0.00002402	0.1384
Transport Cross Section (barns)	25.14	29.76	30.66	29.86
Transfer Cross Section (barns)	1.1274		0.333	

determine the minimum enrichment necessary to reach criticality and its associated power split between the two flux groups. It would appear that the core enrichment could be lowered from 50% and the power split reduced to less than half, if this is desired.

The BeO moderated core has no supporting data to indicate that it can

readily produce more than half its power in the thermal group. In the present configuration described in Table 4.4, the ratio of moderator-to-fuel atoms is approximately thirty. When the calculations were performed on a core with approximately ten times this amount of moderation using cross sections corrected to reflect the shift in spectrum, the fast group still accounted for approximately 85% of the total power produced.

The data presented in Table 4.4 for the required microscopic poison cross section to achieve an eigen value of unity (criticality) represents the amount of poison that would have to be spread uniformly throughout the core. The one-dimensional calculation which solves for the radial power distribution and poison cross section for criticality uses as input the homogenized cell properties for the radial region defined in the axial plane at core mid-height. As such it does not indicate any detailed knowledge regarding radial placement of control rods, depth of insertion, local flux distortion due to control rod presence, etc. The purpose of the calculation has been to indicate only that both of the core configurations presented in Table 4.4 will sustain a chain reaction.

Figures 4.6 and 4.7, graphical representations of the axial variation of power density in the annular fuel rods, and the power split between the two neutron spectrum groups, Table 4.4, show that the two configurations discussed are undermoderated. This fact can be used to suggest a means of controlling the power level in the reactor without resorting to the continual adjustment of control rods. The water and steam flowing through the first pass coolant channels can be considered to come from two distinct sources - feedwater and recirculation water. For discussion purposes, the feedwater alone absorbs heat, the recirculation water flowing through the core at constant temperature and enthalpy.

In the design condition at 100% power, the feed-recirculation water

mixture exits from the first pass channels with an average 10% steam quality or with the steam occupying approximately 62% of the cross sectional channel area (the void fraction). If the recirculation flow rate is increased, the density of the first pass inlet mixture would decrease, since the recirculation water is at a higher temperature and lower density than the feedwater. But the steam exit quality and void fraction would decrease, resulting in a higher exit density. (As the recirculation rate is increased, holding the feedwater rate and power level constant, the point in the channel at which boiling occurs is pushed upwards in the channel.) The overall effect is to increase the density of coolant in the channel. Since the reactor is under-moderated, the power level in the reactor would rise. This same effect would be present at other points of operation. Thus, the power level in the reactor can be partially controlled by varying the recirculation rate.

Variation of the feedwater flow rate will also produce the same effect. If the feedwater flow rate is increased, holding the control rod settings and recirculation flow rate constant, the average density in the first pass coolant channel will increase, increasing the moderation in the reactor and consequently causing the power level to increase. A reduction in the feedwater flow rate at constant control rod setting and recirculation rate will cause the point at which boiling first occurs in the channel to move toward the bottom of the core, resulting in a higher exit steam quality and void fraction, decreasing the moderation in the reactor and hence causing the power level to decrease. For the case of the H2O moderated CFR, Figure 4.1, some heat is transferred to the feedwater in the moderator region through the outer cladding surrounding the first pass coolant channel. At the design condition for full power operation, the feedwater in the moderator region enters the first pass inlet plenum in the subcooled state, no boiling occurring in the moderator region. When the feedwater flow rate is increased, the temperature rise

in the moderator region is lowered, thus increasing the average moderator density and contributing to a subsequent rise in power level.

4.6 Flow When Second Pass Coolant Channel Is Blocked

One of the accidents which may occur to any reactor is the blockage of a coolant channel. For the concept of the CFR, this question is of concern since each fuel element has two distinctly defined coolant channels. Studies were made of the consequences of such an event occurring to the second pass coolant channel. It is readily apparent that blockage of a first pass channel will yield much higher calculated fuel or cladding temperatures in the associated fuel tube. It would also appear that the possibility of complete blockage of a first pass channel is less likely because of the annular shape of the channel.

Comparison of the radial power distribution across the core when all the second pass coolant channels defined by "Radial Region 1" are blocked with the curves of Figure 4.5 for all open flow showed almost no variance. The second pass coolant under normal operating conditions occupies a small percentage of the total volume of the core; additionally, it is of low average density, thus not having a strong influence on the power distribution. For the configurations studied, the neutron spectrum is above thermal which also tends to mitigate the effect of local property variation.

The calculated maximum cladding and fuel temperatures for the two configurations described in Table 4.4 with no flow through the second pass channels of "Radial Region 1" are as follows:

	Moderator	
Temperature (^{o}F)	H_2O	BeO
Maximum First Pass Cladding	570.3	563.9
Maximum Fuel	5427.	9492.
Maximum Second Pass Cladding	5427.	9492.

These calculations show that the core cannot withstand this type of event without damage to the fuel and the inner fuel cladding. The design constraint on maximum fuel temperature is 4500°F. The results quoted are for the steady state case and do not incorporate any provision for temperature peaking as the temperature profile goes from that of the open flow, both channels, to that of blocked flow, second pass channel.

The second pass channel radius (Table 4.4) is 0.332 cm for the H_2O moderated core and 0.388 cm for the BeO moderated core. It is not possible to predict the mechanism which would have to occur to cause a blockage of these channels. The most likely place for such a blockage to occur would be in the upper steam plenum (Figures 4.1 and 4.2) by which a piece of rust or scale from the pressure vessel heat became lodged over the entrance to the channel. No restrictor is present at the entrance to the second pass channels and no protuberances exist in the channel between the upper steam plenum and the lower second pass exhaust plenum so that if any type of particulate matter did reach the second pass side, one would expect it to be swept through to the lower steam exhaust plenum. It is anticipated that any particulate carry-over from the first pass mixing plenum to the upper steam plenum would be negligible since it would have to transit both the steam-water interface in the upper mixing plenum and the steam separators.

One possible mechanism to cause blockage would be the collapse of the second pass coolant-cladding material. The mechanism of failure would be brought about by rupture of the cladding material due to swelling of the fuel. Approximate burn-up calculations indicate that the core life would be limited not be reactivity considerations but by the effects of swelling. Swelling occurs in UO_2 at about 60,000 to 80,000 MWD/T; burn-up calculations indicate that the reactivity lifetime of the two core confirurations may be as much as an order of magnitude greater. During the early core life, the coolant

pressure on both sides of the annular fuel element tends to push the cladding firmly against the fuel material. As more fuel is expended, fission gas will eventually cause the fuel material to swell, pushing against the cladding materials and tending to force them out into their respective coolant channels against the restraining action of the coolant pressures. Eventually the cladding materials would be ruptured. One would expect that the first cladding material to fail under this action would be that for the second pass channel since it is subjected to compressive stresses and possible buckling. At this point, the question of second pass coolant blockage and the temperature excursion beyond the design constraints become somewhat academic. Rupture of the cladding would release radioactive material into the coolant channel.

4.7 Reactor Start-Up

The procedure for start-up of the CFR requires that a detailed knowledge of the transient behavior, including both nuclear and temperature, be available. As stated in Chapter 1, the development and especially the application of the mathematics necessary to provide such detailed knowledge is beyond the scope of this study. Nevertheless, it is possible to determine roughly how much time will be expended to bring the reactor from zero power at ambient temperature to full power at operating conditions by making simplifying assumptions.

During start-up, the recirculating pumps will be used to assure flow through the first pass channels of the core. The ambient temperature of all components will be assumed to be 70°F. Using the condition that only first pass cooling is available, it can be shown that the maximum power that can be used, if inlet reactor temperature is 520°F, to give a maximum second pass cladding and fuel temperature of 1250°F is 14.9% for the H_2O moderated reactor and 8.15% for the B_eO moderated reactor of full power in the steady state condition. Based on the heat capacity, mass and change in energy of the

various constituents involved, the times involved to heat to the condition of 1250 °F maximum fuel temperature are 9.3 minutes and 1.1 hours for the H_2O and BeO moderated reactors, respectively. It has been assumed that first pass coolant is being circulated through the core at full flow, after circulation has been started control rods are withdrawn to a position yielding 10% of design power, and that during the time the coolant temperature is increasing the cladding and fuel temperatures do not exceed the final steady state values. No saturated steam is generated during this step.

Because of the larger mass of fuel, radial thickness of the fuel material annulus and the low thermal conductivity of the fuel, the BeO moderated CFR configuration will not be discussed further. The comparison of times in the initial heat-up phase shows that this configuration takes significantly longer.

After the initial heat-up phase is completed, power is held at the point of 20% of design power. The system is closed until such time as saturated steam is produced, then this steam passes up through the steam separators to the dry steam plenum and back down through the core for second pass heating. Initially, no cooling is present on the second pass side of the annular fuel elements. After second pass steam enters the core, some cooling commences. Upon first entry of second pass steam, the heat transfer coefficient between the second pass steam and the inner fuel cladding is low because of the low mass flux. The temperature of the second pass cladding remains high, which tends to keep more of the heat flowing to the first pass coolant, producing more saturated steam. An equilibrium will be reached at which the flow rate has not changed but the reactor is now producing about 2% saturated steam on the first pass side, which means that about 20% of the design second pass flow has been achieved but not the design exit temperature.

Power can now be increased gradually from 20% of the design value to full power over about a 20 minute period, which corresponds to an increase in

reactor power of about 8.8×10^6 Btu/hr per minute. If a lumped parameter transient model is assumed to describe the temperature behavior, all roots are negative and have values ranging from 1.2/hr to $3/4 \times 10^5$/hr for the assumed ramp-type power rise. In determining some of the characteristic parameters for transient behavior, it was assumed that heat transfer coefficients were constant with time and that second pass flow was initially at its full design value when this power increase was applied. This latter assumption is necessary in order to achieve a manual solution without resorting to a computer aided numerical approach; the difficulty which prompts this assumption is the condition of second pass flow rate and temperature when the system of differential equations is transformed during the solution process. If the second pass flow had been variable in this analysis, another root would have been added; the addition of this root would change the complexion of the solution. Without going through a detailed analysis, it is not possible to determine if the resultant solution would be stable or unstable.

This simplified approach indicates that a time of 30 minutes to an hour may be required to get the reactor on the line at full power. If a more detailed model were developed, the time required could be explored more exactly and procedural steps for start-up could be varied to obtain the shortest start-up time, staying within the constraints of metallurgical limitations and stability.

Chapter 5

REMARKS ON DIRECT CYCLE SHIELDING AND CONTAINMENT

5.1 Limitations

The utilization of a direct cycle nuclear power plant (in contrast to an indirect cycle plant) imposes certain constraints on the arrangement of the plant. These limitations will determine to a large extent whether the direct cycle concept can be applied to a marine power plant, in which they are relatively more severe because of the mobility of the plant and hence the increased probability of damage to the plant.

When locating the machinery space within the ship, the number of alternative choices is reduced from that of the indirect cycle plant. This is caused by the recommended requirement that the containment vessel be located a minimum distance inboard of the hull equal to one-fifth the beam measured at right angles to the centerline at the level of the deep load line.[1] Additionally, side shielding must be provided and a cofferdam is necessary to restrict the effects of a possible explosion. Meeting these plus any specific arrangement requirements peculiar to the ship fixes the location of the machinery space within a limited section of the ship's length.

In contrast to the indirect cycle plant in which the reactor coolant never enters the machinery space, the direct cycle concept necessarily requires that the turbomachinery be automated or incorporate provisions for remote control. For a water cooled reactor, the water becomes radioactive and decays with the emission of a fast neutron or gamma ray. Accessibility to the direct cycle machinery space must be restricted during plant operations to limit exposure to these distributed sources of radioactivity.

In addition to the requirement that side shielding be provided, shielding must also be provided to limit the exposure to which all personnel aboard the ship would be subjected. This would at first imply that shielding must be

provided all around the machinery space. For an indirect cycle plant, the length on the ship's hull would be smaller since only the compartment housing the reactor, main coolant pumps or blowers, the heat exchanger through which power is transferred, etc., would have to be shielded. The spatial distribution of the reactor coolant in the direct cycle plant not only includes those components noted above, but also all turbomachinery in the machinery space through which the coolant flows.

The remainder of this chapter will be devoted to the estimation of secondary shield weights required and comments on containment provisions. The fact that the weights calculated are only estimates must be stressed. A detailed determination of the shield configuration, containment techniques, and coolision protection system would require a comprehensive analysis that is beyond the scope of this study. The results obtained here do, however, lead to some general conclusions of significance.

5.2 Distributed Radioactivity

Pure water becomes radioactive when subjected to neutron irradiation, as previously mentioned. This activation primarily results from the activation of the different oxygen isotopes present. A small additional source of activity is produced by neutron capture of hydrogen, but this is so small that it can be neglected in comparison with that from oxygen activation. Oxygen activation results in a 1 Mev neutron and two gamma rays at 1.1 Mev and 5.3 Mev. In a water-cooled direct cycle plant, this source of activity is distributed through the machinery space.

If a cladding failure occurs within the core, the coolant acts as the vehicle for transporting fission fragments outside the reactor shield. The fission fragments that would escape from the reactor would be in the form of soluble or insoluble gasses or solid particles. The attendant problem they would cause would be due to the increased isotopic radioactive half-lives

present in the machinery space after plant shutdown. Operational experience with a direct cycle boiling water reactor indicated that a serious problem did not result when the fuel cladding failed. The increase in radiation level at the turbine which resulted from deposition of fission fragments on the blading was comparable to that from a radium dial watch.[2]

The phase segregation taking place in the upper mixing plenum of the CFR as the first pass coolant leaves the core in the saturated state is identical with that in the boiling water reactor. The liquid vapor interface has been demonstrated to be extremely effective in preventing the further transfer of non-volatile fission fragments. Fragments introduced through a cladding rupture on the first pass coolant side of the fuel tube will be largely confined to the small flow loop defined by the reactor and recirculation line. On the second pass side (inside the annular fuel tube of the CFR), the all vapor mixture can be expected to carry solid particles introduced into this stream outside the reactor. These will be deposited at various positions along the flow loop. The maintenance of cladding integrity on the second pass side of the fuel tube thus imposes more stringent design criteria than that for the first pass side.

5.3 Estimation of Secondary Shield Weight

An accurate evaluation of the radioactivity level caused by coolant decay within the machinery space but outside the reactor requires specific knowledge of the machinery and piping arrangements and the cycle conditions. Without this knowledge, it is possible only to make an order-of-magnitude estimate of the required secondary shield weight.

The first step in determining this estimate is to calculate the number of coolant atoms which are decaying outside the reactor. A simplified model has been postulated (Appendix F) to determine this rate. The basic assumptions of the model are that the flux throughout the reactor is flat and that

the time a coolant atom spends within any given section of the flow loop is proportional to the mass of coolant within that section of the flow loop. The results of applying this model to a 50% enriched UO_2 CFR core, moderated with either water or BeO, are shown in Table 5.1, the volume ratio of moderator-to-fuel for the water moderated core taken as 2.0 and for the BeO moderated core as 10.0.

To apply the results of Table 5.1 in estimating the required secondary plant shield weight, assumptions must be made regarding the size and arrangement of the machinery space and the dose rate allowable outside the machinery space.

First, it will be assumed that the machinery space is 75' in length, 30' in heighth and 35' in breadth. Within this rectangular solid, all components through which radioactive coolant flows are located. Surrounding this space on all sides, except the bottom, a uniform layer of secondary shielding material will be placed. The incident flux of radiation, either gamma rays or neutrons, is assumed to be normally and uniformly incident over the

Table 5.1

ESTIMATED ISOTOPIC RADIOACTIVITY DECAY RATES

Number of Fissions/MW_t = 3.0×10^{16} Reactor Power = 60.0 MW_t

	Moderator	
	H_2O	BeO
Coolant Cycle Time/Reactor Transit Time	200	200
Reactor Coolant Mass/Fuel Mass	0.213	0.1847
Reactor Transit Time, Seconds	3.41	3.82
1.1 Mev Gammas/Second from O^{18}	5.80×10^{10}	4.11×10^{11}
5.3 Mev Gammas/Second from O^{16}	1.239×10^{12}	8.92×10^{12}
1.0 Mev Neutrons/Second from O^{17}	1.129×10^{8}	7.92×10^{8}

different sides of the machinery space.

These assumptions then preclude the presence of local "hot" spots within the space. In the case of fast neutrons, it will be relatively correct. Where large volumes of feedwater or condensate occur, the very fact that they do exist means that self-shielding takes place. In the case of water at standard conditions, the mean free path for removal of fast neutrons is approximately two inches. As a first approximation, it can be said that all neutrons born within two mean free paths of the boundary of the volume escape but all those originating within this circumferential thickness are trapped within the volume and do not escape.

"Hot" spots will occur due to gamma radiation. Whereas fast neutron energy is reduced to thermal values primarily by elastic collisions with the nuclei of the material they are transiting, gamma rays are attenuated by interaction with the orbital electrons of the material. Fast neutrons originate in a medium which exerts a strong influence on their subsequent behavior. Gamma rays are born in an environment which exerts relatively little influence on their physical behavior within this medium. Thus, where large volumes of feedwater or condensate occur, these volumes produce "gamma hot spots". The structural metal of the different components, although possessing a high electron density for gamma interaction, will not generally be thick enough to appreciably affect the local gamma fluxes which originate within their boundaries. Thus, a discrete pattern of areas on the secondary shield bulkheads will be present, caused by gamma rays. The assumption of a uniform incident gamma ray flux on the shield bulkheads allows only a rough estimate of the total shield weight.

The biological limit of exposure to a flux of 1 Mev neutrons is fixed at 60 neutrons/cm^2/sec based on a 40-hour week. For a ship at sea, the movement of personnel onboard is limited. The allowable flux level at the outside of

the secondary shield has been set a one-third the value found by converting from a 40-hour week to a 168-hour week, i.e., 4.76 neutrons/cm^2/sec.[3]

In calculating the requisite shield thickness for gamma radiation, it has been assumed that the allowable dose rate at the outer shield boundary will be 100 mrad/week. Again, this level is predicated on a man being continuously present at the shield boundary. Since this assumption is highly remote, it tends to make the shielding thickness conservative. It is anticipated that the total shield weight found by these assumptions will be greater than that which would result from a detailed analysis which considers both gamma "hot" spots and a more realistic appraisal of the exposure time outside the shielded space.

Taking the gamma decay rates resulting from the transmutation of O^{16} and O^{18}, Table 5.1 shows that the rate from O^{16} is approximately two orders of magnitude greater than that from O^{18}. Also, the harder 5.3 Mev gamma from O^{16} is more difficult to shield against than the 1.1 Mev gamma from O^{18}. Therefore, the contribution of gammas from O^{18} to the gamma shield weight has been neglected with small resultant inaccuracy in the estimated shield weight.

The results of applying the data generated in Table 5.1 and the assumptions delineated above regarding distribution on the shield and allowable exposure rates are shown in Table 5.2.[4] Comparison of the estimated weight shown for secondary shielding against neutrons and 5.3 Mev gammas shows that the major input to the required shield weight arises as a result of the 5.3 Mev gamma rays.

The gamma shield weight estimates point up the fact that the utilization of a separate and distinct gamma shield is not practical. This severely limits the possible ship types which could incorporate a direct cycle water-cooled nuclear plant. Because of the volume and weight required for a water

Table 5.2

ESTIMATED SECONDARY SHIELD PARAMETERS

Compartment Length 75'	Width 35'		Height 30'	
Moderator	H_2O		BeO	
Shield Material	Water	Lead	Water	Lead
1.0 Mev Neutrons from O^{17}				
Thickness (inches)	1.5		5.6	
Volume (ft^3)	1153		4305	
Weight (long tons)	32.7		122.2	
5.3 Mev Gammas from O^{16}				
Thickness (inches)	100	5.13	138	7.09
Volume (ft^3)	76900	3940	106100	5440
Weight (long tons)	2180	1264	3010	1748

blanket or the weight for a lead blanket, the utilization of a non-revenue producing material as the secondary shielding agent appears impractical.

5.4 Cargo Shielding

One solution to the problem of how to provide a direct cycle nuclear plant with the requisite gamma shield is to consider the use of the cargo itself as the shielding agent. This method has been described previously, particularly in the study of direct cycle plants using boiling water reactors.[5]

The requirement that the shield must provide a continuous belt around the machinery space limits the type of ship in which a direct cycle plant can be fitted to tankers. The amount of shielding protection that any material provides is roughly proportional to the weight of the material per unit surface area between the radioactive source and the point being shielded. A tanker appears to be satisfactory since, if it is empty and must proceed to a different port to load cargo, the empty tanks can be filled with ballast sea water for the trip and the required shielding achieved to permit operation

Table 5.3

COMPARISON OF DIRECT AND INDIRECT CYCLE SHIP WEIGHTS

Power Plant Cycle Containment	Conventional Steam Direct	PWR SAVANNAH Type Indirect Primary	BWR Natural Circ. Direct Primary	BWR Natural Circ. Direct Mach'y Space	BWR Forced Circ. Direct Primary
Light Ship Wt:					
Steel	6430	6555	6620	6650	6620
Outfit	1360	1320	1290	1290	1290
Machinery	970	955	720	720	720
Reactor Plant		480	170	170	170
Containment		200	170	(a)	170
Shielding: Primary		110	850	850	850
Secondary		1830	(b)	(b)	(b)
Total	8760	11400	9820	9680	9820
Deadweight:					
Cargo	19580	19080	20660	20800	20660
Fuel Oil	2460	320	320	320	320
Stores, Effects, Crew, Misc.	600	600	600	600	600
Total	22640	20000	21580	21720	21580
% Gain Cargo	Base	-2.5	5.5	6.2	5.5

(a) Included with structural steel. (b) Included in deadweight.

of the machinery plant.

When considering the different ramifications of cargo shielding, the possible activation of the cargo must be brought up. The weights estimated for the required fast neutron shield are not too large to be prohibitive, indeed with the conservative assumptions made for their determination it is expected that they would be high. They indicate that it is possible to provide a fast neutron shield which can protect the cargo against activiation.

Table 5.3 is taken from a study that considered the use of boiling water reactors as the power source for a marine plant. The deadweights of the direct cycle plant compare favorably with both the conventional oil-fired ship and the SAVANNAH type nuclear ship. The shield arrangement used did not provide for overhead shielding of the machinery space. Consequently, the deck

area over the machinery space also has limited accessibility. If the same philosophy is applied to the weights estimated in Table 5.2, their values can be reduced by approximately 30%.

A sectional view through the machinery space showing the arrangement of the shielding tanks is illustrated in Figure 5.1. This arrangement reflects the philosophy used to generate the data given in Table 5.3 for the direct cycle boiling water plants and shows that only wing tanks are present to provide shielding abeam of the space with no protection provided above the space.

The question of the possible collision at sea in which the cargo shield tanks might be holed is valid. To avoid the immobilization of the ship at sea after such an occurrence, the plant must be provided with an auxiliary non-nuclear power source. The inclusion of a diesel engine to act as an emergency power source is not unrealistic. Normal design philosophy for any marine plant is to provide some alternate means of take-home power in the event of an equipment failure precluding operation of the normal propulsion plant. For the nuclear plant, the loss of secondary shielding can be considered to be such a failure. From this standpoint, wing tanks to provide secondary shielding are feasible. If the reactor pressure vessel is not ruptured, the primary shield encompassing the reactor will furnish the necessary protection against core activity.

5.5 Containment and Collision Protection

To prevent the free egress of fission products from the nuclear fuel to the atmosphere, three barriers placed in series have to be overcome. The flow diagram indicating how these barriers would be penetrated is shown:

Fission Products in the Fuel	⟶	Cladding Failure	⟶	Piping or Equipment Rupture	⟶	Containment Vessel Rupture	⟶	Fission Products in the Atmosphere

Cladding has been provided around the fuel already. "Piping or Equipment

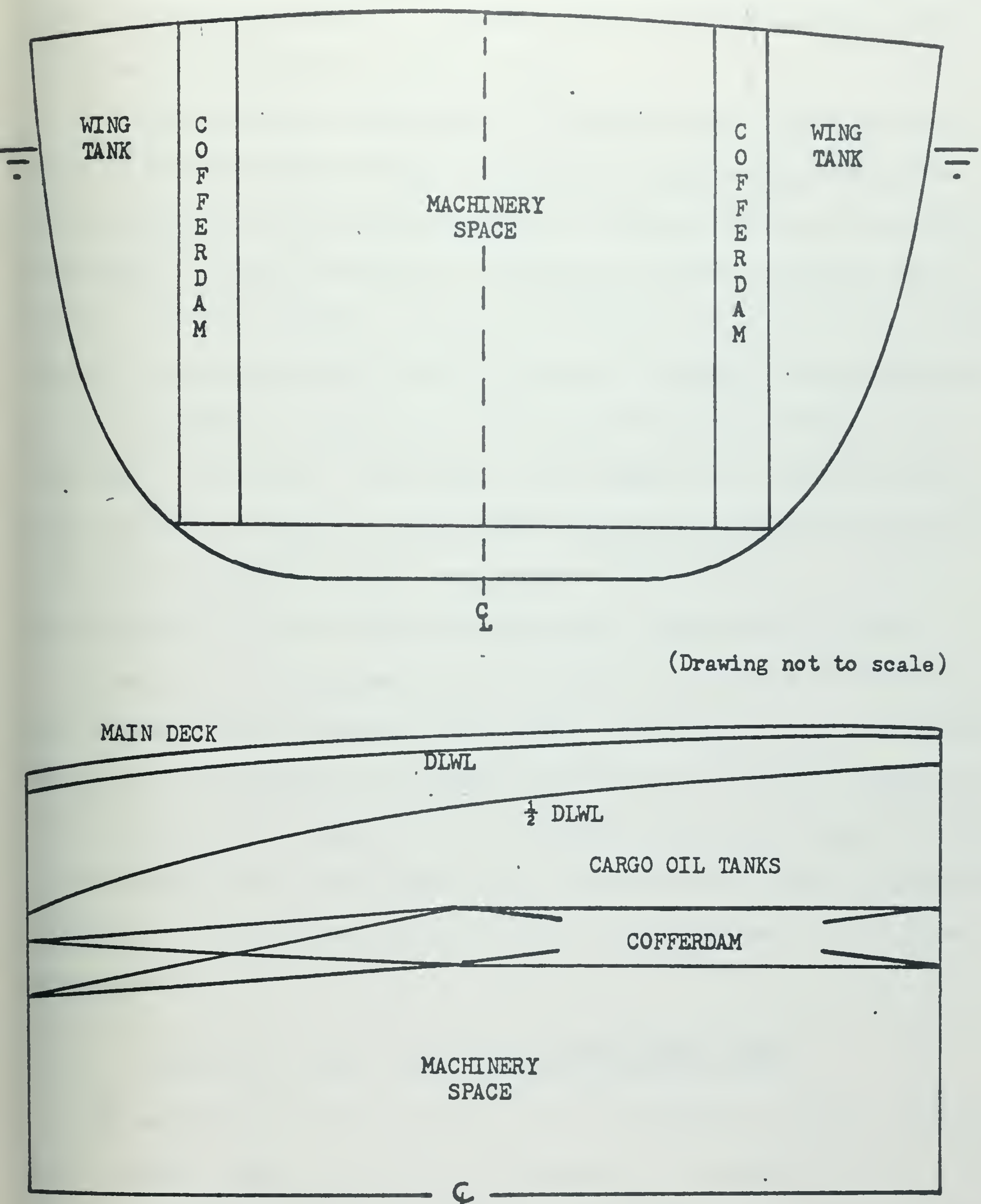

CROSS SECTION OF SHIP THROUGH THE MACHINERY SPACE

Figure 5.1

Rupture" is meant to indicate either a rupture of reactor pressure vessel, a break in the piping system or a rupture of one of the turbomachinery equipment items through which the coolant flows.

The requirement for restricting the dispersal of any fission products that have transited the first two barriers in the direct cycle application favors designing the whole periphery of the machinery space as the containment vessel. In the first place, a breakdown of the first fission product barrier, the fuel cladding, results in a possible circulation of the products through the space along the coolant flow path. Secondly, if this condition occurs, there will be some escape of the volatile products into the open environment of the space through gland seal leakage and as non-condensable gases from the air ejector. Thus, total containment appears more realistic than reactor containment only. Even without cladding rupture, a break in flow loop results in the release of radioactive coolant into the spaces.

A method for accomplishing this containment protection is to incorporate this requirement into the structural design of the ship in way of the machinery space. The pressure to which the containment vessel would be subjected can be estimated by assuming that it is proportional to the available thermodynamic energy of the coolant within the reactor pressure vessel and inversely proportional to the volume enclosed by the containment vessel. With these assumptions:

$$\text{Explosion Pressure} \propto \frac{\text{Coolant Thermodynamic Energy}}{\text{Containment Vessel Volume}}$$

The separate containment vessel for the NS SAVANNAH plant has a calculated internal volume of 3.8×10^4 ft^3 (length = 51', diameter = 35'). At a mean temperature of 508 °F within the pressure vessel, the estimated coolant weight is 8030 lbs at an average energy of 505.3 Btu/lb.[6]

For the CFR system, under the concept of total containment for a compartment of dimensions 75' x 35' x 30' (= 7.9×10^4 ft^3), the weight of

coolant and average specific energy for the H_2O moderated and BeO moderated cores are (1662 lbs, 522.3 Btu/lb) and (1551 lbs, 537.8 Btu/lb), respectively.

Scaling against the SAVANNAH's containment vessel design pressure of 185 psig, the estimated pressures to which the containment vessel of the direct cycle CFR system might be subjected are 6.2 psig and 5.7 psig for the H_2O and BeO moderated cores, respectively, assuming that the final expansion results in saturated liquid at atmospheric pressure (180.02 Btu/lb). The estimated pressure should be considered low, since an explosion does not occur in the idealized manner assumed. The effect of the larger expansion volume and the smaller mass of coolant, which result from the direct cycle CFR application with total containment, are illustrated by the pressure estimates.

When faced with pressures of this order-of-magnitude, a feasible approach is to consider integrating this requirement into the structural design of the hull. A cofferdam (void space) will separate the machinery spaces from the cargo tanks. Stiffening the inboard bulkheads of the cofferdam to withstand explosion pressures of the magnitude estimated above presents no great problem and will not materially contribute to the overall structural weight of the ship.

The longer length of the radioactive machinery space in the direct cycle concept requires collision protection over a greater percentage of the ship's length than is necessary for a PWR or other indirect cycle nuclear plant. If additional steel had to be utilized specifically for collision protection at the same rate of tons/foot, this item would drive up the operating expense for the direct cycle because of revenue loss. The requirement that cargo shielding is necessary to make this concept at all feasible plays a favorable role for collision protection. The fact that there necessarily is a large

separation between the hull plating and longitudinal bulkheads defining the machinery space reduces the amount of steel that must charged to collision protection; part of the weight involved can be charged to the tank structure itself.

The data presented in Table 5.3 points up what would appear to be an advantage in designing for total containment of a direct cycle plant and incorporating this feature plus collision protection into the overall structural requirements of the ship. In the case of the SAVANNAH type plant the light ship weight for steel and containment totals 6755 tons whereas for the direct cycle natural circulation BWR plant these light ship weights are 6650 tons; for the case of the direct cycle BWR plant with primary containment and natural or forced circulation the light ship weights are 6790 tons.

5.6 Concluding Remarks

These preceding sections have been written to indicate some of the problem areas associated with the design of a direct cycle, steam driven nuclear marine power plant. In this respect, the most difficult design problem that has to be solved is that concerning secondary shielding. With the application of the direct cycle plant to tankers, the only feasible way to achieve an economical ship is by means of burying the plant among the cargo tanks. This does not solve the problem since the large thickness or weight of secondary shielding material over the radioactive machinery space appears to be prohibitive, hence deletion of the overhead shield seems necessary and a new set of problems concerning access to a radioactive main deck area is introduced.

Chapter 6

CONCLUSIONS AND RECOMMENDATIONS

6.1 Summary

The CFR reactor appears to be an entirely feasible concept. Results shown in Chapter 4 indicate that it can produce superheated steam within the constraints of metallurgical temperatures.

The H_2O moderated core leads to a smaller reactor than does the BeO moderated core. In the two configurations chosen for discussion, the H_2O moderated core, though smaller, has a lower modal neutron temperature than the BeO moderated core. For both configurations, an enrichment of 50% U^{235} was used. The results of evaluation indicate that a lower enrichment in the neighborhood of 30% will cause more than half of the power produced to arise from fissions induced by neutrons with an energy of less than 1.85 ev, the boundary energy used in the two-group model used, for the same geometrical size of the H_2O moderated core described in Table 4.4. Reduction of the power split between the two groups for the BeO moderated core to this level cannot be achieved without increasing the core size.

The power density achieved with the H_2O and BeO moderated core are 45.3 kw/liter and 6.01 kw/liter, respectively. For the two configurations studied, the second pass exit velocities were of the order of 100 ft/sec and 300 ft/sec. The slower exit velocity yields a core of smaller length. On the other hand, the dimensions of the corresponding flow paths are reduced and the number of flow paths (i.e., number of annular fuel elements) must be increased. Consequently, the ratio of cladding/fuel volume within the core increases and more neutrons are parasitically absorbed. The choice of the configuration was based on minimum core volume, which turned out to be limited by the second pass cladding temperature. Because of the increase in parasitic absorption, only an economic analysis of fuel cycle costs can determine

whether the minimum volume core will in fact be the optimum core.

It has been stated that as the second pass steam exit velocity decreased, the required fuel rod length for a given maximum cladding temperature decreased. This statement was based upon holding the second pass channel radius r_1 fixed. If the number of fuel elements is held fixed (the product of $V_2 r_1^2$), inspection of the results quoted in Table 2.2 will show that for a given maximum cladding temperature, the required fuel rod length will increase as the steam exit velocity, ratio of fuel tube radii (r_3/r_2) and second pass channel radius decrease. In this comparison, the percentage of fuel volume within the core decreases as the steam exit velocity decreases. Thus, the H_2O moderated core appears more feasible at low steam exit velocities than the BeO moderated core, since H_2O is a more efficient moderator than BeO.

In comparison with the typical pressurized water and boiling water reactors in use today, the H_2O moderated CFR appears favorably. The pressurized water plant in the NS SAVANNAH, the only non-military marine plant in existence today, has a calculated power density of 21.1 kw/liter. Additionally, the fact that the steam exit conditions are superheated produces a cycle efficiency which is approximately 1.4 times the efficiency of the SAVANNAH cycle.[1]

An off-shoot of the Aircraft Nuclear Propelled Program has been the study of the "630A Steam Generator". This study deals with the application of an indirect cycle, air cooled, water moderated fully enriched reactor to produce superheated steam at the same design conditions as the CFR. The active core dimensions are 47.8" diameter and 27.4" height, producing 67.4 MW_t for 30,000 SHP. The power density for this core is calculated to be 83.4 kw/liter, or about 1.8 times that of the H_2O moderated core of this study. Overall cycle efficiency for this plant is approximately equal to

that of the CFR plant. Some economic studies indicate that this type installation will be competitive with conventionally fired marine plants. A review of the core configuration indicates that the reactor would be classified as fast.[2]

The figures of Chapter 4 show the power and temperature distributions for a typical CFR core. Near second pass exit at the bottom of the core, power peaking is evident. This tends to limit the advantage of the counter flow arrangement since the heat flux from the second pass coolant to the first pass coolant becomes relatively less. Increasing the moderator/fuel atom ratio will decrease the amount of power peaking, making the axial distribution more uniform and permitting a shorter active length to achieve the design exit conditions.

Control of the direct cycle CFR plant must be accomplished automatically or by remote features. An economic analysis of a boiling water direct cycle reactor plant for a marine installation indicates that automatic control is economically feasible.[3] The power level in the CFR can be varied by changing the feedwater flow rate or the recirculation flow rate. Control rods must enter the core from the bottom, rather than the top, in order to reduce the effects of axial power peaking and permit the reactor to be operated at full power.

Shielding of a direct cycle CFR plant presents many problems. The only practical installation indicates that tankers would be the sole ship type available. Even if the tanker type is chosen, the reactor and turbomachinery must be buried in the cargo tanks and limited access will result in areas above the machinery space.

6.2 Recommendations

Heat transfer can be said to play the controlling part in the engineering evaluation of the counterflow reactor concept. Heat is removed from

the fuel element by two counterflowing coolants, which at various positions during their transit of the core are in the pressurized water, two-phase steam-water and dry superheated steam conditions. It is particularly important that the heat transfer coefficient between cladding and coolant can be accurately predicted. Correlations for doing this for the two-phase steam-water mixture are limited; the majority of published technical literature deals with the burnout heat flux and not with the prediction of the actual heat transfer coefficient. The correlations that do exist generally show wide variations for the same conditions. It becomes almost mandatory that more work be done to develop a consistent and reliable means for predicting two-phase heat transfer over all quality regions in order that the CFR concept can be fully justified.

Many variables were arbitrarily fixed during the study of the CFR. These included the nominal first pass inlet velocity, first pass steam exit quality, and second pass exit velocity. An increase in the first pass inlet velocity will make the core smaller and increase the pressure drop from inlet to mixing plenum. The first pass steam exit quality determines the heat transfer coefficient, recirculation rate and second pass flow rate. The second pass steam exit velocity determines the heat transfer coefficient to the second pass coolant, the size of the channel and the power produced in the associated annular fuel element. Additional scoping studies are recommended which would include these terms as variables in the selection of an optimized core.

The fuel used in this study was a ceramic. One area of further investigation that needs to be fully explored is that of using dispersed fuel in a metallic lattice. Because of the great variance in thermal conductivity between the two types, the curves of required core length shown in Chapter 2 will be entirely different.

The study of transient behavior of the reactor will determine whether the concept is sound. Preliminary investigation of this behavior in conjunction with the remarks made on the start-up procedure indicate that this is the case. This investigation was made using a crude lumped parameter model. The transient study of the CFR concept needs much more work to be able to define with reasonable accuracy the transient peaks during power variation. A detailed investigation of the behavior using numerical analysis techniques appears to be not feasible because of the small time increments that are required to insure stability of the solution. Refinement of the lumped parameter model by describing smaller and smaller volumes within the core appears to offer the most promise in achieving a theoretical tool for predicting transient behavior.

Whether the concept will be adopted depends on its economic potential. The FORTRAN program listed in Appendix G can be modified to assist in this evaluation. It can be coupled to a fuel cycle or burn-up code. This coupling should be such as to allow the reactor to produce power for a specified time increment, calculate the change in composition of the constituents and fission products, homogenize the results so that the CFR program can again be entered to determine the fine details of the power distribution, and then repeat the cycles until criticality is lost.

The steam cycle into which the CFR was installed is pertinent to a marine plant. The direct cycle plant is extremely limited for this type of application, primarily due to the shielding requirements. As such, investigation into the use of this concept for an indirect cycle plant may show additional advantages. Such an investigation will require the determination of a new set of cycle parameters for the primary loop, dependent on the temperature pinch points in the heat exchanger and relative flow rates in the two fluid loops. If the core configurations presented in Chapter 4 could

be directly applied to an indirect cycle plant, the overall cycle efficiency would fall because of the lowering of the maximum practical turbine inlet steam temperature and the machinery weight of the plant would increase due to the steam generators and primary coolant pumps required.

APPENDICES

APPENDIX A

NUCLEAR ANALYSIS

A.1 Choice of Model

The mathematical model describing the steady state neutronic behavior is that of two-group diffusion theory. Diffusion theory has been chosen because of the relative simplicity with which it can be applied and a solution obtained, in contrast to the greater complexity which results when a higher order transport theory approximation is used. The results obtained from this theory are not as precise as might be desired, particularly in the fuel regions. This sacrifice is necessary to permit a digital computer program to be written (1) that is not of such length that it will exceed the machine storage capacity, taking into account the fact that the coupled nuclear, thermodynamic and hydrodynamic problem must be solved simultaneously, and (2) that the necessary computational time per data set conforms to those restrictions imposed by the MIT Computation Center that a maximum number of parametric values can be studied.

A.2 Formulation of the Basic Equations

The general multigroup steady state diffusion equation is written in terms of the physical processes which define the flux level ϕ for neutrons in energy group j at some spatial point x. Energy group 1 denotes neutrons with the highest kinetic energy, whereas energy group N, N being the number of discrete groups into which the energy spectrum has been divided (two for this problem), refers to neutrons of thermal energy. A conservation equation is written for the neutron density, which defines these processes within an infinitesimally small volume at x[1].

Diffusion theory approximates the number of neutrons which are diffusing

away from the volume centered at x per unit time and per unit volume as

$$\text{Diffusion rate} = \nabla\cdot\left[D^j(x)\ \nabla\phi^j(x)\right]$$

The rate at which neutrons are absorbed by constituent nuclei within the volume by fission or non-fission capture is

$$\text{Absorption rate} = \Sigma_a^j(x)\ \phi^j(x)$$

In addition, there is also a pseudo-absorption process in which the neutrons of group j are removed from this group to groups of lower energy (higher group number) through the mechanisms of elastic and inelastic scattering. The rate at which this removal process contributes to the conservation equation is

$$\text{Scattering absorption rate} = \sum_{k=j+1}^{N}\left[\Sigma_s^{j\rightarrow k}(x)\ \phi^j(x)\right]$$

Just as the neutron density is lowered by downscattering to lower energy groups, the density in these lower groups is increased by this mechanism. The contribution to the density of group j by all higher groups is given by

$$\text{Scattering source rate} = \sum_{k=1}^{j-1}\left[\Sigma_s^{k\rightarrow j}(x)\ \phi^k(x)\right]$$

In addition to the downscattering source term, neutron production is also occurring due to fission, if the region under consideration at point x contains a fissionable material. Because of the statistical nature of the fission process, fissions induced by neutrons of group k produce neutrons in group j. Representing the probability that, of all the neutrons born by fission, over all possible energies, the fraction of fissions born directly into group j is given by $X^j(x)$, the fission source is

$$\text{Fission source rate} = X^K(x)\sum_{k=1}^{N}\left[\nu^k(x)\ \Sigma_f^k(x)\ \phi^k(x)\right]$$

Combining these terms through a conservation equation based on the rate of change of density with time,

0 = Production - Absorption - Leakage

the general multigroup steady state diffusion equation can be formulated in continuous space as

$$0 = \nabla \cdot \left[D^j(x) \ \nabla \phi^j(x) \right] - \Sigma_a^j(x) \ \phi^j(x) - \sum_{k=j+1}^{N} \left[\Sigma_s^{j \to k}(x) \right] \phi^j(x)$$

$$+ \chi^j(x) \sum_{k=1}^{N} \left[\nu^k(x) \ \Sigma_f^k(x) \ \phi^k(x) \right] + \sum_{k=1}^{j-1} \left[\Sigma_s^{k \to j}(x) \ \phi^k(x) \right] \quad \text{(A-1)}$$

Certain boundary conditions have to be applied within the reactor to describe the behavior of the neutron density and flux for all energy groups at an interface between two different materials. Since an interface possesses no finite thickness, the density cannot change across it. Because the density does not change, the rate at which neutrons traverse the interface must be the same on both sides, i.e., the current must be continuous. These conditions then are expressed mathematically as

$$\phi^j(x) \Big|_{\text{left}} = \phi^j(x) \Big|_{\text{right}} \quad \text{(A-2a)}$$

$$D^j(x) \ \nabla \phi^j(x) \Big|_{\text{left}} = D^j(x) \ \nabla \phi^j(x) \Big|_{\text{right}} \quad \text{(A-2b)}$$

The local power generation rate at any point, due to stopping of the fission products in the region of the fissioned nucleus, is defined from the condition that

$$P(x) = C \sum_{k=1}^{N} \left[\Sigma_f^k(x) \ \phi^k(x) \right] \quad \text{(A-3)}$$

Equations (A-1) - (A-3) form the basis of the subsequent development to define the flux and power distributions within the reactor. To

determine these distributions, the continuous equations must be reformulated as finite difference equations.

A.3 Reactor Subdivision

The reactor is in the form of a right circular cylinder. This configuration has been chosen to yield the maximum neutron economy and a minimum of heat removal problems. In this shape, the variation of parameters around the radial centerline is assumed to be rotationally symmetric, so that equation (A-1) can be written in two-dimensional cylindrical (r,z) coordinates. This assumption presupposes that the effect of a discrete number of control rods around the reactor centerline can be represented by considering them to be smeared out over an annular ring. As a result of the discrete character, the fission rate and burn-up in the neighborhood of a control rod shows an angular variation. These two effects are neglected by this assumption. This neglect does not change the overall flux distribution within the reactor, but introduces an additional fine structure which alters the local power distribution rate.

The reactor is divided into M_R radial regions and M_Z axial regions as shown in Figure A.1. The properties of any region within the reactor can be specified by the double subscript (I,J). The lower plenum is denoted by J = 1, the upper by J = M_Z. The radial reflector is denoted by I = M_R. The core regions are then specified by I = 1 to I = M_R - 1 and J = 2 to J = M_Z - 1. The properties of all radial subdivisions pertinent to the lower plenum have the same value. The same is true for the upper plenum regions or the radial reflector regions.

Figure A.2 shows a horizontal cross section of one of the cells within the reactor core. All regions across the cell can be described by a

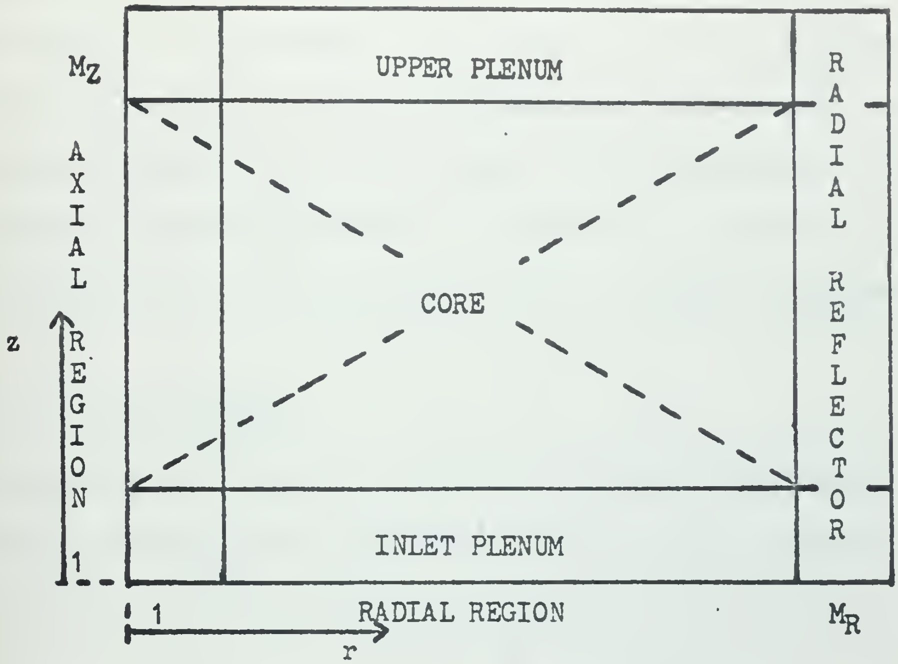

REACTOR SUBDIVISION

Figure A.1

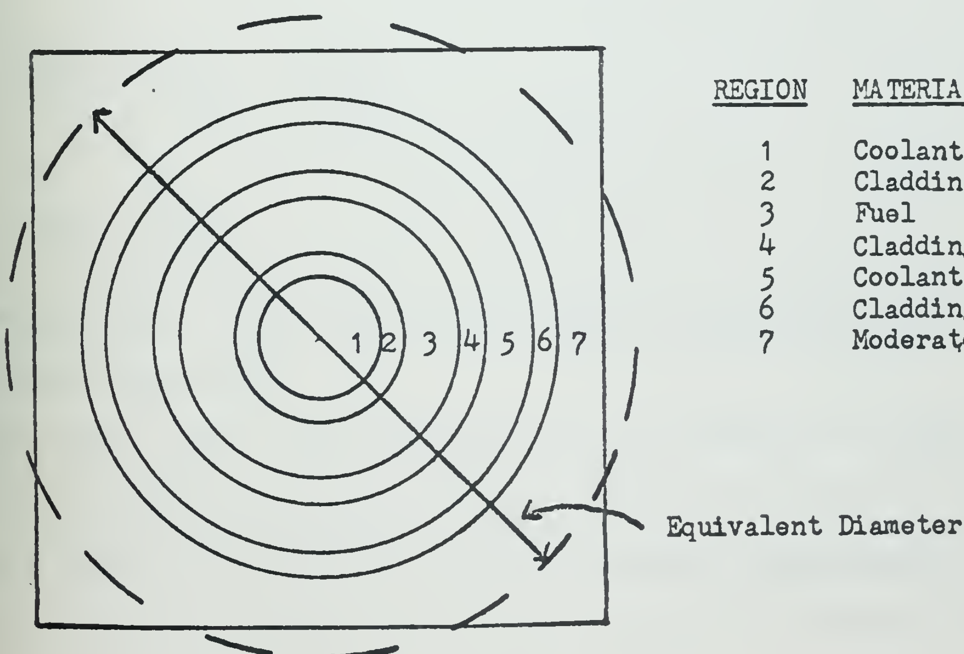

REGION	MATERIAL
1	Coolant
2	Cladding
3	Fuel
4	Cladding
5	Coolant
6	Cladding
7	Moderator

CELL SUBDIVISION

Figure A.2

set of concentric circles. To simplify the mathematical treatment, the moderator region is also assumed to be annular and the equivalent diameter of the square cross section is defined such that the area enclosed by the circumscribing circle is equal to the cell pitch squared. This permits describing the cell properties in terms of cylindrical coordinates in two dimensions by again assuming rotational symmetry.

A.4 Reduction to One-Dimension

Within any given core subdivision volume, the nuclear properties of the constituent material are independent of position and equation (A-1) can be written in (r,z) coordinates within this volume as

$$0 = D^j(\nabla_r^2 + \nabla_z^2)\, \phi^j(r,z) - \left[\Sigma_a^j + \sum_{k=j+1}^{N} (\Sigma_s^{j\to k})\right] \phi^j(r,z)$$
$$+ \sum_{k=1}^{j-1}\left[\Sigma_s^{k\to j}\, \phi^k(r,z)\right] + \chi^j \sum_{k=1}^{N}\left[\nu^k\, \Sigma_f^k\, \phi^k(r,z)\right] \qquad \text{(A-4)}$$

where

$$\nabla_r^2 = \frac{\partial^2}{\partial r^2} + \frac{1}{r}\frac{\partial}{\partial r} \qquad \text{(A-5a)}$$

and

$$\nabla_z^2 = \frac{\partial^2}{\partial z^2} \qquad \text{(A-5b)}$$

The two-dimensional nature of the flux variation is introduced by the Laplacian operators ^{2}.

Physically, these operators account for the diffusion or leakage away from a given point. Because of their presence in (A-4), the total number of space mesh points that must be considered, when formulating the equations in terms of finite differences, is equal to the product of the

number of mesh points in the radial direction and the number of mesh points in the axial direction. To reduce the total number of space points, it is advantageous to define a macroscopic leakage cross section Σ_1^j which will account for the two-dimensional effect and p ermit reducing equation (A-4) to a one-dimensional difference equation without an inordinate decrease in accuracy.

To accomplish this reduction, the direction in which the flux mapping is to be performed is either described in terms of plane (z) or polar (r) coordinates. Then, defining a Laplacian operator ∇^2, which is in this direction of calculation, the leakage cross section will account for neutron flow in a direction transverse to the calculational directional. ∇^2 is defined by equation (A-5a) or (A-5b), depending upon whether the geometry is polar (r) or plane (z).

In terms of the leakage cross section, equation (A-4) is written as

$$0 = D^j \nabla^2 \phi^j(x) - \left[\Sigma_a + \Sigma_1^j + \sum_{k=j+1}^{N} (\Sigma_s^{j\to k})\right] \phi^j(x) + \sum_{k=1}^{j-1}\left[\Sigma_s^{k\to j}\, \phi^k(x)\right] + X^j \sum_{k=1}^{N}\left[\nu^k \Sigma_f^k\, \phi^k(x)\right] \qquad \text{(A-6)}$$

which is one-dimensional with respect to the Laplacian operator, but two-dimensional with the inclusion of the leakage cross section. The method of defining the leakage cross section is derived in Sections A.12 and A.13.

A.5 Formulation of the Difference Equations

Using the method of finite central differences,[3] the first difference for some function f at some mesh point k is given by

$$f_k = f_{k+\frac{1}{2}} - f_{k-\frac{1}{2}}$$

The second central difference about point k is

$$\Delta^2 f_k = \Delta(\Delta f_k) = f_{k+1} - 2 f_k + f_{k-1}$$

With these definitions, the Laplacian operators in plane or polar coordinates take the form

$$\nabla^2 f\Big|_{z=z_k} = \frac{f_{k+1} - 2 f_k + f_{k-1}}{\Delta z^2} \tag{A-7}$$

and

$$\nabla^2 f\Big|_{r=r_k} = \frac{f_{k+1} - 2 f_k + f_{k-1}}{\Delta r^2} + \frac{1}{r_k} \frac{f_{k+\frac{1}{2}} - f_{k-\frac{1}{2}}}{\Delta r} \tag{A-8}$$

The half spacing in (A-8) is inconvenient, so it is replaced by

$$\frac{f_{k+\frac{1}{2}} - f_{k-\frac{1}{2}}}{\Delta r} \qquad \frac{f_{k+1} - f_{k-1}}{2 \Delta r}$$

giving for the polar Laplacian

$$\nabla^2 f\Big|_{r=r_k} = (1 + \frac{\Delta r}{2r_k}) \frac{f_{k+1}}{\Delta r^2} - \frac{2}{\Delta r^2} f_k + (1 - \frac{\Delta r}{2r_k}) \frac{f_{k-1}}{\Delta r^2} \tag{A-9}$$

The similarity between equations (A-7) and (A-9) is apparent. The geometrical correction factor ($\Delta r_k/2r_k$), which appears in (A-9), can also be written as

$$(1 - \frac{\Delta r}{2r_k}) = (1 - \frac{G \Delta r}{2 r_k}) \tag{A-10}$$

where G is defined to be unity if the coordinate system is polar. Defining G to be zero for plane geometry, a general one-dimensional Laplacian operator can be written in terms of central differences as

$$\nabla^2 f = \left(1 + \frac{G\Delta x}{2x_k}\right) \frac{f_{k+1}}{\Delta x^2} - \frac{2f_k}{\Delta x^2} + \left(1 - \frac{G\Delta x}{2x_k}\right) \frac{f_{k-1}}{\Delta x^2} \tag{A-11a}$$

where

$$G = 0 \quad \text{plane geometry} \tag{A-11b}$$

$$G = 1 \quad \text{polar geometry} \tag{A-11c}$$

Using these definitions, the difference equation equivalent of (A-6) in terms of plane or polar geometry at some position $x = x_k$ becomes

$$\begin{aligned} 0 = {} & \frac{D^j}{\Delta x^2}\left(1 + \frac{G\Delta x}{2x_k}\right) \phi^j_{k+1} + \frac{D^j}{\Delta x^2}\left(1 - \frac{G\Delta x}{2x_k}\right) \phi^j_{k-1} \\ & - \left[\frac{2D^j}{\Delta x^2} + \Sigma^j_a + \Sigma^j_l + \sum_{m=j+1}^{N} \left(\Sigma_s^{j\to m}\right)\right] \phi^j_k \\ & + \sum_{m=1}^{j-1} \left(\Sigma_s^{m\to j}\, \phi^m_k\right) + \chi^j \left[\sum_{m=1}^{N} \left(\nu^j\, \Sigma^j_f\, \phi^j_k\right)\right] \end{aligned} \tag{A-12}$$

A.6 Induction Formula to Invert Flux Difference Equations

The basic mathematical technique to invert a one-dimensional set of equations in the form of (A-12) has been previously developed.[4] A brief outline of this method is given below. The difference in the method of solution, as required by the inclusion of the leakage cross section Σ^j_l, is noted.

Within a region the cross sections and diffusion coefficients are constant. The variable parameter is the flux. The last two terms in equations (A-12) represent the source terms for group j and position k. These two terms are denoted by S^j_k:

$$S^j_k = \sum_{m=1}^{j-1} \left(\Sigma_s^{m\to j}\, \phi^m_k\right) + \chi^j \left[\sum_{m=1}^{N} \left(\nu^m\, \Sigma^m_f\, \phi^m_k\right)\right] \tag{A-13}$$

Denoting the total removal cross section from group j, disregarding the influence of diffusion in the direction of calculation, and leakage perpendicular to this direction, by the symbol Σ_T^j, the mathematical definition becomes

$$\Sigma_T^j = \Sigma_a^j + \sum_{m=j+1}^{N} \left[\Sigma_s^{j\to m} \right] \qquad \text{A-14)}$$

The leakage cross section Σ_l^j in (A-12) introduces a variation in the treatment between this method and that previously referenced. If the leakage cross section is negative and there is a net flow of neutrons into the region under consideration, it is possible for a condition to arise where

$$\left| \Sigma_\ell^j \right| > \Sigma_a^j + \sum_{m=j+1}^{N} \left(\Sigma_s^{j\to m} \right)$$

When this situation occurs, the total cross section for absorption, downscattering and leakage becomes negative and direct inversion by the methods of (4) leads to a mathematical instability in the difference equation representation.

To preclude this occurrence, the following technique is employed. The value of the leakage cross section Σ_l^j is tested to determine whether it is positive or negative. When Σ_l^j is greater than zero, the source term and total removal cross section term are modified to

$$S_k^j = \sum_{m=1}^{j-1} \left(\Sigma_s^{m\to j} \phi_k^m \right) + X^j \sum_{m=1}^{N} \left(\nu^m \Sigma_f^m \phi_k^m \right) \qquad \text{(A-15a)}$$

$$\Sigma_T^j = \Sigma_a^j + \Sigma_\ell^j + \sum_{m=j+1}^{N} \left(\Sigma_s^{j\to m} \right) \qquad \text{(A-15b)}$$

On the other hand, if Σ_ℓ^j is negative, Σ_ℓ^j is included with the source

term so that

$$S_k^j = -\Sigma_t^j \phi_k^j + \sum_{m=1}^{j-1} (\Sigma_s^{m\to j} \phi_k^m) + X^j \sum_{m=1}^{N} (\nu^m \Sigma_f^m \phi_k^m) \tag{A-16a}$$

$$\Sigma_T^j = \Sigma_a^j + \sum_{m=j+1}^{N} (\Sigma_s^{j\to m}) \tag{A-16b}$$

Using the appropriate set of either (A-15) or (A-16), equation (A-12) is rewritten as

$$\begin{aligned} 0 = {} & \frac{D^j}{\Delta x^2}\left(1 + \frac{G\Delta x}{2x_k}\right)\phi_{k+1}^j + \frac{D^j}{\Delta x^2}\left(1 - \frac{G\Delta x}{2x_k}\right)\phi_{k-1}^j \\ & - \left(\frac{2D^j}{\Delta x^2} + \Sigma_T^j\right)\phi_k^i + S_k^j \end{aligned} \tag{A-17}$$

Equation (A-17) is solved for the flux at the point k + 1.

$$\phi_{k+1}^j = \frac{\left(\frac{2D^j}{\Delta x^2} + \Sigma_T^j\right)}{\frac{D^j}{\Delta x^2}\left(1 + \frac{G\Delta x}{2x_k}\right)}\phi_k^j - \frac{\left(1 - \frac{G\Delta x}{2x_k}\right)}{\left(1 + \frac{G\Delta x}{2x_k}\right)}\phi_{k-1}^j - \frac{S_k^j}{\frac{D^j}{2x_k}\left(1 + \frac{G\Delta x}{2x_k}\right)} \tag{A-18}$$

Defining the quantities a_k^j, b_k^j and c_k^j by analogy, (A-18) is rewritten as

$$\phi_{k+1}^j = a_k^j \phi_k^j - b_k^j \phi_{k-1}^j - c_k^j \tag{A-19}$$

To invert the matrix defined by (A-19), an induction formula is assumed.

$$\phi_k^j = \frac{\phi_{k+1}^j + A_k^j}{B_{k+1}^j} \tag{A-20}$$

Inserting this assumption into (A-19) and solving for ϕ_k^j gives

$$\phi_k^j = \phi_{k+1}^j + \frac{\left(c_k^j + b_k^j \dfrac{A_k^j - 1}{Bk}\right)}{a_k^j - \dfrac{b_k^j}{B_k^j}} \tag{A-21}$$

which establishes the relationship between the A_k's and B_k's.

$$A_k^j = c_k^j + b_k^j \frac{A_{k-1}^j}{B_k^j} \tag{A-22a}$$

$$B_{k+1}^j = a_k^j - \frac{b_k^j}{B_k^j} \tag{A-22b}$$

A.7. Difference Equations at an Interface

At an interface between two regions of different properties, the boundary conditions of diffusion theory (A-2a,b) must be satisfied. In the subsequent development let primed quantities denote properties to the right of the interface and unprimed quantities denote properties to the left of the interface.

To solve this problem, assume that the interface is centered at the point x_k and write the diffusion equation for the left hand region using central differences and define a ficticious value of the flux at the point x_{k+1} in terms of the properties of the left hand region. Let superscript f additionally identify the point at x_{k+1}

$$\phi_{k+1}^{j\,f} = a_k^j \phi_k^j - b_k^j \phi_{k-1}^j - c_k^j \tag{A-23}$$

Following the same procedure for the region to the right of the interface and defining a fictional flux at the point X_{k-1} yields

$$\phi_{k+1}^{j\prime} = a_k^{j\prime} \phi_k^{j\prime} - b_k^{j\prime} \phi_{k-1}^{j\prime f} - c_k^{j\prime} \tag{A-24}$$

In difference form, the boundary conditions at the interface are written as

$$\phi_k^j = \phi_k^{j'} \tag{A-25a}$$

$$\frac{D^j}{2\Delta x}\left[\phi_{k+1}^{j\,f} - \phi_{k-1}^{j}\right] = \frac{D^{j'}}{2\Delta x'}\left[\phi_{k+1}^{j'} - \phi_{k-1}^{j'\,f}\right] \tag{A-25b}$$

Using (A-21) and (A-22a,b), the bracketed term on the left hand side of (A-25b) can be rewritten as

$$\phi_{k+1}^{j\,f} - \phi_{k-1}^{j} = \left[a_k^j - \frac{(1+b_k^j)}{B_k^j}\right]\phi_k^j - \left[c_k^j + \frac{(1+b_k^j)\,A_{k-1}^j}{B_k^j}\right] \tag{A-26a}$$

and the bracketed term on the right hand side as

$$\phi_{k+1}^{j'} - \phi_{k-1}^{j'\,f} = \frac{(1+b_k^{j'})}{b_k^{j'}}\,\phi_{k+1}^{j'} - \frac{a_k^{j'}}{b_k^{j'}}\,\phi_k^{j'} + \frac{c_k^{j'}}{b_k^{j'}} \tag{A-26b}$$

Requiring flux continuity at the interface, inserting (A-26a) and (A-26b) into (A-25b), and solving for the flux at the interface gives

$$\phi_k^j = \frac{\phi_{k+1}^{j'} + A_k^j}{B_{k+1}^j} \tag{A-27}$$

where

$$A_k^j = \frac{c_k^{j'}}{1+b_k^{j'}} + \frac{D^j}{D^{j'}}\,\frac{\Delta x'}{\Delta x}\,\frac{b_k^{j'}}{(1+b_k^{j'})}\left[c_k^j + \frac{(1+b_k^j)\,A_{k-1}^j}{B_k^j}\right] \tag{A-28a}$$

$$B_{k+1}^j = \frac{a_k^{j'}}{(1+b_k^{j'})} + \frac{D^j}{D^{j'}}\,\frac{\Delta x'}{\Delta x}\,\frac{b_k^{j'}}{(1+b_k^{j'})}\left[a_k^j - \frac{1+b_k^j}{B_k^j}\right] \tag{A-28b}$$

The particularly advantageous feature of (A-27) and (A-28) is the

preservation of the recursion formula defined in (A-20) and (A-22).

A.8. Derivation of the Difference Equations at the Origin

Two boundary conditions can be specified at the origin - either zero flux or zero current. The zero flux assumption neglects the effect of extrapolation distance but introduces negligible error, particularly when considering the uncertainties later introduced through the heat transfer correlations. These two boundary conditions at $x = o$, denoted in the difference notation by $K = 1$, are

$$\phi_1^j = 0 \qquad \text{(zero flux)} \tag{A-29a}$$

$$\phi_1^j = 0 \qquad \text{(zero current)} \tag{A-29b}$$

Evaluating the condition of zero flux first, equation (A-20) is used and K is set equal to 2.

$$\phi_2^j = \frac{\phi_3^j + A_2^j}{B_3^j} \tag{A-30}$$

Setting $K = 2$ in (A-19) and remembering that $\phi_1^j = 0$ yields

$$\phi_3^j = a_2^j \phi_2^j - c_2^j \tag{A-31}$$

which can be rewritten as

$$\phi_2^j = \frac{\phi_3^j + c_2^j}{a_2^j} \tag{A-32}$$

Thus, the recursion factors A_2^j and B_3^j are defined.

$$A_2^j = c_2^j \tag{A-33a}$$

$$B_3^j = a_2^j \tag{A-33b}$$

The condition of zero current is not as direct. To determine the finite difference representation, a neutron balance equation has to be written. The cylindrical geometry introduces slightly more complexity than plane geometry, so the boundary formulation will be developed for this geometry, and then generalized to include both plane and cylindrical geometry through the use of the geometry function G.

The net number of neutrons that result from production and removal per unit time over the circular area of radius x/2 and unit height is

$$\text{Production} - \text{Removal} = 2\pi\int_0^{\Delta x/2} \left[S_1^j - \Sigma_T^j \ \phi_1^j \right] r \, dr \qquad \text{(A-34)}$$

The net number of neutrons diffusing out of this volume is determined by the current at $\Delta x/2$ multiplied by the cylindrical area. This, then, yields

$$\text{Leakage} = -2\pi \ (\Delta x/2) \ D^j \nabla \phi^j_{3/2} \qquad \text{(A-35)}$$

The conservation equation is, in steady state,

$$0 = \text{Production} - \text{Removal} - \text{Leakage}$$

or, in mathematical terms,

$$0 = \int_0^{\Delta x/2} \left[S_1^j - \Sigma_T^j \ \phi_1^j \right] r \ dr + \frac{\Delta x}{2} \ D^j \nabla \phi^j_{3/2} \qquad \text{(A-36)}$$

In the integrations of equations (A-34) or (A-36), the source and flux are assumed to be constant over the range from 0 to $\Delta x/2$. To calculate the flux gradient at $\Delta x/2$, the flux is first expanded in a Taylor series about some point x_0.

$$\phi^j(x) = \phi^j(x_o) + \phi^{j\prime}(x_o)(x - x_o) + 1/2\, \phi^{j\prime\prime}(x_o)(x-x_o)^2 + .. \quad \text{(A-37)}$$

where primes denote differentiation with respect to k. Setting x_o = $\Delta x/2$ corresponding to index 3/2 and evaluating the flux at $x = \Delta x$ (K=2) and $x = 0$ (K=1), the gradient at the half space can be evaluated.

$$\phi^j_2 = \phi^j_{3/2} + \frac{\Delta x}{2} \phi^{j\prime}_{3/2} + \frac{\Delta x^2}{8} \phi^{j\prime\prime}_{3/2} + \cdots \quad \text{(A-38a)}$$

$$\phi^j_1 = \phi^j_{3/2} - \frac{\Delta x}{2} \phi^{j\prime}_{3/2} + \frac{\Delta x^2}{8} \phi^{j\prime\prime}_{3/2} + \cdots \quad \text{(A-38b)}$$

Subtracting (A-38b) from (A-38a) gives

$$\nabla \phi^j_{3/2} = \phi^{j\prime}_{3/2} = \frac{\phi^j_2 - \phi^j_1}{\Delta x} \quad \text{(A-39)}$$

which is valid through second order terms. Equation (A-39) could have been derived directly by taking central differences about the point $x = \Delta x/2$, but this would not have demonstrated the second order validity.

Integrating (A-36) and using (A-39) gives

$$0 = \frac{\Delta x^2}{8} \left[S^j_1 - \Sigma^j_T \phi^j_1 \right] + \frac{D^j}{2} \left[\phi^j_2 - \phi^j_1 \right] \quad \text{(A-40)}$$

which can be solved for ϕ^j_1.

$$\phi^j_1 = \frac{\phi^j_2 + \dfrac{\Delta x^2 S^j_1}{4}}{1 + \dfrac{\Sigma^j_T \Delta x^2}{4 D^j}} \quad \text{(A-41)}$$

Equation (A-41) is valid for cylindrical geometry only, but can be generalized to both plane or cylindrical geometry by incorporating the definition of G

$$\phi_1^j = \frac{\phi_2^j + \dfrac{\Delta x^2 S_1^j}{2(1+G)}}{1 + \dfrac{\sum_T^j \Delta x^2}{2(1+G)D^j}} \tag{A-42}$$

Again, the identity with (A-20) appears and the appropriate recursion coefficients can be defined.

$$A_1^j = \frac{\Delta x^2 \; S_1^j}{2\;(1+G)} \tag{A-43a}$$

$$B_2^j = 1 + \frac{\sum_T^j \Delta x^2}{2\;(1+G)\;D^j} \tag{A-43b}$$

The use of equations (A-33a,b) and (A-43a,b) permits definition of all recursion coefficients of higher index.

A.9. Derivation of the Difference Equations at the Periphery

Again, as with the conditions at the origin, two options are available - zero flux and zero current. Let m denote the index corresponding to the edge of system under consideration.

The trivial solution for the case of zero flux is simply

$$\phi_m^j = 0 \tag{A-44}$$

For the condition of zero current at the edge, a Taylor series expansion is made for the flux in terms of the flux at the edge of x_m.

$$\phi^j(x) = \phi^j(x_m) + \phi^{j\prime}(x_m)\;(x-x_m) + 1/2\;\phi^{j\prime\prime}(x_m)\;(x-x_m)^2 + \ldots . \tag{A-45}$$

Evaluating this expression in difference symbolism for the point at $x = x_m - x$ (index m-1) and remembering that $\phi_m^j = 0$ gives

$$\phi_{m-1}^j = \phi_m^j + \frac{\Delta x^2}{2} \quad \phi_m^{j\prime\prime} + \ldots .. \tag{A-46}$$

through second order terms. Solving for $\phi_m^{j''}$,

$$\phi_m^{j''} = \frac{2}{\Delta x^2} \left(\phi_m^j - \phi_{m-1}^j\right) \tag{A-47}$$

The flux at m-1 can be eliminated from (A-47) using (A-20)

$$\phi_m^j = \frac{2}{\Delta x^2} \left[\frac{1 - B_m^j}{B_m^j}\right] \phi_m^j + \frac{2}{\Delta x^2} \frac{A_{m-1}^j}{B_m^j} \tag{A-48}$$

Writing the diffusion equation for the point at $x = x_m$

$$0 = D^j \phi_m^{j''} - \Sigma_T^j \phi_m^j + S_m^j \tag{A-49}$$

and substituting from (A-48) yields

$$0 = \frac{2D^j}{\Delta x^2} \left[\frac{1 - B_m^j}{B_m^j}\right] \phi_m^j + \frac{2\,D^j}{\Delta x^2} \frac{A_{m-1}^j}{B_m^j} - \Sigma_T^j \phi_m^j + S_m^j \tag{A-50}$$

Equation (A-50) can be solved for ϕ_m^j.

$$\phi_m^j = \frac{S_m^j + \dfrac{2\,D^j}{\Delta x^2} \dfrac{A_{m-1}^j}{B_m^j}}{\Sigma_T^j - \dfrac{2\,D^j}{\Delta x^2} \left[\dfrac{1 - B_m^j}{B_m^j}\right]} \tag{A-51}$$

A.10. Method of Defining the Two-Dimensional Flux and Power Distribution

Figure A.1, Reactor Subdivision, has given an indication of the method of attack that will be used to define the flux distribution. It involves homogenizing the constituents in each of the core subdivisions. By describing the flux distribution through the use of a one-dimensional formulation, corrected for the two-dimensional character by the yet to be defined leakage cross section Σ_ℓ^j, a marching type approach can be used.

The solution proceeds as follows. For the first time through the

nuclear calculations, the power distribution both within the core and across the fuel tubes is assumed to be constant. With this assumption the average coolant density in each of the different core subdivisions and the upper plenum is determined. This information then permits defining the macroscopic nuclear properties for cell regions 1 and 5 (Figure A.2) for all subdivisions. On subsequent iterations, the density variation is determined from an extrapolation of the previous calculated power distribution.

To proceed with the method, the radial region denoted by index 1 is considered. The calculation starts with axial region 2 and homogenizes the properties in this subdivision as defined by the cell properties determined by a cell producing power at a rate characteristic of the average rate for all cells in radial region 1, subject to the condition that the total power produced in the length defined by axial region 2 was determined by the previous power distribution calculation along this length. The cell region defined by this length is considered to be infinite and the homogenization is performed by calculating an equivalent diameter for the square cell, based on cross sectional area, and doing a radial flux calculation across the cell, subject to the conditions of zero current at the origin and edge of the cell. As a result of this flux calculation, the homogenized constituents of this region define the macroscopic properties for this larger reactor region.

After this homogenization is performed, the calculation steps to axial region 3 and the process is repeated until all the core subdivisions in radial region 1 have been homogenized. Then, an axial flux calculation in the z direction of Figure A.1 geometry in which the presence of the lower and upper plenums are included and the flux is set equal to zero at the

bottom and top of the reactor. As a result of this flux calculation, the fraction of the total power generated in each axial subdivision is determined by integrating equation (A-3). Letting P_A (I,J) be the integrated value of (A-3) over axial length J in radial region I, the fraction of power generated in axial zone J is

$$F_A(I,J) = \frac{P_A(I,J)}{\sum_{J=2}^{M_z-1} P_A(I,J)} \tag{A-52}$$

When the $F_A(I,J)$ is defined for all (I=1, J=2 → M_z - 1) subdivisions, the calculation steps to (I=2, J=2) and the subdivision homogenization and power fraction determination is repeated. Thus, the fractional power distribution is determined for all core subdivisions based upon the axial flux traverses.

After the distribution has been obtained for the outermost core radial region, the homogenized properties at the core midplane for each of the radial regions plus the properties of the radial reflector are used to determine the radial flux and power distribution across the reactor. For this case, the boundary conditions are zero current at the origin and zero flux at the edge. When the flux distribution has been determined across the core, the power distribution is again obtainable from (A-3).

Denote the fraction of the total power that is contributed by each of radial core zones as $F_R(I)$, where

$$F_R(I) = \frac{P_R(I)}{\sum_{I=1}^{M_R-1} P_R(I)} \tag{A-53}$$

Using this definition, a two-dimensional histogram can be obtained by

multiplying (A-52) and (A-53) to obtain the fraction of reactor power that is produced in each core subdivision.

Each cell within a given radial zone is assumed to be producing power at a constant rate. Let A_c be the cross sectional area of a cell and $A(I)$ be area of radial zone I. Then the power produced in an axial length, denoted by J, by an "average" cell in radial zone I is

$$Q\ (I,J) = \left[\frac{A_c\ F_R(I)\ F_A(I,J)}{A(I)} \right] P_R \tag{A-54}$$

where the non-indexed symbol P_R is the reactor power generation rate.

A.11. Homogenization of Cell Properties

The square section of a typical cell is replaced by an equivalent diameter as noted in Figure A.2. This permits formulating the necessary difference equations in terms of a one-dimensional model.

To obtain a representative set of nuclear cross-section values which will characterize the processes occurring within a cell, the cross sections for the different regions are averaged with the integrated flux and volume. Thus, the homogenized cross sections are determined by the reaction rates which are taking place in each of the cell regions

$$\overline{\Sigma} = \frac{\int \Sigma \phi^j dV}{\int \phi^j dV} \tag{A-55}$$

Equation (A-55) is valid for fission, absorption and scattering cross sections.

The determination of a homogenized diffusion coefficient for the cell is more uncertain. If one starts with a homogeneous mixture of material,

the energy dependent but spatially independent diffusion coefficient for the mixture be defined by mathematical models, which are generally accepted. However, starting with a heterogeneous mixture, the method of determining a diffusion coefficient is not so well understood and at the present time is under experimental and analytical investigation.[5]

In the context of diffusion theory as used in this analysis, a relative simple approach can be taken. The errors generated in this approach are caused by the shortcomings of diffusion theory, particularly in the case of heavily loaded cells. Diffusion theory relates the diffusion coefficient of a homogeneous assemblage of isotopes to their transport cross section by[6]

$$\frac{1}{D^j} = 3 \sum_i \left[\Sigma^j_{tri} \right] \tag{A-56}$$

where i denotes the ith isotope in the mixture. The isotopic transport cross section is given by

$$\Sigma^j_{tri} = (\Sigma^j_{ai} + \Sigma^j_{si}) (1 - \bar{\mu}_{oi}) \left[1 - \frac{4}{5} \frac{\Sigma^j_{ai}}{(\Sigma^j_{ai} + \Sigma^j_{si})} + \frac{\Sigma^j_{ai}}{(\Sigma^j_{ai} + \Sigma^j_{si})} \frac{\bar{\mu}_{oi}}{(1 - \bar{\mu}_{oi})} + \dots \right] \tag{A-57}$$

where $\bar{\mu}_{oi}$ is average cosine of the scattering angle in the laboratory system of coordinates and Σ^j_{si} is the scattering cross section.

The isotopic microscopic transport cross section of each constituent is determined by defining the density of that constituent based upon the total cell volume. Using this density, the energy dependent absorption cross section is defined from an appropriate set of spatially independent

flux equations. The constituent density is determined by not only weighting with the ratio of regional volume to total cell volume, but also by a flux utilization factor. In other words, the density is flux and volume weighted, but the flux is not known so a guess must be made regarding its level in each of the cell regions for the two energy groups.

Knowing the values of the constituent density and the scattering and absorption cross sections, the flux-volume weighted isotopic transport cross section can be determined from (A-57). The volume representative diffusion coefficient of the cell can be obtained from (A-56) by summing over all the constituents of the cell.

Using (A-56), the diffusion coefficient for each region in the cell can also be obtained. If the other cross sections for each region are known, equation (A-12) can be solved for the flux distribution, subject to zero current at the origin and periphery of the cell, to yield a new set of flux levels for each of the regions. Based upon the new flux levels, a new set of constituent densities is obtained for the isotopic and the spectral dependent cross sections can again be calculated, including the transport cross section and the diffusion coefficient for the total cell assembly. This is a reiteration process.

To simplify the determination of the diffusion coefficient for the cell, the iterations have been stopped after the second trial. Thus, the representative densities are calculated across the cell, and the energy dependent cross sections are calculated. The macroscopic cross sections and diffusion coefficients for each region are determined, and (A-12) is solved. To determine the spatially representative cell diffusion coefficient, the microscopic transport cross section of each

isotopic constituent is assumed to remain constant but the flux-volume weighted density changes due to any change in the regional flux level. Under these conditions, a new average transport cross section is obtained for the cell by weighting in (A-55).

$$\overline{\Sigma}^{j}_{tr} = \frac{\int \Sigma^{j}_{tr} \; \phi^{j} dV}{\int \phi^{j} \, dV} \tag{A-58}$$

In terms of the average and regional diffusion coefficients, equation (A-58) can be written as

$$\overline{D^{j}} = \frac{\int \phi^{j} \, dV}{\int \frac{1}{D^{j}} \; \phi^{j} dV} \tag{A-59}$$

A.12. Calculation of the Radial Leakage Cross Section

Explicitly included in equation (A-54) is the assumption that the power distribution within each subdivision of the core is proportional to the product of the axial flux distribution in a given radial region and the radial flux distribution across the core. Then, designating the axial flux level at some point k in radial region I by the notation $\phi^{j}_{A^k}$ (I) and the radial flux level at some point m by the notation $\phi^{j}_{R^m}$, the two-dimensional variation of the flux in radial region I is given by

$$\phi^{j}_{m,k} = \phi^{j}_{Rm} \quad \phi^{j}_{Ak} (I) \tag{A-60}$$

To preclude distortion between the different radial regions, the axial flux is integrated over the reactor height such that

$$\int \phi^{j}_{Ak} (I) \; dz = 1 \tag{A-61}$$

Thus in equation (A-60), the term ϕ_{Ak}^{j} (I) is a shape factor for the axial variation and the magnitude is determined by ϕ_{Rm}^{j}. The variation of ϕ_{Rm}^{j} for different energy groups j determines the coupling between the groups in $\phi_{m,k}^{j}$.

The determination of ϕ_{Ak}^{j} (I) in (A-12) involves a calculation over the height of the reactor which must simultaneously include the effect of the radial flow of neutron across the core at different heights and the influence this radial flow exerts on the shape of the axial flux distribution. For instance, in radial region I = 3 and axial region J = 3, there can be a net gain or loss of neutrons in the radial direction to region (I = 2, J = 3) or to region (I = 4, J = 3). The problem is to formulate a cross section for region (I = 3, J = 3) which will account for this radial flow and by which the flow can be represented by the product of this cross section with the flux level in region (3,3). This is the previously denoted leakage cross section Σ_{ℓ}^{j}.

To make the analysis easier to follow and to simplify the notation, attention is first focussed on a particular subdivision of the core. Arbitrarily, radial region I = 3 and axial region J = 3 is chosen. It is assumed that radial region I = 4 is also in the core. Let primed quantities denote values to the right of an interface and unprimed quantities to the left of an interface.

Since one of the boundary conditions on the solution of the diffusion equation is that the current is continuous at an interface, its value can be calculated on either the right or left side of that interface. Using diffusion theory and the definition of current, the following expression is valid.

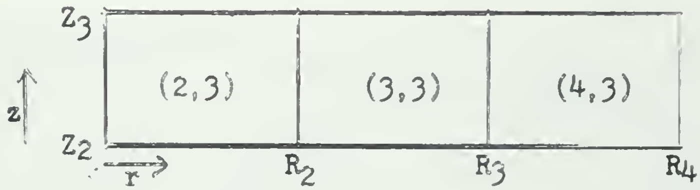

GEOMETRICAL DEFINITIONS FOR DETERMINING LEAKAGE CROSS SECTION AT (I=3, J=3)

Figure A.3

Net number of neutrons diffusing from region (3,3) to (2,3) per unit time $= 2\pi R_2 D^j(2,3) \int_{Z_1}^{Z_2} \left[\frac{\partial}{\partial r} \phi_2^j(z) \Big|_{r=R_2} \right] dz$ (A-62)

where $D^j(2,3)$ is the homogenized diffusion for radial region I = 2 and J = 3 and energy group j and $\phi_2^j(z)$ is the continuous counterpart of discrete flux distribution defined in (A-61). Since the flux has been written as the product of two terms, the integration in (A-62) can be reduced to

$$\int_{Z_1}^{Z_2} \left[\frac{\partial}{\partial r} \phi_2^j(z) \Big|_{r=R_2} \right] dz = \left[\frac{\partial}{\partial r} \phi_R^j(r) \Big|_{r=R_2} \right] \int_{Z_1}^{Z_2} \phi_{A2}^j(z)\, dz \qquad \text{(A-63)}$$

In simplified notation and using the result of (A-63), the following relationships can be written.

Net number of neutrons diffusing from region (3,3) to (2,3) per unit time $= 2\pi R_2 D^j(2,3) \frac{\partial}{\partial r}\phi_R^j(R_2) \int_{Z_1}^{Z_2} \phi_{A2}^j(z)dz$ (A-64)

$$= 2\pi R_2 D^j(3,3) \frac{\partial}{\partial r}\phi_R^j(R_2) \int_{Z_1}^{Z_2} \phi_{A3}^j(z)dz \qquad \text{(A-65)}$$

Net number of neutrons diffusing from region (3,3) to (4,3) per unit time $= - 2\pi R_3 D^j(3,3) \frac{\partial}{\partial r}\phi^j_R(R_3) \int_{Z_1}^{Z_2} \phi^j_{A3}(z)dz$ (A-66)

$$= - 2\pi R_3 D^j(4,3) \frac{\partial}{\partial r}\phi^j_R(R_3) \int_{Z_1}^{Z_2} \phi^j_{A4}(z)dz \tag{A-67}$$

If the assumption of a product type representation of the flux was exact within diffusion theory, the results of (A-64) and (A-65) would be equal and the results of (A-66) would equal those of (A-67). These conditions of equality are not obtained since the flux representation is only approximate. As an averaging correction to this discrepancy, the following assumption is used.

Net number of neutrons diffusing from region (3,3) to (2,3) per unit time $= \frac{1}{2}\left[(A-64) + (A-65)\right]$

Net number of neutrons diffusing from region (3,3) to (4,3) per unit time $= \frac{1}{2}\left[(A-66) + (A-67)\right]$

Writing these expressions in mathematical terms and finding the total diffusion away from region (3,3) in the radial direction gives

Net number of neutrons diffusing radially from (3,3) per unit time $= \pi\Big\{ R_2 D^j(2,3) \frac{\partial}{\partial r}\phi^j_R(R_2) \int_{Z_1}^{Z_2} \phi^j_{A2}(z)dz$ (A-68)

$$+ D^j_A(3,3)\left[R_2 \frac{\partial}{\partial r}\phi^j_R(R_2) + R_3 \frac{\partial}{\partial r}\phi^j_R(R_3)\right]\int_{Z_1}^{Z_2} \phi^j_{A3}(z)dz$$

$$- R_3 D^j_A(4,3) \frac{\partial}{\partial r}\phi^j_R(R_3) \int_{Z_1}^{Z_2} \phi^j_{A4}(z)dz \Big\}$$

Introducing the quantity $\Sigma_{\ell}^{j}(3,3)$, the number of neutrons which are lost from region (3,3) to regions (2,3) or (4,3) is defined by

$$\begin{array}{l}\text{Number of neutrons diffusing} \\ \text{radially from (3,3) per} \\ \text{unit time}\end{array} = \int_{Z_2}^{Z_3} \int_{R_2}^{R_3} 2\pi\Sigma_{\ell}^{j}(2,3)\phi_R^j(r)\phi_{A3}^j(z)rdrdz$$

$$= 2\pi\Sigma_{\ell}^{j}(3,3)\int_{Z_2}^{Z_3} \phi_{A3}^j(z)dz \int_{R_2}^{R_3} \phi_R^j(r)\, rdr \tag{A-69}$$

Equating (A-68) and (A-69) and solving for $\Sigma_{\ell}^{j}(3,3)$ gives

$$\Sigma_{\ell}^{j}(3,3) = \frac{\text{Right hand side of (A-68)}}{2\pi\int_{Z_2}^{Z_3} \phi_{A3}^j(z)\, dz \int_{R_2}^{R_3} \phi_R^j(r)rdr} \tag{A-70}$$

The right hand side of equation (A-68) can take several forms depending upon how many radial regions the core has been divided into and at which radial position the calculation is being performed. To generalize (A-68) replaces the radial index 2 by I-1, radial index 3 by I, radial index 4 by I + 1 and axial index 3 by J. If index I is greater than 1 and is bounded on the right by another core region, equation (A-68) is written, with only the indices replaced.

$$\Sigma_{\ell}^{j}(I,J) = \frac{\left\{ \begin{array}{l} R_{I-1}\, D^j(I-1,J)\frac{\partial}{\partial r}\phi_R^j(R_{I-1}) \int_{Z_{J-1}}^{Z_J} \phi_{AI-1}^j(z)dz \\ + D_A^j(I,J)\left[R_{I-1}\frac{\partial}{\partial r}\phi_R^j(R_{I-1}) - R_I\frac{\partial}{\partial r}\phi_R^j(R_I)\right]\int_{Z_{J-1}}^{Z_J}\phi_{AI}^j(z)dz \\ - R_I\, D_A^j(I+1,J)\frac{\partial}{\partial r}\phi_R^j(R_I)\int_{Z_{J-1}}^{Z_J}\phi_{AI+1}^j(z)dz \end{array}\right\}}{2\int_{Z_{J-1}}^{Z_J}\phi_{AI}^j(z)\, dz \int_{R_{I-1}}^{R_I}\phi_R^j(r)\, rdr} \tag{A-71}$$

If radial region I is greater than 1 but index I + 1 corresponds to the radial reflector, the form of equation (A-66) is used but there is no averaging with (A-67) since no axial flux calculation is done in the radial reflector. The resulting formulation is

$$\Sigma_{\ell}^{j}(I,J) = \frac{\left\{ R_{I-1}\, D_A^j(I-1,J) \frac{\partial}{\partial r} \phi_R^j(R_{I-1}) \int_{Z_{J-1}}^{Z_J} \phi_{AI-1}^j(z)dz + D_A^j(I,J)\left[R_{I-1} \frac{\partial}{\partial r} \phi_R^j(R_{I-1}) - 2\, R_I \frac{\partial}{\partial r} \phi_R^j(R_I)\right] \int_{Z_{J-1}}^{Z_J} \phi_{AI}^j(z)dz \right\}}{2 \int_{Z_{J-1}}^{Z_J} \phi_{AI}^j(z)dz \int_{R_{I-1}}^{R_I} \phi_R^j(r)\, r\, dr} \tag{A-72}$$

When I=1 and the region I = 2 is part of the core, the leakage cross section becomes

$$\Sigma_{\ell}^{j}(1,J) = \frac{R_1 \left\{ D_A^j(1,J) \frac{\partial}{\partial r} \phi_R^j(R_1) \int_{Z_{J-1}}^{Z_J} \phi_{A1}^j(z)dz + D_A^j(2,J) \frac{\partial}{\partial r} \phi_R^j(R_2) \int_{Z_{J-1}}^{Z_J} \phi_{A2}^j(z)dz \right\}}{2 \int_{Z_{J-1}}^{Z_J} \phi_{A1}^j(z)\, dz \int_0^{R_1} \phi_R^j(r)\, r\, dr} \tag{A-73}$$

If I=1, and I=2 corresponds to the radial reflector, the leakage cross section becomes independent of the axial flux distribution and is given by

$$\Sigma_{\ell}^{j}(1,J) = \frac{R_1\, D^j(1,J) \frac{\partial}{\partial r} \phi_R^j(R_1)}{\int_0^{R_1} \phi_R^j(r)\, r\, dr} \tag{A-74}$$

This last equation provides the simplest and least satisfying result. It demonstrates the error involved by assuming a product type solution for the flux distribution.

The transverse leakage perpendicular to a one-dimensional flux calculation is frequently denoted by the term $D^j B_R^{2j}$, where B_R^{2j} denotes the "buckling" of the system. Based on this definition, it is possible to define a radial regional "buckling" within the core as

$$B_R^{2j}(I,J) = \frac{\Sigma_\ell^j(I,J)}{D^j(I,J)} \tag{A-75}$$

For the condition that $\Sigma_\ell^j(I,J)$ is negative, based on the appropriate equation, the physical interpretation is that more neutrons are crossing into region (I,J) from regions (I-1,J) and (I + 1,J) than are leaving. For this case, the leakage is negative and $^i(I,J)$ is treated as a source term and leads to the definitions of equation (A-16). On the other hand, when $\Sigma_\ell^j(I,J)$ is positive, the leakage is truly acting as a neutron absorber and equations (A-15) are used.

The integrations and differentiations designated in this section have been described in terms of continuous functions. The solution for the flux has been defined in terms of discrete values, so these integrations and differentiations are numerical. Differentiations to the left of an interface is done by backward difference equations and to the right by forward differences.

A.13. Calculation of the Axial Leakage Cross Sections

For the condition of axial leakage when performing the radial flux calculation across the core and reflector mid-plane, the leakage cross section has been defined in terms of the so-called system "buckling B_A^2," and the diffusion coefficient $D^j(I)$ of the mid-plane.

The fast group axial buckling for all the radial regions has been defined in terms of the geometrical height of the reactor. Thus

$$B_A^{2F}(I) = \frac{\pi^2}{(\text{Reactor Height})^2} \qquad \text{(A-76)}$$

In terms of a leakage cross section,

$$\Sigma_\ell^F(I) = D^F(I)\, B_A^{2F}(I) \qquad \text{(A-77)}$$

This leakage cross section is always positive, so equations (A-15) are used. Note that the only variation of $\Sigma_\ell^F(I)$ occurs through variation of the diffusion coefficient $D^F(I)$ across the reactor.

For neutrons in the thermal group, the axial buckling for the core regions is described in terms of the reactor height H_r and the lower and upper plenum properties which define a "reflector savings". For the case of water in the upper and lower plenums, the thermal diffusion length is relatively small compared to the plenum thicknesses so that from the nuclear viewpoint the plenums are essentially infinitely thick for thermal neutrons.

The reflectors savings δ^T for this condition is defined from[6]

$$\delta^T \approx \frac{D_c^T}{\sqrt{D_r^T\, \Sigma_{ar}^T}} \qquad \text{(A-78)}$$

where subscript c denotes the core and subscript r denotes the reflector. Equation (A-78) is written for the same reflector properties on both sides of the core. For the condition at hand, the properties of the two plenums are quite different because of the change in density of the water coolant. To account for this, the thermal savings δ^T is approximated as follows, remembering that the index $J = 1$ refers to the lower plenum and $J = M_z$ refers to the upper plenum.

$$\zeta^T(I) \approx \frac{D^T(I)}{2}\left[\frac{1}{\sqrt{D^T(I,1)\Sigma_a^T(I,1)}} + \frac{1}{\sqrt{D^T(I,M_z)\Sigma_a^T(I,J)}}\right] \quad (A\text{-}79)$$

With this definition, the axial buckling for the thermal group is determined from

$$B_A^{2T}(I) = \frac{\pi^2}{(H_r + 2\zeta^T(I))^2} \quad (A\text{-}80)$$

The cross section for the axial leakage when the radial flux calculation is performed then is defined by

$$\Sigma_\ell^T(I) = D^T(I)\ B_A^{2T}(I) \quad (A\text{-}81)$$

Again, all values of $\Sigma_\ell^T(I)$ are positive, so equations (A-15) are used.

In the radial reflector, the buckling and leakage cross section for the thermal group are assumed to be equal to those for the fast group so that equations (A-76) and (A-77) define the thermal properties for this region.

The assumptions involved in equations (A-76) and (A-80) have been compared with more precise calculations. The method of this latter calculation followed the pattern established in the preceding section. This simply involved rotating the direction of calculation 90° from that in the preceding section and proceeded by determining the integrated flux in a radial region and the loss out the top and bottom faces of the reactor by integrating the currents out over these areas. The results of the two methods were sufficiently close to permit the use of equations (A-76) and (A-80), simpler formulations which take less computer calculation time.

A.14. Energy Dependent Cross Sections

The program has been formulated as a two-group problem. The mathematical treatment for a higher number of groups simply increases the number N appearing in (A-12), but does not change the methods discussed in all previous sections. The number of groups was selected as two to give a representative picture of the power distribution and at the same time to hold down the computation time; two groups are also necessary, in this latter connection, to keep computer storage requirements to a minimum, one problem associated with the MIT system tape for the IBM 7090 which limits the core storage available to the programmer to roughly 24.5K registers.

To determine the energy dependent isotopic microscopic cross sections of the cell constituents, the program GAM-1 was used.[7] The spatially homogenized densities of the constituents were obtained as discussed in the section "Homogenization of Subdivision Properties". GAM-1 provided the isotopic microscopic cross sections of the fast group $j = 1$ for fission, absorption, transport and downscattering and the number of neutrons produced per fission for fuel material. These microscopic cross sections were then used to define the macroscopic properties of the different cell regions (Figure A.2).

The thermal absorption and fission cross sections were obtained by averaging over a Wilkin's spectrum with the use of a program available at MIT known as THERMIT. The density inputs to this program were also determined by the method previously described. The absorption cross section for each of the isotopes were taken from BNL-325[8]; fission cross sections, in the case of fuel material, also came from this report. The individual scattering cross sections of the different isotopes were

assumed to be constant over the thermal range. The results of this calculation provided the thermal macroscopic properties of the different cell regions.

Within the core, the density of the coolant changes. This consequently changes the shape of the two flux spectrums determined in GAM-1 and THERMIT and also leads to an infinite number of combinations of cell constituent densities and cross sections. The approach taken in this study has been to define an average coolant density in the core by assuming a flat power distribution and a given reactor power level. Since all other physical densities within the cell are fixed, the cross sections applicable to a given reactor size, power, and inlet flow conditions are based on this mean coolant density. When the reactor power distribution is defined, the only spectral influence to the flux determination occurs through the variation of the coolant density and the resultant change in the macroscopic properties of cell regions 1 and 5. The microscopic cross sections are assumed not to change.

A.15. Evaluation of the Mean Chord Length for Resonance Absorption

The geometry of a fuel element influences the magnitude of the resonance absorption cross section of any fertile material, which is included in the element. In the energy range for resonance absorption, there is a strong selective absorption as the neutrons proceed into the fuel, away from the moderator. This decrease of the resonance energy flux reduces the effect of the resonance material within the fuel element. To account for this decrease in effectiveness, the effective resonance integral I_{eff} for a fuel element is often expressed in the form

$$I_{eff} = A + B\ (S/M) \tag{A-82}$$

where A and B are experimentally determined constants, dependent on the material structure of the element, and M and S are the mass enclosed within the surface and the surface area of the element, respectively. For a given density of the fuel material, the ratio of (M/S) represents a characteristic dimension of a solid fuel element.

When the fuel element is an annular cylinder surrounding a moderator, the calculation of the spectrum dependent resonance absorption cross section becomes more undefined. The manner of including the effect of the fuel element geometry is dependent not only on the physical dimensions of the fuel, but also on the properties of the enclosed moderator.

The method of determining the resonance cross section of the fertile material (U^{238}) has been through the use of the program GAM-1. The geometrical input, which characterizes the fuel element for the determination of the resonance absorption cross section, is the mean chord length $\bar{l}$ for a neutron transiting the fuel material. Although different methods have been proposed to account for the (S/M) ratio in a formulation defining I_{eff}, a search of the literature reveals no analytical representation defining the mean chord length $\bar{l}$. In lieu of a more refined analysis, the following simplified model is proposed.

Consider first the case of a neutron with energy in the resonance range which enters the fuel from the region exterior to the annular element. As seen in Figure A.4, a plane of symmetry can be defined longitudinally through the element, which passes through the center of the element and the point of entrance. Then, as indicated in the figure,

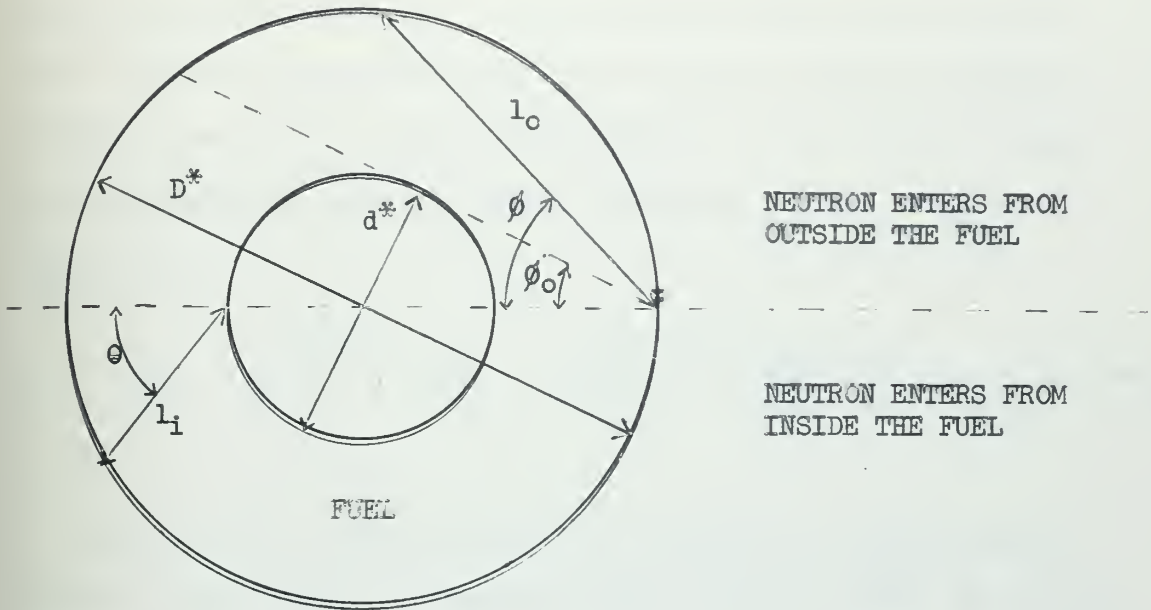

CHORD LENGTH GEOMETRY FOR AN ANNULAR FUEL ELEMENT

Figure A.4

---

the possible angular variation within one of the symmetrical regions of the direction than can be taken in traversing the fuel element is from 0° to 90°. Assuming that the distribution over these possible angles is constant, the probability that a neutron will enter the fuel element such that its angle of flight lies between ϕ and $\phi + d\phi$ is

$$p(\phi)\, d\phi = \frac{2\, d\phi}{\pi} \tag{A-83}$$

The length of the fuel material traversed (i.e., the chord length) before the neutron leaves the fuel region, either going to the moderator filled circular zone in the interior or the moderator zone on the outside, can be written in terms of the two diameters d^* and D^* and the angle of flight ϕ. When the inside diamter d^* has a value greater than zero, there is a discontinuity present in the magnitude of the chord length as ϕ

varies across the angle ϕ_o. Determining the chord length l_o for a given angle ϕ, the mean chord length in the fuel region is found by weighting the length at ϕ by the probability of the flight at angle ϕ, and integrating over all possible values of ϕ. The resultant expression is

$$\frac{\bar{l}_o}{D^*} = \frac{1}{\pi}\int_0^{\phi_o}\left[\cos\phi - \sqrt{\cos^2\phi - 1 + \frac{d^{*2}}{D^{*2}}}\right] d\phi + \frac{2}{\pi}\int_{\phi_o}^{\pi}\cos\phi \, d\phi \tag{A-84}$$

When (d^*/D^*) equals zero, the fuel element is a solid rod, and the mean chord length for outside entrance $(\bar{l}_o/D^*) = 2/\pi$. As (d^*/D^*) approaches unity, $(\bar{l}_o/D^*)$ goes to zero. For finite values of (d^*/D^*) less than unity, the first integral on the LHS of (A-84) cannot be evaluated in closed form.

When the flight path is from the inside moderator across the fuel element to the outside moderator region, a plane of symmetry can again be defined. The possible variation of the angle θ is from 0^o to 90^o and, if the distribution is assumed to be constant over this range, the probability that the angle of flight will lie between θ and $\theta + d\theta$ is given by

$$p(\theta)\, d\theta = \frac{2\, d\theta}{\pi} \tag{A-85}$$

The chord length l_i for some angle θ can be evaluated also in terms of d^* and D^*, and the mean chord length $\bar{l}_i$ is determined by weighting each possible length l_i with the probability for the occurrence of this length and integrating over the range of 0^o to 90^o. The geometrical determination for the chord length l_i is simpler in this case, since there

is no discontinuity caused by sweeping across a tangent boundary angle. For the case of inside entrance, the mean chord length is given by

$$\frac{\bar{l}_i}{D^*} = \frac{1}{\pi}\int_0^{\pi/2}\left[-x\cos\theta + \sqrt{x^2\cos^2\theta + 1 - x^2}\right]d\theta \tag{A-86}$$

where

$$x = (d^*/D^*) \tag{A-87}$$

In the limit of (d^*/D^*) going to zero, the value of $(\bar{l}_i/D^*)$ approaches $D^*/2$. As (d^*/D^*) goes to unity, the mean chord length $(\bar{l}_i/D^*)$ goes to zero.

For any given set of conditions, the mean chord length for a neutron transiting the fuel region is fixed. But as just seen, the calculated value of the geometrical length is dependent on whether the point of entry to the annular fuel region is from the interior or exterior moderator region. To resolve this difficulty, it is necessary to postulate a physical model which predicts the mean chord length for a resonance neutron entering the fuel from either moderator region.

Diffusion theory defines the resonance neutron current in the positive radial direction as

$$J^+ = \frac{\phi}{4} - \frac{D}{2}\frac{\partial\phi}{\partial r} \tag{A-88}$$

and in the negative radial direction as

$$J^- = \frac{\phi}{4} + \frac{D}{2}\frac{\partial\phi}{\partial r} \tag{A-89}$$

Denoting $J^+(d^*/2)$ as the outward directed current at the inside radius

of the fuel tube and $J^{-}(D^{*}/2)$ as the inwardly directed current at the outside radius of the fuel tube, the fraction of the total number of neutrons entering the fuel tube from the exterior moderator region is given by

$$\text{Fraction entering from the outside region } f_o = \frac{D^{*}J^{+}(D^{*}/2)}{D^{*}J^{+}(D^{*}/2) + d^{*}J^{+}(d^{*}/2)} \tag{A-90}$$

With this definition, the mean chord length can be written as

$$(\bar{l}/D^{*}) = f_o\ (\bar{l}_o/D^{*}) + f_i\ (\bar{l}_i/D^{*}) \tag{A-91}$$

where

$$f_i = 1.0 - f_o \tag{A-92}$$

Unfortunately, the current values have to be determined from the spatial distribution of the resonance flux. The flux distribution is dependent on the resonance cross section, which is the quantity that is ultimately to be determined after defining a mean chord length, so the problem is of an iterative nature.

If it is assumed that the current values at the inner and outer boundary are equal, the fraction of neutrons entering from the exterior moderator region is given simply by

$$f_o = \frac{1.0}{1.0 + (d^{*}/D^{*})} \tag{A-93}$$

This assumption postulates that the number of neutrons entering from either the exterior or interior moderator region is proportional only to the surface area of the outside or inside fuel material boundary.

As a first approximation, this assumption has intuitive appeal. The direction of the error which it introduces into the calculated chord length and resonance cross section can be demonstrated as follows. The boundary conditions for a radial plot of the resonance flux require that the flux have zero current at the origin (center of the enclosed moderator region) and at the edge of the exterior moderator region. Consider that the fast flux is constant across the cell, that the resonance source terms in the separated moderator regions are equal, and that there is no source term for resonance neutrons in the fuel region. All slowing down takes place in the moderator regions. The downscattering cross sections in the two moderator regions are assumed to be equal and represent the "absorption" cross sections for these regions. The resonance absorption cross section in the fuel is assumed to be larger than the moderator cross sections.

With this set of conditions, which represent the physical situation quite reasonably, it can be demonstrated that the current $J^{+}(d^{*}/2)$ is less than $J^{-}(D^{*}/2)$. This result shows that the value of f_o, as determined in (A-93) is too high. As previously shown, the value of $(\overline{I}_o/D^{*})$ is greater than $(\overline{I}_i/D^{*})$ when (d^{*}/D^{*}) is zero. Table A.1 indicates that $(\overline{I}_o/D^{*})$ is always greater than $(\overline{I}_i/D^{*})$ for all values of (d^{*}/D^{*}). The assumption of equal currents predicts a value of mean chord length, which is high. Thus, the calculated resonance absorption cross section will be low.

When defining the effective resonance integral I_{eff} for the condition of a hollow fuel element filled with a moderator, it has been suggested that all the material within the exterior fuel surface be homogenized. This procedure thus decreases the density of the resonance material by

Table A.1

MEAN CHORD LENGTH FOR AN ANNULAR FUEL ELEMENT AVERAGED BY EQUATION (A-93)

(d^*/D^*)	$(\bar{\lambda}_o/D^*)$	$(\bar{\lambda}_i/D^*)$	$(\bar{\lambda}/D^*)$
0.0	0.6366	0.5000	0.6366
0.1	0.6023	0.4669	0.5900
0.2	0.5629	0.4313	0.5410
0.3	0.5184	0.3931	0.4895
0.4	0.4685	0.3520	0.4352
0.5	0.4129	0.3080	0.3779
0.6	0.3510	0.2604	0.3170
0.7	0.2820	0.2087	0.2518
0.8	0.2044	0.1516	0.1809
0.9	0.1151	0.0865	0.1016
1.0	0.0000	0.0000	0.0000

considering it to be distributed over a larger volume. If at the same time, the chord length were calculated on the basis of a solid element, the net result would be to doubly decrease the magnitude of the resonance cross section.

By calculating the density of resonance absorbers, based on their actual physical density in the fuel element, and the chord length, as predicted by (A-91) and (-93), the two inputs for the resonance calculation cause opposite effects and tend to cancel. The determination of the final discrepancy would require a more exact analysis and is beyond the scope of this thesis.

A.16. Criticality Determination

Whether a given assembly of cells will sustain a nuclear chain reaction is determined from the results of the radial flux mapping across the mid-plane of the reactor. If the reactor under consideration is just critical with an effective multiplication factor k_{eff} of 1.0, then the

total neutron production within the reactor is equal to the total absorption plus leakage out of the top and bottom faces of the reactor. For values other than unity, k_{eff} is defined by the integrations across the ractor as

$$k_{eff} = \frac{\sum_{j=1}^{n} \int \nu^j \Sigma_f^j \; \phi^j \; dV}{\sum_{j=1}^{n} \int \left[\Sigma_a^j + \Sigma_\ell^j\right] \phi^j dV} \tag{A-94}$$

From an arbitrary value of k_{eff}, other than zero, the concentration of a poison distributed somewhere within the reactor is assumed and this concentration is added to the absorption cross section. Given an assumed value of the concentration and some desired k_{eff} the problem can be solved by trial-and-error to within specified limits of convergence to define the magnitude of the concentration.

With the method of calculation followed, how this "mathematical" poison is put in the reactor has a physical counterpart. For the case of a burnable poison, the intuitive approach is to load a cell region with the assumed poison. Most probably, the cell region containing the poison would be the solid moderator region. Through the homogenization of the cell properties to define the reactor subdivision properties, the effect of the poison enters. On the other hand, when synthesizing a ring of control rods around the reactor centerline, the approach would be to load the poison directly into the specified radial region and proceed with the calculation of (A-94).

A.17. Errors

The effect of initially assuming a two-dimensional rotationally symmetric characterization for the flux and nuclear properties would not

introduce appreciable error into the problem unless the reactor operator had, for some unforeseeable reason programmed the control rods to cause a large skewing of the flux or that the distribution of fuel around the centerline had considerable variation. The major error is introduced through the assumption of a product type flux representation.

This error becomes more severe as the corner regions of the core are approached. A true two-dimensional representation of the flux would show more peaking of the thermal flux in this region than as predicted by this model. This effect is brought more clearly by equation (A-74), which describes the radial flow of neutrons when mapping the flux in the axial direction for a one radial subdivision core. The exact magnitude of this error cannot be readily stated, since a program for comparing the model developed here with a two-dimensional model is not available. Any power peaking radially across the core is accentuated by this lack of correct representation, if the peak power is in the central region of the core. From the standpoint of conservatism, this limits the core performance and underestimates the ability of the core to provide a given power, subject to certain engineering constraints.

The energy produced per fission is assumed to be confined to the point at which the fission occurred. This neglects the effect of heating in the solid moderator region by slowing down and gamma heating and the effect of gamma heating in the reflector. This assumption places more stringent requirements on the coolant to remove heat from the fuel region. But it also imposes a requirement to remove heat from the moderator and reflector. The amount of energy involved for this requirement is of the

order of 10 - 15 Mev out of approximately 200 Mev recoverable from each fission that occurs. This assumption introduces an error in the calculated power distribution of approximately 6%.

The effect of axial flux streaming when homogenizing the constituents of a cell has also been neglected. More error is introduced for those regions in the neighborhood of the plenums than in the interior core regions. This is particularly true for the fast flux (group 1), which follows, more or less, the usual cosine representation. A two-dimensional description here would also furnish more exact knowledge than has been assumed by the purely one-dimensional method of homogenizing the different reactor subdivision cell properties.

Other errors have been mentioned throughout this Appendix, which arise as a result of the simplifications necessitated by the limitations of Section A.1.

A.18. Credits

The programming of certain of the mathematical equations was based on the previously written program AIM-5.[9] Those sections of the program CFR (Appendix G) of this thesis involved with the flux difference equations and their convergence were rewritten from AIM-5 to fit this problem.

APPENDIX B

FUEL TEMPERATURE PROFILES

B.1. Introduction

The wall temperatures of an annular nuclear fuel element are controlled by the local temperatures of the two counterflowing coolants surrounding the fuel element. The variation of the two coolant temperatures is determined by the amount of power that is produced in a given length of fuel element, the fraction of this power which goes to the coolant stream inside or outside the fuel element, and the transfer of heat across the fuel element between the coolant streams caused by their temperature difference.

The temperature gradients within the fuel and cladding material are much steeper in a direction perpendicular to the direction of coolant flow than in a direction parallel to it. The longitudinal temperature distribution is determined by the longitudinal variation of the cladding-coolant interface temperature and the variation of the heat generation rate.

Within a conducting region, the temperature distribution is determined by the Fourier heat conduction equation.

$$\left[\frac{\partial^2}{\partial r^2} + \frac{1}{r}\frac{\partial}{\partial r} + \frac{\partial^2}{\partial Z^2}\right] T(r,z) = -\frac{H(r,z)}{k} \qquad \text{(B-1)}$$

which has been written to indicate the case of a rotationally symmetric distribution assuming a constant value of thermal conductivity k. Rotational symmetry is a result of the definition of the flux distribution across a particular axial position of a cell.

Using the knowledge that the longitudinal gradients are not as

steep as the radial ones, equation (B-1) can be written in the form

$$\frac{1}{r}\,\frac{d}{dr}\left[r\,\frac{dT}{dr}(r,z)\right] = -\frac{H(z)\,f(r,z)}{k} \tag{B-2}$$

where $H(z)$ is the total heat production in a unit length of fuel element centered at axial position z and $f(r,z)$ is a normalized shape function for the radial distribution at height z. Equation (B-2) can be integrated to yield the expression

$$T(r,z) = C_1(z)\,\ln(r) + C_2(z) - H(z)\,C_3\,(r,z) \tag{B-3}$$

The radial "constants" C_1 and C_2 are evaluated by the appropriate boundary conditions specified by the coolant temperatures or heat fluxes. C_3 is found by performing the mathematical operations indicated in (B-2) on the shape factor $f(r,z)$.

To estimate the errors involved with the assumptions that are made in (B-3), consider the following numerical example. A solid fuel element of diameter 0.1 feet and thermal conductivity $k = 1.0$ Btu/hr/ft/$^{\circ}$F is assumed to be producing heat uniformly at the rate of 100.0 Btu/hr/ft of length. This heat is removed on the outside by a coolant flow of 10.0 lb/hr; the coolant is assumed to have a specific heat of 1.0 Btu/lb/$^{\circ}$F and to undergo no phase or flow pattern change, so the heat transfer coefficient at the fuel - coolant interface is constant.

Neglecting for the nonce the heat flow axially through the fuel element, the temperature rise of the coolant is found to be 10°F/ft. Since the heat transfer coefficient was assumed to be constant, this gradient also represents the axial temperature rise in the fuel elememt. From (B-3) the radial temperature rise from the fuel-coolant interface

to the centerline is approximately $8^{o}F$, which represents an average radial gradient of $160^{o}F/ft$. With these numbers, the amount of heat produced in a one-foot length that flows axially out along the fuel material is approximately 0.08%.

When a phase or flow pattern change occurs in the coolant, or the longitudinal variation of heat production changes in the fuel, a change occurs in the axial gradient. This variation does not introduce any appreciable error in the formulation (B-3). However, at the ends of the fuel material, a step change is made in the heat production rate (for a reactor with axial reflectors) and a local error is present. This error is confined to a relatively short segment of fuel material, approximately two diameters in length. For a reactor which has an upper and lower coolant plenum, which are adjacent to the ends of the fuel elements, the fuel temperature will be lower than those predicted by (B-3).

The spatial distribution of heat production across the fuel material is determined by equation (A-3), a one-dimensional representation which is assumed to be rotationally symmetric and found from the solution of the flux difference equations. The one-dimensional counterpart of (B-1) could also be written in terms of a difference equation by utilizing the discrete heat generation values at the different space mesh points. For the problem at hand, it is desirable to define the radial heat generation rate across the fuel in terms of a continuous function.

A polynomial has been chosen to represent the distribution of the heat generation rate. In order to reduce the order of the polynomial which is necessary, the discrete values of heat generation rate have been fitted by the method of least squares. This leads to a functional

relationship of the form

$$H(r,z) = H(z) \sum_{i=1}^{n} a_i(z)\, r^{i-1} \qquad (B-4)$$

in which $H(z)$ is heat produced per unit length and per unit time in the fuel material and the coefficients $a_i(z)$ in conjunction with the distance r define the shape of the power distribution radially across the fuel. The coefficients $a_i(z)$ are normalized such that

$$2\pi \int_{R_2}^{R_3} \left(\sum_{i=1}^{n} a_i r^{i-1} \right) r dr = 1 \qquad (B-5)$$

where R_2 and R_3 represent the geometrical limits of fuel material, as seen in Figure B.1.

One reason for formulating the heat generation distribution in this fashion is because of the trial-and-error method of solution necessary to define the coolant temperatures and hence the fuel temperature. From the preceding nuclear calculation the shape of the distribution is known. With the shape defined, it is possible to determine the fractional heat split across the fuel, i.e., the fraction of total heat produced that goes either to the inside or outside coolant. Keeping the shape factor constant, the problem can be reiterated until the fractional heat split does not change, within specified convergence limits. The change between these iterations then is only influenced by the variation of the coolant states and their associated heat transfer coefficients at the two cladding-coolant interfaces.

The second reason for formulating the heat generation shape distribution in this manner is to reduce the necessary computational time. When determining the coefficients $a_i(z)$ in equation (B-4), the following

set of n simultaneous linear equations are necessary in making the least square fit of the m points in the fuel.

$$\underline{X}\ \underline{A} = \underline{B} \tag{B-6}$$

$$x_{ij} = \sum_{k=1}^{m} r_k^{\,i+j-2} \tag{B-7a}$$

$$b_i = \sum_{k=1}^{m} P_k\, r_k^{\,i-1} \tag{B-7b}$$

The coefficients of $\underline{A}$ are the desired values of the fitted coefficients. Equation (B-6) can be inverted by a triangularization method similar to a Gauss-Jordan reduction.[2] This method is well-suited to computer programming techniques.

Once the distribution of heat generation across the fuel is known and the fraction of the total heat produced going to either of the two coolant streams is determined, the fuel temperature profile can be calculated using (B-3).

In defining the conduction equation, it has been tacitly assumed that the thermal conductivity k in each region is constant and has been determined such that it represents an average of the total regional variations.

Figure B1 shows the geometrical distances involved when calculating the temperature profile across the fuel. Cross-hatching at the interfaces indicates a temperature discontinuity represented by a heat transfer coefficient. Between the fuel and cladding, the temperature discontinuity is caused by gas accumulation and non-perfect contact between the two materials.

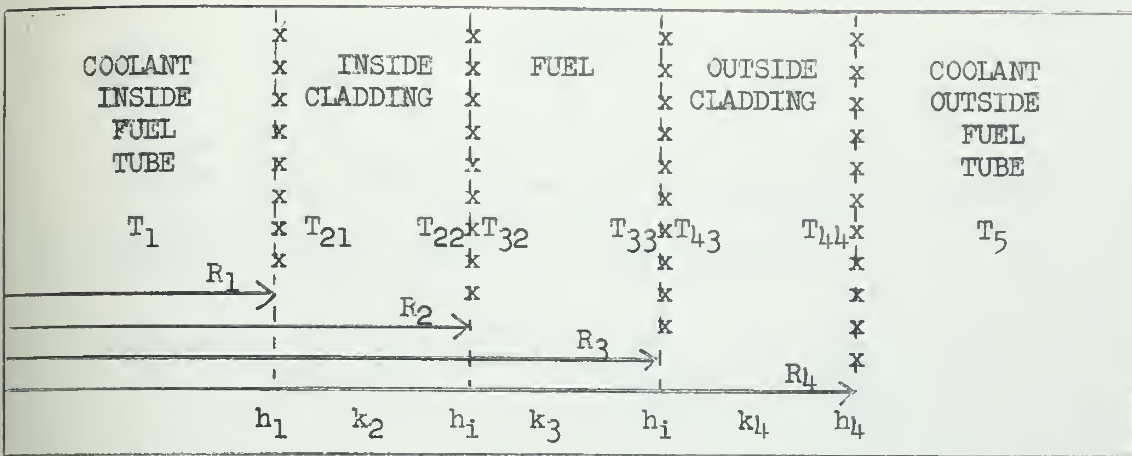

GEOMETRY FOR FUEL TEMPERATURE DETERMINATION

FIGURE B.1

B.2. Fuel Temperatures at the Cladding-Fuel Interfaces

Let Q_1 and Q_5 be the heat flowing per unit length and per unit time to the inside and outside coolant streams, respectively. Using the concept of thermal resistances, the temperature differences between fuel temperatures at the fuel-cladding interfaces can be written in terms of Q_1 and Q_5 and the heat transfer properties defined in Figure B.1 as

$$T_{32} - T_1 = \frac{Q_1}{2\pi}\left[\frac{1}{R_1h_1} + \frac{\ln(R_2/R_1)}{k_2} + \frac{1}{R_2h_i}\right] \tag{B-8a}$$

$$T_{33} - T_5 = \frac{Q_5}{2\pi}\left[\frac{1}{R_4h_4} + \frac{\ln(R_4/R_3)}{k_4} + \frac{1}{R_3h_i}\right] \tag{B-8b}$$

In equations (B-8), equivalent heat transfer coefficients can be written for the bracketed terms such that

$$\frac{1}{R_2h_2} = \frac{1}{R_1h_1} + \frac{\ln(R_2/R_1)}{k_2} + \frac{1}{R_2h_i} \tag{B-9a}$$

$$\frac{1}{R_3h_3} = \frac{1}{R_4h_4} + \frac{\ln(R_4/R_3)}{k_4} + \frac{1}{R_3h_i} \tag{B-9b}$$

At this point, define the temperature difference across the fuel material, a value needed in the next section.

$$T_{33} - T_{32} = (T_5 - T_1) + \frac{Q_5}{2\pi R_3h_3} - \frac{Q_1}{2\pi R_2h_2} \tag{B-10}$$

B.3. Determination of the Heat Flow Fraction

At some given height in the cell, the temperature distribution is defined in the fuel material by (B-3), where the quantity C_3 is determined from the polynomial representation in (B-4). When the mathematical operations have been performed, the fuel temperature $T_3(r)$ is given by

$$T_3(r) = C_1\ln(r) + C_2 - \frac{H}{k_3}\left[\sum_{i=1}^{n} \frac{a_i r^{i+1}}{(i+1)^2}\right] \tag{B-11}$$

To determine the fuel temperature, both C_1 and C_2 must be evaluated. For determining the fraction of heat going to the outer channel, only the integration constant C_1 needs to be evaluated. To find C_1, evaluate (B-10) at $r = R_3$ and $r = R_2$, take the difference of the two expressions and solve for C_1, yielding

$$C_1 = \frac{T_{33} - T_{32}}{\ln(R_3/R_2)} + \frac{H}{k_3\ln(R_3/R_2)} \sum_{i=1}^{n}\left[\frac{a_i}{(i+1)^2}\left(R_3^{i+1} - R_2^{i+1}\right)\right] \tag{B-12}$$

The quantity Q_5 can be evaluated as

$$Q_5 = -2 R_3 k_3 \pi \left.\frac{dT_3(r)}{dr}\right|_{r = R_3} \tag{B-13}$$

which permits writing C_1 in terms of Q_5.

$$C_1 = \frac{H}{k_3} \sum_{i=1}^{n} \left[\frac{a_i R_3^{\,i+1}}{(i+1)} \right] - \frac{Q_5}{2\pi k_3} \tag{B-14}$$

In steady state,

$$Q_1 + Q_5 = H \tag{B-15}$$

Eliminating C_1 from (B-12) and (B-14) and using (B-10) to replace the fuel temperature difference gives

$$\begin{aligned} \frac{Q_5}{2\,k_3} + \frac{1}{2\pi \ln(R_3/R_2)} \frac{Q_5}{R_3 h_3} - \frac{1}{2\pi \ln(R_3/R_2)} \frac{Q_1}{R_2 h_2} \\ = - \frac{T_5 - T_1}{\ln (R_3/R_2)} + \frac{H}{k_3} \sum_{i=1}^{n} \left[\frac{a_i R_3^{\,i+1}}{(i+1)} \right] \\ - \frac{H}{k_3 \ln(R_3/R_2)} \sum_{i=1}^{n} \left[\frac{a_i}{(\,i+1\,)^2} \left(R_3^{\,i+1} - R_2^{\,i+1}\right) \right] \end{aligned} \tag{B-16}$$

Q_1 can be eliminated from (B-16) using the result of (B-15). Before solving for Q_5, it is advantageous to define an effective thermal conductivity k_e between the two bulk coolant temperatures. This value is defined to be

$$\frac{1}{k_e} = \frac{1}{R_2 h_2} + \frac{\ln (R_3/R_2)}{k_3} + \frac{1}{R_3 h_3} \tag{B-17}$$

Using this definition, Q_5 is specified.

$$Q_5 = -2\pi k_e (T_5 - T_1) + \frac{H k_e}{R_2 h_2} + 2\pi \frac{k_e}{k_3} H \ln(R_3/R_2) \sum_{i=1}^{n} \frac{a_i R_3^{i+1}}{(i+1)}$$
$$- 2\pi \frac{k_e}{k_3} H \sum_{i=1}^{n} \left[\frac{a_i}{(i+1)^2} (R_3^{i+1} - R_2^{i+1}) \right] \qquad \text{(B-18)}$$

The first term on the RHS of (B-18) represents the heat flow per unit length and per time that would take place in a conventional counter-flow heat exchanger. The remainder of the terms on the RHS determine the heat flow to the outer coolant stream, dependent only on the relative magnitude of the thermal barriers which are encountered and the shape function of the heat generation rate. The fraction of heat produced in the fuel material, which goes to the outside coolant channel, is given by

$$\frac{Q_5}{H} = \frac{\left\{ \left[\frac{1}{R_2 h_2} + \frac{\ln(R_3/R_2)}{k_3} \right] \sum_{i=1}^{n} \frac{a_i R_3^{i+1}}{(i+1)} - \frac{1}{R_2 h_2} \sum_{i=1}^{n} \frac{a_i R_2^{i+1}}{(i+1)} - \frac{1}{k_3} \sum_{i=1}^{n} \left[\frac{a_i}{(i+1)^2} (R_3^{i+1} - R_2^{i+1}) \right] \right\}}{\frac{1}{k_e} \sum_{i=1}^{n} \left[\frac{a_i}{(i+1)} (R_3^{i+1} - R_2^{i+1}) \right]} \qquad \text{(B-19)}$$

B.4. Influence of Fuel Thermal Conductivity on Heat Flow Fraction

An effective thermal conductivity k_e of the material separating the two coolant streams was defined in (B-18). This was shown to be made up of three terms, one of which directly related to the thermal conductivity of the fuel material and the remaining two to the cladding conductivity and the interface heat transfer coefficients.

To demonstrate how the heat flow fraction is influenced through the relative magnitude of k_3, consider the two cases when $k_3 = 1.0$ Btu/hr/ft/$^{\circ}$F and $k_3 = 25.0$ Btu/hr/ft/$^{\circ}$F. The first case has a value typical of a ceramic fuel, such as UO_2, while the second is more representative of a

metallic fuel. Arbitrarily, assign the following values to the other geometrical and heat transfer parameters.

$(R_2/R_1) = 1.1$

$R_2 = 0.02$ ft

$(R_3/R_2) = 3.0$

$(R_4/R_3) = 1.05$

$K_2 = K_4 = 10.0$ Btu/hr/ft/°F

$h_1 = h_2 = h_3 = h_4 = 1000.0$ Btu/hr/ft^2/°F

Using the assumed values, the following numbers are calculated.

$$\frac{1}{R_2h_2} = 0.1145 \qquad \frac{1}{R_3h_3} = 0.0375$$

$$\left.\frac{\ln(R_3/R_2)}{k_3}\right|_{k_3=1.0} = 1.1 \qquad \left.\frac{\ln(R_3/R_2)}{k_3}\right|_{k_3=25} = 0.044$$

When k_3 has a low value, it predominates in the expression for k_e and the heat flow faction to the outer coolant channel becomes relatively unaffected by the heat transfer coefficients at the cladding - coolant interface. If k_3 is large, the reverse is true. The heat transfer flow fraction is, of course, influenced by the shape of the heat generation rate across the fuel.

B.5. Limiting Case for Heat Flow Fraction

If the fuel has a low thermal conductivity, a simple relationship can be derived for the flow faction to the rate coolant when the assumption is made that the power distribution is constant across the fuel material. With the assumption of a flat power distribution, only the polynomial coefficient a_1 has a finite positive value; all other coefficients are identically zero. For these conditions, equation (B-19) can be simplified to

$$\frac{Q_5}{H} = \frac{-(x^2-1) + x^2 \ln(x^2)}{(x^2-1)\ln(x^2)} \tag{B-20a}$$

where

$$x = (R_3/R_2) \tag{B-20b}$$

The variation of (Q_5/H) for this condition is shown below.

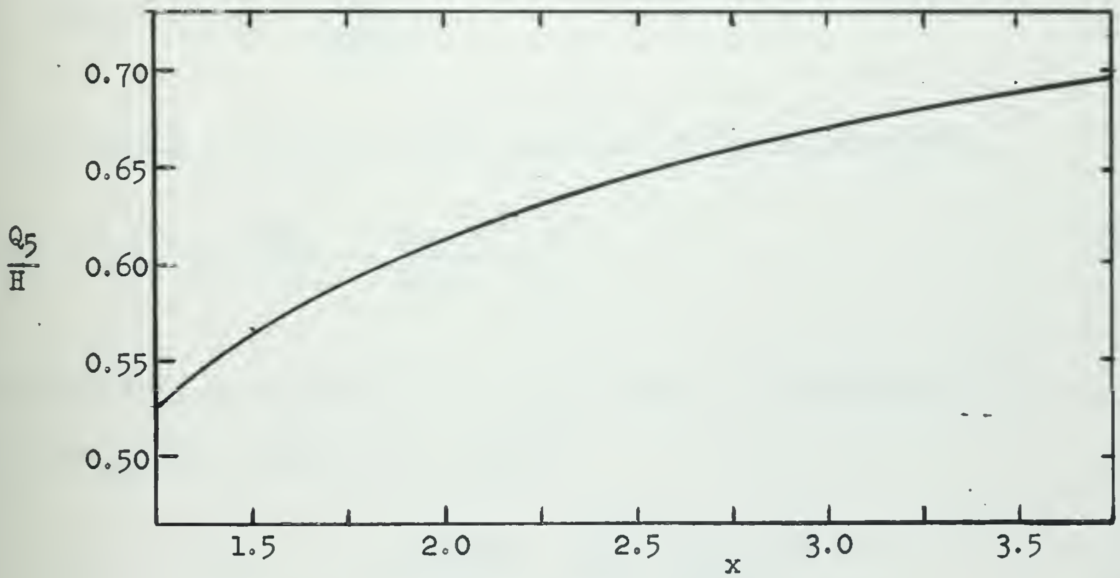

HEAT FLOW FRACTION PREDICTED BY EQ. (B-20a)

FIGURE B.2

B.6. Fuel Temperature Distribution

When Q_5 has been determined in (B-19), the integration constant C_1 can be found in (B-14). Once C_1 is known, the second integration constant C_2 can be found in (B-11) from evaluation with the fuel temperature at either fuel - cladding interface. The temperature distribution at any point in the fuel is then identically fixed with (B-11).

B.7. Fuel Temperature Distribution when Outside Coolant Flow is Blocked

As a limiting case for this situation, it is assumed that the temperature gradient is zero at the position $r = R_3$ and all heat produced in the fuel leaves radially at $r = R_2$. When this occurs, the fuel temperature T_{32} at $r = R_2$ is given by substituting H in (B-8a) to give for T_{32}

$$T_{32} = T_1 + \frac{H}{2\pi R_2 h_2} \tag{B-21}$$

The boundary condition on the slope at $r = R_3$ requires that

$$C_1 = \frac{H}{R_3} \sum_{i=1}^{n} \left[\frac{a_i {R_3}^{i+1}}{(i+1)} \right] \tag{B-22}$$

The constant C_2 is evaluated at $r = R_2$ to yield as the expression for no cooling on the outside fuel surface

$$\begin{aligned} T_3(r) &= T_{32} + \frac{H \ln(r/R_2)}{k_3} \sum_{i=1}^{n} \frac{a_i {R_3}^{i+1}}{i+1} \\ &- \frac{H}{k_3} \sum_{i=1}^{n} \left[\frac{a_i}{(i+1)^2} \left(r^{i+1} - {R_2}^{i+1}\right) \right] \end{aligned} \tag{B-23}$$

B.8. Fuel Temperature Distribution when Inside Coolant Flow is Blocked

This situation is just the reverse of the preceding one. Now the temperature slope is assumed to be zero at $r = R_2$, so that all heat produced in the fuel must be carried away by the outside coolant. This condition results in the expressions

$$T_{33} = T_5 + \frac{H}{2\pi R_3 h_3} \tag{B-24}$$

$$T_3(r) = T_{33} - \frac{H \ln(R_3/r)}{k_3} \sum_{i=1}^{n} \frac{a_i {R_2}^{i+1}}{(i+1)} + \frac{H}{k_3} \sum_{i=1}^{n} \left[\frac{a_i \left({R_3}^{i+1} - r^{i+1}\right)}{(i+1)^2} \right] \tag{B-25}$$

APPENDIX C

HEAT TRANSFER AND FLUID FLOW

C.1 Introduction

The magnitude of the two coolant heat transfer coefficients plays a determining role in defining the heat flow fraction for the power produced in the fuel tube which goes to the two coolant streams. Because of this influence, a consistent and reliable method must be employed in order to properly size the dimensional parameters of the fuel tube and coolant channels to achieve the desired steam exit conditions.

As indicated by equation (B-19), the formulation of the heat flow fraction is more properly expressed in terms of thermal resistances, rather than conductivities or "heat transfer coefficients." The following sections present selected correlations used to predict the heat transfer coefficients and the temperature differential between the bulk coolant and heat transfer surface for a given heat flux. The temperature differential is directly proportional to the product of the effective thermal resistance (defined from the "heat transfer coefficient") and the heat transferred per unit length of coolant channel.

Convective heat transfer is functionally dependent on the velocity or flow profile of the coolant. This dependence is particularly noticeable at transition points for two-phase flow, in which the flow pattern undergoes relatively sharp changes. The coupling between flow profile and pressure drop is represented through a force equation written for an elemental length of coolant channel. For two-phase flow, a description of the velocity profile is necessary not only for heat transfer but also for pressure loss calculations.

C.2 Numerical Description of the Physical Properties of Water and Steam

When describing the heat transfer coefficients or thermal resistance at the coolant-heating surface interface, the quantities $\underline{k}$ thermal conductivity,

$\underline{u}$ dynamic viscosity and $\underline{c}$ specific heat at constant pressure appear. Additionally, either the specific volume $\underline{v}$ or density $\underline{\rho}$ and surface tension $\underline{\sigma}$ may be required in the physical correlation. In the subsequent discussion, the liquid phase will be denoted by subscript $\underline{f}$ and the vapor phase by subscript $\underline{g}$.

The data for the values of specific heat $\underline{c}$ and specific volume $\underline{v}$ have been taken directly from the "Steam Tables".[1] The values associated with a given value of pressure and enthalpy, these two being necessary to completely specify the thermodynamic state of the coolant, are obtained by linear interpolation. Internally, the program reads in as data a set of steam table cards encompassing the region from 100 °F to the critical pressure and from 100 to 1500 psia over a selected range of 14 temperatures. The value of specific volume $\underline{v}$ is determined directly by interpolating between successive spanning data points. For the specific heat at constant pressure $\underline{c}$, the quantity is calculated for the coolant, when it is in the subcooled or saturated state, by

$$c_f = \frac{H_{f,j+1} - H_{f,j}}{T_{j+1} - T_j} \tag{C-1}$$

where $H_{f,j+1}$ and $H_{f,j}$ are the enthalpy values of saturated liquid above and below the actual liquid enthalpy and T_{j+1} and T_j are the corresponding temperatures above and below the point. Defining the specific heat for the liquid in this manner is not quite correct, since there is in fact an increase in pressure P between the points T_j and T_{j+1}.

The value of the specific heat at constant pressure for the vapor c_g is calculated by two-way linear interpolation. The pressure is held constant, thus introducing only the error associated with the assumption of linear variation between the four points, two pressure and four enthalpy, circumscribing the actual state point.

The variables σ, k and u have been determined by making least square

fits yielding a polynomial representation for their values at a given pressure and phase, if appropriate, as a function of temperature.[2,3] In this representation, the variable

$$T' = T/100 \qquad (C-2)$$

has been used. T is the bulk coolant temperature in degrees Fahrenheit. For each of these quantities, represented generally by the symbol X, the describing polynomial is written as

$$X = A_1 + A_2 T' + A_3 T'^2 + A_4 T'^3 \qquad (C-3)$$

The polynomial coefficients are dimensional. The respective units arising for these variable definitions are:

σ	lb/ft
k	Btu/hr/ft/$^\circ$F
u	lb/hr/ft

Coefficients for the liquid phase properties are given in Table C.1. The liquid viscosity u_f can be represented by only one curve, defined at the saturation point, between the saturation pressure and 5000 psia to within $\pm$ 5%. For the case of thermal conductivity, the value corresponding to pressures above and below the actual state pressure is calculated and linear interpolation is used to define the state point conductivity.

The dimensional coefficients for the polynomial representation of the vapor dynamic viscosity and thermal conductivity are given in Table C.2. Again, linear interpolation is used to define the values, when the polynomial coefficients are pressure dependent.

The method of interpolation is illustrated in Figure C.1. Consider that it is necessary to find the value of the vapor viscosity at the state 1300 psia, 600 $^\circ$F. A glance at the steam tables reveals that the saturation temperature at 1300 psia is 577.46 $^\circ$F. Thus, the state point lies between the saturation temperatures at 1000 and 2000 psia. For this particular set of

Table C.1

POLYNOMIAL COEFFICIENTS DESCRIBING LIQUID HEAT TRANSFER PROPERTIES

Quantity	A_1	A_2	A_3	A_4
σ	5.274×10^{-6}	-3.448×10^{-7}	-1.435×10^{-7}	1.457×10^{-8}
k (saturated)	3.153×10^{-1}	6.137×10^{-2}	-1.186×10^{-2}	1.632×10^{-4}
k (1000 psia)	3.153×10^{-1}	6.166×10^{-2}	-1.136×10^{-2}	6.842×10^{-5}
k (2000 psia)	3.217×10^{-1}	5.488×10^{-2}	-8.766×10^{-3}	-1.601×10^{-4}
u (saturated)	3.049	-1.849	4.046×10^{-1}	-2.974×10^{-2}

Table C.2

POLYNOMIAL COEFFICIENTS DESCRIBING VAPOR HEAT TRANSFER PROPERTIES

Quantity	A_1	A_2	A_3	A_4
k (saturated)	-3.289×10^{-3}	1.317×10^{-2}	-3.171×10^{-3}	3.537×10^{-4}
k (250 psia)	1.639×10^{-2}	7.114×10^{-4}	1.215×10^{-4}	-1.341×10^{-6}
k (1000 psia)	8.672×10^{-2}	-2.010×10^{-2}	2.221×10^{-3}	-7.211×10^{-5}
k (1500 psia)	1.703×10^{-1}	-4.385×10^{-2}	4.487×10^{-3}	-1.443×10^{-4}
u (saturated)	1.319×10^{-2}	1.419×10^{-2}	-3.571×10^{-3}	5.185×10^{-4}
u (0 psia)	1.939×10^{-2}	6.546×10^{-3}	-3.158×10^{-4}	1.243×10^{-5}
u (1000 psia)	7.692×10^{-2}	-3.426×10^{-3}	3.569×10^{-4}	9.390×10^{-9}
u (2000 psia)	2.074×10^{-1}	-3.684×10^{-2}	3.743×10^{-3}	-1.194×10^{-4}

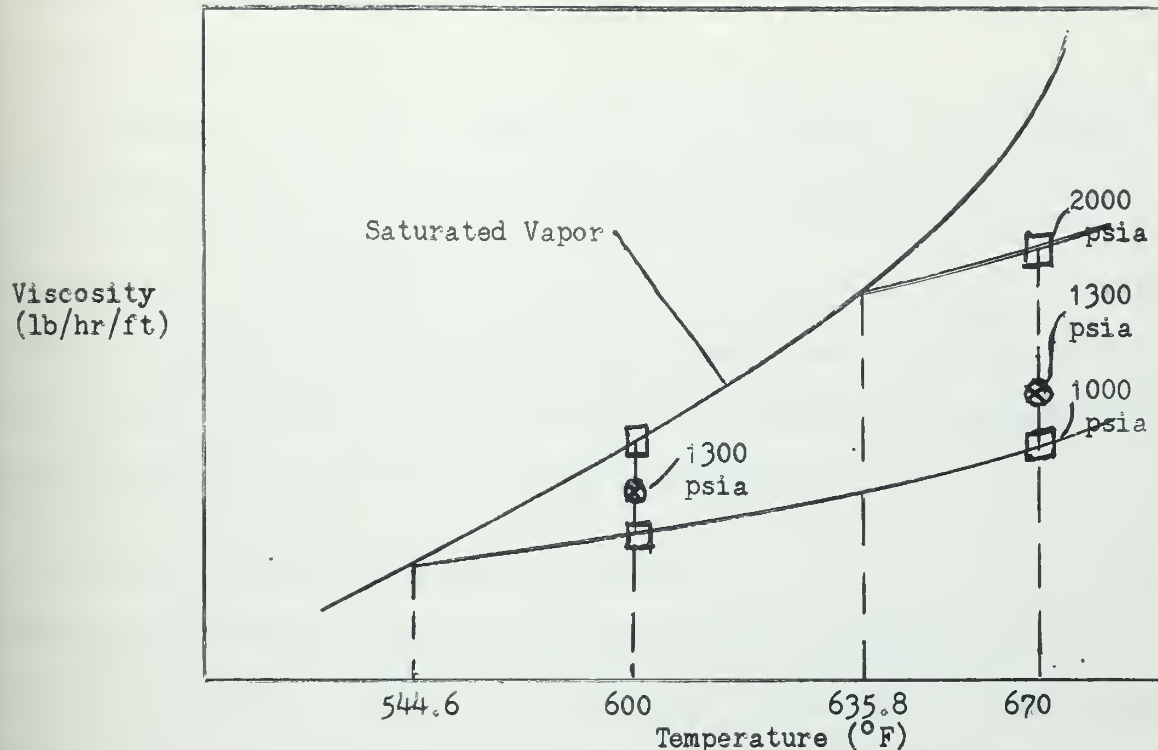

INTERPOLATION METHOD FOR DETERMINING VISCOSITY OF VAPOR

Figure C.1

coordinates, the viscosity is found by calculating the viscosity at the points along the curve u (1000 psia) and along the curve u (saturated). At 600 °F, the saturation pressure of water is 1542.9 psia. The viscosity at 1300 psia is found by interpolating on pressure between these two points.

On the other hand, for the point at 1300 psia, 670 °F, as shown on Figure C.1, the viscosity at 670 °F for the curves u (1000 psia) and u (2000 psia) is calculated. Interpolation on pressure to 1300 psia is then performed between these two lines of constant pressure.

C.3 Forced Convection Non-Boiling Heat Transfer

The study of non-boiling heat transfer has resulted in different correlations which predict the temperature difference between the heated surface and the bulk coolant. The general form for these correlations is basically the same. Functionally, their variations result from the consideration of

the temperature-sensitive properties of the coolant and the mathematical description of the velocity profile in the turbulent stream.

The commonly used representation of the forced convection non-boiling turbulent heat transfer coefficient is given by the Colburn equation[3]

$$Nu = 0.023\ Re^{0.8}\ Pr^{1/3} \tag{C-4}$$

expressed in terms of the dimensionless groupings of the Nusselt Nu, Reynolds Re, and Prandtl Pr numbers. Written in terms of dimensional parameters, the Colburn equation predicts the heat transfer coefficient h as

$$h_C = 0.023\ (k/D)\ (VD/vu)^{0.8}\ (cu/k)^{1.3} \tag{C-5}$$

The average bulk coolant velocity V and the hydraulic diameter D are the new symbols appearing in (C-5). The velocity V and specific volume v define the mass flux G.

$$G = V/v \tag{C-6}$$

Thus, the wall temperature of the heated surface T_W is determined in terms of the bulk coolant temperature T_c, the heat flux at the wall (Q/A) and the Colburn heat transfer coefficient h_C.

$$T_W = T_c + (Q/A)/h_C \tag{C-7}$$

For the first pass flow of the CFR core, the flow path is annular with the majority of heat supplied to the coolant by transfer across the inner surface of the flow channel. A small percentage of heat is also generated in the solid moderator region, due to gamma heating and the kinetic energy of neutrons as they are slowed down. This heating is neglected, thus imposing more stringent demands on the heat transfer surface separating the fuel material and the first pass coolant.

The effect of the annular geometry can be neglected without appreciable loss in accuracy.[4] Using

$$h_A = 0.020\,(r_o/r_i)^{1/2}\,Re^{0.8}\,Pr^{1/3} \qquad \text{(C-8)}$$

where r_o and r_i are the outer and inner radii defining the annular region and h_A a corrected heat transfer coefficient for an annular region heated on the inner wall, it is apparent that the ratio (r_o/r_i) does not appreciably affect the unmodified Colburn heat transfer coefficient h_C (C-5) until

$$(r_o/r_i) \geqslant (0.023/0.020)^2 = 1.323 \qquad \text{(C-9)}$$

For the CFR core, the value of (r_o/r_i) is not reached at which the annular effect causes a significant variation in the heat transfer coefficient predicted by (C-5). Non-boiling heat transfer coefficients are subsequently predicted using the Colburn formulation (C-5).

The heat transfer coefficient for vapor flowing down through the interior of the fuel tube for the second pass heating can also be predicted by (C-5). In this case the geometry is circular with heat added to the coolant from only one wall. This situation is similar to that previously considered, except that the one-phase coolant flow is now all vapor rather than pressurized or subcooled water.

More detailed predictions of the heat transfer coefficient for water vapor appear in the literature. For example, one recent proposed correlation for steam is given by[5]

$$Nu = 0.0157\,Re^{0.84}\,Pr^{1/3}\,(L/D)^{-0.04} \qquad \text{(C-10a)}$$

when the length L falls in the range $6 < L/D < 60$ and

$$Nu = 0.0137\,Re^{0.84}\,Pr^{1/3} \qquad \text{(C-10b)}$$

for $L/D > 60$. In equations (C-10), the properties of the steam are evaluated at the mean film temperature (i.e., at $0.5\,T_c + 0.5\,T_w$). Checking these correlations against the experimental data from which they arose results in a prediction quoted to be valid to within $\pm$ 10%. On the other

hand, it was found that when the Colburn equation (C-5) was used, the properties also being evaluated at the mean film temperature, the predicted value of h_c was 11.5% high at Reynolds numbers in the region of 2.5×10^4 and 1.8% high at 3.7×10^5. Because no significant increase in accuracy results from going to correlations other than the Colburn, equation (C-5) is retained and used in predicting one-phase heat transfer coefficients.

C.4 Incidence of Boiling

When the coolant is in the compressed liquid or subcooled state, boiling can occur at the heated surface, providing the heat flux and wall temperature are high enough to produce bubbles with the requisite amount of superheat. For the case of subcooled boiling the bubbles, formed at the heated surface and swept into the coolant stream, collapse when the bulk coolant temperature is below the saturation point, resulting in a net steam quality of zero.

When the wall temperature is sufficiently higher than the saturation temperature of the liquid coolant, the coolant at the wall may possess the necessary amount of superheat to produce bubbles. When this situation exists, the mode of heat transfer changes and the Colburn equation is no longer applicable.

Several empirical formulations have been proposed to predict the requisite wall temperature or heat flux necessary to produce vapor bubbles at the wall. McAdams fitted the results of experiments at 90 psia for an internally heated annulus of 0.25-in. ID, thickness 0.09 to 0.26-in., for 20 to 150 °F subcooling when the upward coolant velocity was between 1 and 36 ft/sec by[6]

$$T_w - T_{sat} = 1.97\,(Q/A)^{0.26} \qquad \text{(C-11)}$$

Buchberg has proposed a correlation for subcooled water in a 0.26-in. ID type 347 stainless steel tube at 2000 psia as[7]

$$(Q/A) = 0.0027\,(G^{0.8}/D^{0.2})\,(T_c^{\,0.32})\,(646 - T_c) \qquad \text{(C-12)}$$

Utilizing the Colburn equation and McAdams correlation, the incidence of boiling is predicted whenever

$$T_c + (Q/A)/h_C \geqslant T_{sat} + 1.97\,(Q/A)^{0.26} \qquad \text{(C-13)}$$

For the set of assumed values:

$T_c = 500\ {}^\circ F$ $\qquad$ $T_{sat} = 544.6\ {}^\circ F$ (1000 psia)

$G = 1.765 \times 10^6$ lb/hr/ft^2 $\qquad$ $D = 0.01667$ ft

$h_C = 5310$ Btu/hr/ft^2/$^\circ$F

boiling occurs, as predicted by (C-13) according to the numerical inequality

$$(Q/A)/5310 \geqslant 44.6 + 1.97\,(Q/A)^{0.26}$$

Solving for the limiting value of (Q/A) yields a heat flux of 5.63×10^5 Btu/hr/ft^2. Using the direct calculation of the Buchberg correlation, the limiting heat flux is predicted as 6.48×10^5 btu/hr/ft^2.

A comparison between McAdams' and Buchberg's correlations for the assumed set of values given above indicates that no significant difference exists when the two correlations are extrapolated to 1000 psia. Considering that Buchberg's correlation is supposedly valid to within $\pm$ 10% at 2000 psia, the choice of which to use is not well defined.

McAdams' correlation has been artibrarily chosen for the prediction of the incidence of boiling. On this basis, whenever

$$T_c \geqslant T_{sat} + 1.97\,(Q/A)^{0.26} - (Q/A)/h_C \qquad \text{(C-14)}$$

local boiling is assumed to occur and the prediction of the wall temperature using the Colburn formula is no longer valid.

C.5 Boiling Heat Transfer

A schematic representation of the heat transfer coefficient and flow profile variation for a once-through system (i.e., subcooled inlet, superheated exit) is shown in Figure C.2.[8] The more or less abrupt changes in

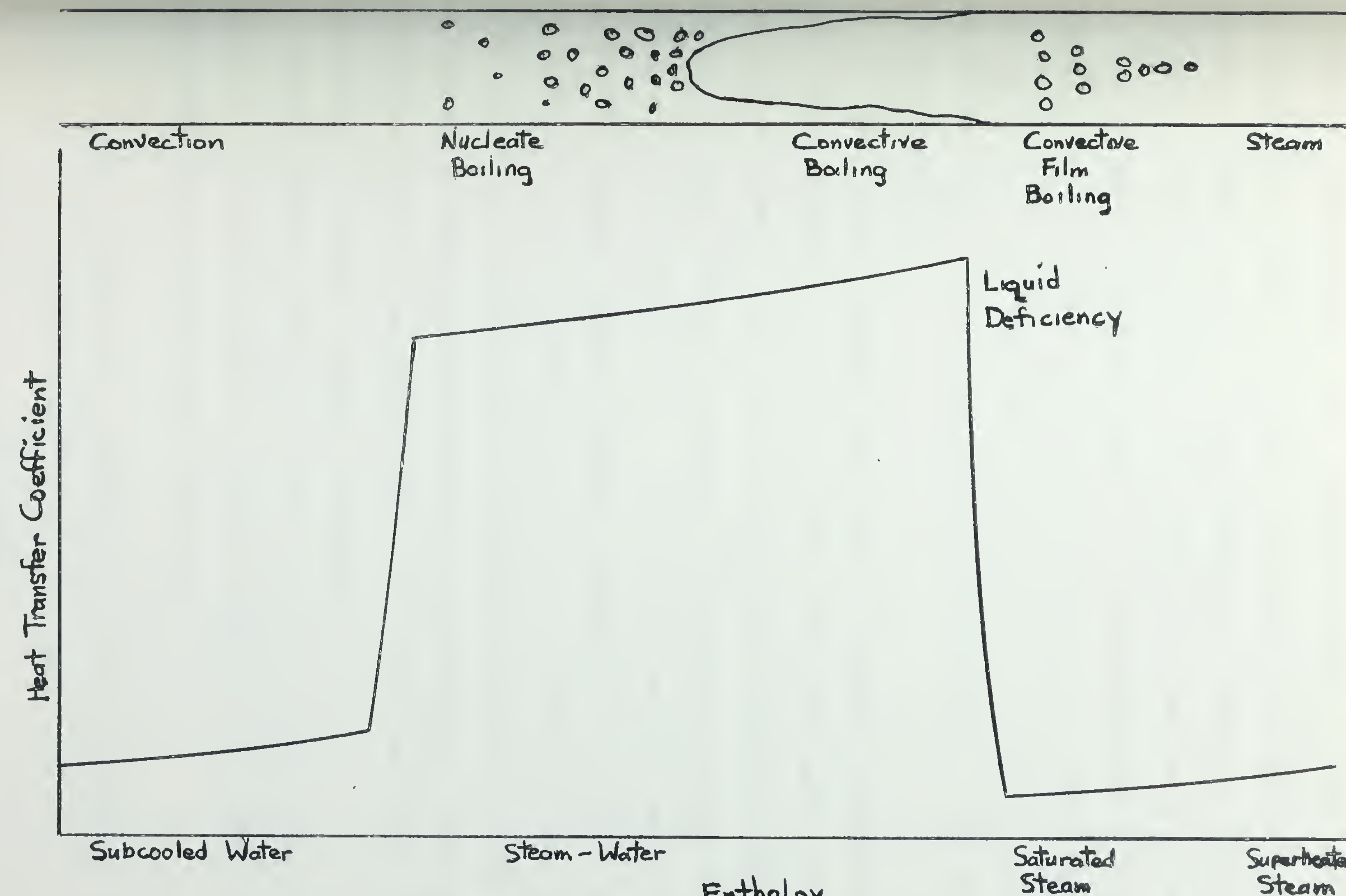

HEAT TRANSFER IN A ONCE-THROUGH SYSTEM

Figure C.2

the heat transfer coefficient over the saturated region signify that the application of any single correlation to describe this variation is highly unlikely. Because of this, it becomes necessary to attempt to describe separately each of the successive regions through which the heated coolant flows.

The literature abounds in reports of the experimental and theoretical work that has been devoted to the study of boiling heat transfer, particularly over the period of the last ten to fifteen years. The wealth of material present has almost come to the point where bibliographies of bibliographies are being published.

In order to make a partial comparison of the reports encountered in the search for a consistent and reliable method of describing boiling heat transfer in the CFR system, only a few of the many works encountered will be mentioned. The rapid advances of knowledge in this field may outmode the final selection that has been made here. The choice of a suitable combination of correlations becomes extremely difficult, obscured by the fact that the majority of work that has been published was done at relatively low pressures. Of those reports that present results at pressures applicable to the CFR system, the majority of work has been concentrated in determining the conditions resulting in "burn out" and little effort seems to have been devoted to the description of local heat transfer coefficients.

Specifically for the region of forced convection subcooled boiling, in addition to the work of McAdams and Buchberg referenced in Section C.4, some other correlations that have been suggested are[9,10]

$$(Q/A) = \Big[(c_f/\mathrm{Const.})^3 \, (u_f/(H_{fg}^{\,2}\, Pr^{5.1}))\, ((\rho_f - \rho_g)/\sigma)^{\frac{1}{2}} \times \times (T_w - T_{sat})^3\Big] + h_C\, (T_w - T_c) \qquad (C\text{-}15)$$

$$T_w - T_{sat} = 1.9\, (Q/A)^{1/4}\, e^{-p/900} \qquad (C\text{-}16)$$

$$T_w - T_{sat} = 123 - 35 \log(p) \qquad \text{(C-17)}$$

$$T_w - T_{sat} = 28 - 0.012\ p \qquad \text{(C-18)}$$

The superposition technique of Rosenhow and Clark in (C-15) is clearly evidenced by the two terms present, the first for boiling heat transfer, the second for non-boiling heat transfer.

In the region of net steam generation, it has been observed that the heat transfer coefficient increases up to a certain vapor quality and then falls off sharply, the so-called burn-out condition. This effect is clearly evidenced in Figure C.2; at the point where the heat transfer coefficient falls, the liquid film on the heated surface has been burned off or dynamic instabilities cause it to break off. The flow profile of the liquid and vapor undergoes a change and, as has been observed, the remaining liquid in this higher quality region is carried as droplets in a flowing steam medium.

The results of several correlations for the region of net steam generation (the two-phase region) are given below.[11-14] In the subsequent discussion the vapor quality x is defined by

$$x = W_g / (W_f + W_g) \qquad \text{(C-19)}$$

where W is the mass flow rate, and the void fraction α is described by

$$\alpha = A_g / (A_f + A_g) \qquad \text{(C-20)}$$

where A is the cross sectional flow area. The subscript tp denotes two-phase.

$$h_{tp} = h_f\ ((1 - x)/(1 - \alpha))^{0.8} \qquad \text{(C-21)}$$

$$h_{tp} = 0.060\ (v_g/v_f)^{0.28}\ (k_f/D)\ (xD/A\ u_f)^{0.87}\ Pr_f^{\ 0.4} \qquad \text{(C-22)}$$

$$h_{tp} = C\ (k_g/D)\ Re_g^{\ 0.8} \qquad \text{(C-23)}$$

In equation (C-23), $C = 0.840$ for $0.4 < x < 0.5$, 0.887 for $0.55 < x < 0.65$ and 0.904 for $0.7 < x < 0.8$.

$$h_{tp} = (k_f/D)\,(4.3 + 0.005\,x\,(v_g/v_f)^{0.64}) \\ ((Q/A)/(G\,H_{fg}))^{0.464}\,(GD/u_f)^{0.808} \qquad \text{(C-24)}$$

$$(Q/A)_b = k_f\,c_f\,\rho_f^{\,2}\,(1 - x)\,(T_w - T_{sat})^3 \\ (H_{fg} + c_f\,(T_{sat} - T_c))/(\sigma\,T_{sat}\,(\rho_f - \rho_g)\,B_L\,H_{fg}) \qquad \text{(C-26)}$$

In equation (C-26), B_L is a free parameter, graphically represented as a function of the vapor density and heat of vaporization.

For the region of liquid deficiency (Figure C.1), Parker and Grosh report that two distinct types of heat transfer are present, depending on the relative magnitude of the wall temperature.[15] The Leidenfrost effect was observed for high wall temperatures, for which the heat transfer coefficient was experimentally observed to be almost identical with that found with dry saturated steam. When the liquid droplets in the mist flow did not achieve the spheroidal state, the droplets striking the wall provided a local wetting action and heat transfer coefficients of the order of 3 to 6 times those for dry steam were observed.

The correlations indicated in equations (C-24) to (C-26) cannot represent the transitional effect of the loss of the liquid film on the heat transfer surface. The point at which the liquid film is lost has been variously reported as occurring between qualities of 0.45 to 0.80, being a function of the mass flux and the heat flux.[12]

The results of the correlations indicated above all showed wide discrepancies over their region of investigation, principally being of the order of ± 20%. Microscopically, the complex phenomena associated with the boiling process are not understood and the dimensional or dimensionless groupings

are an engineering attempt to describe the observed experimental results. As noted previously, the data has been fitted generally to systems operating under pressures of 200 psia.

The pr cure adopted here to consistently evaluate the local heat transfer coefficients for regions of subcooled boiling or net steam generation has used the Levy correlation (C-26). For qualities up to 70%, this formulation is assumed to be valid. Above 70%, the heat transfer coefficient is predicted using the Colburn formulation for an all vapor flow, following the results of Parker and Grosh.

In the description of the heat flux (Q/A), the superposition technique is frequently employed.

$$(Q/A)_{total} = (Q/A)_{boiling} + (Q/A)_{non-boiling} \qquad \text{(C-27)}$$

This is the technique demonstrated in the Rosenhow correlation (C-15). Assuming a given wall temperature T_W, (C-27) would be solved by trial-and-error to define an equivalent heat transfer coefficient $\underline{h_e}$, where

$$h_e = (Q/A)_{total}/(T_W - T_c) \qquad \text{(C-28)}$$

The errors associated with the formulation of (C-26) may play a deciding role in the size configuration of the CFR fuel element. To insure that the value of the equivalent heat transfer coefficient, for the subcooled and two-phase boiling regions is not over predicted, the assumption has been made that the heat transfer mechanism is dependent only on the "boiling" process. A typical value for the non-boiling heat transfer coefficient will be of the order of 1500 to 5000 Btu/hr/ft^2/$^{\circ}$F, while in the low quality region the boiling heat transfer coefficient will be roughly 10,000 to 30,000 Btu/hr/ft^2/$^{\circ}$F. Disregarding the effect of the non-boiling convective heat transfer mechanism introduces a conservative note in the calculational

procedure, increasing the thermal resistance for heat flow to the first pass coolant and subsequently raising the wall temperatures for both the first and second pass heating surfaces.

The evaluation of the equivalent heat transfer coefficient $\underline{h_e}$ is obtained by inserting the calculated value of (Q/A) for (C-26) into (C-28). The free parameter B_L has been mathematically fitted from the data presented in the Levy paper using the method of least squares. Defining the parameter $\underline{y}$

$$y = H_{fg} / (1000\, v_g) \tag{C-29}$$

the quantity $1/B_L$ is mathematically described by

$$1/B_L = -0.6163 + 2.297\, y - 0.5857\, y^2 + 0.03481\, y^3 \tag{C-30}$$

C.6 Burnout Prediction - The Critical Heat Flux Ratio

The controlling constraint on the performance of a water-cooled reactor is often the so-called "DNB (Danger, Nucleat Boiling)-ratio". Changes in the flow profile within a heated channel can lead to an extreme decrease of the heat transfer coefficient resulting in an inordinately high wall temperature.

The continuation of the use of the nomenclature "DNB-ratio" to define the point beyond which the coolant is unable to remove heat from a fuel rod or pin should be discarded. More realistically, the limiting constraint for heat transfer would be defined the "critical heat flux" or the "critical enthalpy rise". At its inception, the term "DNB-ratio" had physical meaning because of the constraint imposed on the pressurized-water reactor system and the fact that the early extremely conservative design approach did not allow for nucleate boiling to occur. The design of present day power reactors to operate with the coolant in the saturated state has its limiting

constraints, but these are not caused only by heat transfer problems due to nucleate boiling but rather changes in the coolant flow profiles and the wetness or dryness of the heat transfer surface. In this sense, the term "DNB-ratio" has little physical significance.

Extensive research has been and is being carried out in order to gain information that will lead to more precise empirical or semi-analytical correlations that can be used to predict this constraint on reactor performance.[16-19] Presently, the microscopic behavior of what is happening within the channel is still not understood, just as with heat transfer prediction for two-phase flow. Thus, it becomes necessary to use an empirical correlation which can predict the critical conditions with a reasonable degree of accuracy.

The prediction of the critical heat transfer condition in this study is made using the formulation of Tong et al. These formulations are based on two different constraints, either heat flux or enthalpy rise.

For the case of saturated outputs, the critical enthalpy rise ΔH_c is predicted by

$$\begin{aligned} \Delta H_c = \; & 0.529(H_f - H_{in}) + H_{fg}(0.825+2.36e^{-204D_e})e^{-1.5G/10^6} \\ & + H_{fg}(0.548-0.41e^{-0.0048L/D_e} - 1.12v_f/v_g) \end{aligned} \tag{C-31}$$

The value of ΔH_c was found to be sensibly independent of the variation of heat flux along the channel. The range of applicability of (C-31) is given below:

Geometries: circular tube, rectangular channel and rod bundles

Axial heat flux distribution: uniform and non-uniform

Mass velocity: 0.2×10^6 to 4.0×10^6 lb/hr/ft^2

Pressure: 800 to 2750 psia

L/D_e ratio: 21 to 656

Inlet subcooling ($H_f - H_{in}$): 0 to 400 Btu/lb

Local heat flux: 0.1×10^6 to 1.8×10^6 Btu/hr/ft^2

Exit quality: 0 to 90 weight percent

Equivalent diameter: 0.1 to 0.54 inches

Heated-to-wetted perimeter ratio: 0.88 to 1.0

Although the first pass outlet condition is, on the average, in the saturated state for the CFR system, it is conceivable that the local exit condition from some channel could be in the subcooled state. For this situation, the critical heat flux $(Q/A)_c$ is given by

$$\begin{aligned}(Q/A)_c = {} & (0.23 \times 10^6 + 0.095\, G)\,(3.0 + 0.01\, \Delta T_{sc}) \\ & (0.435 + 1.23\, e^{-0.0093 L/D_e}) \\ & (1.7 - 1.4\, e^{-0.0532 (H_f - H_{in})/H_{fg}})^{3/4}\, (v_f/v_g)^{-1/3}\end{aligned} \qquad (C\text{-}32)$$

For the condition of uniform heat flux, $(Q/A)_c$ yields values within $\pm$ 20% at a 95% confidence level. For non-uniform heat fluxes, the calculated values of $(Q/A)_c$ were approximately 40% lower than those observed experimentally. The range of applicability of (C-32) is:

Geometries: circular tube, rectangular channel and rod bundle

Mass velocity: $0.2 \times 10^6 - 8.0 \times 10^6$ lb/hr/ft^2

Pressure: 800 to 2000 psia

L/D_e ratio: 21 -365

Inlet subcooling ($H_f - H_{in}$): 0 to 700 Btu/lb

Subcooling at DNB (ΔT_{sc}): 0 to 228°F

Local heat flux: 0.4×10^6 to 4.0×10^6 Btu/hr/ft^2

Equivalent diameter: 0.1 to 0.54 inches

Heated-to-wetted perimeter ratio: 0.88 to 1.0

The CFR first pass channel geometry does not specifically conform to the limits of heated-to-wetted perimeter ratio. For the CFR design, this value is less than 0.5. The correlation of Tong is used, however, for lack of a reliable correlation more closely fitting the CFR geometry.

In the final determination of the controlling heat transfer constraint, the values of $(\Delta H_{actual})/(\Delta H_c)$ and $(Q/A)_{actual}/(Q/A)_c$ are both calculated. Above 10% quality, only (C-31) is assumed to be valid. For outlet conditions below 10% quality, the values of the two ratios are compared. The ratio with the higher value is taken to be the limiting constraint, and is designated the "Critical heat flux ratio" in the printout of computer results.

Because the "burnout" condition is described locally in the final answer statement, the general determination of whether the "critical heat flux ratio" is a limiting constraint on the system performance should be based only on the calculated result shown for the complete passage through the heat transfer channel. This appraisal is based on the discrepancies noted for the prediction of the values for non-uniform channel heating.

It should also be noted that second pass coolant critical heat flux ratios will appear which are negative. These numbers are generated by the following situation. As the saturated vapor enters the channel entrance for second pass heating, the pressure drops and a high quality two-phase mixture is present. The program does not distinguish the fact that the "inlet subcooling" on the second pass is negative and that the final steam quality is unity, i.e., in fact superheated. The second pass calculated values of the critical heat flux ratio have thus no physical meaning.

<u>C.7 Void Fraction Representation</u>

The introduction of the void fraction $\underline{\alpha}$ into the calculation of either

heat transfer or pressure drop equations is an attempt to describe the slip flow present in a two-phase stream. The vapor velocity is different from that of the liquid. This then is a refinement of the homogeneous model in which a uniform bulk velocity is ascribed to both the liquid and vapor phases.

The influence of the void fraction on the overall thermodynamic and pressure balance quations for the dimension and sizes of the CFR system is small. The primary importance in describing the effect is reflected in the nuclear calculations, where the total mass of water present at a given axial position along the first pass channel is a function of the void fraction. This is not to say, however, that the influence on the two-phase pressure gradient is not negligible.

The "classical" work describing the variation of the void fraction is that of Martinelli and Nelson.[20] In that paper, the void fraction is derivable from a set of curves which are pressure and quality dependent.

The fact that the first pass channel dimensions are small provides some flexibility in the representation of the void fraction. In the CFR system, the fuel elements are vertical, which presupposes that the flow profile distribution around the element centerline is, on the average, rotationally symmetric. One suggested representation of the void fraction by Armand[21] correlates the specific volumes and quality parameters.

$$\alpha = (0.833 + 0.167\, x)\ x\, v_g/(v_f + x\, v_{fg}) \qquad \text{(C-33)}$$

The Armand correlation has been incorporated into the subsequent calculations.

The explicit definition of the void fraction in (C-33) makes the calculation very straight forward, without the necessity of extensive curve fitting to define a polynomial or other type representation or of tabular

data defining the property. This correlation is, however, strictly not correct for the type of calculations involved with the CFR core. It was determin by measuring void fractions in horizontal heated pipe flows, rather than vertical. The general trends of this correlation have been borne out in vertical flow channels. It is, of course, accurate at the positions x = 0 and x = 1.0.

The void fraction, as given in (C-33), is assumed to be a smooth continuous function of the vapor quality.

C.8 Velocity Profile with Slip Flow

The definition of the quality x and void fraction α fixes the velocity of the non-homogeneous liquid and vapor flow when the mass flow rate and cross sectional flow area are specified.

For the liquid velocity V_f, the describing equation is derived from

$$\rho_f \quad V_f \quad A_f \equiv W_f \tag{C-34}$$

$$V_f = v_f W_f/A_f \tag{C-35}$$

$$V_f = v_f G (1 - x)/(1 - \alpha) \tag{C-36}$$

where G is the total mass flux. In the limit of x approaching unity (an all vapor flow), the quantity $(1 - x)/(1 - \alpha)$ goes to zero.

For the vapor velocity V_g, the describing equation is derived from

$$\rho_g V_g A_g = W_g \tag{C-37}$$

$$V_g = v_g W_g/A_g \tag{C-38}$$

$$V_g = v_g G x/\alpha \tag{C-39}$$

Again, the slope of the void fraction is finite for the quality x going to zero, and V_g is zero for x = 1.0.

C.9 Two-Phase Friction Factor

As shown in Section D.1, the two-phase pressure gradient is caused

by the sum of two terms, the first reflecting the influence of momentum changes of the coolant as its thermodynamic state changes, the second the effect of shear along the confining walls of the channel.

The definition of the two-phase frictional gradient depends on the choice of the frictional coefficient. As with the Martinelli et al. work, the ratio of the two-phase frictional gradient is sometime represented as a functional multiplier times the all liquid frictional gradient.

Shrock and Grossman have experienced a measure of success in describing the frictional gradient in the conventional manner, that is, as a function of a friction factor.[22] In their work, the fraction coefficient $\underline{C_F}$ is defined as a pseudo-Fanning friction factor, where

$$C_F = 0.046/Re^{0.2} \tag{C-40}$$

when the Reynolds number $\underline{Re}$ is defined from the total flow through the system. The dynamic viscosity for the definition is based on the quality of the mixture, such that

$$1/u = x/u_g + (1 - x)/u_f \tag{C-41}$$

The definition of $\underline{C_F}$ in (C-41) is used subsequently for determining the two-phase friction factor. Note that for one-phase flow, either all liquid or all vapor, the Reynolds number is defined in terms of a one-phase fluid.

APPENDIX D

ENERGY BALANCE AND PRESSURE LOSS WITHIN THE CFR CORE

D.1 Introduction

The method of defining the thermodynamic coolant properties at any position in the core must be compatible with the nuclear analysis of Appendix A. This limits the description of the coolant state within any given axial retion of a cell to a set of values, which must represent the average state of the coolant within that region. In this fashion, the analysis proceeds.

The energy balance that is used to describe the steady state operation of the system includes not only the consideration of the power produced in the fuel itself, but also the heat exchanger effect caused by the flow of two fluid streams of different temperature separated by a conducting wall.

The energy equation which must be satisfied at all points along a flow channel is derived from[1]

$$dH + d(V^2)/(2gJ) + dz/J + dQ - dW_x = 0 \qquad (D\text{-}1)$$

In equation (D-1), the following terms are understood:

H - enthalpy

V - bulk coolant velocity

J - conversion factor

z - height above some given datum line

Q - heat added

W_x - shaft work removed from the system.

Each of these terms must be considered. W_x is zero since no work is taken from the coolant while it is within the core. The effect of height change can be neglected in comparison to the variation in the enthalpy term H. The kinetic energy variation (the second term on the LHS of (D-1)) could also be neglected. However, because of the close relationship between the

kinetic energy and momentum flux terms, the effect of kinetic energy variation is included in the calculations with little additional computational effort. Under this set of assumptions, (D-1) becomes

$$dH + d(V^2)/(2gJ) + dQ = 0 \tag{D-2}$$

where the terms in (D-2) are written per unit mass of coolant.

Distinct from the energy balance considerations, the force balance on an element of coolant is not directly coupled to the physical processes that are occurring on the other side of the fuel tube. There is, however, an indirect coupling through the energy balance between the two streams. Primarily this coupling is exerted through the variation of the coolant density and its influence on the momentum flux term in the force balance equation. The basic force balance equation can be written as

$$0 = -\frac{\partial}{\partial z}\left(\frac{\rho V^2 A}{g}\right) dz - \frac{\partial}{\partial z}(pA)\, dz - \frac{\partial}{\partial z}(p_s A)\, dz \tag{D-3}$$

where

ρ - coolant density

A - flow area

p - pressure

and subscript s represents the pressure magnitude variation introduced by shear at the confining channel walls. The change in pressure due to gravitational head is not included in (D-3), since it can be neglected in comparison with the variation of the other terms.

A tacit assumption made in the subsequent development is that the pressure across the fluid stream is constant, regardless of the flow profile or state of the coolant.

D.2 General Characterization of Kinetic Energy in One- or Two-Phase Flow

When the reactor coolant is water and the reactor core is designed to

produce superheated steam, the state of the coolant as it flows through the core varies from compressed liquid to a two-phase saturated mixture to a one-phase all vapor flow. This section is devoted to the development of a relationship which is valid for any of these states and defines the kinetic energy term.

The steam quality x is defined in terms of flow rates, where

$$x = W_g / W \qquad \text{(D-4)}$$

where W is the total flow rate through the channel and subscript g denotes the vapor phase and f the liquid phase. The total flow rate W is simply

$$W = W_f + W_g \qquad \text{(D-5)}$$

Conceptually, one can consider that $x = 0$ for an all liquid flow and $x = 1$ for an all vapor flow. The intermediate values of x then denote a two-phase flow. Note that with the definition of (D-4), in which the quality is defined in terms of flow rates rather than enthalpies, the concept is directly expressed mathematically.

Using the definition of the void fraction α (C-33), the velocity of the vapor phase can be written as

$$V_g = v_g \, x \, W / (\alpha A) \qquad \text{(D-6)}$$

and for the liquid phase as

$$V_f = v_f (1 - x) W / ((1 - \alpha) A) \qquad \text{(D-7)}$$

The kinetic term in (D-2) was written on a per unit mass basis. If the total energy (kinetic) flowing through some cross section of the coolant channel is considered, the following relationship is developed:

$$W V^2 / (2 g J) = (W_f V_f^2 + W_g V_g^2)/(2 g J) \qquad \text{(D-8)}$$

Note that this definition tacitly assumes that a slug of liquid is flowing

at the rate of W_f lb/hr with an average velocity V_f ft/hr while at the same cross section a slug of vapor is flowing at the rate of W_g lb/hr at an average velocity of V_g ft/hr.

Factoring out the flow rate W from the RHS of (D-8) by using the definition of quality x yields

$$W\,V^2/(2\,g\,J) = (x\,V_g^{\,2} + (1-x)\,V_f^{\,2})\,W/(2\,g\,J) \qquad \text{(D-9)}$$

When the definitions of the liquid and vapor velocities are inserted in (D-9),

$$\frac{W\,V^2}{2gJ} = \frac{W\,G^2}{2gJ}\left((1-x)^3\,v_f^{\,2}/(1-\alpha)^2 + x^3\,v_g^{\,2}/\alpha^2\right) \qquad \text{(D-10)}$$

The mass flux is denoted by G. In equation (D-10) the flow rate W can be cancelled from both sides, leaving an expression for the kinetic energy KE, again on a per unit mass basis.

$$KE = \left((1-x)^3\,v_f^{\,2}/(1-\alpha)^2 + x^3\,v_g^{\,2}/\alpha^2\right)G^2/(2\,g\,J) \qquad \text{(D-11)}$$

It immediately is apparent that (D-11) is valid for liquid, liquid-vapor flow and all vapor flow. For the all liquid case, (D-11) reduces to

$$KE)_f = G^2\,v_f^{\,2}/(2\,g\,J) \qquad \text{(D-12)}$$

while for the all vapor case

$$KE)_g = G^2\,v_g^{\,2}/(2\,g\,J) \qquad \text{(D-13)}$$

D.3 General Characterization of Momentum Flux in One- or Two-Phase Flow

The previous section developed a general relation for the kinetic energy term in the steady flow energy equation. In this section, a general equation will be developed to characterize the momentum flux at a given cross section in a flow channel. The notation of the previous section is employed here.

Let $\dot{MF}$ denote the momentum flux. Mathematically, it is expressed as

$$MF = V\,(\rho V A)/(A\,g) \tag{D-14}$$

or simply as

$$MF = W\,V/(A\,g) \tag{D-15}$$

The total momentum passing through a given section is then the product of (D-15) and the flow area A.

$$\text{Total Momentum} = W\,V/g \tag{D-16}$$

which can be broken into a liquid and vapor component as

$$\text{Total Momentum} = (W_f\,V_f + W_g\,V_g)/g \tag{D-17}$$

Using the definition of quality x

$$\text{Total Momentum} = ((1 - x)\,V_f + x\,V_g)\,W/g \tag{D-18}$$

and finally the velocity relationships

$$\text{Total Momentum} = ((1 - x)^2 v_f/(1 - \alpha) + x^2 v_g/\alpha)\,W^2/(gA) \tag{D-19}$$

Dividing this equation through by the flow area A yields the average momentum flux through the section.

$$MF = ((1 - x)^2\,v_f/(1 - \alpha) + x^2\,v_g/\alpha)\,G^2/g \tag{D-20}$$

D.4 Differential Equations for Counterflow Energy Balance

The coupled differential equations defining the energy balance in the CFR core are best defined by first considering the geometrical sketch shown in Figure D.1. The physics of the situation can be envisioned quickly from this sketch.

Defining the total energy term U such that

$$U = H + KE \tag{D-21}$$

where subscripts 1 and 2 denote first and second pass flow, respectively, the differential equations for the two coolant streams over an incremental

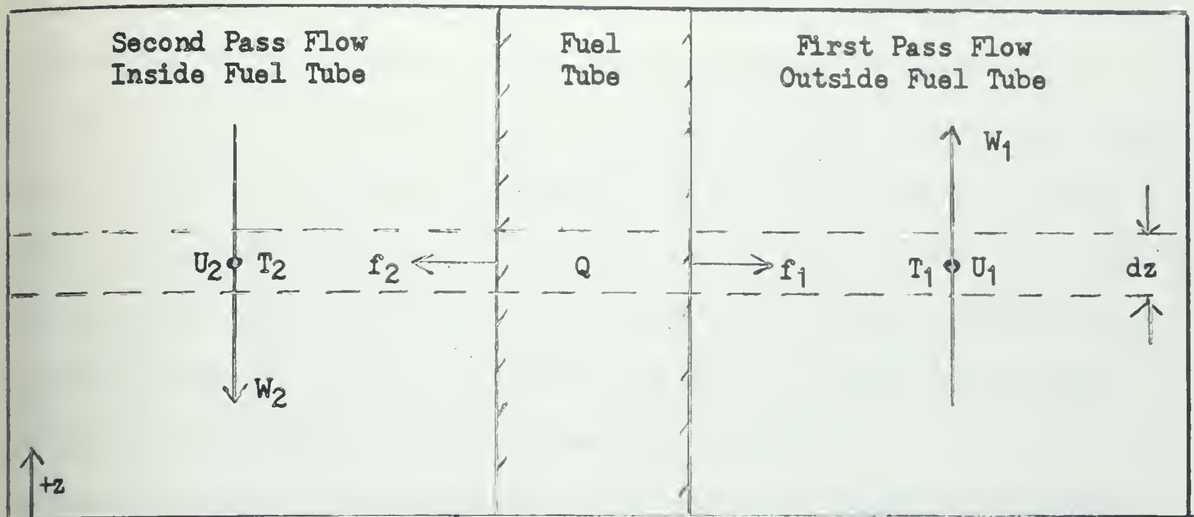

SCHEMATIC OF COUNTERFLOW ENERGY BALANCE

Figure D.1

length of fuel tube dz are:

$$W_1 \frac{dU_1}{dz} = f_1 Q + 2 \pi k_e (T_2 - T_1) \qquad \text{(D-22)}$$

$$- W_2 \frac{dU_2}{dz} = f_2 Q - 2 \pi k_e (T_2 - T_1) \qquad \text{(D-23)}$$

where all the terms in (D-22) and (D-23) are functions of the height z, except the flow rates W_1 and W_2. The negative sign for the term on the LHS of (D-23) appears because the flow is opposite to the direction of positive height z.

The terms f_1 and f_2 are defined in Appendix B. For the case of first pass flow entering from the region outside the fuel tube, as shown in Figure D.1 and incorporated into the equations (D-22) and (D-23), the term

$$f_1 = Q_5 / H \qquad \text{(D-24)}$$

where the RHS of (D-24) is defined by (B-19) and previous definitions of that appendix. The quantity f_2 is then simply

$$f_2 = 1.0 - f_1 \qquad \text{(D-25)}$$

The effective thermal conductivity k_e of (D-22) and (D-23) is defined by (B-17) and prior relations. Given the temperature differential $(T_2 - T_1)$, the second term on the RHS of (D-22) and (D-23) accounts for the heat transferred from the "hot" second pass channel coolant to the "cold" first pass coolant across the fuel tube. (If no heat were produced in the fuel tube, only the second term on the RHS of (D-22) and (D-23) would be present, and the result would be a set of differential equations identical with those describing a "conventional" counterflow heat exchanger.)

D.5 Simplification of Equations for a Constant Axial Power Distribution

If the kinetic energy term is neglected in (D-21) and one considers the total energy of a coolant stream can be described an any axial position only by its enthalpy H, (D-22) and (D-23) become

$$W_1 \frac{dH_1}{dz} = f_1 Q + 2 \pi k_e (T_2 - T_1) \quad \text{(D-26)}$$

$$- W_2 \frac{dH_2}{dz} = f_2 Q - 2 \pi k_e (T_2 - T_1) \quad \text{(D-27)}$$

If one assumes that there is no sensible variation of the first pass coolant temperature T_1 over the length of the channel L, which presupposes (1) that there is not a large amount of first pass subcooling when one considers the mixed inlet temperature of the feedwater and recirculating water relative to the saturation temperature of the first pass stream, and (2) pressure drop during the first pass does not appreciably lower the saturation temperature at which boiling first commences, then the quantity T_1 can be considered a constant.

Assuming further that the water that is continuously recirculated through the core (i.e., $W_1 = W_2$) loses no heat and defining the term H_{fw} to represent the inlet feedwater enthalpy to the core from the last stage feedwater preheater, the LHS of (D-26) can be rewritten as $W_2\, dH_1/dz$, referring

the incremental change in H_1 only to that water which goes through the second pass, yielding the new set

$$W_2 \frac{dH_1}{dz} = f_1 Q + 2 \pi k_e (T_2 - T_1) \qquad \text{(D-28)}$$

$$-W_2 \frac{dH_2}{dz} = f_2 Q - 2 \pi k_e (T_2 - T_1) \qquad \text{(D-29)}$$

The ratio of the second pass enthalpy rise to the total enthalpy rise of the coolant which flows through the core can be described by

$$f_e = (H_{out} - H_g) / (H_{out} - H_{fw}) \qquad \text{(D-30)}$$

where H_g is the enthalpy of saturaged vapor at the first pass pressure.

If one assumes that the enthalpy change of the second pass vapor coolant is proportional to the temperature rise, an average specific heat of the coolant c_2 can be defined such that

$$c_2 = (H_{out} - H_g) / (T_{out} - T_g) \qquad \text{(D-31)}$$

where, by previous assumption

$$T_g = T_1 \qquad \text{(D-32)}$$

As a final simplification, the power generation rate in the fuel tube over any incremental length dz is assumed constant and the terms defining f_1 and f_2 are also assumed to be constant. Under these conditions, (D-29) becomes

$$\frac{dT_2}{dz} - \frac{2 \pi k_e (T_2 - T_1)}{W_2 c_2} = - \frac{f_2 Q}{W_2 c_2} \qquad \text{(D-33)}$$

Defining the variable X to represent the temperature differential between the two streams

$$X = T_2 - T_1 \qquad \text{(D-34)}$$

where

$$X = T_{out} - T_g \quad \text{at } z = 0 \tag{D-35}$$

and

$$X = 0 \quad \text{at } z = L \tag{D-36}$$

equation (D-33) can be integrated to give, in terms of an integration constant X_o,

$$X = X_o \, e^{+\beta z} + \frac{f_2 \, Q}{2 \pi k_e} \tag{D-37}$$

where

$$\beta = 2 \pi k_e \, / \, (W_2 \, c_2) \tag{D-38}$$

With the assumption that all parameters relative to the coolants and the heat transfer process are constant over the whole length of the channel, the term Q, the average power gradient in the fuel tube, is simply

$$Q = W_2 \, (H_{out} - H_{fw}) \, / \, L \tag{D-39}$$

Using the boundary condition (D-35) to eliminate the integration constant X_o and substituting the definition of (D-34) into the boundary condition (D-36) results in the transcendental equation

$$\frac{f_e}{f_2} = \frac{1 - e^{-\beta L}}{\beta L} \tag{D-40}$$

By choosing the radial dimensions of the fuel tube and coolant channels and calculating values of representative heat transfer coefficients of the two coolant streams, equation (D-40) determines the length of the channel L necessary to achieve the required final outlet temperature or enthalpy for a given flow rate W_2 and ratio of second pass enthalpy rise to total enthalpy rise.

Physically, (D-40) gives considerable insight to the energy transfer and balance process. First, it mathematically demonstrates that for the system to yield the required heat split between the first and second pass

streams, the LHS must be less than unity. Then depending on how great this deviation is from unity, the length of the channel is varied, changing the axial power generation gradient, so that the heat flux caused by the temperature differential between the two streams results in the desired system performance. With reasonable judgment the constant parameters appearing in (D-40) can be evaluated and parametric studies performed to make a preliminary determination of the optimum dimensions for the system characteristics without the necessity of going into the fine details of the complete coupled nuclear-thermodynamic-heat transfer calculations.

D.6 Difference Equation Representation of the Energy Balance Equations

The variation of the coefficients in equations (D-22) and (D-23) makes the integration of these equations impractical if a detailed study is made on the energy balance of the system. Consequently, a set of difference equations are necessary to their evaluation. These equations are formulated in a manner consistent with the nuclear analysis of Appendix A.

The difference equation analog of Figure D.1 is shown in Figure D.2. Using this figure as a guide, the derivation of the difference equations becomes more meaningful.

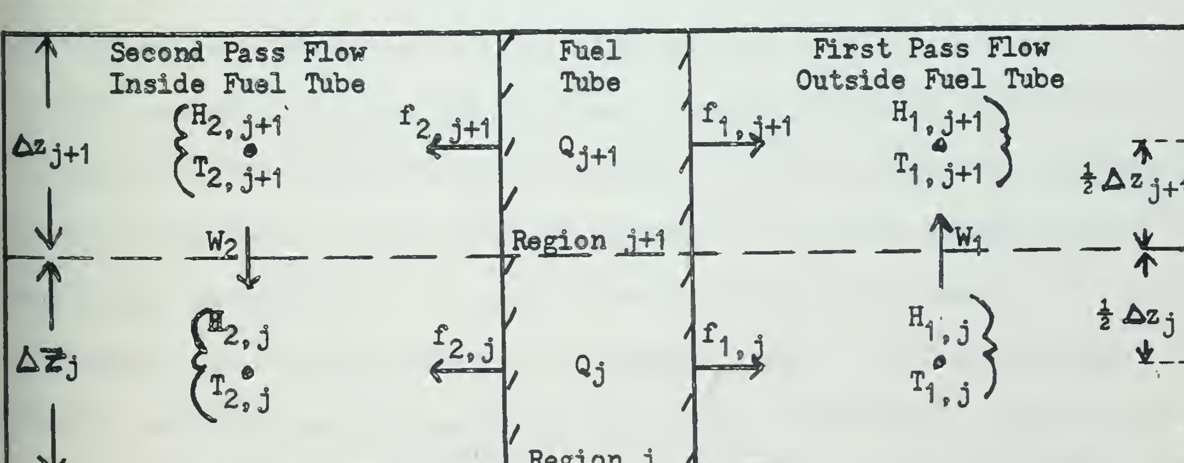

COUNTERFLOW ENERGY BALANCE MESH POINT QUANTITIES

Figure D.2

Figure D.2 again shows the case for first pass flow in the region outside the fuel tube and second pass flow inside the fuel tube.

Equations (D-22) and (D-23) are integrated in terms of forward differences. For the second pass flow, the index steps down rather than up since the flow is opposite to the direction of positive length.

Letting subscript j represent one axial subdivision of the fuel tube and j+1 the region immediately above it, equation (D-22) for the first pass flow is written as

$$U_{1,j+1} = U_{1,j} + \left[\frac{f_{1,j+1}\, Q_{j+1}\, \Delta z_{j+1} + f_{1,j}\, Q_j\, \Delta z_j}{2\, W_1}\right]$$
$$+ \frac{\pi}{W_1}\left[k_{e\,j+1}\,(T_{2,j+1} - T_{1,j+1})\Delta z_{j+1} + k_{e\,j}(T_{2,j} - T_{1,j})\Delta z_j\right] \quad \text{(D-41)}$$

and for the second pass flow (D-23) gives

$$U_{2,j} = U_{2,j+1} + \left[\frac{f_{2,j+1}\, Q_{j+1}\, \Delta z_{j+1} + f_{2,j}\, Q_j\, \Delta z_j}{2\, W_2}\right]$$
$$- \frac{\pi}{W_2}\left[k_{e\,j+1}(T_{2,j+1} - T_{1,j+1})\Delta z_{j+1} + k_{e\,j}(T_{2,j} - T_{1,j})\Delta z_j\right] \quad \text{(D-42)}$$

The method of integration in (D-41) and (D-42) is not strictly that of forward differences. The characterization of properties for each of the regions is based on their average value. Thus, the assumption is tacitly made that property variation over each of the axial regions is linear.

This method of integration more realistically expresses the variation of properties. The value for each sub-region then represents the properties that are found when half the total power from the fuel and counterflowing coolant have been added as the coolant passes through the region.

However, this type of integration scheme leads to a trial-and-error method of solution, as is apparent in both (D-41) and (D-42). The temperature of the coolant, if it isn't in the two-phase region, is a strong measure of the total energy U. In (D-41) one sees that $U_{1,j+1}$ is defined in

terms of $T_{1,j+1}$ and $T_{2,j+1}$, while in (D-42) $U_{2,j}$ is expressed as a function of $T_{2,j}$ and $T_{1,j}$. In both cases, the temperatures with the same axial index as the total energy's index are unknown.

D.7 Pressure Drop Due to Friction

The last term on the RHS of (D-3) represents the change in force on the coolant stream due to friction. Using the definition of the friction factor C_F in (C-40), the pressure gradient due to friction can be defined.

In the usual description of the frictional pressure gradient, when the Fanning Friction Factor is used, the pressure drop is written as

$$\Delta p_f = 2\, C_F\, (L/D_e)\, (\rho \overline{V^2}/g) \qquad \text{(D-43)}$$

where the quantity (L/D_e) is interpreted to mean the number of equivalent hydraulic diameters through which the fluid flows. The gradient then is

$$\frac{\Delta p_f}{L} = \frac{2\, C_F}{D_e} \frac{\rho \overline{V^2}}{g} \qquad \text{(D-44)}$$

For the situation in which two-phase flow may exist, the general description of (D-44) is written for either one- or two-phase flow as

$$\frac{\Delta p_f}{L} = \frac{2\, C_F}{D_e}\, MF \qquad \text{(D-45)}$$

where the momentum flux MF is defined by (D-14) and (D-20).

D.8 Numerical Representation of the Force Balance Equation

The differential relationship of the force balance equation of the coolant stream is given by (D-3). The representation subsequently used in this section is identical with that of Section D.6. In Figure D.2, the quantity pressure p can be substituted for total energy U.

Using the results of the preceding section, the frictional gradient can be written in terms of the momentum flux. Putting this into (D-3) and writing in a difference notation, the pressure at position j+1 for the first

pass coolant becomes

$$P_{1,j+1} = P_{1,j} + \left\{MF\left[1 - \frac{C_F \Delta z}{D_e}\right]\right\}\Bigg|_{1,j+1} - \left\{MF\left[1 + \frac{C_F \Delta z}{D_e}\right]\right\}\Bigg|_{1,j} \tag{D-46}$$

(D-46) illustrates the same principle of integration that was used in (D-41) and (D-42). The properties in any region are defined at the "mid-point" of that region. To complete the details, the second pass flow pressure at position j is simply

$$P_{2,j} = P_{2,j+1} + \left\{MF\left[1 - \frac{C_F \Delta z}{D_e}\right]\right\}\Bigg|_{2,j+1} - \left\{MF\left[1 + \frac{C_F \Delta z}{D_e}\right]\right\}\Bigg|_{2,j} \tag{D-47}$$

The coupling between the first and second pass flow is through the variation of the momentum flux. This coupling is directly caused by changes in the thermodynamic energy state, i.e., specific volume, quality and void fraction, as they are influenced by the heat transferred between the two coolant streams. The coupling is therefore not as direct as in (D-41) and (D-42), where the total energy of the system was considered. However, (D-46) and (D-47) again point up the fact that with this integration scheme, a trial-and-error method of solution is necessary.

D.9 Solution of the Energy Balance and Force Balance Equations

The method of solving the coupled set of heat balance and pressure drop equations initially assumes the temperature of the two counterflowing cooling streams is known from the previous iteration. Under this condition, the problem revolves into one of two-way interpolation on enthalpy and pressure, in which the counterflow effect has been completely uncoupled.

Letting Q_t be the total heat added to the coolant stream (due to both

power production in the fuel tube and the temperature differential between the streams), the set of equations defining the enthalpy and pressure at position j+1 for the first pass coolant is simply

$$H_{1,j+1} + KE)_{1,j+1} = H_{1,j} + KE)_{1,j} + Q_t \qquad (D-48)$$

$$P_{1,j+1} + \left\{ MF\left[1 + \frac{C_F \Delta z}{D_e}\right]\right\}\Bigg|_{1,j+1} = P_{1,j} + \left\{ MF\left[1 + \frac{C_F \Delta z}{D_e}\right]\right\}\Bigg|_{1,j} \qquad (D-49)$$

Defining error terms associated for both enthalpy and pressure, (D-48) and (D-49) can also be written as

$$e_H = \text{RHS (D-48)} - \text{LHS (D-48)} \qquad (D-50)$$

$$e_p = \text{RHS (D-49)} - \text{LHS (D-49)} \qquad (D-51)$$

When the correct combination of $(H_{1,j+1}, P_{1,j+1})$ have been selected, the two error terms are zero.

Several methods were tried to find the "best" method of solving (D-50) and (D-51). These included, among others, linear interpolation and parabolic interpolation. However, none of these methods proved satisfactory.

The method finally determined as yielding the fastest method of solution involved the direct calculation of e_H and e_p. If e_H and e_p did not fall within specified convergence limits, a new iteration was started. For this and any subsequent iterations, the new trial enthalpy $H_{1,j+1}$ was set equal to the sum of the previous value of $H_{1,j+1}$ and the calculated error term e_H. The new trial pressure value was found in the same manner. It was found that under most circumstances, this two-way interpolation procedure would converge to limits of 0.01 (a relative figure based for enthalpy on $|e_H/Q_t|$ and for pressure on $e_p/|P_{1,j+1} - P_{1,j}|$) within three iterations.

The counterparts of (D-48),(D-49) and (D-50),(D-51) were also written for the second pass flow side to define values at the point j.

D.10 Calculational Procedure and Macroscopic Heat Balance

The method solving the property variation between the sub-regions has been described in the preceding sections. As pointed out, the sequence of calculations used as a starting point the results of the preceding iteration.

Prior to the first radial sweep across the core, the temperature of the coolant is assumed to be zero. For any subsequent iterations during the first radial sweep the temperature differential across the fuel tube is set to zero, uncoupling the heat exchanger effect. This approximation was necessary to avoid extrapolating the calculated enthalpy values of the second pass coolant out of the steam table data cards. Before this feature was incorporated into the routine, the first time through the procedure both the enthalpy values of the coolant and the least-square-fitted coefficients defining the thermal conductivity and dynamic viscosity of the coolant were extended beyond their range of applicability and, in certain situations, resulted in negative enthalpy, conductivity, or viscosity values. After the first radial sweep has been completed and the first iteration power distribution as determined by the nuclear properties has been calculated, the heat exchanger effect with a finite temperature differential between the two counterflowing coolant streams is included in the calculations.

The calculation first starts by assuming that the thermal resistance between the cladding wall and coolant is zero (infinite heat transfer coefficients) for both the first and second pass flow. Then, the calculation starts with a cell in radial region 1, first pass side and marches up the cell subdivisions to the upper mixing plenum. The procedure is repeated on the first pass side for all the radial core regions. The bulk mixed enthalpy of the first pass flow is calculated, which in turn fixes the second pass total flow rate. The calculation then marches back down the core on the

second pass side to the point of second pass outlet and across the core for all the radial regions.

In determining whether the final thermodynamic profile of the coolant has been achieved within the core for the given nuclear power distribution, the total energy gained by both coolant streams is not calculated. Instead the method of testing is a little more indirect. In the testing process the fraction of heat that flows to the coolant stream outside the fuel tube is calculated, based upon the heat transfer coefficients (or thermal resistances) of the just completed iteration. These values are then checked point wise for all the core subdivisions, both radial and axial, against the heat flow fraction determined from the previous iteration. If agreement is not achieved, the problem is reiterated, using the new value of $f_{1,j}$ or $f_{2,j}$, depending on whether the flow enters from the outside or inside the fuel tube on the first pass. This process is repeated until the relative absolute magnitude of the difference between two successive iterations for all points in the core meets the desired convergence criterion. The value of the coolant state is then reflected in the testing procedure through its influence on the heat transfer coefficient between the cladding wall and the coolant.

APPENDIX E

RADIAL FLOW DISTRIBUTION ACROSS THE REACTOR

E.1 Instability

When a fluid flows through a confined heated channel, pressure drop occurs due to friction. Additionally, when the fluid state undergoes large thermodynamic changes, the effect of momentum change must be considered, introduced through the variation in the density or specific volume of the coolant.

An example of this effect can be demonstrated when one considers liquid water entering a heated channel. Assuming the inlet thermodynamic state and power generation rate in the channel are kept fixed, the outlet thermodynamic enthalpy will vary inversely as the flow rate through the channel. If the flow rate is sufficiently reduced, the exit condition of the coolant will be in the two-phase region. For this situation, the gradient of pressure with flow rate becomes negative and an instability is present if more than one channel is connected in parallel between the inlet and exit plenums.

The pressure change along the channel can be approximately represented by

$$\Delta p = W^2((v_2 - v_1) + C_F (v_2 + v_1)L/D_e)/(A^2 g) \qquad \text{(E-1)}$$

where
- W = mass flow rate
- A = cross sectional flow area
- g = gravitational constant
- v = specific volume
- C_F = Fanning friction factor

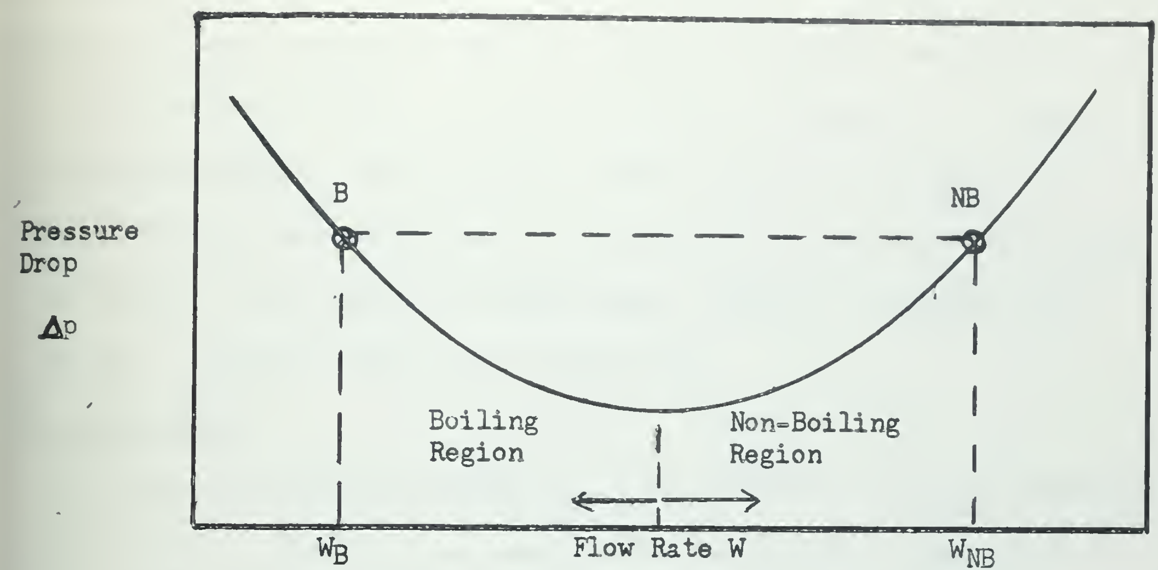

PRESSURE DROP THROUGH A HEATED CHANNEL VS FLOW RATE

Figure E.1

L = channel length

D_e = equivalent hydraulic diameter

and subscripts 1 and 2 denote the inlet and exit conditions, respectively.

A schematic representation of this effect is shown in Figure E.1. For an assumed pressure drop across the channel, as indicated by the horizontal dashed line connecting points B and NB, two flow rates through the channel are possible, either W_B or W_{NB}, respectively.

The flow rate at the point W_B is unstable. For regions to the left of the vertical dashed line, the negative slope of Δp vs W produces this instability. If, with no other flow resistance in series with the channel, the flow at the point W_B may change due to either a statistical or external perturbation. If the flow rate should fall slightly, the pressure drop across the channel increases, decreasing the flow rate even more. If, on

the other hand, the flow rate should rise slightly, the pressure will decrease and the flow rate through the channel will first accelerate down to the minimum point on the curve and then decelerate up to the point designated W_{NB}. The condition of the flow rate falling or the pressure differential rising leads to burnout, since the exit temperature of the leaving vapor becomes extremely high, causing an attendant rise in the heat transfer surface wall temperature.

E.2 Flow Control

The means of avoiding a hydraulic instability for a forced convection boiling channel is to place an external flow resistance in series with the heated channel. This resistance has the characteristic that the pressure drop across it always has a positive slope for all through rates. Thus, with the resistance in series, the pressure drop curve of Figure E.1 would be changed to that shown in Figure E.2.

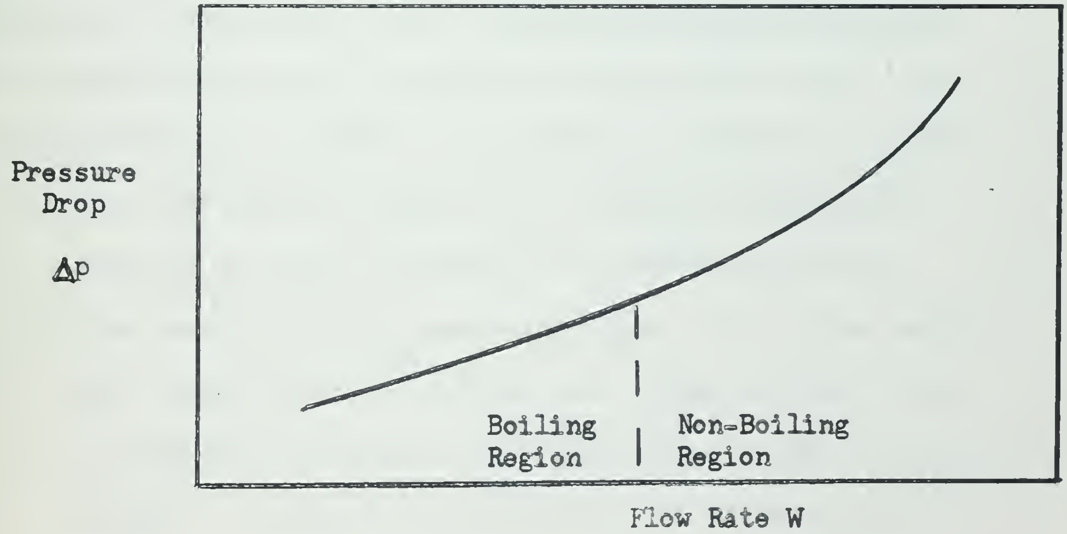

PRESSURE DROP THROUGH A HEATED CHANNEL VS FLOW RATE WITH AN EXTERNAL FLOW RESISTANCE IN SERIES WITH THE CHANNEL

Figure E.2

For this case, the pressure drop vs flow rate is positive over all expected flow rates through the channel for a given channel power. Thus, the instability is removed with the resistance in series.

The treatment subsequently is to consider the use of nozzles at each of the channel entrances to provide a stable flow pattern across the reactor. All the nozzles are assumed to have the same throat diameter. This has the disadvantage that for relatively hot channels additional flow is not received to decrease the exit quality or temperature. The utilization of variable throat diameters to regulate the final exit conditions is an area for further investigation.

The nozzles that are used cause the system overall to exhibit a stable flow pattern. With a non-uniform power distribution radially across the core, sufficient pressure drop across the nozzles must be provided to ensure that the momentum changes of the coolant do not cause a negative slope for the quantity $d\Delta p/dW$.

E.3 Mathematical Formulation of the Pressure Drop Across the Nozzles

In the description of the model used to analytically predict the pressure drop through the nozzles, the following assumptions are made:

1) Flow through the nozzle can be considered homogeneous even if in fact it results in a saturated discharge.
2) The nozzle is of the converging type. The section beyond the throat can be considered as a sudden expansion and be described using non-compressible flow theory to roughly predict the heat loss associated with this expansion.
3) The treatment of the flow of the relatively hot water through the first pass nozzles can be considered to be described by non-compressible flow theory down to the saturation pressure.

If the pressure drop associated with the necessary flow rate takes the pressure below the saturation pressure, the flow is then described using homogeneous compressible flow theory.

Starting with a pressure p_e and a temperature T_e and liquid specific volume v_{fe} (corresponding to the saturation temperature T_e), the decrease in pressure is described by

$$\Delta p = V_1^2/(2\ g\ v_{fe}) \tag{E-2}$$

The velocity of the coolant in the plenum is considered neglibible. The velocity at the throat V_1 is found by

$$V_1 = v_{fe}\ W/A_t \tag{E-3}$$

where $\underline{W}$ is the mass flow rate through the nozzle and $\underline{A_t}$ is the cross sectional area for flow at the throat. Putting this relation into (E-2) yields

$$\Delta p = v_{fe}\ W^2/(2\ g\ A_t^{\ 2}) \tag{E-4}$$

The preliminary estimated pressure at the throat is then equal to

$$p_t = p_e - \Delta p \tag{E-5}$$

If the value of p_t determined from (E-5) is greater than the saturation pressure corresponding to the temperature T_e, the analysis skips to the calculation of the pressure loss resulting from the sudden expansion beyond the nozzle. For this case, the enthalpy of the coolant at the throat is assumed to be the same as that in the preceding plenum.

However, if the value of p_t in (E-5) is found to lie below the satur-

tion pressure corresponding to T_e, the analysis then dictates that the two-phase condition be considered. For this case, the velocity corresponding to a pressure drop down to the saturation pressure is calculated.

$$V_{sat}^2 = 2 g v_f (p_e - p_{sat}) \quad \text{(E-6)}$$

From this point, the calculation proceeds assuming two-phase homogeneous flow. The calculation assumes that ideally the expansion is isentropic. Thus, the reference entropy value is that of saturated liquid s_{fe}, or if for second pass flow the entropy of saturated vapor s_{ge}, at a temperature T_e. A trial pressure value p is assumed, below the saturation pressure, and the quality of the mixture is calculated.

$$X = (s_{fe} - s_f)/s_{fg} \quad \text{(E-7)}$$

(The discussion is based on first pass entrance. For second pass entrance, the only change is to replace the subscript f with the subscript g.) The enthalpy at the point of ideal expansion H_s is given by

$$H_s = H_f + x H_{fg} \quad \text{(E-8)}$$

A velocity term V_2 is then defined such that

$$V_2^2 = 2 g J e (H_{fe} - H_s) \quad \text{(E-9)}$$

where J is a conversion factor and e is the efficiency of the nozzle. (It should be noted that the nozzle efficiency for both the second and first pass flow is the same.) Including the velocity term from (E-6), a new total velocity term V^2 is found by summing with (E-9).

$$V^2 = V_{sat}^2 + V_2^2 \quad \text{(E-10)}$$

The conversion of thermodynamic to kinetic energy is represented by the term $\underline{V_2}^2$. Under this condition, the final enthalpy of the flow $\underline{H}$ including the effect of a non-ideal expansion is represented by

$$H = H_{fe} - e\,(H_{fe} - H_s) \tag{E-11}$$

and a two-phase quality

$$x = (H - H_f)/H_{fg} \tag{E-12}$$

The specific volume of the homogeneous flowing mixture is defined by

$$v = v_f + x\,v_{fg} \tag{E-13}$$

Under the conditions stated, the calculated value of mass flow rate through the throat W_t is given by

$$W_t^2 = V^2 A_t^2/v^2 \tag{E-14}$$

If W_t^2 does not agree with the actual flow rate W^2, the assumed pressure to which the expansion takes place is varied until convergence within specified limits is obtained.

The expansion following the converging nozzle section is predicted using a pseudo non-compressible flow theory. The mass flux through the throat G_t is defined by

$$G_t = W_t/A_t \tag{E-15}$$

whereas in the channel the mass flux G_c is given by

$$G_c = W_t/A_c \tag{E-16}$$

where A_c is the channel cross sectional flow area.

At the throat before the sudden expansion takes place due to the increased flow area of the channel, the momentum term M_t in the force balance equation is given by

$$M_t = v\, G_t^2/g \tag{E-17}$$

and the kinetic energy term E_t by

$$E_t = v^2\, G_t^2/(2\, g\, J) \tag{E-18}$$

The total energy entering the region of sudden expansion is $\underline{\underline{H}}$ plus E_t, while the total "force" is p plus M_t. Using non-compressible flow theory, the final pressure p_3 and enthalpy H_3 after the sudden expansion are found from a solution of the set of equations:

$$H_3 = H + E_t - G_c^2\, (v_{f3}^2(I - x_3)^3/(1 - \alpha_3)^2 + v_{g3}^2\, x\, {}_3^3/\alpha_3^2)) \tag{E-19}$$

$$p_3 = p + M_g - G_c^2(v_{f3}^2\, (1 - x_3)^2/(1 - \alpha_3) + v_{g3}\, x_3^2/\alpha_3) + (2.0\, (A_t/A_c)^2 - (A_t/A_c)^2)M_t \tag{E-20}$$

The last term on the RHS of (E-20) accounts for the pressure loss associated with the sudden expansion.

E.4 Mathematical Formulation of the Pressure Drop at Channel Exit

The analytical method used to describe the expansion process at the point when the flow suddenly starts into the plenum is the same as that previously described for the phenomenon after passage through the control nozzle. For this case, the fluid is assumed to be decelerated to zero

velocity, that is, to assume that the area/channel is infinite in the plenum.

Under this assumption, equation (E-19) and (E-20) reduce to

$$H_3 = H + E_c \tag{E-21}$$

$$p_3 = p_c + M_c \tag{E-22}$$

and they are solved by trial-and-error according to the methods of Appendix B.

E.5 Numerical Programming Techniques

The first pass channels all start from a common plenum and exhaust to a common plenum. Under this arrangement, the pressure drop for all the channels must be same, on the average, since they are all connected in parallel. The same is true for the second pass channels.

Starting with the plenum pressure and the area ratios of the throat to channel dimensions, the maximum value of V^2 (E-10) is calculated. Since the flow is compressible, a plot of V^2 vs Δp, the pressure drop across the nozzle, is calculated. The results of such a calculation are schematically shown in Figure E.3.

Because the flow is compressible, the value of W_t or W_t^2 goes through a maximum. For a given plenum pressure p_e, the maximum flow rate through a channel is calculated, before the actual pressure drop across the channel or the flow rate through the different channels is varied to achieve equal pressure drop.

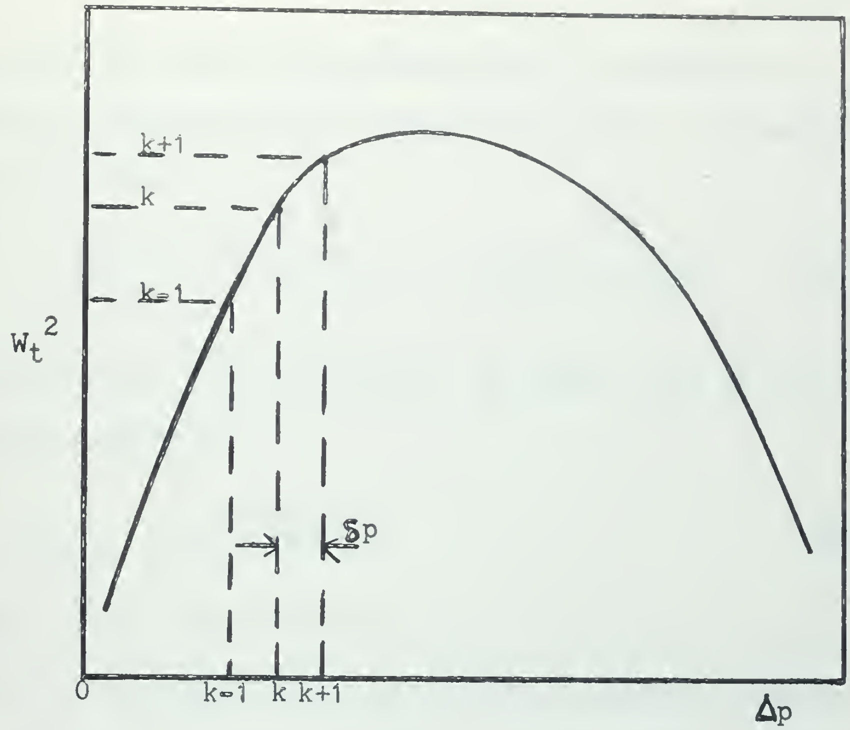

MASS FLOW RATE (COMPRESSIBLE) THROUGH A NOZZLE AS A

FUNCTION OF PRESSURE DROP

Figure E.3

To determine the point of zero slope, the quantity W_t^2 is considered to be a function of Δp. Thus,

$$W_t^2 = f(\Delta p) \tag{E-23}$$

Numerically, some particular value of Δp is designated p_k and the values of p_{k+1} and p_{k-1} are defined which are an amount δp above and below the pressure drop p_k. Corresponding to each of these assumed pressure drops, the flow rate term $W_{t,k}{}^2$ is determined.

The derivative of W_t^2 with Δp at the point p_k isdefined to be

$$W_t^2 = (W_{t,k+1}{}^2 - W_{t,k-1}{}^2)/(2\delta p) \tag{E-24}$$

which is the central difference approximation made in Appendix A. Differentiation with respect to Δp is denoted by primes. The second derivative of W_t^2 is then

$$W_t^{2''} = (W_{t,k+1}^2 + W_{t,k-1}^2 - 2 W_{t,k}^2)/(\delta p^2) \qquad (E\text{-}25)$$

Using Newton's rule for interpolation, the value of Δp at which the slope is zero is given by

$$\Delta p = p_k - W_{t,k}^{2'}/W_{t,k}^{2''} \qquad (E\text{-}26)$$

To ascertain that value of Δp at which the slope is zero is in fact a maximum for W_t^2, the curvature of the curve must be concave downward, i.e., the value of $W_{t,k}^{2''}$ must be negative. The programming technique employed has been to start at the lower values of pressure in the data steam table deck and to successively increase the pressure until the curvature is concave downward. As soon as the pressure drop has been decreased to this region, (E-26) is applied until the maximum is attained.

If the flow, which is assumed to go through the nozzle, is not choked, the pressure drop through the nozzle corresponding to this flow is determined. This type of calculation is based on that portion of the curve of Figure E.3 which lies between the origin and the point of zero slope. Newton's rule is again applied.

If W_a^2 is the square of the flow rate that has been set for the channel and W_t^2 is the flow rate squared through the nozzle corresponding to some pressure drop Δp, the equation below is successively applied until $W_t^2 = W_a^2$.

$$\Delta p = p_k - (W_{t,k}^2 - W_a^2)/W_{t,k}^{2'} \qquad (E-27)$$

For the determination of the distribution of flow across the core channels, as a function of the radial power distribution, the initial assumption is made that the flow through each of the channels is identical. Based on this assumption, the power distribution, determined from nuclear calculations is made. On the second and subsequent iterations, the pressure drop across the channels may vary due to this uneven heating.

On the first sweep across the core, an average pressure drop is calculated. Then the method of calculation is to start another sweep across the core, during which the flow through each of the channels is varied until the average pressure drop is achieved. When this second type of sweep has been completed, the flow through all the channels is summed and the calculated flow is checked against the specified flow. If the two do not agree, interpolation to a new average pressure drop is made using Newton's method. This type of calculation proceeds until the calculated and specified flow rates agree and yield an equal (to within specified convergence limits) pressure drop across the first or second pass core coolant channels. When this condition has been achieved, a new nuclear calculation commences and a new power distribution is begun, which may introduce a new radial power distribution across the core and necessitate a repetition of the procedure just described.

APPENDIX F

DIRECT CYCLE COOLANT ACTIVITY MODEL

F.1 Assumptions

When water flows through the interior of a reactor and is exposed to fast neutron irradiation, it becomes radioactive. This radioactivity is carried outside the reactor primary shielding by the coolant. In the direct cycle application using steam from the reactor in the turbomachinery, it is necessary to determine the activity level, which is introduced into the machinery space by the activated coolant, to estimate the secondary shielding requirements.

To make this estimation, the physics of the process must be considered. Writing the flow parameters of the coolant inside the reactor in an Eulerian system of coordinates, the space and time-dependent equation describing this situation is

$$\frac{\partial}{\partial t}\left(n_i(x,t)\,\rho(x,t)\right) = \rho(x,t)\,\phi(x,t)\,\sigma_i - \lambda_i\, n_i(x,t)\,\rho(x,t) - \nabla\cdot\left[\left(n_i(x,t)\,\rho(x,t)\;\underline{V}(x,t)\right)\right] \tag{F-1}$$

where ρ is the density of coolant atoms, n_i is the fraction of isotope type i that is radioactive, ϕ is a characteristic one-group neutron flux, σ_i is the cross section for activation of the i^{th} isotope, λ_i is the radioactive decay constant, and $\underline{V}$ is the vector coolant velocity. The symbol x denotes spatial position and t time.

A detailed solution of equation (F-1) requires laborious calculations, since it implied a knowledge of both spatial and time variation of the parameters. As an obvious simplification to this dilemna, the estimation of the time variation of the coolant activity will be made by assuming a lumped parameter model in which the spatial influence does not enter

directly in the calculations.

To predict the level which will be attained with this model, it is assumed that the coolant is initially completely free of activity. The reactor then begins producing power at a constant rate. This rate is held constant and the coolant reaches a saturated level of activity after an infinite time has elapsed.

F.2 Lumped Parameter Coolant Activity Concentration

Let N(t) be the number of radioactive nuclei within the reactor at any time t. With the lumped parameter approximation, it is assumed that the production rate of radioactive nuclei within the reactor is independent of position. Let P be the constant rate at which this production is occurring. Then, the general time-dependent equation for the change of N(t) with time is

$$\frac{dN(t)}{dt} = P - \lambda N(t) \tag{F-2}$$

Equation (F-2) can be integrated directly for the condition that N(t) is zero for all time prior to power production and that at time t = 0, the production term in (F-2) undergoes a step change to a constant value for all subsequent time. This gives

$$N(t) = P \lambda (1 - e^{-\lambda t}) \tag{F-3}$$

Letting T_R be the time it takes the coolant to transit the reactor and M_c the mass of coolant within the reactor, both quantities representing their representative statistical averages, after the assumed start-up procedure, the number of radioactive atoms per unit coolant mass in the reactor after its first complete transit through the reactor becomes

$$\frac{N(T_R)}{M_c} = \frac{P \lambda}{M_c} (1 - e^{-\lambda T_R}) \tag{F-4}$$

Following a specific mass of coolant around the coolant flow loop, the number of radioactive nuclei in this mass begins to decrease as soon as it leaves the reactor. Outside the reactor, the production term in (F-2) is zero. If T_S is the time it takes this mass to make a complete cycle of the coolant flow loop, the number of radioactive nuclei per unit mass of coolant remaining after the first complete coolant pass is

$$\left.\frac{N(T_R, T_S)}{M_c}\right|_1 = \frac{P\lambda}{M_c}\,(1 - e^{-\lambda T_R})\,e^{-\lambda T_S} \qquad \text{(F-5)}$$

But at the same time, the coolant is again subjected to a step change in the production rate and an additional number of new radioactive nuclei are produced as predicted by (F-4). This phenomenon is qualitatively illustrated in Figure F.1.

To determine the steady state concentration per unit mass of coolant either of two techniques can be employed, both methods yielding the same result. The first and most elegant mathematical method is to formulate a general time-dependent differential equation in terms of step functions and solve for the steady state concentration by the methods of Laplace transforms.[1]

The second method, based on an understanding of the physics of the process, is to recognize that each time that the mass of coolant leaves the core an additional amount of activity is introduced into the mass. This additional amount of activity is given by equation (F-5), except that the cycle time is now denoted by nT_S. This increment is

$$\frac{\Delta N(T_R, T_S)}{M_c} = \frac{P\lambda}{M_c}\,(1 - e^{-\lambda T_R})\,e^{-\lambda n T_S} \qquad \text{(F-6)}$$

Equation (F-6) can be summed for an infinate number of cycles n in closed form to yield

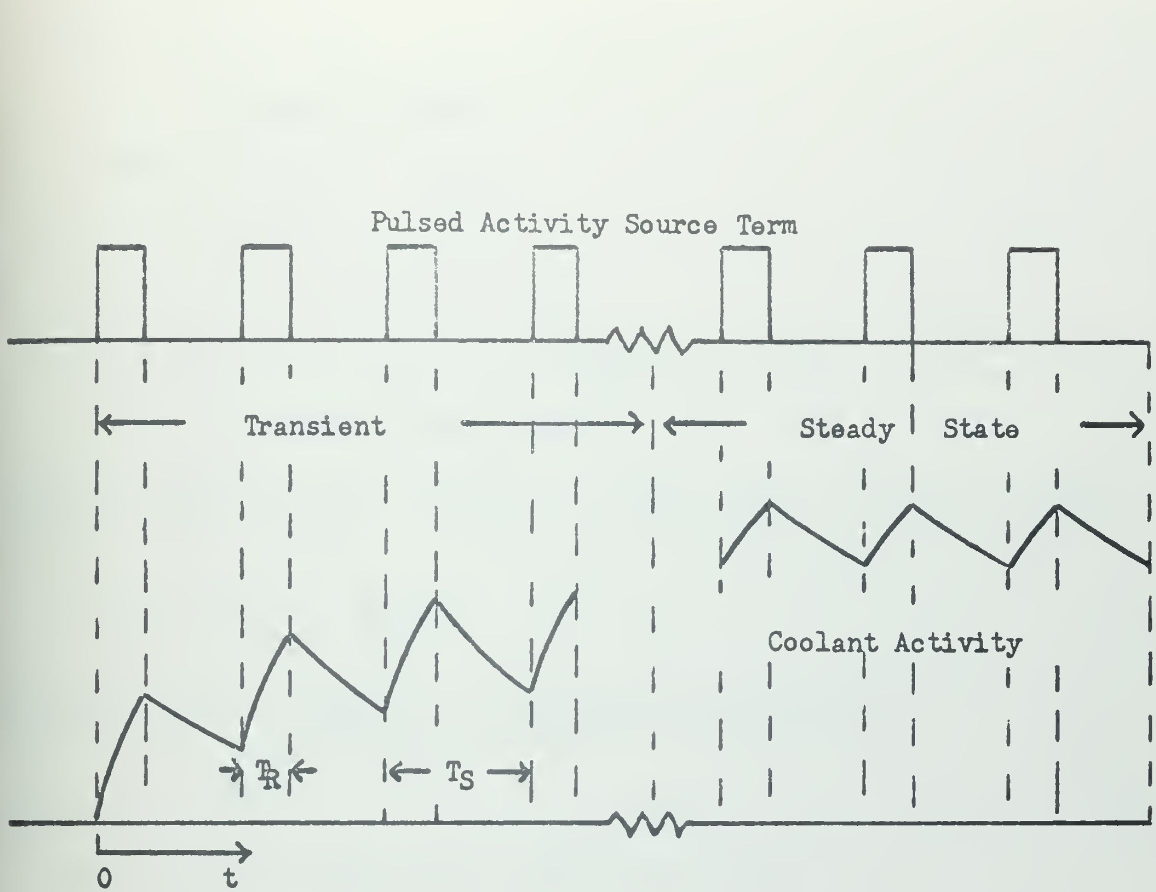

VARIATION OF RADIOACTIVITY FOR A GIVEN MASS OF COOLANT VS TIME

Figure F.1

$$\left.\frac{N(T_R, T_S)}{M_c}\right|_{\infty} = \frac{P\lambda(1 - e^{-\lambda T_R})}{M_c(1 - e^{-\lambda T_S})} \qquad \text{(F-7)}$$

F.3 Coolant Activity Production Rate

The production rate P in (F-2) can be estimated by homogenizing the reactor constituents and using a one-group model. Using the definition of Avogadro's number, the number of coolant or fuel molecules can be determined.

Let

v = reactor volume

η = Avogadro's number

A = molecular weight

M = mass within the reactor

N = number of molecules within the reactor

ρ = homogenized mass density

Then, the average molecular density of a particular isotope can be predicted by

$$\frac{N}{v} = \frac{\eta \rho}{A} = \frac{\eta M}{Av} \tag{F-8}$$

The total number of molecules of this type is predicted by

$$N = \frac{\eta M}{A} \tag{F-9}$$

The ratio of coolant-to-fuel molecules is then

$$\frac{N_c}{N_f} = \frac{M_c}{M_f} \frac{A_f}{A_c} \tag{F-10}$$

The rate at which the coolant is being activated will be proportional to its activation cross section σ_c, while the number of fissions taking place is proportional to the fission cross section σ_f. If the constant C denotes the fission rate to produce a specified reactor power, the production rate P is determined.

$$P = C \frac{M_c}{M_f} \frac{A_f}{A_c} \frac{\sigma_c}{\sigma_f} \tag{F-11}$$

F.4 Decay Rate Outside the Reactor

Let M_S be the total mass of coolant in the flow loop, which encompasses the reactor and turbomachinery. Equation (F-7) gave the concentration of radioactive coolant atoms leaving the reactor after an infinite number of

passes through the reactor. The concentration an amount of time $(T_s - T_R)$ later is the number of active atoms present after traversing the loop external to the reactor. Letting D represent the total number of decays that have taken place during the time increment $(T_S - T_R)$ in a mass of coolant $(M_S - M_R)$, the radioactive source level in the machinery space is determined.

$$D = \frac{(M_S - M_R)}{(T_s - T_R)} \frac{P\lambda}{M_c} \frac{(1 - e^{-\lambda T_R})}{(1 - e^{-\lambda T_S})} (1 - e^{-\lambda(T_S - T_R)}) \qquad \text{(F-12)}$$

F.5 Estimation of Reactor Transit and Cycle Times

To gain a representative description of the reactor transit time for the coolant, a mixing volume for the process can be determined. When considering the removal of heat from a reactor, a coolant flow rate W is specified. The mass of coolant within the reactor M_c can be calculated from the geometry and a knowledge of the coolant property profile within the reactor.

When the mass M_c has been determined, the reactor transit time for the coolant is simply

$$T_R = M_c / W \qquad \text{(F-13)}$$

A similar approach can be used for the determination of the total coolant cycle time T_S, when the total mass of coolant in the flow loop is given or calculated. This yields

$$T_S = M_S / W \qquad \text{(F-14)}$$

The combination of (F-13) and (F-14) show that, to estimate the radioactive source level D, the number of parameter permutations can be reduced by considering

$$(T_s / T_R) = (M_S / M_R) \qquad \text{(F-15)}$$

With this relationship, (F-12) can be reduced to

$$D = \frac{P\lambda\,(1 - e^{-\lambda T_R})}{T_R\,(1 - e^{-\lambda T_S})}\,(1 - e^{-\lambda(T_S - T_R)}) \qquad \text{(F-16)}$$

and then studied parametrically for different values of T_R and the ratio of (T_S/T_R).

F.6 Refinement of the Model

Additional refinements can be introduced in the simplified model used, primarily in the area of estimating the spatial effects. A more exact analysis of the reactor transit and cycle time is the more obvious correction.

Errors will be introduced in the production rate P in the reactor, if only volumetric considerations are used to define the "effective" mass of coolant or fuel present in (F-10). The contribution to the total activity that is caused by coolant traversal through a given section of the reactor is not only dependent on the local neutron flux spectrum and its correlation with the activation cross section but also on the time spent in that region. The local spatial variation is demonstrated by the general differential equation (F-1). The total coolant mass should thus be weighted not only by the local one-group flux magnitude but also with a flux spectrum correction factor.

The activation of the different isotopes is also proportional to their natural abundance. If the quantity r_i represents their natural abundance, the cross section for activation must be written as $r_i\sigma_i$.

APPENDIX G

LISTING OF THE PROGRAM CFR

To shorten the amount of space necessary to list the program, the following deviation has been made from the actual manner in which the FORTRAN cards would appear when compiling the source check. The program is too long for one main program on the IBM 7090 using the MIT system tape, so it had to be broken into a two-link chain job. To permit data transmission from one link of the program to the other and between subprograms, most variables are stored in COMMON. This necessitates the appearance of the same 23 DIMENSION, 4 COMMON, and 77 EQUIVALENCE cards in each main program and subroutine. Rather than repeating these 104 cards in each subprogram, they are listed completely only once below and then indicated in each subprogram by the 3 cards DIMENSION, COMMON, and EQUIVALENCE.

The main program and subroutine appearing in the first link of the chain job on tape B1 are:

CHAIN (1, B1)

Main Program: CFR1

Subroutines: START, DATIN, DATA1, DATA2, DATA3, DATA4, DAPR, BEGIN, THERMO

The second link of the chain on tape B2 includes:

CHAIN (2, B2)

Main Program: CFR2

Subroutines: THERMO, SSHTR, SSHTR1, SSHTR2, SSHTR3, SSHTR4, CNOZ, CNOZ1, CNOZ2, CNOZ3, PEXP, PXHTR, HTRAN, BURN, AIM, SIGMA, CONS, FLUX, EIVAL, CONV, CRIT, RING, RING1, RING2, CELAX, CELL, AXIAL, ANPRAX

Note that SUBROUTINE THERMO appears in both chain links 1 and 2.

As another means of shortening space, SUBROUTINE THERMO is shown

only in the listing for chain link 1.

DIMENSION, COMMON AND EQUIVALENCE Statements

```
 DIMENSION A(2512),AC1(7),AC2(7),AC3(7,2),AC4(7,2),AC5(7,2),AC6(7,2
1),AC7(7,2),AC8(7,2),AC9(7),AC10(7),AMAT(5,6),ASTO(773),BETA(101),B
2MAT(6,6,5),BUCKCH(6,7,2),BUCK2(7,2),BUCK2A(7,2),BUCK2C(7,2),BUCK2R
3(7,2),C(5),CHI(7,2),D(101),DELR(7),DELRA(7),DELRC(7),DELRR(7),DELT
4(3,21),DELTA(101),DEN(6,7,2),DIF(7,2),DIFA(7,2),DIFC(7,2),DIFCH(6,
57,2),DIFR(7,2)DP(7),DPHI(101,2),DPHO(7,2),DUMMY(6,6),DZ(7),ENTH(6
6,7,2),FAREA(2),FL(101),FLOW(6,2),FLP(101),FRAC(6,7),FRACT(6,6),G(1
701),GP(7),G1(101),G1P(7),HDIAM(2),HEAT(1611),HF(123),HG(123),HSUP(
814,29),HT(2),HTR(6,7,2),L(169),LB(7),LBA(7),LBC(7),LBR(7),LBS(7),L
9BSA(7),LBSC(7),LBSR(7),NN(5),NPO(11),PHI(101,2),POWER(6,7)
 DIMENSION POWP(101,2),POWR(7,2),PRES(6,7,2),PSAT(123),PSUP(29),R(1
101),RA(101),RAREA(7),RC(101),RHTR(2),RI(101),RIA(101),RIC(101),RIN
2T(7,3),RIR(101),RR(101),SIGA(7,2),SIGAA(7,2),SIGAC(7,2),SIGAR(7,2)
3,SIGAW(2),SIGPT(7),SIGPTA(7),SIGPTC(7),SIGPTR(7),SIGT(7,2),SIGTRW(
42),SMU(13),SOP(7),SOPA(7),SOPC(7),SOPP(7),SOPR(7),SOU(101),SOUA(10
51),SOUC(101),SOUP(101),SOUR(101),T(2),TA(2),TC(2),TEMC(6,7,2),TEMW
6(6,7,2),TERM(6,6,4),TFMX(6,7),TR(2),TRANS(7,1,2),TRANSA(7,1,2),TRA
7NSC(7,1,2),TRANSR(7,1,2),TSAT(123),TSUP(14),U(9,21),VF(123),VG(123
8),VSUP(14,29),VU(7,2),VUA(7,2),VUC(7,2),VUR(7,2),VUSIG(7,2),VUSIGA
9(7,2),VUSIGC(7,2),VUSIGR(7,2),VUSIG(2),VUW(2),ZSTO(1276)
 DIMENSION DNB(6,7,2),SF(123),SG(123),DCOR1(7,2),DCOR2(7,2),DCOR3(7
1,2)
 DIMENSION APOWP(6,101),APOWR(6,7),DISTL(21),TFBAR(6,7)
 COMMON A,ASTO,HEAT,ITA1,ITA0,ITA1,ITA2,ITA3,ITA4,L,NDS,NOG,SUM1,SU
1M2,SUM3,SUM4,SUM5,SUM6,SUM7,SUM8,ZSTO
 COMMON SF,SG,DCOR1,DCOR2,DCOR3,ENOZ,RUSQ,DNBMAX
 COMMON APOWP,APOWR,DISTL,TFBAR
 EQUIVALENCE (A(1),VUSIG),(A(15),VU),(A(22),TRANS),(A(36),SIGA),(A(
150),DIF),(A(64),SIGPT),(A(71),T),(A(73),EIGEN2),(A(74),R),(A(175),
2RI),(A(276),DELR),(A(283),PIM),(A(284),P),(A(285),BUCK2),(A(299),S
3OU),(A(400),SOP),(A(407),EIGEN1),(A(408),EIGEN),(A(409),C1),(A(410
4),C2),(A(411),C3),(A(412),C4),(A(413),C5),(A(414),C6),(A(415),C7),
5(A(416),C8),(A(417),C9),(A(418),C10),(A(419),C11),(A(420),C12),(A(
6421),ERR),(A(422),SUM),(A(423),FAC),(A(424),FAC1),(A(425),FAC2),(A
7(426),FAC3),(A(427),FAC4),(A(428),CON1),(A(429),CON2),(A(430),CON3
8),(A(431),CON4),(A(432),CON5),(A(433),CON6),(A(434),GAM),(A(435),G
9AM1),(A(436),ALPHA),(A(437),A1),(A(438),B1),(A(439),W),(A(440),W1)
 EQUIVALENCE (A(441),W2),(A(442),PSI1),(A(443),PSI2),(A(444),DET),(
1A(445),CHI),(A(459),VUSIGC),(A(473),VUC),(A(480),TRANSC),(A(494),S
2IGAC),(A(508),DIFC),(A(522),SIGPTC),(A(529),TC),(A(532),RC),(A(633
3),RIC),(A(734),DELRC),(A(743),BUCK2C),(A(757),SOUC),(A(858),SOPC),
4(A(865),VUSIGA),(A(879),VUA),(A(886),TRANSA),(A(900),SIGAA),(A(914
5),DIFA),(A(928),SIGPTA),(A(935),TA),(A(938),RA),(A(1039),RIA),(A(1
6140),DELRA),(A(1149),BUCK2A),(A(1163),SOUA),(A(1264),SOPA),(A(127)
7),VUSIGR),(A(1285),VUR),(A(1292),TRANSR),(A(1306),SIGAR),(A(1320),
8DIFR),(A(1334),SIGPTR),(A(1341),TR),(A(1344),RR),(A(1445),RIR),(A(
```

```
91546),DELRR),(A(1555),BUCK2R),(A(1569),SOUR),(A(1670),SOPR)
 EQUIVALENCE (A(1715),VUSIGW),(A(1717),VUW),(A(1719),TRANSW),(A(172
10),SIGAW),(A(1722),SIGTRW),(A(1724),ESP1),(A(1725),ESP2),(A(1726),
2ESP3),(A(1727),THETA),(A(1728),POW1),(A(1729),FLO),(A(1730),RAT1),
3(A(1731),TCIN),(A(1732),TCFU),(A(1733),TCOU),(A(1734),HINT),(A(173
45),TFMAX),(A(1736),PPUMP),(A(1737),HPUMP),(A(1738),DCDEN),(A(1739)
5,RRDEN),(A(1740),RINT),(A(1761),HIN),(A(1762),RECIRC),(A(1763),HTO
6P),(A(1764),PTOP),(A(1765),HOUT),(A(1766),POUT),(A(1767),HDIAM),(A
7(1769),FAREA),(A(1771),CAREA),(A(1772),RAREA),(A(1779),DZ),(A(1786
8),POWER),(A(1828),TEMC),(A(1912),TEMW),(A(1996),TFMX),(A(2038),ENT
9H),(A(2122),FLOW),(A(2134),DEN),(A(2218),FRAC),(A(2260),HTR)
 EQUIVALENCE (A(2344),PRES1,(A(2428),DNB),(A(2512),WATE)
 EQUIVALENCE (ASTO(1),AC1),(ASTO(8),AC2),(ASTO(15),AC3),(ASTO(29),A
1C4),(ASTO(43),AC5),(ASTO(57),AC6),(ASTO(71),AC7),(ASTO(85),ACB),(A
2STO(99),AC9),(ASTO(106),AC10),(ASTO(113),BETA,G),(ASTO(214),D),(AS
3TO(315),DELTA,G1),(ASTO(416),DP),(ASTO(423),FL),(ASTO(524),FLP),(A
4STO(625),GP),(ASTO(632),G1P),(ASTO(639),SIGT),(ASTO(653),SMU),(AST
5O(666),SOPP),(ASTO(673),SOUP)
 EQUIVALENCE (HEAT(1),TSAT),(HEAT(124),PSAT),(HEAT(247),VF),(HEAT(3
170),VG),(HEAT(493),HF),(HEAT(616),HG),(HEAT(739),TSUP),(HEAT(753),
2PSUP),(HEAT(782),VSUP),(HEAT(1188),HSUP),(HEAT(1594),P2),(HEAT(159
35),H2),(HEAT(1596),T2),(HEAT(1597),TSATU2),(HEAT(1598),VL2),(HEAT(
41599),VV2),(HEAT(1600),HL2),(HEAT(1601),HV2),(HEAT(1602),CL2),(HEA
5T(1603),CV2),(HEAT(1604),TCL2),(HEAT(1605),TCV2),(HEAT(1606),VISL2
6),(HEAT(1607),VISV2),(HEAT(1608),RBL2),(HEAT(1609),SURT2),(HEAT(16
710),QUAL2),(HEAT(1611),VOID2)
 EQUIVALENCE (L(1),N1),(L(2),N2),(L(3),N3),(L(4),N7),(L(5),N),(L(6)
1,NM1),(L(7),NM2),(L(8),MM1),(L(9),ICT),(L(10),TCT1),(L(11),ICT2),(
2L(12),ICT3),(L(13),ILK),(L(14),M),(L(15),LB),(L(22),NB),(L(23),LBS
3),(L(30),MICT),(L(31),MICT2),(L(32),N4),(L(33),N5),(L(38),NCELL),(
4L(39),NCE),(L(41),MCE),(L(47),MCELL),(L(48),LBC),(L(55),NBC),(L(56
5),LBSC),(L(71),NAXIAL),(L(72),NAXI),(L(74),MAXI),(L(80),MAXIAL),(L
6(81),LBA),(L(88),NBA),(L(89),LBSA),(L(104),NRING),(L(105),NRI),(L(
7107),MRI),(L(113),MRING),(L(114),LBR),(L(121),N8R),(L(122),LBSR),(
8L(133),ITERM),(L(134),IPR),(L(135),IPU),(L(136),ITER),(L(137),N34)
9,(L(138),N35),(L(139),LB1),(L(140),LB2),(L(141),LB3),(L(142),LB5)
 EQUIVALENCE (L(143),N100),(L(144),N101),(L(145),M80,II),(L(146),M8
11),(L(147),NN),(L(152),NPO),(L(163),NAA),(L(164),NCR),(L(165),NSKP
2),(L(166),MODEH),(L(167),ITEST),(L(168),MAXIA),(L(169),MRIN)
 EQUIVALENCE (ZSTO(1),AMAT),(ZSTO(31),BMAT),(ZSTO(311),BUCKCH),(ZST
1O(295),C),(ZSTO(300),DELT,H1),(ZSTO(301),P1),(ZSTO(302),ENK1),(ZST
2O(303),PK1),(ZSTO(304),ENK2),(ZSTO(305).PK2),(ZSTO(306),Q1),(ZSTO(
3307),Q2),(ZSTO(308),POWER2),(ZSTO(309),FRACZ),(ZSTO(310),DTC22),(Z
4STO(311),D2),(ZSTO(312),PISIGN),(ZSTO(313),GSQP),(ZSTO(314),GSQE),
5(ZSTO(315),H3),(ZSTO(316),P3),(ZSTO(317),DZ1),(ZSTO(318),DZ2),(ZST
6O(319),TW2),(ZSTO(320),RH2),(ZSTO(321),R1),(ZSTO(322),HD),(ZSTO(32
73),GHD),(ZSTO(324),FLOC),(ZSTO(325),AH1),(ZSTO(326),AP1),(ZSTO(327
8),ERRH1),(ZSTO(328),ERRH2),(ZSTO(329),ERRP1),(ZSTO(330),ERRP2),(ZS
9TO(331),XXX),(ZSTO(332),XINT),(ZSTO(333),VINT),(ZSTO(334),TCL1)
 EQUIVALENCE (ZSTO(335),TCV1),(ZSTO(336),VISV1),(ZSTO(337),E1),(ZST
1O(338),E2),(ZSTO(339),E3),(ZSTO(340),E4),(ZSTO(341),V1),(ZSTO(342)
2,V2),(ZSTO(343),V3),(ZSTO(344),V4),(ZSTO(345),PS),(ZSTO(346),TRED)
```

DIMENSION, COMMON AND EQUIVALENCE (Continued)

```
3,(ZSTO(347),TRED2),(ZSTO(348),TRED3),(ZSTO(349),TE),(ZSTO(350),ENT
4),(ZSTO(351),VOLUM),(ZSTO(363),DIFCH),(ZSTO(447),DPHI,POWP),(ZSTO(
5649),DPHO,POWR),(ZSTO(663),DUMMY),(ZSTO(699),FRACT),(ZSTO(735),HT)
6,(ZSTO(737),PHI),(ZSTO(939),RHTR),(ZSTO(941),TERM),(ZSTO(1085),U),
7(ZSTO(1274),TWOGJ),(ZSTO(1275),TWOG),(ZSTO(1276),FULOG),(ZSTO(352)
8,ARAT),(ZSTO(353),DNB2)
```

CHAIN LINK (1, B1)

```
*     CHAIN(1,B1)
*     LIST
*     FORTRAN
*     LABEL
CCFR1  - STEADY STATE NUCLEAR / POWER PROGRAM
      DIMENSION
      COMMON
      EQUIVALENCE
    1 FORMAT (80H
     1                                    )
    2 FORMAT (F10.4)
    3 READ 2.A1
      IF(A1)11,11,10
   10 CALL START
   11 READ INPUT TAPE ITAI,1
      WRITE OUTPUT TAPE ITAO,1
      ITA3=0
   12 CALL DATIN
      IF(N100)13,13,3
   13 CALL DAPR
   14 CALL BEGIN
      C1=334722E-2
      TRANSW=C1*TRANSW
      DO 15J=1,NOG
      VUSIGW(J)=C1*VUSIGW(J)
      SIGAW(J)=C1*SIGAW(J)
   15 SIGTRW(J)=C1*SIGTRW(J)
      WRITE OUTPUT TAPE ITAO,1
      IF(POW1)16,16,19
   16 ITEST=1
      H2=HPUMP
      P2=PPUMP
   17 CALL THERMO
      C1=1.0/(62.43*(QUAL2*VV2+(1.0-QUAL2)*VL2))
      DO 18K=1.2
      DO 18J=1,MAXIAL
      DO 18I=1,MRI
   18 DEN(I,J,K)=C1
   19 ITER=0
  500 CALL CHAIN(2,B2)
      END
```

CHAIN LINK (1,B1) - Continued.

```
*     LIST
*     FORTRAN
*     LABEL
      SUBROUTINE START
      DIMENSION
      COMMON
      EQUIVALENCE
C
C     SET A AND L MATRICES = 0
C
      DO 1I=1,2512
    1 A(I)=0.0
      DO 2I=1,169
    2 L(I)=0
C
C     DEFINE FISSION SPECTRUM
C
      DO 3I=1,7
    3 CHI(I,1)=1.0
C
C     SET UP EXTRAPOLATION FACTOR,NUMBER OF GROUPS FOR DOWNSCATTERING,
C     NUMBER OF GROUPS,NUMBER OF ITERATIONS FOR FLUX AND CRITICALITY
C     SEARCHES AND POWER DISTRIBUTION
      THETA=0.8
    4 NOG=2
      NDS=1
    5 ITERM=25
      L(134)=1
      L(162)=5
    6 RUSQ=0.0
      A(1343)=1.0
    7 DO 8I=1,3
      J=30+33*I
      L(J)=50
      J=J+1
    8 L(J)=15
C
C     SET UP TAPE NUMBERS
C     ITAI=INPUT TAPE          ITAO=OUTPUT TAPE
C
      ITAI=4
      ITAO=2
C
C
      DO 9I=65,131,33
    9 L(I)=1
C
C     READ IN STEAM TABLES
C
   10 FORMAT (8F10.4)
   11 FORMAT (4F10.4)
   12 FORMAT (2F12.5)
      READ INPUT TAPE ITAI,10,(TSAT(I),PSAT(I),VF(I),VG(I),HF(I),HG(I),S
     1F(I),SG(I),I=1,123)
```

```
      READ INPUT TAPE ITAI,11,((TSUP(1),PSUP(J),VSUP(I,J),HSUP(I,J),J=1,
     129),I=1,14
      READ INPUT TAPE ITAI,12,DNBMAX,ENOZ
C
  500 RETURN
      END

*     LIST
*     FORTRAN
*     LABEL
      SUBROUTINE DATIN
      DIMENSION
      COMMON
      EQUIVALENCE
      N100=0
    1 CALL DATA1
      IF(N100)2,2,5
    2 CALL DATA2
      IF(N100)3,3,5
    3 CALL DATA3
      IF(N100)4,4,5
    4 CALL DATA4
      IF(N100)500,500,5
    5 READ INPUT TAPE ITAI,6
    6 FORMAT (1H)
  500 RETURN
      END

*     LIST
*     FORTRAN
*     LABEL
      SUBROUTINE DATA1
      DIMENSION
      COMMON
      EQUIVALENCE
    1 FORMAT (2I1,I10,5I12)
    2 FORMAT (2I1,I10,5E12.5)
    3 FORMAT (60H0    ERROR, ADDRESS FORMAT FOR FIXED POINT DATA CARD NU
     1MBER I3)
    4 FORMAT (63H0    ERROR, ADDRESS FORMAT FOR FLOATING POINT DATA DARD
     1 NUMBER I3)
      K=0
   31 K=K+1
      READ INPUT TAPE ITAI,1,NR,LC,NA,(NN(I),I=1,5)
      IF(NR)32,32,33
   32 WRITE OUTPUT TAPE ITAO,3,K
      N100=1
      GO TO 37
   33 IF(NR-5)34,34,32
   34 IF(NA)32,32,35
   35 NA=NA-1
      DO 36I=1,NR
      J=NA+1
   36 L(J)=NN(I)
```

```
   37 IF(LC)31,31,38
   38 K=0
   39 K=K+1
      READ INPUT TAPE ITAI,2,NR,LC,NA,(C(I),I=1.5)
      IF (NR)40,40,41
   40 WRITE OUTPUT TAPE ITAO,4,K
      N100=1
      GO TO 45
   41 IF(NR-5)42,42,40
   42 IF(NA)40,40,43
   43 NA=NA-1
      DO 44I=1,NR
      J=NA+I
   44 A(J)=C(I)
   45 IF(LC)39,39,500
  500 RETURN
      END

*     LIST
*     FORTRAN
*     LABEL
      SUBROUTINE DATA2
      DIMENSION
      COMMON
      EQUIVALENCE
    5 FORMAT (22H0    ERROR, ADDRESS L(I3,48H), NUMBER OF CELL REGIONS M
     1UST BE EQUAL TO SEVEN)
    6 FORMAT (22H0    ERROR, ADDRESS L(I3,65H), NUMBER OF AXIAL REGIONS
     1MUST BE EQUAL TO OR GREATER THAN THREE)
    7 FORMAT (22H0    ERROR, ADDRESS L(I3,64H), NUMBER OF RADIAL REGIONS
     1 MUST BE EQUAL TO OR GREATER THAN TWO)
    8 FORMAT (22H0    ERROR, ADDRESS L(I3,32H), NUMBER OF REGIONS IS TOO
     1LARGE)
    9 FORMAT (22H0    ERROR, ADDRESS L(I3,38H), NUMBER OF SPACE POINTS 1
     1S TOO LARGE)
   10 FORMAT (22H0    ERROR, ADDRESS L(I3,32H), INTERFACE NUMBERS MUST B
     1E ODD)
   11 FORMAT (22H0    ERROR, ADDRESS L(I3,42H), NUMBER OF POINTS IN REGI
     1ON IS TOO LARGE)
   12 FORMAT (22H0    ERROR, ADDRESS L(I3,42H), NUMBER OF POINTS IN REGI
     1ON IS TOO SMALL)
   13 FORMAT (22H0    ERROR, ADDRESS L(I3,41H), NUMBER OF CONTROL REGION
     1S IS TOO LARGE)
   14 FORMAT (22H0    ERROR, ADDRESS L(I3,45H), CONTROL REGIONS MUST BE
     1IN ASCENDING ORDER)
  145 FORMAT (22H0    ERROR, ADDRESS L(I3,35H), CRITICALITY OPTION NOT S
     1PECIFIED)
C
C     FIXED POINT DATA CHECK
C
   47 IF(L(47)-7)48,49,48
   48 I=47
      WRITE OUTPUT TAPE ITAO,5,1
      N100=1
```

CHAIN LINK (1,B1) - Continued.

```
   49 IF(L(80)-3)50,51,51
   50 I=80
      WRITE OUTPUT TAPE ITAO,6,1
      N100=1
   51 IF(L(113)-2)52,53,53
   52 I=113
      WRITE OUTPUT TAPE ITAO,6,1
      N100=1
   53 DO 70NR=1,3
      NCR=33*NR
      J=NCR+13
      DO 54I=14,29
      J=J+1
   54 L(I)=L(J)
      M=M
      IF(M-7)56,56,55
   55 J=14+NCR
      WRITE OUTPUT TAPE ITAO,8,J
      N100=1
   56 LB1=LB(M)
      IF(LB1-101)58,58,57
   57 J=14+M+NCR
      WRITE OUTPUT TAPE ITAO,9,J
      N100=1
   58 DO 60I=1,M
      LB1=LB(I)/2
      LB1=2*LB1
      IF(LB1-LB(I))60,59,59
   59 J=14+I+NCR
      WRITE OUTPUT TAPE ITAO,10,J
      N100=1
   60 CONTINUE
      LB1=1
      DO 64I=1,M
      LB2=LB(I)-LB1
      J=14+I+NCR
      IF(NR-1)601,601,62
  601 IF(I-3)62,602,62
  602 IF(LB2-20)62,64,61
   61 WRITE OUTPUT TAPE ITAO,11,J
      N100=1
      GO TO 64
   62 IF(LB2-6)63,64,64
   63 WRITE OUTPUT TAPE ITAO,12,J
      N100=1
   64 LB1=LB(I)
      IF(N8-M)66,66,65
   65 J=22+NCR
      WRITE OUTPUT TAPE ITAO,13,J
      N100=1
   66 IF(N8)70,70,67
   67 LB1=0
      DO 69I=1,NB
      IF(LBS(I)-LB1)68,68,69
```

CHAIN LINK (1,B1) - Continued.

```
   68 J=22+I+NCR
      WRITE OUTPUT TAPE ITAO,14,J
      N100=1
   69 LB1=LBS(I)
   70 CONTINUE
      IF(L(132))701,701,500
  701 K=132
      WRITE OUTPUT TAPE ITAO,145,K
      N100=1
  500 RETURN
      END

*     LIST
*     FORTRAN
*     LABEL
      SUBROUTINE DATA3
      DIMENSION
      COMMON
      EQUIVALENCE
C
C     FLOATING POINT DATA CHECK OF NUCLEAR DATA
C
   15 FORMAT (70HO    ERROR, NO POSITIVE VALUES OF NU*SIGMA FISSION FOR
     1CELL OR COOLANT)
   16 FORMAT (22HO    ERROR, ADDRESS A(I4,31H), NU*SIGMA FISSION IS NEGA
     1TIVE)
   17 FORMAT (72HO    ERROR, NO POSITIVE VALUES OF SIGMA TRANSFER FROM G
     1ROUP 1 TO GROUP 2/24H      FOR CELL OR COOLANT)
   18 FORMAT (22HO    ERROR, ADDRESS A(I4,38H), SIGMA TRANSFER (1 TO 2)
     1IS NEGATIVE)
   19 FORMAT (70HO    ERROR, NO POSITIVE VALUES OF SIGMA ABSORPTION FOR
     1CELL OR COOLANT)
   20 FORMAT (22HO    ERROR, ADDRESS A(I4,31H), SIGMA ABSORPTION IS NEGA
     1TIVE)
   21 FORMAT (22HO    ERROR, ADDRESS A(I4,41H), DIFFUSION COEFFICIENT IS
     1 ZERO/NEGATIVE)
   22 FORMAT (22HO    ERROR, ADDRESS A(I4,43H), COOLANT SIGMA TRANSPORT
     1IS ZERO/NEGATIVE)
   23 FORMAT (22HO    ERROR, ADDRESS A(I4,31H), NU*SIGMA FISSION IS POSI
     1TIVE/22H         ADDRESS A(I4,22H), NU IS ZERO/NEGATIVE)
   24 FORMAT (22HO    ERROR, ADDRESS A(I4,27H), SIGMA POISON IS NEGATIVE
     1)
   25 FORMAT (22HO    ERROR, ADDRESS A(I4,41H), POISON CROSS SECTION RAT
     1IO IS NEGATIVE)
  255 FORMAT (22HO    ERROR, ADDRESS A(I4,30H), EIGENVALUE MUST BE POSIT
     1IVE)
  702 M=MCELL
      J=458
      DO 71I=1,72
      J=J+1
   71 A(I)=A(J)
      DO 73J=1,NOG
      DO 72I=1,M
      IF(VUSIG(I,J))72,72,74
```

CHAIN LINK (1,B1) - Continued.

```
72 CONTINUE
   IF(VUSIGW(J))73,73,74
73 CONTINUE
   WRITE OUTPUT TAPE ITAO,15
   N100=1
74 DO 78J=1,NOG
   DO 76I=1,M
   IF(VUSIG(I,J))75,76,76
75 K=45+I+7*J
   WRITE OUTPUT TAPE ITAO,16,K
   N100=1
76 CONTINUE
   IF(VUSIGW(J))77,78,78
77 K=1714+J
   WRITE OUTPUT TAPE ITAO,16,K
   N100=1
78 CONTINUE
   DO 79I=1,M
   IF(TRANS(I,1,2))79,79,81
79 CONTINUE
   IF(TRANSW)80,80,81
80 WRITE OUTPUT TAPE ITAO,17
   N100=1
81 DO 83I=1,M
   IF(TRANS(I,1,2))82,83,83
82 K=486+1
   WRITE OUTPUT TAPE ITAO,18,K
   N100=1
83 CONTINUE
   IF(TRANSW)84,85,85
84 K=1719
   WRITE OUTPUT TAPE ITAO,18,K
   N100=1
85 DO 87J=1,NOG
   DO 86I=1,M
   IF(SIGA(I,J))86,86,88
86 CONTINUE
   IF(SIGAW(J))87,87,88
87 CONTINUE
   WRITE OUTPUT TAPE ITAO,19
   N100=1
88 DO 92J=1,NOG
   DO 90I=1,M
   IF(SIGA(I,J))89,90,90
89 K=486+I+7*J
   WRITE OUTPUT TAPE ITAO,20,K
   N100=1
90 CONTINUE
   IF(SIGAW(J))91,92,92
91 K=1719+J
   WRITE OUTPUT TAPE ITAO,20,K
   N10C=1
92 CONTINUE
```

CHAIN LINK (1,B1) - Continued.

```
      DO 97J=1,NOG
      DO 95I=2,M
      IF(I-5)93,95,93
   93 IF(DIF(I,J))94,94,95
   94 K=500+I+7*J
      WRITE OUTPUT TAPE ITAO,21,K
      N100=1
   95 CONTINUE
      IF(SIGTRW(J))96,96,97
   96 K=1721+J
      WRITE OUTPUT TAPE ITAO,22,K
      N100=1
   97 CONTINUE
      DO 105J=1,NOG
      DO 102I=2,M
      IF(I-5)98,102,98
   98 IF(VUSIG(I,J))102,102,99
   99 IF(VU(I,J))100,100,102
  100 K=451+I+7*J
      M80=14+K
      WRITE OUTPUT TAPE ITAO,23,K,M80
      N100=1
  102 CONTINUE
      IF(VUSIGW(J))105,105,103
  103 IF(VUW(J))104,104,105
  104 K=1714+J
      M80=K+2
      WRITE OUTPUT TAPE ITAO,23,K,M80
      N100=1
  105 CONTINUE
      DO 109NA=1,3
      NCR=522+406*(NA-1)
      NAA=6+NCR
      DO 107I=NCR,NAA
      IF(A(I))106,107,107
  106 K=I+NCR-1
      WRITE OUTPUT TAPE ITAO,24,K
      N100=1
  107 CONTINUE
      NAA=NAA+1
      IF(A(NAA))108,109,109
  108 WRITE OUTPUT TAPE ITAO,25,NAA
      N100=1
  109 CONTINUE
      IF(A(1343))1095,1095,500
 1095 K=1343
      WRITE OUTPUT TAPE ITAO,255,K
      N100=1
  500 RETURN
      END
```

CHAIN LINK (1, B1) - Continued.

```
*     LIST
*     FORTRAN
*     LABEL
      SUBROUTINE DATA4
      DIMENSION
      COMMON
      EQUIVALENCE
   26 FORMAT (22HO    ERROR, ADDRESS A(I4,15H), VALUE OF ESPI1,13H IS TO
     1O SMALL)
   27 FORMAT (22HO    ERROR, ADDRESS A(I4,36H), PUMP EXHAUST PRESSURE IS
     1 TOO HIGH)
   28 FORMAT (22HO    ERROR, ADDRESS A(I4,35H), PUMP EXHAUST ENTHALPY IS
     1 TOO LOW)
   29 FORMAT (22HO    ERROR, ADDRESS A(I4,59H), QUANTITY MUST BE POSITIV
     1E FOR NON-ZERO POWER CALCULATION)
   30 FORMAT (22HO    ERROR, ADDRESS A(I4,43H), GEOMETRICAL DISTANCES MU
     1ST BE INCREASING)
C
C     TEST OF CONVERGENCE LIMITS
C
 1096 DO 111I=1,3
      J=1723+I
      IF(A(J)-0.00001)110,111,111
  110 WRITE OUTPUT TAPE ITAO,26,J,I
      N100=1
  111 CONTINUE
C
C     TEST OF PUMP EXHAUST PROPERTIES
C
      J=1736
      IF(A(J)-2000.0)113,113,112
  112 WRITE OUTPUT TAPE ITAO,27,J
      N100=1
  113 J=1737
      IF(A(J)-68.0)114,115,115
  114 WRITE OUTPUT TAPE ITAO,28,J
      N100=1
  115 IF(POW1)1185,1185,116
C
C     TEST OF HEAT TRANSFER PROPERTIES
C
  116 DO 118J=1729,1734
      IF(A(J)117,117,118
  117 WRITE OUTPUT TAPE ITAO,29,J
      N100=1
  118 CONTINUE
C
C     TEST OF GEOMETRICAL INPUTS
C
 1185 DO 121J=1.3
      R1=0.0
      K=14+33*J
      M=L(K)
```

```
      DO 120I=1,M
      IF(RINT(I,J)-R1)119,119,120
  119 K=1732+I+7*J
      WRITE OUTPUT TAPE ITAO,30,K
      N100=1
  120 R1=RINT (I,J)
  121 CONTINUE
  500 RETURN
      END

*     LIST
*     FORTRAN
*     LABEL
      SUBROUTINE DAPR
      DIMENSION
      COMMON
      EQUIVALENCE
    1 FORMAT (59H5                  POWER/HEAT TRANSFER/THERMODYNAMIC PROPER
     1TIES//46H      POWER GENERATION RATE                        1PE13.5,7H
     2BTU/HR/46H      INLET PLENUM PRESSURE                       1PE13.5,11
     3H PSIA      /46H      INLET PLENUM ENTHALPY                       1PE1
     43.5,7H BTU/LB)
    2 FORMAT (38H      COOLANT FLOW RATE OUT SECOND PASS1PE32.5,6H LB/HR/
     140H      ADDITIONAL FIRST PASS FLOW FRACTIONOPF30.5/53H      FIRST P
     2ASS NOZZLE/ORIFICE AREA CONTRACTION RATIOF17.5/54H      SECOND PASS
     3 NOZZLE/ORIFICE AREA CONTRACTION RATIOF16.5/43H      THERMAL CONDUC
     4TIVITY OF INNER CLADDING1PE27.5,18H BTU/HR/FT/(DEG F)/33H      THER
     5MAL CONDUCTIVITY OF FUELE37.5,18H BTU/HR/FT/(DEG F)/43H      THERMA
     6L CONDUCTIVITY OF OUTER CLADDINGE27.5,18H BTU/HR/FT/(DEG F)/40H
     7  INTERFACE HEAT TRANSFER COEFFICIENTE30.5,23H BTU/HR/(FT**2)/(DEG
     8 F)//21H      DRY CORE DENSITYE39.5,11H LB/(FT**3)/29H      RADIAL R
     9EFLECTOR DENSITYE41.5,11H LB/(FT**31))
    3 FORMAT (49HE                                  GEOMETRICAL INPUTS/70HO
     1                CELL                     AXIAL                   RADI
     2AL/78H     REGION  INTERFACE  DISTANCE    INTERFACE  DISTANCE    I
     3NTERFACE  DISTANCE/76H     NUMBER   NUMBER      (CMS)        NUMBER
     4     (CMS)       NUMBER     (CMS))
    4 FORMAT (1H I7,I10,1PE15.5,2(I8,E15.5))
    5 FORMAT (1H I7,I10,1PE15.5,I31,E15.5)
    6 FORMAT (1H I7,I10,1PE15.5,I8,E15.5)
    7 FORMAT (1H I7,I10,1PE15.5)
    8 FORMAT (59H1                        NUCLEAR MICROSCOPIC COOLANT PROPER
     1TIES/61H                                   GROUP 1               GROU
     2P 2/21H      NU*SIGMA FISSION1PE23.5,E20.5/7H      NUE37.5,E20.5/21H
     3      SIGMA ABSORPTIONE23.5,E20.5/20H      SIGMA TRANSPORTE24.5,E20.
     45/28H      SIGMA TRANSFER (1 TO 2)E16.5)
    9 FORMAT (57H3                        NUCLEAR MACROSCOPIC CELL PROPERTI
     1ES/61H                                   GROUP 1               GROUP
     22)
   10 FORMAT (26HO                      REGIONI2/21H      NU*SIGMA FISSION1P
     1E23.5,E20.5/7H      NUE37.5,E20.5/21H      SIGMA ABSORPTIONE23.5,E20
     2.5/26H      DIFFUSION COEFFICIENTE18.5,E20.5/28H      SIGMA TRANSFER
     3 (1 TO 2)E16.5)
```

```
  105 FORMAT (41H1     THE EIGENVALUE TO BE SEARCHED FOR IS1PE15.5)
   11 FORMAT (70H0     POISON CRITICALITY SEARCH        REGIONS -
    1              )
   12 FORMAT (70H+                                   CELL
    1              )
   14 FORMAT (70H+                                   RADIAL
    1              )
   15 FORMAT (70H+
    1IN ALL REGIONS )
   16 FORMAT (47H+
   17 FORMAT (42H0     REGION          SIGMA POISON (GROUP 2))
   18 FORMAT (1H I7,1PE29.51)
   19 FORMAT (53H0     RATIO OF POISON CROSS SECTIONS (GROUP 1/GROUP 2)1P
    1E19.5)
   20 FORMAT (56H3                                  CELL       AXIAL      RADIA
    1L)
   21 FORMAT (25H      CONVERGENCE TESTING I7,111,110)
   22 FORMAT (38H0     MAXIMUM NUMBER OF FLUX ITERATIONSI22/45H      MAXIM
    1UM NUMBER OF CRITICALITY ITERATIONSI15/51H     MAXIMUM NUMBER OF E
    2NTHALPY/PRESSURE ITERATIONSI9/36H     MAXIMUM NUMBER OF RADIAL SWE
    3EPS124///22H      FLOW INLET OPTIONI38/24H      BLOCKED FLOW OPTION1
    436/24H      BLOCKED SIDE OPTION136/26H      BLOCKED REGION OPTIONI34
    5)
   23 FORMAT (31H0     CONVERGENCE LIMIT FOR FLUX1PE29.5/38H      CONVERGE
    1NCE LIMIT FOR CRITICALITYE22.5/32H     CONVERGENCE LIMIT FOR POWER
    2E28.5)
C
C
C
      WRITE OUTPUT TAPE ITAO,1,POW1,PPUMP,HPUMP
      IF(POW1)25,25,24
   24 WRITE OUTPUT TAPE ITAO,2,FLO,RECIRC,HOUT,RATI,TCIN,TCFU,TCOU,HINT,
    1DCDEN,RRDEN
   25 WRITE OUTPUT TAPE ITAO,3
      IF (MAXIAL-MRING)26,27,28
   26 LB2=MAXIAL
      N1=1
      GO TO 29
   27 LB2=MAXIAL
      N1=2
      GO TO 29
   28 LB2=MRING
      N1=3
   29 DO 30I=1,LB2
   30 WRITE OUTPUT TAPE ITAO,4,I,LBC(I),RINT(I,1),LBA(I),RINT(I,2),LBR(I
    1),RINT(I,3)
      LB1=LB@+1
   31 IF(LB)-MCELL)32,32,39
   32 IF(N1-2)33,35,37
   33 LB2=MRING
      DO 34I=LB1,LB2
   34 WRITE OUTPUT TAPE ITAO,5,I,LBC(I),RINT(I,1),BR(I),RINT(I,3)
      LB1=LB2+1
      N1=2
      GO TO 31
```

```
   35 LB2=MCELL
      DO 36I=LB1,LB2
   36 WRITE OUTPUT TAPE ITAO,7,I,LBC(I),RINT(I,1)
      GO TO 39
   37 LB2=MAXIAL
      DO 38I=LB1,LB2
   38 WRITE OUTPUT TAPE ITAO,6,I,LBC(I),RINT(I,1),LBA(I),RINT(I,2)
      LB1=LB2+1
      N1=2
      GO TO 31
   39 WRITE OUTPUT TAPE ITAO,8,VUSIGW(1),VUSIGW(2),VUW(1),VUW(2),SIGAW(1
     1),SIGAW(2),SIGTRW(1),SIGTRW(2),TRANSW
      WRITE OUTPUT TAPE ITAO,9
      DO 41I=2,MCELL
      IF(I-5)40,41,40
   40 WRITE OUTPUT TAPE ITAO,10,I,VUSIGC(I,1),VUSIGC(I,2),VUC(I,1),VUC(I
     1,2),SIGAC(I,1),SIGAC(I,2),DIFC(I,1),DIFC(I,2),TRANSC(I,1,2)
   41 CONTINUE
      I=1343
      WRITE OUTPUT TAPE ITAO,105,A(I)
      WRITE OUTPUT TAPE ITAO,11
      N5=L(132)
      J=13+33*N5
      DO 42I=14,29
      J=J+1
   42 L(I)=L(J)
      J=115+406*N5
      M80=J+1
      DO 43I=64,72
      J=J+1
   43 A(I)=A(J)
      IF(N5-1)44,44,46
   44 WRITE OUTPUT TAPE ITAO,12
      GO TO 47
   46 WRITE OUTPUT TAPE ITAO,14
   47 IF(N8)48,48,49
   48 WRITE OUTPUT TAPE ITAO,15
      N8=M
      LB1=22+33*N5
      L(LB1)=M
      LB2=M80-1
      DO 481I=1,M
      LB1=LB1+1
      LB2=LB2+1
      A(LB2)=A(M80)
      LBS(I)=1
  481 L(LB1)=I
      GO TO 50
   49 WRITE OUTPUT TAPE ITAO,16,(LBS(I),I=1,N8)
   50 WRITE OUTPUT TAPE ITAO,17
      DO 501I=1,N8
      LB1=LBS(I)
  501 WRITE OUTPUT TAPE ITAO,18,LB1,SIGPT(LB1)
      WRITE OUTPUT TAPE ITAO,19,T(1)
      WRITE OUTPUT TAPE ITAO,20
      WRITE OUTPUT TAPE ITAO,21,L(65),L(98),L(131)
```

CHAIN LINK (1,B1) - Continued.

```
      MICT=L(129)
      MICT2=L(130)
      WRITE OUTPUT TAPE ITAO,22,MICT,MICT2,ITERM,L(162),(L(I),I=152,155)
      WRITE OUTPUT TAPE ITAO,23,ESP1,ESP2,ESP3
      RETURN
      END

*     LIST
*     FORTRAN
*     LABEL
      SUBROUTINE BEGIN
      DIMENSION
      COMMON
      EQUIVALENCE
C
C     SET FIXED OPTIONS
C     C
C     N1,N2,N3,N7,N5,
C
      L(34)=2
      L(67)=1
      L(100)=2
      L(35)=1
      L(68)=2
      L(101)=1
      L(36)=2
      L(69)=1
      L(102)=1
      L(37)=1
      L(70)=2
      L(103)=3
      L(66)=0
      L(99)=0
C
C     POINTWISE DISTANCES AND N,NM1,NM2,MM1
C
      DO 11I=1,3
      R(1)=0.0
      J=13+33*I
      DO 1K=14,21
      J=J+1
    1 L(K)=L(J)
      SUM1=0.0
      M80=1
      LB1=2
      DO 3J=1,M
      K=LB(J)
      R(K)=RINT(J,I)
      SUM2=K-M80
      LB2=K-1
      DELR(J)=(R(K)-SUM1)/SUM2
      DO 2K=LB1,LB2
```

```
    2 R(K)=R(K-1)+DELR(J)
      LB1=LB2+2
      M80=LB2+1
    3 SUM1=R(M80)
      J=530+406*(I-1)
      A(J)=1.0
      M=M
      MM1=M-1
      N=LB(M)
      NM1=N-1
      NM2=N-2
      M80=5+33*1
      M81=M80+3
      J=4
      DO 4K=M80,M81
      J=J+1
    4 L(K)=L(J)
      IF(I-2)5,7,5
    5 P=1.0
      PIM=6.2831853
      DO 6K=1,N
    6 RI(K)=R(K)
      GO TO 9
    7 P+0.0
      PIM=1.0
      DO 8K=1,N
    8 RI(K)=1.0
    9 M80=126+406*I
      M81=210+M80
      J=73
      DO 10K=M80,M81
      J=J+1
   10 A(K)=A(J)
   11 CONTINUE
C
C     AMAT
C
      LB1=LBC(2)
      LB2=LBC(3)
      J=0
      DO 12I=LB1,LB2
      J=J+1
      U(1,J)=1.0
      U(2,J)=(3.2808E-2)*RC(1)
      DO 12K=3.9
   12 U(K,J)=U(K-1,J)*U(2,J)
      M80=1+LB2-LB1
      DO 13I=1.9
      G(I)=0.0
      DO 13J=1,M80
   13 G(I)=G(I)+U(I,J)
      DO 14I=1,5
      DO 14J=1,5
```

```
      K=I+J-1
   14 AMAT(I,J)=G(K)
      DO 20I=1,5
      DO 20J=1,5
      K=1
      IF(I-J)15,18,18
   15 AMAT(I,J)=AMAT(I,J)/AMAT(I,I)
   16 IF(K-I)17,20,20
   17 AMAT(I,J)=AMAT(I,J)-AMAT(I,K)*AMAT(K,J)/AMAT(I,1)
      K=K+1
      GO TO 16
   18 IF(K-J)19,20,20
   19 AMAT(I,J)=AMAT(I,J)-AMAT(I,K)*AMAT(K,J)
      K=K+1
      GO TO 18
   20 CONTINUE
C
C     DEFINE THE RADIAL REFLECTOR PROPERTIES
C
      MCELL=MCELL
      MAXIAL=MAXIAL
      MRING=MRING
      BUCK2R(MRING,1)=(3.14159265/RINT(MAXIAL,2))**2
      BUCK2R(MRING,2)=BUCK2R(MRING,1)
C
C     FIRST GUESS FOR CHANNEL BUCKLING TERMS
C
      DO 23K=1,NOG
      DO 23J=1,MAXIAL
      DO 23I=1,MRI
   23 BUCKCH(I,J,K)=0.0
C
C     GENERATE SOURCE TERMS
C
      DO 24I=1,101
      SOUC(I)=0.0
      SOUA(I)=0.0
   24 SOUR(I)=0.0
      LB1=LBC(2)+1
      LB2=LBC(3)-1
      C1=1.0/(3.14159265*(RINT(3,1)*RINT(3,1)-RINT(2,1)*RINT(2,1)))
      DO 25I=LB1,LB2
   25 SOUC(I)=C1
      MAXI=MAXI
      LB1=LBA(1)+1
      LB2=LBA(MAXI)-1
      C1=1.0/(RINT(MAXI,2)-RINT(1,2))
      DO 26I=LB1,LB2
   26 SOUA(I)=C1
      MRI=MRI
      LB2=LBR(MRI)-1
      C1=1.0/(3.14159265*RINT(MR1,3)*RINT(MRI,3))
```

CHAIN LINK (1,B1) - Continued.

```
      DO 27I=1,LB2
   27 SOUR(I)=C1
C
  500 RETURN
      END
*     LIST
*     FORTRAN
*     LABEL
      SUBROUTINE THERMO
      DIMENSION
      COMMON
      EQUIVALENCE
C     INTERPOLATION CALCULATION
C
      LLLLL=1
      IHEAT=2
      XXX=P2
    1 JSAT=123*IHEAT
      XINT=JSAT
      VINT=HEAT(JSAT)
      ISAT=JSAT-122
    2 VISL1=ISAT
      ISAT=(1.0+VISL)+(XINT-VISL1)*(XXX-HEAT(ISAT))/(VINT-HEAT(ISAT))
      IF(HEAT(ISAT)-XXX)2,2,3
    3 JSAT=ISAT-1
      IF(HEAT(JSAT)-XXX)5,5,4
    4 ISAT=ISAT-1
      GO TO 3
    5 XINT=(XXX-HEAT(JSAT))/(HEAT(ISAT)-HEAT(JSAT))
      ISAT=ISAT-123*(IHEAT-1)
      JSAT=ISAT-1
      IF(LLLLL-1)10,10,58
   10 IF(IHEAT-2)11,11,13
   11 TSATU2=TSAT(JSAT)+XINT*(TSAT(ISAT)-TSAT(JSAT))
      HL2=HF(JSAT)+XINT*(HF(ISAT)-HF(JSAT))
      HV2=HG(JSAT)+XINT*(HG(ISAT)-HG(JSAT))
      IF(HL2-H2)16,17,12
   12 MODEH=1
      QUAL2=0.0
      VOID2=0.0
      IHEAT=5
      XXX=H2
      GO TO 1
   13 T2=TSAT(JSAT)+XINT*(TSAT(ISAT)-TSAT(JSAT))
   14 CL2=(HF(ISAT)-HF(JSAT))/(TSAT(ISAT)-TSAT(JSAT))
      ISUP=0
      JSUP=P2/50.0
  141 IF(PSUP(JSUP)-P2)142,142,143
  142 JSUP=JSUP+1
      GO TO 141
  143 ISUP=ISUP+1
      IF(HSUP(ISUP,JSUP))143,143,144
```

```
 144 VINT=(P2-PSUP(JSUP-1))/(PSUP(JSUP)-PSUP(JSUP-1))
     VISL1=HSUP(ISUP,JSUP-1)+VINT*(HSUP(ISUP,JSUP)-HSUP(ISUP,JSUP-1))
     CV2=(VISL1-HV2)/(TSUP(ISUP)-TSATU2)
     VL2=VF(JSAT)+XINT*(VF(ISAT)-VF(JSAT))
     VV2=VG(JSAT)+XINT*(VG(ISAT)-VG(JSAT))
     IF(MODEH-1)100,100,15
  15 QUAL2=(H2-HL2)/(HV2-HL2)
     VOID2=(0.833+0.167*QUAL2)*(QUAL2*VV2)/(VL2+QUAL2*(VV2-VL2))
     GO TO 100
  16 IF(HV2-H2)50,17,17
  17 MODEH=2
     T2-TSATU2
     GO TO 14
  50 MODEH=3
     QUAL2=1.0
     VOID2=1.0
     JSUP=P2/50.0
  51 IF(PSUP(JSUP)-P2)52,52,53
  52 JSUP=JSUP+1
     GO TO 51
  53 ISUP=1
  54 IF(HSUP(ISUP,JSUP)-H2)55,55,56
  55 ISUP=ISUP+1
     GO TO 54
  56 E1=HSUP(ISUP-1,JSUP-1)
     V1=VSUP(ISUP-1,JSUP-1)
     E2=HSUP(ISUP-1,JSUP)
     V2=VSUP(ISUP-1,JSUP)
     E3=HSUP(ISUP,JSUP-1)
     V3-VSUP(ISUP,JSUP-1)
     E4=HSUP(ISUP,JSUP)
     V4=VSUP(ISUP,JSUP)
     IF(E2)57,57,62
  57 XXX=PSUP(JSUP)
     IHEAT=2
     LLLLL=2
     GO TO 1
  58 TE=TSAT(JSAT)+XINT*(TSAT(ISAT)-TSAT(JSAT))
     VOLUM=VG(JSAT)+XINT*(VG(ISAT)-VG(JSAT))
     ENT=HG(JSAT)+XINT*(HG(ISAT)-HG(JSAT))
     XINT=(TSUP(ISUP-1)-TE)/(TSUP(ISUP)-TE)
     IF(LLLLL-2)59,59,61
  59 E2=ENT+XINT*(HSUP(ISUP,JSUP)-ENT)
     V2=VOLUM+XINT*(VSUP(ISUP,JSUP)-VOLUM)
     IF(E1)60,60,62
  60 XXX=PSUP(JSUP-1)
     IHEAT=2
     LLLLL=3
     TO TO 1
  61 E1=ENT+XINT*(HSUP(ISUP,JSUP-1)-ENT)
     V1=VOLUM+XINT*(VSUP(ISUP,JSUP-1)-VOLUM)
  62 XINT=(P2-PSUP(JSUP-1))/(PSUP(JSUP)-PSUP(JSUP-1))
```

CHAIN LINK (1,B1) - Continued.

```
      E1=E1+XINT*(E2-E1)
      V1-V1+XINT*(V2-V1)
      E2=E3+XINT*(E4-E3)
      V2=V3+XINT*(V4-V3)
      XINT=(H2-E1)/(E2-E1)
      T2=TSUP(ISUP-1)+XINT*(TSUP(ISUP)-TSUP(ISUP-1))
      VV2=V1+XINT*(V2-V1)
      CV2=(E2-E1)/(TSUP(ISUP)-TSUP(ISUP-1))
  100 IF(ITEST)1000,1000,121
 1000 TRED=T2/100.0
      TRED2-TRED*TRED
      TRED3=TRED*TRED2
      IF(T2-705.4)150,151,151
  150 ISAT=(T2/5.0)-18.0
  101 JSAT=ISAT-1
      IF(TSAT(JSAT)-T2)103,103,102
  102 ISAT=ISAT-1
      GO TO 101
  103 XINT=(T2-TSAT(JSAT))/(TSAT(ISAT)-TSAT(JSAT))
      PS=PSAT(JSAT)+XINT*(PSAT(ISAT)-PSAT(JSAT))
  151 IF(MODEH-2)104,108,109
  104 IF(P2-1000.0)106,105,105
  105 TCL1=0.31533+0.061663*TRED-0.011357*TRED2+0.000068420*TRED3
      TCL2=0.32170+0.054882*TRED-0.0087762*TRED2-0.00016007*TRED3
      XINT=(P2-1000.0)/1000.0
      GO TO 107
  106 TCL1=0.31527+0.061374*TRED-0.011858*TRED2+0.00016320*TRED3
      TCL2=0.31533+0.061663*TRED-0.011357*TRED2+0.000068420*TRED3
      XINT=(P2-1000.0)/(PS-1000.0)
  107 TCL2=TCL1+XINT*(TCL2-TCL1)
      VISL2=3.0491-1.8409*TRED+0.40457*TRED2-0.029744*TRED3
      SURT2=(5.20406E-3)-(2.13922E-4)*TRED-(2.24004E)*TRED2+(3.43981E-
     15)*TRED3-(1.69209E-6)*(TRED*TRED3)
      TRED=(HV2-HL2)/)1000.0*VV2)
      IF(TRED-0.003)202,201,201
  201 RBL2=2.063E-3
      GO TO 121
  202 TRED2=TRED*TRED
      TRED3=TRED*TRED2
      RBL2=-(1.88225E-5)+(3.39739E-4)*TRED+(1.47490E-3)*TRED2-(8.19500E-
     14)*TRED3+(1.22556E-4)*(TRED*TRED3)
      GO TO 121
  108 TCV2=-0.0032887+0.013173*TRED-0.0031711*TRED2+0.00035368*TRED3
      VISV2=0.013192+0.014194*TRED-0.0035711*TRED2+0.00051849*TRED3
      GO TO 106
  109 IF(P2-1000.0)117,110,110
  110 TCV1=0.086720-0.020103*TRED+0.0022207*TRED2-0.000072108*TRED3
      VISV1=0.076922-0.0034264*TRED+00.00035689*TRED2+TRED3*9.3899E-9
      IF(T2-596.23)112,111,111
  111 TCV2=0.17027-0.043853*TRED+0.0044871*TRED2-0.00014428*TRED3
      XINT=(P2-1000.0)/1000.0
      GO TO 113
```

CHAIN LINK (1,B1) - Continued.

```
  112 TCV2=-0.0032887+0.013173*TRED-0.0031711*TRED2+0.00035368*TRED3
      XINT=(P2-1000.0)/(PS-1000.0)
  113 IF(T2-544.61)115,114,114
  114 VISV2=0.20737-0.036836*TRED+0.0037431*TRED2+0.00011943*TRED3
      VINT=(P2-1000.0)/500.0
      GO TO 120
  115 VINT=(P2-1000.0)/(PS-1000.0)
  116 VISV2-0.013192+0.014194*TRED-0.0035711*TRED2+0.0051849*TRED3
      GO TO 120
  117 TCV1=0.016393+0.00071136*TRED+0.00012148*TRED2-0.0000013415*TRED3
      VISV1=0.019394+0.0065459*TRED-0.00031585*TRED2+0.000012432*TRED3
      IF(T2-544.61)119,118,118
  118 TCV2=0.086720-0.020103*TRED+0.0022207*TRED2-0.000072108*TRED3
      XINT=(P2-250.0)/750.0
      VINT=P2/1000.0
      VISV2=0.076922-0.0034264*TRED+0.00035689*TRED2+TRED3*9.3899E-9
      GO TO 120
  119 TCV2=-0.0032887+0.013173*TRED-0.0031711*TRED2+0.00035368*TRED3
      XINT=(P2-250.0)/(PS-250.0)
      VINT=P2/PS
      GO TO 116
  120 TCV2=TCV1+XINT*(TCV2-TCV1)
      VISV2=VISV1+VINT*(VISV2-VISV1)
  121 RETURN
      END
```

CHAIN LINK (2,B2)

```
*     CHAIN (2,B2)
*     LIST
*     FORTRAN
*     LABEL
CCFR2 - STEADY STATE NUCLEAR/POWER PROGRAM
      DIMENSION
      COMMON
      EQUIVALENCE
    1 FORMAT (80H
     1                                )
    2 FORMAT (26H0    THE REACTOR POWER IS 1PE12.4,7H BTU/HR)
    3 FORMAT (69H1    CALCULATION FAILED, MAXIMUM NUMBER OF RADIAL ITERA
     1TIONS EXCEEDED)
  301 FORMAT (21H1    RADIAL ITERATIONI3)
      IF(NPO(1))302,302,303
  302 K1=0
      K2=1
      GO TO 304
  303 K1=3
      K2=-1
  304 MRI=MRI
      MAXI=MAXI
      MCELL=MCELL
      MAXIAL=MAXIAL
      SUM3=RINT(MRI,3)**2
```

```
      SUM2=0.0
      DO 4I=1,MRI
      SUM1=SUM2
      SUM2=RINT(I,3)**2
    4 DUMMY(I,1)=(SUM2-SUM1)/SUM3
      READ INPUT TAPE ITAI,1
      IF(POW1)7,7,5
    5 SUM1=(RINT(MCELL,1))**2
      SUM2=(3,2808E-2)*(RINT(MAXI,2)-RINT(1,2))
      SUM5=POW1*(SUM1/SUM3)/SUM2
      DO 6J=2,MAXI
      DO 6I=1,MRI
    6 DUMMY(I,J)=SUM5
      WRITE OUTPUT TAPE ITAD,2,POW1
    7 ITER=ITER+1
      IF(ITER-NPO(11))9,9,8
    8 WRITE OUTPUT TAPE ITAD,3
      GO TO 37
    9 IF(IPR)902,902,901
  901 WRITE OUTPUT TAPE ITAD,301,ITER
  902 IF(POW1)10,10,11
   10 IF(ITER-1)12,12,14
   11 CALL SSHTR
      IF(N100-2)12,45,45
   12 K=0
      DO 13I=1,MAXIAL,MAXI
      K=K+1
      C1=DEN(1,I,K)
      TRANSA(I,1,2)=C1*TRANSW
      DO 13J=1,NOG
      VUSIGA(I,J)=C1*VUSIGW(J)
      VUA(I,J)=VUW(J)
      SIGAA(I,J)=C1*SIGAW(J)
   13 DIFA(I,J)=1.0/(3.0*C1*SIGTRW(J))
   14 DO 31IMRIN=1,MRI
      MRIN=IMRIN
      IF(POW1)15,15,17
   15 IF(ITER-1)17,17,16
   16 IF(L(132)-1)24,17,24
   17 J=33
      DO 18I=1,33
      J=J+1
   18 L(I)=L(J)
      J=458
      DO 19I=1,406
      J=J+1
   19 A(I)=A(J)
      DO 23IMAXIA=2,MAXI
      MAXIA=IMAXIA
      K=K1
      DO 20I=1,5,4
      K=K+K2
```

CHAIN LINK (2,B2) - Continued.

```
      C1=DEN(IMRIN,IMAXIA,K)
      TRANS(I,1,2)=C1*TRANSW
      DO 20J=1,NOG
      VUSIG(I,J)=C1*VUSIGW(J)
      VU(I,J)=VUW(J)
      SIGA(I,J)=C1*SIGAW(J)
   20 DIF(I,J)=1.0/(3.0*C1*SIGTRW(J))
   21 CALL AIM
      IF(N100-2)22,45,45
   22 IF(POW1)24,24,23
   23 CONTINUE
   24 J=66
      DO 25I=1,33
      J=J+1
   25 L(I)=L(J)
      J=864
      DO 26I=1,406
      J=J+1
   26 A(I)=A(J)
      DO 27J=1,NOG
      DO 27I=1,MAXIAL
   27 BUCK2(I,J)=BUCKCH(IMRIN,I,J)
   28 CALL AIM
      IF(N100-2)29,45,45
   29 IF(ITER-1)30,30,31
   30 IF(NPO(2))32,32,31
   31 CONTINUE
   32 J=99
      DO 33I=1,33
      J=J+1
   33 L(I)=L(J)
      J-1270
      DO 34I=1,444
      J=J+1
   34 A(I)=A(J)
   35 CALL AIM
      IF(N100-1)36,7,45
   36 IF(N101)37,37,7
   37 IF(POW1)45,45,38
   38 DO 40IMRIN=1,MRI
      MRIN=IMRIN
      WRITE OUTPUT TAPE ITAO,1
      WRITE OUTPUT TAPE ITAO,2,POW1
   39 CALL ANPRAX
   40 CONTINUE
   45 C1=3.34722E-2
      TRANSW=TRANSW/C1
      DO 46J=1,NOG
      VUSIGW(J)=VUSIGW(J)/C1
      SIGAW(J)=SIGAW(J)/C1
   46 SIGTRW(J)=SIGTRW(J)/C1
  500 CALL CHAIN(1,B1)
      END
```

```
*     LIST
*     FORTRAN
*     LABEL
      SUBROUTINE SSHTR
      DIMENSION
      COMMON
      EQUIVALENCE
C
    1 FORMAT (62H2    MAXIMUM NUMBER OF ITERATIONS EXCEEDED IN SUBROUTIN
     1E SSHTR)
    2 FORMAT (34H     PROGRAM TERMINATED IN CHANNELI2,19H (INNER=1, OUTE
     1R=2))
    3 FORMAT (33H1    RESULTS WHEN PROGRAM STOPPED)
    4 FORMAT (18H     RADIAL REGIONI6,5I20/10H     AXIAL/11H     REGION)
    5 FORMAT (28H          POWER DISTRIBUTION)
    6 FORMAT (50H          FRACTION OF POWER GOING TO OUTER CHANNEL)
    7 FORMAT (18H          PRESSURE)
    8 FORMAT (18H          ENTHALPY)
    9 FORMAT (19H          FLOW RATE)
   91 FORMAT (19H          DNB-RATIO)
   92 FORMAT (26H          WALL TEMPERATURE)
   93 FORMAT (34H          MAXIMUM FUEL TEMPERATURE)
   10 FORMAT (I8,6E20.5)
   11 FORMAT (I8,6E20.5/E28.5,5E20.5)
C
      I1=0
      N100=0
      MAXIAL=MAXIAL
      IF(ITER-1)12,12,13
   12 IF(ITA3)121,121,13
  121 CALL SSHTR1
      I2=0
      I3=1
      IF(NPO(1))123,123,122
  122 I3=2
  123 IF(NPO(2))13,13,124
  124 I2=NPO(4)
      IF(I2)13,13,125
  125 IF(NPO(1))126,126,127
  126 IF(NPO(3)-1)128,128,129
  127 IF(NPO(3)-1)129,129,128
  128 C13=1.0
      GO TO 13
  129 C13=0.0
   13 PIM=6.2831853
      DO 133J=2,MAXI
      DO 133I=1,MRI
      IF(I-12)132,131,132
  131 FRAC(I,J)=C13
      GO TO 133
  132 FRAC(I,J)=(TERM(I,J,4)-TERM(I,J,3)+(FULOG+HTR(I,J,I3))*TERM(I,J,1)
     1-HTR(I,J,I3)*TERM(I,J,2))/((FULOG+HTR(I,J,1)+HTR(I,J,2))*TERM(I,J
     2,1)-TERM(I,J,2)))
```

```
  133 CONTINUE
      WATE=WATE-C(5)
   14 I1=I1+1
      IF(I1-ITERM)17,17,15
   15 N100=2
      WRITE OUTPUT TAPE ITAO,1
   16 WRITE OUTPUT TAPE ITAO,3
      WRITE OUTPUT TAPE ITAO,4,(I,I=1,6)
      WRITE OUTPUT TAPE ITAO,5
      WRITE OUTPUT TAPE ITAO,10,(J,(POWER(I,J),I=1,6),J=2,MAXIAL)
      WRITE OUTPUT TAPE ITAO,6
      WRITE OUTPUT TAPE ITAO,10,(J,(FRAC(I,J),I=1,6),J=2,MAXI)
      WRITE OUTPUT TAPE ITAO,7
      WRITE OUTPUT TAPE ITAO,11,(J,((PRES(I,J,K),I=1,6),K=1,2),J=1,MAXIA
     1L)
      WRITE OUTPUT TAPE ITAO,8
      WRITE OUTPUT TAPE ITAO,11,(J,((ENTH(I,J,K),I=1,6),K=1,2),J=1,MAXIA
     1L)
      WRITE OUTPUT TAPE ITAO,9
      J=0
      WRITE OUTPUT TAPE ITAO,11,J,((FLOW(I,K),I=1,6),K=1,2)
      WRITE OUTPUT TAPE ITAO,3
      WRITE OUTPUT TAPE ITAO,91
      WRITE OUTPUT TAPE ITAO,11,(J,((DNB(I,J,K),I=1,6),K=1,2),J=1,MAXIAL
     1)
      WRITE OUTPUT TAPE ITAO,92
      WRITE OUTPUT TAPE ITAO,11,(J,((TEMW(I,J,K),I=1,6),K=1,2),J=2,MAXI)
      WRITE OUTPUT TAPE ITAO,93
      WRITE OUTPUT TAPE ITAO,10,(J,(TFMX(I,J),I=1,6),J=2,MAXI)
      GO TO 500
C
   17 C(5)=0.0
      DO 30K=1,2
      II=K
      ITEST=1
      R1=RHTR(K)
      HD=HDIAM(K)
      ARAT=FAREA(K)/CAREA
      CON1=ARAT
      IF(K-1)18,18,19
   18 H2=HIN
      P2=PPUMP
      PISIGN=-PIM
      N1=0
      N2=1
C     HOUT - CONTRACTION RATIO AT INLET
      FAC2=HOUT
      FAC1=ARAT*FAC2
      GO TO 22
   19 HTOP=0.0
      C1=0.0
      DO 21I=1,MRI
      HTOP=HTOP+FLOW(I,1)*RAREA(I)*ENTH(I,MAXIAL,1)
```

CHAIN LINK (2,B2) - Continued.

```
      C1=C1+FLOW(I,1)*RAREA(I)
      DO 20J=2,MAXI
   20 FRACT(I,J)=FRAC(I,J)
   21 CONTINUE
      HTOP=HTOP/C1
      H2=HTOP
      P2=PTOP
      PISIGN=PIM
      N1=1+MAXIAL
      N2=-1
      FAC1=RAT1*ARAT
      FAC2=RAT1
   22 CALL THERMO
      IF(K-2)221,222,222
  221 C(K)=1.0/(QUAL2*VV2+(1.0-QUAL2)*VL2)
      GO TO 225
  222 IF(H2-HL2)221,221,223
  223 IF(H2-HV2)224,224,221
  224 HTOP=HV2
      H2=HTOP
      C(K)=1.0/VL2
  225 J=N1+N2
      C1=C(K)/62.43
      DO 23I=1,MRI
      PRES(I,J,K)=P2
      ENTH(I,J,K)=H2
      TEMC(I,J,K)=T2
   23 DEN(I,J,K)=C1
   28 CALL SSHTR2
      IF(N100)30,30,29
   29 WRITE OUTPUT TAPE ITAO,2,II
      GO TO 16
   30 CONTINUE
      DO 31I=1,MRI
      IF(I-I2)301,31,301
  301 DO 302J=2,MAXI
  302 FRAC(I,J)=(TERM(I,J,4)-TERM(I,J,3)+(FULOG+HTR(I,J,I3))*TERM(I,J,1)
     1-HTR(I,J,I3)*TERM(I,J,2))/((FULOG+HTR(I,J,1)+HTR(I,J,2))*(TERM(I,J
     2,1)-TERM(I,J,2)))
   31 CONTINUE
      DO 32I=1,MRI
      IF(I-I2)311,32,311
  311 DO 313J=2,MAXI
  312 ERR=ABSF(FRACT(I,J)/FRAC(I,J)-1.0)
      IF(ERR-ESP3)313,313,14
  313 CONTINUE
   32 CONTINUE
      SUM3=0.0
      DO 33I=1,MRI
   33 SUM3=SUM3+RAREA(I)
      SUM3=SUM3*(DZ(1)*C(1)+DZ(MAXIAL)*C(2))
      C(5)=C(5)+SUM3
```

```
      WATE=WATE+C(5)
   34 CALL SSHTR4
  500 RETURN
      END
*     LIST
*     FORTRAN
*     LABEL
      SUBROUTINE SSHTR1
      DIMENSION
      COMMON
      EQUIVALENCE
      MRING=MRING
      MAXIAL=MAXIAL
      MCELL=MCELL
C
C     INITIAL SET UP
C
    1 HIN=HPUMP
      CON1=3.38149989E-3
      CON2=6.5616E-2
      FAREA(1)=CON1=(RINT(1,1))**2
      FAREA(2)=CON1*(((RINT(5,1))**2)-((RINT(4.1))**2))
      HDIAM(1)=CON2*RINT(1,1)
      HDIAM(2)=CON2*(RINT(5,1)-RINT(4,1))
      RHTR(1)=(3.2808E-2)*RINT(1,1)
      RHTR(2)=(3.2808E-2)*RINT(4,1)
      HT(1)=TCFU*(((LOGF(RINT(2,1)/RINT(1,1)))/TCIN)+1.0/((3.2808E-2)*HI
     1NT*RINT(2,1)))
      HT(2)=TCFU*(((LOGF(RINT(4.1)/RINT(3,1)))/TCOU)+1.0/((3.2808E-2)*HI
     1NT*RINT(3,1)))
      IF(NPO(1))102,102,101
  101 C1=FAREA(1)
      FAREA(1)=FAREA(2)
      FAREA(2)=C1
      C1=HDIAM(1)
      HDIAM(1)=HDIAM(2)
      HDIAM(2)=C1
      C1=RHTR(1)
      RHTR(1)=RHTR(2)
      RHTR(2)=C1
      C1=HT(1)
      HT(1)=HT(2)
      HT(2)=C1
  102 TWOGJ=6.49029989E+11
      TWOG=6.00444058E+10
      FULOG=LOGF(RINT(3,1)/RINT(2,1))
      CAREA=CON1*(RINT(MCELL,1))**2
      SUM2=0.0
      DO 2I=1,MRING
      SUM1=SUM2
      SUM2=CON1*(RINT(I,3))**2
    2 RAREA(I)=SUM2-SUM1
```

```
      SUM4=0.0
      DO 3I=1,MAXIAL
      SUM3=SUM4
      SUM4=(3.2808E-2)*RINT(I,2)
    3 DZ(I)=SUM4-SUM3
      SUM3=SUM3-DZ(1)
      C1=POW1*CAREA/SUM1
      DO 4I=1,MRI
      POWER(I,MAXIAL)C1
      DO 4J=1,MAXI
    4 POWER(I,J)=DUMMY(I,J)
      C2=FLO*CAREA/SUM1
      C1=C2*(1.0+RECIRC)
      DO 5I=1,MRI
      FLOW(I,1)=C1
    5 FLOW(I,2)=C2
      WATE=(SUM1*SUM3*DCDEN)+(RAREA(MRING)*SUM4*RRDEN)
      C(5)=0.0
      DO 6I=1,2
      AC3(1,I)=-0.0093/HDIAM(I)
      AC3(2,I)=-0.0017/HDIAM(I)
    6 AC3(3,I)=-0.0048/HDIAM(I)
      DZ2=0.0
      SUM1=0.0
      AC4(1,1)=0.^
      AC4(MAXIAL,1)=SUM3
      AC4(MAXIAL,2)=0.0
      AC4(1,2)=SUM3
      DO 71=2,MAXI
      DZ1=DZ2
      DZ2=DZ(I)
      SUM1=SUM'+(DZ1+DZ2)/2.0
      AC4(I,1)=SUM1
    7 AC4(I,2)=SUM3-SUM1
      DO 8J=1,2
      DO 8I=1,MAXIAL
      C1=AC3(1,J)*AC4(I,J)
      C2=AC3(2.J)*AC4(I,J)
      C3=AC3(3,J)*AC4(I,J)
      DCOR1(I,J)=0.435+1.236*EXPF(C1)
      DCOR2(I,J)=0.825+2.36*EXPF(C2)
    8 DCOR3(I,J)=-0.41*EXPF(C3)
      LB1=1+LBC(3)-LBC(2)
      C1=U(3,LB1)/2.0
      C2=U(3,1)/2.0
      C3=C1/2.0
      C4=C2/2.0
      DO 9J=2,MAXI
      DO 9I=1,MRI
      TERM(I,J,1)=C1
      TERM(I,J,2)=C2
      TERM(I,J,3)=C3
      TERM(I,J,4)=C4
```

```
      DO 9K=1,2
      TEMC(I,J,K)=0.0
    9 TEMW(I,J,K)=0.0
   12 DO 13K=1,2
      DO 13J=2,MAXI
      DO 13I=1,MRI
   13 HTR(I,J,K)=HT(K)
      IF(NPO(2))500,500,14
   14 I1=NPO(4)
      IF(I1)500,500,15
   15 I2=NPO(3)
      DO 16J=2,MAXI
   16 HTR(I1,J,I2)=0.0
C
  500 RETURN
      END

*     LIST
*     FORTRAN
*     LABEL
      SUBROUTINE SSHTR2
      DIMENSION
      COMMON
      EQUIVALENCE
C
C     SET-UP
C
    1 FORMAT (59H2    MAXIMUM NUMBER OF TRIALS EXCEEDED IN SUBROUTINE S
     1HTR2)
    2 FORMAT (22H     RADIAL FLOW SWEEPI3)
    3 FORMAT (36H     RATIO OF CALCULATED/ACTUAL FLOW2(1PE20.5))
    4 FORMAT (18H     PRESSURE DROP1PE38.5,E20.5)
    5 FORMAT (40H     PROGRAM TERMINATED IN RADIAL REGIONI2)
    6 FORMAT (17H     ASSUMED FLOW1PE32.5,E20.5)
    7 FORMAT (29H     CALCULATED PRESSURE DROP2(1PE20.5))
      II=II
      N35=0
      K1=N1+N2
      K2=N1+N2-MAXIAL
      I1=2
      I2=0
      I3=1
      C1=1.0
      IF(ITER-1)8,8,11
    8 IF(II-1)9,9,11
    9 C20=0.0
      DO 10I=1,MRI
   10 C20=C20+RAREA(I)
      C19=FLO*CAREA/(20.0*C20)
      ASQ=CAREA*CAREA*TWOGJ
      ESP4=1.5*ESP3
      ESP5=2.0*ESP3
```

CHAIN LINK (2,B2) - Continued.

```
   11 IF(NPO(2))15,15,12
   12 IF(NPO(3)-11)15,13,15
   13 I2=NPO(4)
      FLOW(I2,II)=0.0
      DO 131J=2,MAXI
  131 DEN(I2,J,II)=0.0
      C1=C20/(C20-RAREA(I2))
      IF(I2-I3)15,14,15
   14 I3=2
   15 FLOTA=FLO
      IF(II-1)17,17,16
   16 IF(QUAL2)17,17,161
  161 FLOTA=QUAL2*FLO
      C2=FLOTA*CAREA*C1/C20
      DO 164I=1,MRI
      IF(I-I2)163,162,163
  162 IF(II-NPO(3))163,164,163
  163 FLOW(I,II)=C2
  164 CONTINUE
      C1=QUAL2*C1
   17 DFLOW=C1*C19
C
C     START RADIAL SWEEP
C
   18 SUM8=0.0
      N35=N35+1
      IF(N35-ITERM)21,21,19
   19 WRITE OUTPUT TAPE ITAO,1
   20 WRITE OUTPUT TAPE ITAO,2,N35
      WRITE OUTPUT TAPE ITAO,3,FLOW1,FLOW2
      WRITE OUTPUT TAPE ITAO,4,PDROP1,PDROP2
      N100=2
      GO TO 500
   21 IF(N35-2)23,22,23
   22 I1=1
   23 DO 50I=1,MRI
      IF(I-I2)24,50,24
   24 MRIN=I
      N34=0
      FAC3=CON1*RAREA(I)
   25 N34=N34+1
      IF(N34-ITERM)28,28,26
   26 WRITE OUTPUT TAPE ITAO,1
   27 WRITE OUTPUT TAPE ITAO,5,MRIN
      WRITE OUTPUT TAPE ITAO,6,(DPHO(J),J=1,2)
      WRITE OUTPUT TAPE ITAO,7,(PHI(J),J=1,2)
      GO TO 20
   28 IF(I1-1)29,29,30
   29 DP+O(1)=FLOW(I,II)-DFLOW
   30 DP+O(2)=FLOW(I,II)
      DO 32J=I1,2
      FLOC=DPHO(J)
```

```
      FAC4=FLOC/FAREA(II)
      GHD=FAC4*HD
      GSQE=FLOC*FLOC/ASQ
      GSQP=(TWOGJ/TWOG)*GSQE
      C8=FAC4/(1.0E+06)
      C9=(0.23+0.094*C8)*(1.0E+06)
      C10=EXPF(-1.5*C8)
   31 CALL SSHTR3
      IF(N100)32,32,27
   32 PHI(J)=PRES(I3,K1,II)
      IF(NPO(2))33,33,40
   33 IF(ITER-1)34,34,40
   34 IF(ITA3)35,35,40
   35 IF(MRI-2)49,36,36
   36 DO 39K=1,MAXIAL
      DO 39J=2,MRI
      ENTH(J,K,II)=ENTH(1,K,II)
      PRES(J,K,II)=PRES(1,K,II)
      TEMC(J,K,II)=TEMC(1,K,II)
      DNB(J,K,II)=DNB(1,K,II)
      IF(K-1)39,39,37
   37 IF(K-MAXIAL)38,39,39
   38 DEN(J,K,II)=DEN(1,K,II)
      TEMW(J,K,II)=TEMW(1,K,II)
      HTR(J,K,II)=HTR(1,K,II)
   39 CONTINUE
      SUM8=SUM7*C20/RAREA(1)
      GO TO 65
   40 IF(N35-1)49,49,41
C
C     FLOW PERTURBATION TO ACHIEVE DESIRED PRESSURE DROP
C
   41 ERR=PHI(2)-C12
      C1-ABSF(ERR/C12)
      IF(C1-ESP4)49,49,42
   42 IF(ERR)43,49,44
   43 FLOW(I,II)=1.06*DPHD(2)
      GO TO 25
   44 IF(PHI(1)-C12)46,45,45
   45 FLOW(I,II)=0.97*DPHO(1)
      GO TO 25
   46 XINI=(C12-PHI(1))/(PHI(2)-PHI(1))
      FLOW(I,I)=DPHO(1)+XINT*DFLOW
      GO TO 25
   49 SUM8=SUM8+SUM7
   50 CONTINUE
   51 IF(N35-1)52,52,61
C
C     GENERATE AVERAGE PRESSURE DROP
C
   52 C1=0.0
      C2=1.0E+06
```

CHAIN LINK (2,B2) - Continued.

```
      C12=0.0
      C3=C20
      DO 58I=1,MRI
      IF(I-I2)54,53,54
   53 IF(II-NPO(3))54,531,54
  531 C3=C20-RAREA(I)
      GO TO 58
   54 AC1(I)=PRES(I,K1,II)-PRES(1,K2,II)
      C12=C12+AC1(I)*RAREA(I)
      IF(AC1(I)-C1)56,56,55
   55 C1=AC1(I)
   56 IF(C2-AC1(I))58,58,57
   57 C2=AC1(I)
   58 CONTINUE
      C12=C12/C3
      ERR1=0.3/C1
      IF(ERR1-ESP4)59,60,60
   59 ERR1=ESP4
   60 ERR=(C1-C2)/01
      IF(ERR-ERR1)65,65,18
C
C     ADJUST PRESSURE DROP FOR TOTAL FLOW
C
   61 C2=0.0
      DO 62I=1,MRI
   62 C2=C2+FLOW(I,II)*RAREA(I)
      C1=C2/(CAREA*FLOTA)
      C2=ABSF(1.0-C1)
      IF(C2-ESP5)63,63,67
   63 DO 64I=1,MRI
   64 FLOW(I,II)=FLOW(I,II)/C1
   65 C(5)=C(5)+SUM8
      IF(II-1)66,66,500
   66 PTOP=PRES(I3,K2,II)
      GO TO 500
   67 PDROP1=PDROP2
      PDROP2=C12
      FLOW1=FLOW2
      FLOW2=C1
      I=2*(N35/2)
      IF(I-N35)69,68,68
   68 C12=1.05*PDROP2
      GO TO 18
   69 IF(FLOW2-1.0)70,65,71
   70 C12=PDROP1*(1.0+FLOW1)/2.0
      GO TO 18
   71 IF(FLOW1-10)72,72,73
   72 XINT=(1.0-FLOW1)/(FLOW2-FLOW1)
      C12=PDROP1+XINT*(PDROP2-PDROP1)
      GO TO 18
   73 C12=2.0*PDROP1/(1.0+FLOW1)
```

```
      GO TO 18
C
  500 RETURN
      END
*     LIST
*     FORTRAN
*     LABEL
      SUBROUTINE SSHTR3
      DIMENSION
      COMMON
      EQUIVALENCE
    1 FORMAT (39H     PROGRAM TERMINATED IN AXIAL REGIONI3)
      II=II
      MRIN=MRIN
      Q2=0.0
      SUM7=0.0
      IF(N34-1)101,101,7
  101 IF(N35-1)2,2,7
    2 IF(ITER-1)3,3,7
    3 IF(II-1)4,4,7
    4 IF(NPO(1))6,6,5
    5 SIDE1=0.0
      SIDE2=1.0
      GO TO 7
    6 SIDE1=1.0
      SIDE2=-1.0
    7 I=N1+N2
      P2=PRES(MRIN,I,II)
      H2=ENTH(MRIN,I,II)
      ARAT=FAC1
      ITEST=1
      I1=MRIN
      IF(II=NPO(3))8,71,8
   71 IF(NPO(4)-1)8,72,8
   72 IF(MRIN-2)8,73,8
   73 MRIN=1
    8 CALL CNOZ
      MRIN=I1
      IF(N100)10,10,9
    9 WRITE OUTPUT TAPE ITAO,1,I
      GO TO 500
   10 ARAT=FAC2
   11 CALL PEXP
      IF(N100)12,12,9
   12 ITEST=0
      A(1)=H2
      C5=HL2-H2
      C6=VL2/VV2
      C7=HV2-HL2
      IF(C5)13,13,14
   13 C1=1.0
```

```
      GO TO 15
   14 C1=(C5/C7)**0.75
      C1=EXPF(-0.532*C1)
   15 C1=1.4*C1/(C6**0.333(
      C1=1.7-C1
      C2=0.529*C5+C7*(0.548-1.12*C6)
      DO 16J=2,MAXIAL
      I=N1+N2*J
      ACB(I,1)=C2+C7*DCOR3(I,II)
      AC8(I,2)=C7*DCOR2(I,II)
      AC7(I,1)=C1*DCOR1(I,II)
      AC9(I)=C9*AC7(I,1)
   16 AC10(I)=AC8(I,1)+C10*AC8(I,2)
      DO 33K=2,MAXIAL
      I=N1+N2*K
      J=I-N2
      MAXIA=I
      D2=FULOG=HTR(MRIN,I,1)+HTR(MRIN,I,2)
      IF(K-2)17,17,18
   17 DZ1=0.0
      GO TO 20
   18 IF(K-MAXIAL)19,21,21
   19 DZ1=DZ(J)/2.0
   20 DZ2=DZ(I)/2.0
      POWER2=POWER(MRIN,I)
      DTC22=TEMC(MRIN,I,1)-TEMC(MRIN,I,2)
      FRAC2=SIDE2*FRAC(MRIN,I)
      CON4=DZ(I)*FAC3
      GO TO 22
   21 DZ1=DZ(J)/4.0
      DZ2=DZ1
      POWER2=POWER(MRIN,J)
      DTC22=TEMC(MRIN,J,1)-TEMC(MRIN,J,2)
      FRAC2=SIDE1+SIDE2*FRAC(MRIN,J)
   22 IF(II-1)24,24,23
   23 FRAC2=1.0-FRAC2
   24 IF(MRIN-NPO(4))26,25,26
   25 DTC22=0.0
   26 CALL PXHTR
      IF(N100)28,28,27
   27 WRITE OUTPUT TAPE ITA0,1,I
      GO TO 500
   28 IF(K-MAXIAL)29,32,32
   29 C1=1.0/(VOID2*VV2+(1.0-VOID2)*VL2)
      PRES(MRIN,I,II)=P2
      ENTH(MRIN,I,II)=H2
      TEMC(MRIN,I,II)=T2
      SUM7=SUM7+C1*CON4
      DEN(MRIN,I,II)=C1/62.43
   30 CALL HTRAN
      IF(N100)31,31,27
   31 HTR(MRIN,I,II)=TCFU/RH2+HT(II)
```

```
      TEMW(MRIN,I,II)=TW2
   32 CALL BURN
      DNB(MRIN,I,II)=DNB2
   33 CONTINUE
      I=N1+N2*MAXIAL
      ARAT=0.0
      ITEST=1
   34 CALL PEXP
      IF(N100)35,35,9
   35 PRES(MRIN,I,II)=P2
      ENTH(MRIN,I,II)=H2
      TEMC(MRIN,I,II)=T2
  500 RETURN
      END

*     LIST
*     FORTRAN
*     LABEL
      SUBROUTINE SSHTR4
      DIMENSION
      COMMON
      EQUIVALENCE
      IF(ITER-1)1,1,11
    1 IFUEL=1+LBC(3)-LBC(2)
      DISTL(1)=0.0
      DISTL(IFUEL)=FULOG
      I1=IFUEL-1
      DO 2I=2,I1
    2 DISTL(I)=LOGF(U(2,I)/U(2,1))
      IF(NPO(1))3,3,8
    3 I1=1
      I2=2
      IF(NPO(3)-1)4,4,6
    4 I3=2
    5 I4=2
      C13=-FULOG
      C14=I.0
      GO TO 101
    6 I3=1
    7 I4=1
      C13=FULOG
      C14=-1.0
      GO TO 101
    8 I1=2
      I2=1
      IF(NPO(3)-1)9,9,10
    9 I3=2
      GO TO 7
   10 I3=1
      GO TO 5
C
C     FIRST GUESS FOR AVERAGE FUEL TEMPERATURE
C
```

```
  101 ITEST=1
      P2=PPUMP
      H2=HON+POW1/FLC
  102 CALL THERMO
      C1=T2+2000.0
      DO 103J=2,MAXI
      DO 103I=1,MRI
  103 TFBAR(I,J)=C1
      GO TO 500
C
C     CALCULATED AVERAGE AND MAXIMUM FUEL TEMPERATURE
C
   11 DO 22J=2,MAXI
      DO 21I=1,MRI
      C4=POWER(I,J)/TCFU
      IF(I-NPO(4))12,13,12
   12 TFI=TEMC(I,J,I1)+C4*(1.0-FRAC(I,J))*HTR(I,J,I1)/PIM
      TFO=TEMC(I,J,I2)+C4*FRAC(I,J)*HTR(I,J,I2)/PIM
      GO TO 16
   13 D2=TEMC(I,J,I3)+C4*HTR(I,J,I3)/PIM
      DTC22=D2+C4*(C13*TERM(I,J,I4)+C14*(TERM(I,J,3)-TERM(I,J,4)))
      IF(I4-1)15,15,14
   14 TFI=DTC22
      TFO=D2
      GO TO 16
   15 TFI=D2
      TFO=DTC22
   16 C1=TFI+C4*TERM(I,J,4)
      C2=(TFO-TFI+C4*(TERM(I,J,3)-TERM(I,J,4)))/FULOG
      TFMX(I,J)=TFI
      G(1)=TFI
      DO 19K=2,IFUEL
      SUM1=0.0
      DO 17I5=1,5
      C3=(I5+1)*(I5+1)
   17 SUM1=SUM1+BMAT(I,J,I5)*U(I5+2,K)/C3
      C3=C4*SUM1
      G(K)=C1+C2*DISTL(K)-C3
      IF(G(K)-TFMX(I,J))19,19,18
   18 TFMX(I,J)=G(K)
   19 CONTINUE
      SUM1=0.0
      SUM2=0.0
      I5=LBC(2)
      DO 20K=3,IFUEL,2
      I5=I5+2
      SUM1=SUM1+RC(I5-2)+4.0*RC(I5-1)+RC(I5)
   20 SUM2=SUM2+RC(I5-2)*G(K-2)+4.0*RC(I5-1)*G(K-1)+RC(I5)*G(K)
      TFBAR(I,J)=SUM2/SUM1
   21 CONTINUE
   22 CONTINUE
  500 RETURN
      END
```

```
*      LIST
*      FORTRAN
*      LABEL
       SUBROUTINE CNOZ
       DIMENSION
       COMMON
       EQUIVALENCE
       C1=ARAT*ARAT
       GSQE=GSQE/C1
       GSQP=GSQP/C1
       NSKP=15
       C3=5.0
       C4=2.0*C3
       C5=C3*C3
       C6=1.0E-5
       IF(I)-1)1,1,2
     1 P2=PPUMP
       H2=HIN
       GO TO 3
     2 P2=PTOP
       H2=HTOP
     3 P1=P2
       H1=H2
       IF(MRIN-1)4,4,7
     4 IF(N34-1)5,5,7
     5 IF(N35-1)6,6,7
     6 CALL CNOZ1
       IF(NIOO-2)7,500,500
     7 CALL CNOZ2
   500 RETURN
       END

*      LIST
*      FORTRAN
*      LABEL
       SUBROUTINE CNOZ1
       DIMENSION
       COMMON
       EQUIVALENCE
     1 FORMAT (54H2    PROGRAM NOT EQUIPPED TO HANDLE SUPERHEATED PLENUM)
     2 FORMAT (69H2    PROGRAM NOT EQUIPPED TO HANDLE EXPANSION INTO SUPE
      1RHEATED REGION)
     3 FORMAT (42H2    MAXIMUM NUMBER OF ITERATIONS EXCEEDED)
     4 FORMAT (43H     PROGRAM TERMINATED IN SUBROUTINE CNOZ1)
C
C      STORAGE LOCATIONS FOR VARIABLES WHEN SATURATION IS ACHIEVED
C
C      SOU(1)  - PRESSURE
C      SOU(2)  - ENTHALPY
C      SOU(3)  - ENTROPY
C      SOU(4)  - VELOCITY**2
C      SOU(5)  - FLUX**2/G
C      SOU(6)  - SPECIFIC VOLUME
```

```
C       SOU(7)  - QUALITY
C       SOU(8)  - VOID FRACTION
C       SOU(9)  - LIQUID SPECIFIC VOLUME
C       SOU(10) - VAPOR SPECIFIC VOLUME
C
C       STORAGE LOCATIONS FOR CRITICAL FLOW PARAMETERS
C
C       SOU(11) - PRESSURE
C       SOU(12) - ENTHALPY
C       SOU(13) - FLUX**2/G
C       SOU(14) - SPECIFIC VOLUME
C       SOU(15) - QUALITY
C       SOU(16) - VOID FRACTION
C       SOU(17) - LIQUID SPECIFIC VOLUME
C       SOU(18) - VAPOR SPECIFIC VOLUME
C
C       DETERMINE PLENUM CONDITIONS
C
        NAA=2
        XXX=P1
      5 CALL CNOZ3
        IF(N100-2)6,9,9
      6 NAA=NAA
        J=NAA
        I=J+1
        HL2=HF(J)*XINT*(HF(I)-HP(J))
        HV2=HG(J)*XINT*(HG(I)-HG(J))
        IF(H2-HV2)7,13,8
      7 IF(H2-HL2)10,13,13
C
C       PLENUM IS SUPERHEATED
C
      8 WRITE OUTPUT TAPE ITAO,1
      9 WRITE OUTPUT TAPE ITAO,4
        N100=2
        GO TO 500
C
C       PLENUM IS COMPRESSED LIQUID
C
     10 NAA=5
        XXX=H1
     11 CALL CNOZ3
        IF(N100-2)12,9,9
     12 NAA=NAA
        J=NAA
        I=J+1
        P2=PSAT(J)+XINT*(PSAT(I)-PSAT(J))
        VL2=VF(J)+XINT*(VF(I)-VF(J))
        HL2=H1
        HV2=0.0
        V1=TWOG*(P1-P2)*VL2
        GO TO 14
```

```
C
C     PLENUM IS INITIALLY SATURATED
C
   13 P2=P1
      VL2=VF(J)+XINT*(VF(I)-VG(J))
      V1=0.0
C
C     STORE SATURATED PLENUM VARIABLES
C
   14 VV2=VG(J)+XINT*(VG(I)-VG(J))
      SL2=SF(J)+XINT*(SF(I)-SF(J))
      SV2=SG(J)+XINT*(SG(I)-SG(J))
      QUAL2=(H2-HL2)/(HV2-HL2)
      VOIC2=QUAL2
      C1=VL2+QUAL2*(VV2-VL2)
      SOU(1)=P2
      SOU(2)=H2
      SOU(3)=SL2+QUAL2*(SV2-SL2)
      SOU(4)=V1
      SOU(5)=V1/(TWOG*C1*C1)
      SOU(6)=C1
      SOU(7)=QUAL2
      SOU(8)=VOID2
      SOU(9)=VL2
      SOU(10)=VV2
      IF(P2-50.0)141,141,142
  141 VOLUM=C1
      G(3)=SOU(5)
      GO TO 32
C
C     DETERMINE MAXIMUM MASS FLUX
C
  142 S2=SOU(3)
      ICT=0
      I2=0
      P2=P2-5.0
      GO TO 17
  143 P2=50.0
   15 ICT=ICT+1
      IF(ICT-ITERM)17,17,16
   16 WRITE OUTPUT TAPE ITAO,3
      GO TO 9
   17 G1P(1)=P2-C3
      G1P(2)=P2+C3
      G1P(3)=P2
      DO 26K=1,3
      NAA=2
      XXX=G1P(K)
   18 CALL CNOZ3
      IF(N100-2)19,9,9
   19 NAA=NAA
      J=NAA
      I=J+1
```

```
      SL2=SF(J)+XINT*(SF(I)-SF(J))
      SV2=SG(J)+XINT*(SG(I)-SG(J))
      HL2=HF(J)+XINT*(HF(I)-HF(J))
      HV2=HG(J)+XINT*(HG(I)-HG(J))
      I1=0
      QUAL2=(S2-SL2)/(SV2-SL2)
      C1=HL2+QUAL2*(HV2-HL2)
      C1=TWOGJ*ENOZ*(H1-C1)
      V2=V1+C1
   20 I1=I1+1
      IF(I1-NSKP)21,21,16
   21 C2=C1*EXPF(-V2*RUSQ)
      ERRH1=V1+C2-V2
      ERR=ABSF(ERRH1/V2)
      IF(ERR-C6)23,23,22
   22 V2=V2+ERRH1
      GO TO 20
   23 H2=H1+(V1-V2)/TWOGJ
      QUAL2=(H2-HL2)/(HV2-HL2)
      IF(QUAL2-1.0)25,25,24
   24 WRITE OUTPUT TAPE ITAO,2
      GO TO 9
   25 VL2=VF(J)+XINT*(VF(I)-VF(J))
      VV2=VG(J)+XINT*(VG(I)-VG(J))
      VOLUM=VL2+QUAL2*(VV2-VL2)
   26 G(K)=V2/(VOLUM*VOLUM*TWOG)
      C1=(G(2)-G(1))/C4
      C2=(G(2)+G(1)-2.0*G(3))/C5
      IF(ICT-1)261,261,28
  261 IF(I2)33,33,27
   27 IF(C1)32,32,28
   28 ERR=ABSF(C3*C1/G(3))
      IF(ERR-ESP3)32,32,29
   29 IF(C2)31,30,30
   30 P2=G1P(3)+25.0*C1/ABSF(C1)
      GO TO 311
   31 P2=G1P(3)-C1/C2
  311 IF(P2-SOU(1))15,312,312
  312 P2=SOU(1)-10.0
      GO TO 15
   32 SOU(11)=P2
      SOU(12)=H2
      SOU(13)=G(3)
      SOU(14)=VOLUM
      SOU(15)=QUAL2
      SOU(16)=QUAL2
      SOU(17)=VL2
      SOU(18)=VV2
      GO TO 500
   33 C1=(G(2)-G(1))/C4
      ERR=ABSF(C3*C1/G(3))
      IF(ERR-ESP3)32,32,34
```

```
   34 I2=1
      IF(C1)143,32,32
  500 RETURN
      END
*     LIST
*     FORTRAN
*     LABEL
      SUBROUTINE CNOZ2
      DIMENSION
      COMMON
      EQUIVALENCE
C
    1 FORMAT (26H2    NOZZLE FLOW IS CHOKED)
    2 FORMAT (42H2    MAXIMUM NUMBER OF ITERATIONS EXCEEDED)
    3 FORMAT (43H     PROGRAM TERMINATED IN SUBROUTINE CNOZ2)
C
C     DETERMINE ACTUAL PRESSURE DROP
C
      IF(GSQP-SOU(13))7,4,5
    4 P2=SOU(11)
      H2=SOU(12)
      VOLUM=SOU(14)
      QUAL2=SOU(15)
      VOID2=SOU(16)
      VL2=SOU(17)
      VV2=SOU(18)
      GO TO 22
    5 WRITE OUTPUT TAPE ITAO,1
    6 WRITE OUTPUT TAPE ITAO,3
      N100=2
      GO TO 500
    7 IF(GSQP-SOU(5))8,8,9
C
C     COMPRESSED LIQUID EXHAUST
C
    8 H2=SOU(2)
      VOLUM=SOU(6)
      P2=P1-GSQP*VOLUM
      QUAL2=0.0
      VOID2=0.0
      VL2=SOU(9)
      VV2=SOU(10)
      VOLUM=VL2
      GO TO 22
C
C     SATURATED EXHAUST
C
    9 S2=SOU(3)
      V1=SOU(4)
      ICT=0
      P2=SOU(1)-25.0
```

```
   10 ICT=ICT+1
      IF(ICT-ITERM)12,12,11
   11 WRITE OUTPUT TAPE ITAO,2
      GO TO 6
   12 G1P(1)=P2-C3
      G1P(2)=P2+C3
      G1P(3)=P2
      DO 20K=1,3
      NAA=2
      XXX=G1P(K)
   13 CALL CNOZ3
      IF(N100-2)14,6,6
   14 NAA=NAA
      J=NAA
      I=J+1
      SL2=SF(J)+XINT*(SF(I)-SF(J))
      SV2=SG(J)+XINT*(SG(I)-SG(J))
      HL2=HF(J)+XINT*(HF(I)-HF(J))
      HV2=HG(J)+XINT*(HG(I)-HG(J))
      I1=0
      QUAL2=(S2-SL2)/(SV2-SL2)
      C1=HL2+QUAL2*(HV2-HL2)
      C1=TWOGJ*ENOZ*(H1-C1)
      V2=V1+C1
   15 I1=I1+1
      IF(I1-NSKP)16,16,11
   16 C2=C1*EXPF(-V2*RUSQ)
      ERRH1=V1+C2-V2
      ERR=ABSF(ERRH1/V2)
      IF(ERR-C6)18,18,17
   17 V2=V2+ERRH1
      GO TO 15
   18 H2=H1+(V1-V2)/TWOGJ
      QUAL2=(H2-HL2)/(HF2-HL2)
      IF(QUAL2-1.0)19,11,11
   19 VL2=VG(J)+XINT*(VF(I)-VF(J))
      VV2=VG(J)+XINT*(VG(I)-VG(J))
      VOLUM=VL2+QUAL2*(VV2-VL2)
   20 G(K)-V2/(VOLUM*VOLUM*TWOG)
      C1=(G(2)-G(1))/C4
      ERR-ABSF((G(3)/GSQP)-1.0)
      IF(ERR-ESP3)22,22,21
   21 P2=G1P(3)+(GSQP-G(3))/C1
      GO TO 10
C
C     MOMENTUM AND KINETIC ENERGY TERMS
C
   22 ENK2=GSQE*VOLUM*VOLUM
      PK2=GSQP*VOLUM
      VOID2=QUAL2
C
  500 RETURN
      END
```

```
*       LIST
*       FORTRAN
*       LABEL
        SUBROUTINE CNOZ3
        DIMENSION
        COMMON
        EQUIVALENCE
C
C       STEAM TABLE ITERPOLATION ROUTINE
C
      1 FORMAT (51H2    TRIAL VALUE IS TOO HIGH FOR STEAM TABLE VALUES)
      2 FORMAT (50H2    TRIAL VALUE IS TOO LOW FOR STEAM TABLE VALUES)
      3 FORMAT (43H     PROGRAM TERMINATED IN SUBROUTINE CNOZ3)
        NAA=NAA
        J=123*NAA
        XINT=J
        VINT=HEAT(J)
        I=J-122
        IF(NAA-2)4,4,8
      4 IF(XXX-HEAT(J))8,7,5
      5 WRITE OUTPUT TAPE ITAO,1
      6 WRITE OUTPUT TAPE ITAO,3
        N100=2
        GO TO 500
      7 NAA=123
        XINT=0.0
        GO TO 500
      8 IF(HEAT(I)-XXX)11,10,9
      9 WRITE OUTPUT TAPE ITAO,2
        GO TO 6
     10 NAA=1
        XINT=0.0
        GO TO 500
     11 Y=I
        I=(1.0+Y)+(XINT-Y)*(XXX-HEAT(I))/(VINT-HEAT(I))
        IF(HEAT(I)-XXX)11,11,12
     12 J=I-1
        IF(HEAT(J)-XXX)14,14,13
     13 I=J
        GO TO 12
     14 XINT=(XXX-HEAT(J))/(HEAT(I)-HEAT(J))
        NAA=J-123*(NAA-1)
    500 RETURN
        END

*       LIST
*       FORTRAN
*       LABEL
        SUBROUTINE PEXP
        DIMENSION
        COMMON
        EQUIVALENCE
```

CHAIN LINK (2,B2)- Continued.

```
    1 FORMAT (61H2    MAXIMUM NUMBER OF ITERATIONS EXCEEDED IN SUBROUTIN
     1E PEXP)
      C5=ARAT*ARAT
      GSQE=GSQE*C5
      GSQP=GSQP*C5
      AH1=H2+ENK2
      AP1=P2+(2.0*ARAT-C5)*PK2
      I1=0
C
C     TEST NUMBER OF ITERATIONS
C
    2 I1=I1+1
      IF(I1-ITERM)4,4,3
    3 N100=2
      WRITE OUTPUT TAPE ITA0,1
      GO TO 500
C
C     MOMENTUM,ENERGY, AND ERROR TERMS
C
    4 CALL THERMO
      IF(QUAL2)5,5,6
    5 C1=VL2*VL2
      C2=0
      C3=VL2
      C4=0
      GO TO 9
    6 C1=1.0-QUAL2
      IF(C1)7,7,8
    7 C1=0.0
      C2=VV *VV2
      C3=0.0
      C4=VV2
      GO TO 9
    8 C5=C1*VL2/(1.0-VOID2)
      C3=C1*C5
      C1=C3*C5
      C5=QUAL2*VV2/VOID2
      C4=QUAL2*C5
      C2=C4*C5
    9 ENK2=GSQE*(C1+C2)
      PK2=GSQP*(C3+C4)
      ERRH2=AH1-ENK2-H2
      ERRP2=AP1-PK2-P2
      IF(I1-1)12,12,10
C
C     CONVERGENCE TESTING
C
   10 C1=ABSF((ERRH2/H2)
      C2=ABSF((ERRP2/P2)
      IF(C1-ESP3)11,11,12
   11 IF(C2-ESP3)500,500,12
C
```

```
C     NEW VALUES OF PRESSURE AND ENTHALPY
C
   12 P2=P2+ERRP2
      H2=H2+ERRH2
      GO TO 2
C
  500 RETURN
      END

*     LIST
*     FORTRAN
*     LABEL
      SUBROUTINE PXHTR
      DIMENSION
      COMMON
      EQUIVALENCE
C
C     INITIAL SET UP
C
      Q1=Q2
      Q2=(POWER2*FRAC2)+(PISIGN*TCFU*DTC22)/D2
      C11=(Q1*DZ1+Q2=DZ2)/FLOC
      AH1=H2+ENK2+C11
      AP1=P2+PK2
      H2=AH1
      lCT=0
C
C     CALCULATION
C
    1 ICT=ICT+1
    2 CALL THERMO
      IF(QUAL2)3,3,4
    3 C1=VL2*VL2
      C2=0.0
      C3=VL2
      C4=0.0
      GO TO 9
    4 C1=1.0-QUAL2
      IF(C1)5,5,6
    5 C1=0.0
      C2=VV2*VV2
      C3=0.0
      C4=VV2
      GO TO 9
    6 C5=C1*VL2/(1.0-VOID2)
      C3=C1*C5
      C1=C3*C5
      C5=QUAL2*VV2/VOID2
      C4=QUAL2*C5
      C2=C4*C5
      GO TO 9
```

```
    9 C5=(0.092*DZ2/HD)/((GHD*((QUAL2/VISV2)+((1.0-QUAL2)/VISL2)))**0.2)
      ENK2=GSQE*(C1+C2)
      PK2=GSQP*(C3+C4)*(1.0+C5)
      ERRH2=AH1-ENK2-H2
      ERRP2=AP1-PK2-P2
      IF(ICT-1)16,16,10
C
C     TEST ERROR
C
   10 C1=ABSF(ERRH2/H2)
      C2=ABSF(ERRP2/P2)
      IF(C1-ESP3)11,11,13
   11 IF(C2-ESP3)12,12,13
   12 PK2=GSQP*(C3+C4)*(1.0-C5)
      Q1=Q2/(PIM*R1)
      GO TO 500
C
C     TEST NUMBER OF ITERATIONS
C
   13 IF(ICT-ITERM)16,16,14
   14 N100=2
      WRITE OUTPUT TAPE ITAO,15
      GO TO 500
   15 FORMAT (40H2    TOO MANY TRIALS IN SUBROUTINE PXHTR)
C
C     NEW VALUES OF ENTHALPY AND PRESSURE
C
   16 H2=H2+ERRH2
      P2=P2*ERRP2
      GO TO 1
C
  500 RETURN
      END

*     LIST
*     FORTRAN
*     LABEL
      SUBROUTINE HTRAN
      DIMENSION
      COMMON
      EQUIVALENCE
    1 FORMAT (63H2    MAXIMUM NUMBER OF ITERATIONS EXCEEDED IN SUBROUTIN
     1E HTRAN1)
      IF(QUAL2)2,2,6
C
C     PRESSURIZED LIQUID
C
```

```
    2 C1=0.023*(TCL2/HD)*((GHD/VISL2)**0.8)*((CL2*VISL2/TCL2)**0.33)
      C2=T2+)Q1/C1)-1.97*(Q1**0.26)
      IF(C2-TSATU2)3,3,5
    3 TW2=T2+Q1/C1
    4 RH2=R1*C1
      GO TO 500
    5 H1=H2
      C1=T2
      H2=HL2
   51 CALL THERMO
      H2=H1
      T2=C1
      C1=0.0
      GO TO 7
C
C     VAPOR
C
    6 C1=0.023*(TCV2/HD)*((GHD/VISV2)**0.8)*((CV2*VISV2/TCV2)**0.33)
      C1=QUAL2*C1
      IF(QUAL2-0.70)7,3,3
C
C     BOILING
C
    7 C2=778.26*(1.0-QUAL2)*RBL2*(1.0+CL2*(TSATU2-T2)/(HV2-HL2))
      C2=C2*TCL2*CL2*VV2/(SURT2*VL2*(VV2-VL2)*(459.76+TSATU2))
      IF(C1)8,8,10
    8 TW2=TSATU2+(01/C2)**0.33
    9 RH2=R1*Q1/(TW2-T2)
      GO TO 500
C
   10 I1=0
      TW2=TSATU2+30.0
   11 I1=I1+1
      IF(I1-ITERM)13,13,12
   12 N100=2
      WRITE OUTPUT TAPE ITAO,1
      GO TO 500
   13 C3=TW2
      C4=(Q1-C1*(TW2-T2))/C2
      IF(C4)14,14,15
   14 C5=-1.0
      C4=-C4
      GO TO 16
   15 C5=1.0
   16 TW2=TSATU2+C5*(C4**0.33)
      ERR=ABSF((TW2/C3)-1.0)
      IF(ERR-ESP3)9,9,11
C
  500 RETURN
      END
```

```
*     LIST
*     FORTRAN
*     LABEL
      SUBROUTINE BURN
      DIMENSION
      COMMON
      EQUIVALENCE
C
      MAXIAL=MAXIA
C
C     ENTHALPY DNB RATIO
C
      DNB2=(H2-A(1))/AC10(MAXIA)
      IF(QUAL2-0.1)101,101,500
C
C     Q=DNB RATIO
C
  101 C2=0.01*(TSATU2-T2)
      IF(C2)1,2,2
    1 C2=0 0
    2 C2=3.0+C2
      C1=Q1/(C2*AC9(MAXIA))
C
C     FIND MAXIMUM DNB RATIO
C
      IF(C1-DNB2)500,500,3
    3 DNB2=C1
  500 RETURN
      END

*     LIST
*     FORTRAN
*     LABEL
      SUBROUTINE AIM
      DIMENSION
      COMMON
      EQUIVALENCE
    1 CALL SIGMA
      NSKP=0
      IF(N5)6,6,2
    2 DO 3J=1,NOG
      DO 3I=1,M
    3 VUSIG(I,J)=VUSIG(I,J)/EIGEN2
      IF(N5-2)4,4,5
    4 IF(ITER-1)5,5,6
    5 ICT2=1
    6 CALL CONS
      ICT=0
      ICT1=0
      EIGEN=0.0
      EIGEN1=0.0
```

```
    7 CALL FLUX
    8 CALL EIVAL
    9 CALL CONV
      IF(N100-1)7,10,500
   10 IF(N5)16,16,11
   11 CALL CRIT
      IF(N100-1)13,12,500
   12 IF(N5-2)13,13,6
   13 DO 14J=1,NOG
      DO 14I=1,M
   14 VUSIG(I,J)=VUSIG(I,J)*EIGEN2
   15 CALL RING
      GO TO 500
   16 CALL CELAX
  500 RETURN
      END

*     LIST
*     FORTRAN
*     LABEL
      SUBROUTINE SIGMA
      DIMENSION
      COMMON
      EQUIVALENCE
C
      DO 6J=1,NOG
C
C     CALCULATE TOTAL REMOVAL CROSS SECTIONS
C
      DO 4I=1,M
      SIGT(I,J)=SIGA(I,J)+SIGPT(I)-T(J)
      IF(J-1)1,1,2
    1 SIGT(I,J)=SIGT(I,J)+TRANS(I,1,2)
    2 IF(BUCK2(I,J))4,4,3
    3 SIGT(I,J)=SIGT(I,J)*DIF(I,J)*BUCK2(I,J)
    4 CONTINUE
C
C     SET FLUX TO ZERO
C
      DO SK=1,N
    5 PHI(K,J)=0.0
C
    6 CONTINUE
C
  500 RETURN
      END

*     LIST
*     FORTRAN
*     LABEL
      SUBROUTINE CONS
```

```
      DIMENSION
      COMMON
      EQUIVALENCE
C
C
      IF(NSKP)1,1,11
    1 IF(N1-2)2,5,5
C
C     PLANE GEOMETRY
C
    2 DO 3I=2,NM1
      FL(I)=0.0
    3 FLP(I)=1.0
      DO 4I=1,MM1
      AC1(I)=0.0
    4 AC2(I)=1.0
      GO TO 9
C
C     CYLINDRICAL GEOMETRY
C
    5 DO 6I=1,M
    6 AC1(I)=P*DELR(I)
      LB1=1
      LB2=LB(1)
      DO 8I=2,NM1
      FAC2=AC1(LB1)/R(I)
      FLP(I)=1.0/(1.0+FAC2/2.01
      FL(I)=FAC2*FLP(I)
      IF(I-LB@)8,7,7
    7 K=LB1
      LB1=K+1
      LB2=LB(LB1)
      FAC2=AC1(LB1)/R(I)
      AC2(K)=1.0/(1.0+FAC2/2.01
      AC1(K)=FAC2*AC2(K)
    8 CONTINUE
C
C     COMMON CALCULATION
C
    9 DO 10J=1,NOG
      DO 10I=1,MM1
   10 AC5(I,J)=(DIF(I+1,J)*DELR(I))/DIF(I,J)*DELM(I+1))-1.0
C
C
   11 DO 12J=1,NOG
      DO 12I=1,M
      AC3(I,J)=(DELR(I)**2)/DIF(I,J)
   12 AC4(I,J)=AC3(I,J)*SIGT(I,J)
      IF(N2-2)13,18,18
C
C     FLUX GRADIENT ZERO AT ORIGIN
C
```

```
   13 IF(R(1))14,14,15
   14 P2=2.0*(1.0+P)
      GO TO 16
   15 P2=2.0
   16 DO 17J=1,NOG
      AC6(1,J)=AC3(1,J)/P2
   17 AC6(2,J)=SIGT(1,J)*AC6(1,J)
      GO TO 20
C
C     FLUX ZERO AT ORIGIN
C
   18 DO 19J=1,NOG
      AC6(1,J)=AC4(1,J)*FLP(2)-FL(2)+1.0
   19 AC6(2,J)=AC3(1,J)*FLP(2)
C
C     COMMON CALCULATION
C
   20 DO 21J=1,NOG
      DO 21I=1,MM1
      AC7(I,J)=AC2(I)*AC4(I+1,J)-AC1(I)
   21 AC8(I,J)=AC2(I)*AC3(I+1,J)
  500 RETURN
      END

*     LIST
*     FORTRAN
*     LABEL
      SUBROUTINE FLUX
      DIMENSION
      COMMON
      EQUIVALENCE
C
      LOB=2
      N=N
      M=M
    1 DO 29I=1,NOG
    2 K8=1
      K9=LB(1)
      DO 4J=1,N
      D(J)=CHI(K8,I)*SOU(J)
      IF(J-K9)4,3,3
    3 DP(K8)=CHI(K8+1,I)*SOP(K8)
      K8=K8+1
      K9=LB(K8)
    4 CONTINUE
      DO 407J=1,M
      IF(BUCK2(J,I))401,407,407
  401 I2=J-1
      SUM1=-BUCK2(J,I)*DIF(J,I)
      IF(I2)402,402,403
  402 K8=1
      GO TO 404
```

```
  403 I1=LB(I2)
      K8=I1+1
  404 K9=LB(J)
      DO 405K=K8,K9
  405 D(K)=D(K)+SUM1*PHI(K,I)
      IF(I2)407,407,406
  406 DP(I2)=DP(I2)+SUM1*PHI(I1,I)
  407 CONTINUE
    5 IF(I-1)15,15,6
    6 LB3=I-1
      LB2=I-NDS
      IF(LB2-1)7,8,8
    7 LB2=1
    8 DO 10J=1,MM1
      I1=LB(J)
      SUM=0.0
      DO 9K=LB2,LB3
      M80=K-LB2+1
    9 SUM=SUM+TRANS(J+1,M80,I)*PHI(I1,K)
   10 DP(J)=DP(J)+SUM
      I2=LB(1)+1
      I3=1
      DO 14J=1,N
      SUM=0.0
      IF(J-I2)12,11,11
   11 I3=I3+1
      I2=LB(I3)+1
   12 DO 13K=LB2,LB3
      I4=K-LB2+1
   13 SUM=SUM+TRANS(I3,I4,I)*PHI(J,K)
   14 D(J)=D(J)+SUM
   15 IF(N2-2)16,17,17
C
C     DERIVATIVE OF FLUX EQUALS ZERO AT INNER BOUNDARY
C
   16 BETA(1)=D(1)*AC6(1,I)
      DELTA(2)=AC6(2,I)
      GO TO 18
C
C     FLUX EQUALS ZERO AT INNER BOUNDARY
C
   17 BETA(2)=AC6(2,I)*D(2)
      DELTA(2)=AC6(1,I)
      LOB=3
C
C     CALCULATION OF DELTA AND BETA
C
   18 I6=LB(1)
      I7=1
      DO 21J=LOB,NM1
      SM=AC3(I7,I)*D(J)*FLP(J)
```

CHAIN LINK (2,B2) - Continued.

```
      CK=AC4(I7,I)*FLP(J)-FL(J)
      CL=FL(J)
      SL=1.0-CL
      CON1=1.0/(1.0+DELTA(J))
      IF(J-I6)19,20,19
   19 BETA(J)=SL*CON1*BETA(J-1)+SM
      DELTA(J+1)=CK+CON1*(DELTA(J)+CL)
      GO TO 21
   20 CLP=AC1(I7)
      SLP=1.0-CLP
      CKP=AC7(I7,I)
      SMP=AC8(I7,I)*DP(I7)
      GAM=AC5(I7,I)
      GAM1=GAM+1.0
      CON2=0.5*(CK+DELTA(J)*CON1*2.0+CKP+CL*CON1+(GAM+CLP)*(CKP+2.)/SLP)
      CON3=1.0-CLP/2.0
      BETA(J)=(SM+CON1*(2.0-CL)*BETA(J-1)+GAM1*SMP/SLP)*(SLP/(GAM1*(2.0-
     1CLP)))
      DELTA(J+1)=(CON2*SLP-GAM*CON3-CLP/2.0)/(GAM1*CON3)
      I7=I7+1
      I6=LB(I7)
   21 CONTINUE
   22 IF(N3-2)23,24,24
C
C     FLUX EQUALS ZERO AT OUTER BOUNDARY
C
   23 PHI(N,I)=0.0
      GO TO 25
C
C     DERIVATIVE OF FLUX EQUALS ZERO AT OUTER BOUNDARY
C
   24 CON1=1.0+DELTA(N)
      PHI(N,I)=(AC3(M,I)*CON1*D(N)+2.0*BETA(N-1))/(CON1*AC4(M,I)+2.0*
     1DELTA(N))
C
C     START BACKWARD COMPUTATION
C
   25 DO 26J=1,NM2
      I20=N-J
   26 PHI(I20,I)=(PHI(I20+1,I)+BETA(I20))/(1.0+DELTA(I20+1))
      IF(N2-2)28,27,27
   27 PHI(1,I)=0.0
      GO TO 29
   28 PHI(1,I)=(PHI(2,I)+BETA(1))/(1.0+DELTA(2))
   29 CONTINUE
  500 RETURN
      END

*     LIST
*     FORTRAN
*     LABEL
```

```
      SUBROUTINE EIVAL
      DIMENSION
      COMMON
      EQUIVALENCE
C
    1 LB2=LB(1)
    2 M80=1
      DO 7I=1,N
      G(I)=0.0
      DO 3J=1,NOG
    3 G(I)=G(I)+VUSIG(M80,J)*PHI(I,J)
      G1(I)=G(I)*RI(I)
      IF(I=LB2)7,4,4,
    4 IF(I-N)5,7,7
    5 GP(M80)=0.0
      DO 6J=1,NOG
    6 GP(M80)=GP(M80)+VUSIG(M80+1,J)*PHIII,J)
      G1P(M80)=GP(M80)*RI(I)
      M80=M80+1
      LB2=LB(M80)
    7 CONTINUE
C
C     BEGIN CALCULATION OF EIGENVALUE
C
    8 M80=1
      LB2=3
      LB3=LB(1)
      EIGEN=0.0
    9 SUM=0.0
      DO 13I=LB2,LB3,2
      IF(I-LB2)10,10,12
   10 IF(I-3)12,12,11
   11 SUM=SUM+G1P(M80)+4.0*G1(I-1)+G1(I)
      M80=M80+1
      GO TO 13
   12 SUM=SUM+G1(I-2)+4.0+G1(I=1)+G1(I)
   13 CONTINUE
      AC9(M80)=(SUM*DELR(M80))/3.0
      EIGEN=EIGEN+AC9(M80)
      IF(M80-M)14,15,15
   14 LB2=LB3+2
      K80=M80+1
      LB3=LB(K80)
      GO TO 9
   15 EIGEN=EIGEN*PIM
  500 RETURN
      END

*     LIST
*     FORTRAN
*     LABEL
```

```
      SUBROUTINE CONV
      DIMENSION
      COMMON
      EQUIVALENCE
C
      DO 1I=1,N
    1 SOUP(I)=G(I)/EIGEN
      ICT=ICT+1
      DO 2I=1,MM1
    2 SOPP(I)=GP(I)/EIGEN
      IF(N4-2)3,4,4
C
C     EIGENVALUE CONVERGENCE CRITERION
C
    3 ERR=ABSF((EIGEN-EIGEN1)/EIGEN)
      IF(ERR-ESP1)15,15,17
C
C     POINTWISE CONVERGENCE CRITERION
C
    4 TEST1=0.0
      TEST2=1.0E25
      DO 9I=1,N
      IF(SOU(I))9,9,5
    5 FAC=G(I)/SOU(I)
      IF(TEST1-FAC)6,7,7
    6 TEST1=FAC
    7 IF(FAC-TEST2)8,9,9
    8 TEST2=FAC
    9 CONTINUE
      DO 14I=1,MM1
      IF(SOP(I))14,14,10
   10 FAC=GP(I)/SOP(I)
      IF(TEST1-FAC)11,12,12
   11 TEST1=FAC
   12 IF(FAC-TEST2)13,14,14
   13 TEST2=FAC
   14 CONTINUE
      ERR=(TEST1-TEST2)/TEST1
      IF(ERR-ESP1)15,15,17
   15 ICT1=ICT1+1
      IF(ICT1-2)18,16,16
   16 N100=1
      GO TO 500
   17 ICT1=0
   18 IF(ICT-MICT)19,19,24
   19 N100=0
      IF(ICT-2)27,27,20
C
C     SOURCE EXTRAPOLATION
C
   20 FAC=THETA+1.0
```

```
      DO 21I=1,N
   21 SOU(I)=SOUP(I)*FAC-THETA*SOU(I)
      DO 22I=1,MM1
   22 SOP(I)=SOPP(I)*FAC-THETA*SOP(I)
   23 EIGEN1=EIGEN
      GO TO 500
   24 IF(MICT)16,16,25
   25 WRITE OUTPUT TAPE ITAO,26
   26 FORMAT (47HO    MAXIMUM NUMBER OF FLUX ITERATIONS EXCEEDED)
      N100=2
      GO TO 500
   27 DO 28I=1,N
   28 SOU(I)=SOUP(I)
      DO 29I=1,MM1
   29 SOP(I)=SOPP(I)
      EIGEN1=EIGEN
  500 RETURN
      END

*     LIST
*     FORTRAN
*     LABEL
      SUBROUTINE CRIT
      DIMENSION
      COMMON
      EQUIVALENCE
    1 FORMAT (42HO                                          CELL)
    2 FORMAT (42HO                                         AXIAL)
    3 FORMAT (43HO                                         RADIAL)
    4 FORMAT (61H+    CRITICALITY    EIGENVALUE                     THERMAL
     1POISON/60H         COUNT                           REGION    CROSS SEC
     2TION/1H I10,1PE20.5,I10,E19.5)
    5 FORMAT (1H I40,1PE19.5)
    6 FORMAT (54HO    MAXIMUM NUMBER OF CRITICALITY ITERATIONS EXCEEDED)
    7 FORMAT (43HO    SEARCH FAILED - POISON BECAME NEGATIVE)
C
C     SET UP CONTROL REGIONS AND CALCULATE ERROR
C
      IF(N5-2)8,8,11
    8 J=13+33*N5
      DO 9I=14,29
      J=J+1
    9 L(I)=L(J)
      J=115+406*N5
      DO 10I=64,70
      J=J+1
   10 A(I)=A(J)
   11 W=EIGEN-1.0
      ERR=ABSF(W)
C
C     INTERMEDIATE PRINT
```

```
C
      IF(IPR)172,172,12
   12 SUM1=EIGEN*EIGEN2
      IF(N5-2)13,14,15
   13 WRITE OUTPUT TAPE ITAO,1
      GO TO 16
   14 WRITE OUTPUT TAPE ITAO,2
      GO TO 16
   15 WRITE OUTPUT TAPE ITAO,3
   16 LB1=LBS(1)
      WRITE OUTPUT TAPE ITAO,4,ICT2,SUM1,LB1,SIGPT(LB1)
      IF(N8-2)172,17,17
   17 DO 171I=2,N8
      J=LBS(I)
  171 WRITE OUTPUT TAPE ITAO,5,J,SIGPT(J)
  172 IF(ICT2-1)18,18,19
C
C     SET UP FOR FIRST ITERATION
C
   18 LB1=LBS(1)
      SGPT=SIGPT(LB1)
      C10=1.0
      ILK=0
      ICT3=1
      NSKP=1
      C3=1.0
   19 IF(ERR-ESP2)20,20,33
   20 N100=0
      GO TO 23
C
C     CALCULATE NEW POISON VALUES
C
   21 DO 22I=1,N8
      LB1=LBS(I)
   22 SIGP(LB1)=C10*SIGPT(LB1)
      IF(N5-2)23,23,26
C
C     STORE POISON VALUES FOR CELL OR AXIAL REGIONS
C
   23 J=115+406*N5
      DO 24I=64,70
      J=J+1
   24 A(J)=A(I)
      J=112
      DO 25I=14,29
      J=J+1
   25 L(I)=L(J)
      GO TO 500
C
C     CALCULATE NEW VALUE OF SIGT FOR RADIAL CRITICALITY (N5=3)
C
```

```
   26 DO 32J=1,NOG
      LB1=LBS(1)
      LB2=1
      DO 31I=1,M
      IF(LB1-I)31,27,31
   27 SIGT(I,J)=SIGA(I,J)+DIF(I,J)*BUCK2(I,J)+SIGPT(I)*T(J)
      GO TO (28,29),J
   28 SIGT(I,J)=SIGT(I,J)+TRANS(I,1,2)
   29 LB2=LB2+1
      IF(LB2-N8)30,30,32
   30 LB1=LBS(LB2)
   31 CONTINUE
   32 CONTINUE
      GO TO 500
C
C     TEST NUMBER OF CRITICALITY ITERATIONS
C
   33 IF(ICT2-MICT2)35,35,34
   34 WRITE OUTPUT TAPE ITAO,6
      N100=2
      GO TO 500
   35 IF(ICT3-2)36,42,47
C
C     FIRST CHOICE OF SEARCH PARAMETER
C
   36 IF(W)41,37,37
   37 IF(EIGEN-1.25)38,38,40
   38 C4=1.0/(1.0+10.0*W)
   39 C2=C3
      PSI2=EIGEN
      ICT2=ICT2+1
      ICT3=ICT3+1
      GO TO 51
   40 C4=1.0/(1.0-W*(2.62-50.0*W)
      GO TO 39
   41 C4=1.0-10.0*W/EIGEN
      GO TO 39
C
C     SECOND CHOICE OF SEARCH PARAMETER
C
   42 IF(C3)36,36,43
   43 IF(C2)36,36,44
   44 (W1=LOGF(C3)
      W2=LOGF(C2)
      A1=(W2-W1)/(PSI2-EIGEN)
      B1=W1-A1*EIGEN
      FAC=A1+B1
      IF(FAC-88.0)45,45,36
   45 C4=EXPF(FAC)
   46 C1=C2
      PSI1=PSI2
```

```
      GO TO 39
C
C     GENERAL CHOICE OF SEARCH PARAMETER
C
   47 CON1=PSI1-PSI2
      CON2=C1-C2
      CON6=C1*PSI1
      CON4=PSI1-EIGEN
      CON5=C1-C3
      CON3=CON6-C2*PSI2
      CON6=CON6-C3*EIGEN
      DET=CON1*CON5-CON2*CON4
      IF(DET)48,42,48
   48 A1=(CON3*CON5-CON2*CON6)/DET
      B1=(CON1*CON6-CON3*CON4)/DET
      B2=(C1-A1)*(PSI1-B1)
      C4=A1+B2/(1.0-B1)
      IF(C4-A1)50,50,49
   49 IF(C3-A1)42,46,46
   50 IF(C3-A1)46,46,42
C
C     TEST FOR NEGATIVE POISON
C
   51 IF(C4)52,52,54
   52 ILK=ILK+1
      ICT3=1
      C3=1.0
      LB1=LBS(1)
      SGPT=SIGPT(LB1)
      C10=1.0
      ICT2=ICT2-1
      IF(ILK-2)36,36,53
   53 WRITE OUTPUT TAPE IIAO,7
      N100=2
      GO TO 500
C
C     CALCULATE NEW POISON RATIO
C
   54 C12=SGPT/C4
      LB1=LBS(1)
      C10=C12/SIGPT(LB1)
      C3=C4
      N100=1
      GO TO 21
  500 RETURN
      END

*     LIST
*     FORTRAN
*     LABEL
      SUBROUTINE RING
```

```
      DIMENSION
      COMMON
      EQUIVALENCE
C
    1 FORMAT (18H1    RADIAL REGIONI6,5I20/10H     AXIAL/11H     REGION)
    2 FORMAT (28H            POWER DISTRIBUTION)
    3 FORMAT (47H            TRANSVERSE BUCKLING FOR AXIAL MAPPING)
    4 FORMAT (18H            PRESSURE)
    5 FORMAT (18H            ENTHALPY)
    6 FORMAT (19H            FLOW RATE)
    7 FORMAT (I8,6E20.5)
    8 FORMAT (I8,6E20.5/E28.5,5E20.5)
    9 FORMAT (34H6    THERMAL POISON CROSS SECTIONS/1H )
   10 FORMAT (I13,1PE20.5)
      MAXIAL=MAXIAL
      N=N
      IF(ITER-1)11,11,16
   11 IF(ITA3)12,12,16
   12 SUM1=(2.4048/R(N))**2
      DO 13K=1,NOG
      DO 13J=1,MAXIAL,MAXI
      DO 13I=1,MRI
   13 BUCKCH(I,J,K)=SUM1
      IF(POW1)14,14,15
   14 F1=1.0
      F2=0.0
      GO TO 16
   15 F1=0.5
      F2=1.0-F1
C
C     CALCULATE FLUX-VOLUME WEIGHTING TERMS AND RADIAL POWER DISTRIBU-
C     TION
C
   16 LB1=1
      SUM5=0.0
      DO 19I=1,MRI
      POWER(I,1)=0.0
      LB2=LB(I)-2
      DO 18K=1,NOG
      SUM1=0.0
      DO 17J=LB1,LB2,2
   17 SUM1=SUM1+R(J)*PHI(J,K)+4.0*R(J+1)*PHI(J+1,K)+R(J+2)*PHI(J+2,K)
      AC3(I,K)=SUM1*DELR(I)/3.0
   18 POWER(I,1)=POWER(I,1)+AC3(I,K)*VU(I,K)
      SUM5=SUM5+POWER(I,1)
   19 LB1=LB(I)
      DO 20I=1,MRI
   20 POWER(I,1)=POWER(I,1)/SUM5
C
C     REGIONAL POWER DISTRIBUTION
C
      IF(POW1)21,21,23
```

CHAIN LINK (2,B2) - Continued.

```
   21 DO 22J=2,MAXI
      DO 22I=1,MRI
   22 POWER(I,J)=POWER(I,1)*POWER(I,J)
      GO TO 25
   23 SUM1=POW1*CAREA
      DO 24I=1,MRI
      POWER(I,MAXIAL)=POWER(I,1)*SUM1/RAREA(I)
      DO 24J=2,MAXI
   24 POWER(I,J)=POWER(I,J)*POWER(I,MAXIAL)/DZ(J)
C
C     TEST POWER DISTRIBUTION
C
   25 N101=0
      LB1=0
      LB2=0
      DO 30I=1,MRI
      K=MRING-I
      SUM1=ABSF((DUMMY(K,1)/POWER(K,1))-1.0)
      IF(SUM1-ESP3)27,27,26
   26 N101=1
      LB1=1
   27 DO 29J=2,MAXI
      SUM1=ABSF((DUMMY(K,J)/POWER(K,J))-1.01
      IF(SUM1-ESP3)29,29,28
   28 N101=1
      LB2=K
   29 CONTINUE
   30 CONTINUE
      IF(N101)31,31,38
   31 IF(N100)32,32,38
C
C     CONVERGENCE SATISFIED
C
   32 DO 33K=1,NOG
      DO 33I=1,MRI
   33 VU(I,K)=VUSIG(I,K)/VU(I,K)
   34 CALL RING2
      WRITE OUTPUT TAPE ITAO,9
      IF(N5-2)35,36,37
   35 WRITE OUTPUT TAPE ITAO,10,(I,SIGPTC(I),I=1,MCELL)
      GO TO 57
   36 WRITE OUTPUT TAPE ITAO,10,(I,SIGPTA(I),I=1,MAXIAL)
      GO TO 57
   37 WRITE OUTPUT TAPE ITAO,10(I,SIGP(I),I=1,MRING)
      GO TO 57
C
C     CONVERGENCE NOT SATISFIED
C
   38 IF(ITER-NPO(11))381,32,32
  381 CALL RING1
      IF(IPR)39,39,40
```

```
39 IF(LB1)45,45,42
40 WRITE OUTPUT TAPE ITAO,1,(I,I=1,6)
   WRITE OUTPUT TAPE ITAO,2
   WRITE OUTPUT TAPE ITAO,7,(J,(POWER(I,J),I=1,6),J=2,MAXI)
   WRITE OUTPUT TAPE ITAO,3
   WRITE OUTPUT TAPE ITAO,8,(J,((BUCKCH(I,J,K),I=1,6),K=1,2),J=1,MAXI
  1AL)
   IF(POW1)39,39,41
41 WRITE OUTPUT TAPE ITAO,4
   WRITE OUTPUT TAPE ITAO,8,(J,((PRES(I,J,K),I=1,6),K=1,2),J=1,MAXIAL
  1)
   WRITE OUTPUT TAPE ITAO,5
   WRITE OUTPUT TAPE ITAO,8,(J,((ENTH(I,J,K),I=1,6),K=1,2),J=1,MAXIAL
  1)
   J=0
   WRITE OUTPUT TAPE ITAO,6
   WRITE OUTPUT TAPE ITAO,8,J,((FLOW(I,K),I=1,6),K=1,2)
   GO TO 39
42 LB2=1
   SUM1=0.0
   DO 43I=1,MRI
   POWER(I,1)=F1*POWER(I,1)+F2*DUMMY(I,1)
43 SUM1=SUM1+POWER(I,1)
   DO 44I=1,MRI
44 DUMMY(I,1)=POWER(I,1)/SUM1
45 IF(POW1)46,46,50
46 DO 49I=LB2,MRI
   SUM1=0.0
   DO 47J=2,MAXI
   DUMMY(I,J)=F1*POWER(I,J)+F2*DUMMY(I,J)
47 SUM1=SUM1+DUMMY(I,J)
   SUM1=DUMMY(I,1)/SUM1
   DO 48J=2,MAXI
48 DUMMY(I,J)=SUM1*DUMMY(I,J)
49 CONTINUE
   GO TO 500
50 SUM2=POW1*CAREA
   DO 52I=LB2,MRI
   POWER(I,MAXIAL)=SUM2*DUMMY(I,1)/RAREA(I)
   SUM1=0.0
   DO 51J=2,MAXI
   POWER(I,J)=(F1*POWER(I,J)+F2*DUMMY(I,J))*DZ(J)
51 SUM1=SUM1+POWER(I,J)
   SUM1=POWER(I,MAXIAL)/SUM1
   DO 52J=2,MAXI
   POWER(I,J)=POWER(I,J)*SUM1/DZ(J)
52 DUMMY(I,J)=POWER(I,J)
53 CONTINUE
54 J=109
   DO 55I=11,13
   J=J+1
55 L(J)=L(I)
```

```
      J=1678
      DO 56I=409,444
      J=J+1
   56 A(J)=A(I)
   57 DO 58I=1,N
   58 SOUR(I)=SOUP(I)
      DO 59I=1,M
   59 SOPR(I)=SOPP(I)
  500 RETURN
      END

*     LIST
*     FORTRAN
*     LABEL
      SUBROUTINE RING1
      DIMENSION
      COMMON
      EQUIVALENCE
C
      MRI=MRI
      N101=1
C
C     CALCULATE FLUX GRADIENTS TO THE LEFT OF INTERFACES
C
      DO 4JOG=1,NOG
      DO 4IREG=1,MRI
      LB2=LB(IREG)
      LB1=LB2-2
      J=0
      DO 1I=L81,LB2
      J=J+1
    1 DELT(1,J)=PHI(I,JOG)-PHI(I-1,JOG)
      DO 3I=2,3
      DO 2J=I,3
    2 DELT(I,J)=DELT(I-1,J)-DELT(I-1,J-1)
    3 CONTINUE
    4 DFHO(IREG,JOG)=(DELT(1,3)+DELT(2,3)/2.0+DELT(3.3)/3.0)/DELR(IREG)
      IF(MRI-2)11,5,5
C
C     CALCULATE FLUX GRADIENTS TO THE RIGHT OF INTERFACES
C
    5 DO 9JOG=1,NOG
      DO 9IREG=2,MRI
      LB1=LB(IREG-1)
      LB2=LB1+2
      J=0
      DO 6I=LB1,LB2
      J=J+1
    6 DELT(1,J)=PHI(I+1,JOG)-PHI(I,JOG)
      LB2=2
      DO 8I=2,3
```

```
      DO 7J=1,LB2
    7 DELT(I,J)=DELT(I-1,J+1)-DELT(I-1,J)
    8 LB2=LB2-1
    9 DPHI(IREG,JOG)=(DELT(1,1)-DELT(2,1)/2.0+DELT(3.1)/3.0)/DELR(IREG)
C
C     COMMON TERMS FOR BUCKLING
C
C     RIGHT HAND SIDE OF INTERFACE
C
      DO 10I=2,MRI
      SUM1=RINT(I-1,3)/2.0
      DO 10J=1,NOG
   10 AC4(I,J)=SUM1*DPHI(I,J)
C
C     LEFT HAND SIDE OF INTERFACE
C
   11 DO 12I=1,MRI
      SUM1=RINT(I,3)/2.0
      DO 12J=1,NOG
   12 AC5(I,J)=SUM1*DPHO(I,J)
      DO 13J=1,NOG
   13 AC5(MRI,J)=2.0*AC5(MRI,J)
C
C     BUCKLING
C
      DO 19K=1,NOG
      DO 19J=2,MAXI
      IF(MRI-2)14,15,15
   14 BUCKCH(1,J,K)=-AC5(1,K)/AC3(1,K)
      GO TO 19
   15 BUCKCH(1,J,K)=-(DIFCH(1,J,K)*AC5(1,K)+DIFCH(2,J,K)*AC4(2,K))/(DIFC
     1H(1,J,K)*AC3(1,K))
      IF(MRI-2)18,18,16
   16 LB1=MRI-1
      DO 17I=2,LB1
   17 BUCKCH(I,J,K)=(DIFCH(I-1,J,K)*AC5(I-1,K)+DIFCH(I,J,K)*(AC4(I,K)-AC
     15(I,K))-DIFCH(I+1,J,K)*AC4(I+1,K))/(DIFCH(I,J,K)*AC3(I,K))
   18 I=MRI
      BUCKCH(I,J,K)=(DIFCH(I-1,J,K)*AC5(I-1,K)+DIFCH(I,J,K)*(AC4(I,K)-AC
     15(I,K)))/(DIFCH(I,J,K)*AC3(I,K)
   19 CONTINUE
C
  500 RETURN
      END

*     LIST
*     FORTRAN
*     LABEL
      SUBROUTINE RING2
      DIMENSION
      COMMON
      EQUIVALENCE
```

```
C
      M=M
      N=N
      MRI=MRI
C     CALCULATION FOR ANSWER PRINTOUT OF RADIAL PARAMETERS
C
C     PHI(N,1) - RADIAL FAST FLUX TRAVERSE OF THE REACTOR
C     PHI(N,2) - RADIAL THERMAL FLUX TRAVERSE OF THE REACTOR
C     POWP(N,1),POWR(M,1) - POINTWISE RATIO OF FAST TO TOTAL POWER
C     POWP(N,2),POWR(M,2) - POINTWISE RADIAL POWER GENERATION
C     C1 - RATIO OF MAXIMUM TO AVERAGE THERMAL FLUX IN THE REACTOR
C     C2 - RATIO OF MAXIMUM TO AVERAGE POWER DENSITY ACROSS THE CORE
C
      FAC=0.0
      LB1=LB(MRI)
      DO 2J=1,LB1
      IF(PHI(J,2)-FAC)2,2,1
    1 FAC=PHI(J,2)
    2 CONTINUE
      SUM2=3,14159265*(RINT(MRI,3)**2)
      SUM1=0.0
      LB1=1
      DO 4I=1,MRI
      LB2=LB(I)-2
      SUM3=0.0
      DO 3J=LB1,LB2,2
    3 SUM3=SUM3+R(J)*PHI(J,2)+4.0*R(J+1)*PHI(J+1.2)+R(J+2)*PHI(J+2.2)
      SUM1=SUM1+SUM3*DELR(I)*PIM/3.0
    4 LB1=LB(I)
      C1=FAC*SUM2/SUM1
      LB2=N-2
      SUM3=0.0
      DO 5J=LB1,LB2,2
    5 SUM3=SUM3+R(J)*PHI(J,2)+4.0*R(J+1)*PHI(J+1,2)+R(J+2)*PHI(J+2,2)
      SUM1=SUM1+SUM3*DELR(M)*PIM/3.0
      DO 6K=1,NOG
      DO 6J=1,NM1
    6 PHI(J,K)=PHI(J,K)/SUM1
C
C     POINTWISE RADIAL POWER DISTRIBUTION
C
      FAC1=0.0
      SIM1=0.0
      LB1=1
      DO 16I=1,M
      LB2=LB(I)
      CON1=0.0
      CON2=0.0
      IF(VU(I,1))8,8,7
    7 CON1=VUSIG(I,1)/VU(I,1)
    8 IF(VU(I,2))10,10,9
```

CHAIN LINK (2,B2) - Continued.

```
    9 CON2=VUSIG(I,2)/VU(I,2)
   10 DO 14J=LB1,LB2
      CON3=CON1*PHI(J,1)
      POWP(J,2)=CON3+CON2*PHI(J,2)
      IF(POWP(J,2))11,11,12
   11 POWP(J,1)=0.0
      GO TO 14
   12 POWP(J,1)=CON3/POWP(J,2)
      IF(POWP(J,2)-FAC1)14,14,13
   13 FAC1=POWP(J,2)
   14 CONTINUE
      SUM3=0.0
      LB2=LB(I)-2
      DO 15J=LB1,LB2,2
   15 SUM3=SUM3+R(J)*POWP(J,2)+4.0*R(J+1)*POWP(J+1,2)+R(J+2)*POWP(J+2,2)
      SUM1=SUM1+SUM3*PIM*DELR(I)/3.0
      LB1=LB(I)
      POWR(I,1)=POWP(LB1,1)
      POWR(I,2)=POWP(LB1,2)
   16 CONTINUE
      C2=FAC1*SUM2/SUM1
      DO 17I=1,M
   17 POWR(I,2)=POWR(I,2)/SUM1
      DO 18J=1,N
   18 POWP(J,2)=POWP(J,2)/SUM1
C
C     OUTPUT
C
   47 FORMAT (73H1                                                    SOLUTION FOR
     1 RADIAL PARAMETERS)
   48 FORMAT (73H0    RADIAL REGION                                           GRO
     1UP 1       GROUP 2)
   49 FORMAT (1H0I11,24H         NU*SIGMA FISSION1PE25.4,E14.4/22H
     1               NUE39.4,E14.4/36H                        SIGMA ABSORPTION
     2E25.4,E14.4/41H                        DIFFUSION COEFFICIENTE20.4,E14.
     34/28H                   BUCKLINGE33.4,E14.4/49H
     4  SIGMA TRANSFER  (GROUP 1 TO 2)E12.4)
   50 FORMAT (117H0       RADIUS             NORMALIZED                FLUX
     1              FLUX                 POWER           POWER FRACTION/11
     28H       (CMS)             SOURCE TERMS          GROUP 1
     3  GROUP 2            (TOTAL)          (GROUP 1/TOTAL)/1H )
   51 FORMAT (1H 1PE14.5,5E20.5)
   52 FORMAT (67H2    RATIO OF MAXIMUM TO AVERAGE THERMAL FLUX ACROSS TH
     1E CORE     =F8.5)
   53 FORMAT (67H0    RATIO OF MAXIMUM TO AVERAGE POWER GENERATION ACROS
     1S THE CORE =F8.5)
   54 FORMAT (30H0    CORE + REFLECTOR WEIGHT =1PE12.5,4H LBS)
      WRITE OUTPUT TAPE ITAO,47
      WRITE OUTPUT TAPE ITAO,48
      DO 55I=1,M
      WRITE OUTPUT TAPE ITAO,49,I,VUSIG(I,1),VUSIG(I,2),VU(I,1),VU(I,2),
     1SIGA(I,1),SIGA(I,2),DIF(I,1),DIF(I,2),BUCK2(I,1),BUCK2(I,2),TRANS(
```

```
     2I,1,2)
   55 CONTINUE
      WRITE OUTPUT TAPE ITAO,47
      WRITE OUTPUT TAPE ITAO,50
      LB1=1
      DO 57I=1,M
      LB2=LB(I)-1
      WRITE OUTPUT TAPE ITAO,51,(R(J),SOUP(J),PHI(J,1),PHI(J,2),POWP(J,2
     1),POWP(J,1),J=LB1,LB2)
      J=LB(I)
      R(J)=-R(J)
      WRITE OUTPUT TAPE ITAO,51,R(J),SOUP(J),PHI(J,1),PHI(J,2),POWR(I,2)
     1,POWR(I,1)
      IF(M-I)57,57,56
   56 LB1=LB(I)+1
      WRITE OUTPUT TAPE ITAO,51,R(J),SOPP(I),PHI(J,1),PHI(J,2),POWP(J,2)
     1,POWP(J,1)
   57 CONTINUE
      WRITE OUTPUT TAPE ITAO,52,C1
      WRITE OUTPUT TAPE ITAO,53,C2
      IF(POW1)500,500,58
   58 WRITE OUTPUT TAPE ITAO,54,WATE
C
  500 RETURN
      END

*     LIST
*     FORTRAN
*     LABEL
      SUBROUTINE CELAX
      DIMENSION
      COMMON
      EQUIVALENCE
      MAXIA=MAXIA
      IF(N7-2)1,13,500
C
C     FLUX-VOLUME WEIGHTING TERMS
C
    1 DO 5K=1,NOG
      LB1=1
      SUM2=0.0
      DO 3I=1,M
      LB2=LB(I)-2
      SUM1=0.0
      DO 2J=LB1,LB2,2
    2 SUM1=SUM1+R(J)*PHI(J,K)+4.0*R(J+1)*PHI(J+1,K)+R(J+2)*PHI(J+2,K)
      AC3(I,K)=SUM1*DELR(I)
      SUM2=SUM2+AC3(I,K)
    3 LB1=LB(I)
      DO 4I=1,M
    4 AC3(I,K)=AC3(I,K)/SUM2
    5 CONTINUE
```

CHAIN LINK (2,B2) - Continued.

```
C
C     FLUX-VOLUME WEIGHTED PROPERTIES
C
      TRANSA(MAXIA,1,2)=0.0
      DO 6K=1,NOG
      VUSIGA(MAXIA,K)=0.0
      VUA(MAXIA,K)=0.0
      SIGAA(MAXIA,K)=0.0
    6 DIFA(MAXIA,K)=0.0
      DO 10I=1,M
      TRANSA(MAXIA,1,2)=TRANSA(MAXIA,1,2)+AC3(I,1)*TRANS(I,1,2)
      DO 9K=1,NOG
      SUM1=0.0
      IF(VU(I,K))8,8,7
    7 SUM1=VUSIG(I,K)/VU(I,K)
    8 VUSIGA(MAXIA,K)=VUSIGA(MAXIA,K)+AC3(I,K)*VUSIG(I,K)
      VUA(MAXIA,K)=VUA(MAXIA,K)+AC3(I,K)*SUM1
      SIGAA(MAXIA,K)=SIGAA(MAXIA,K)+AC3(I,K)*(SIGA(I,K)+SIGPT(I)*T(K))
    9 DIFA(MAXIA,K)=DIFA(MAXIA,K)+AC3(I,K)/DIF(I,K)
      DIFA(MAXIA,K)=1.0/DIFA(MAXIA,K)
   10 CONTINUE
C
C     CELL ONLY
C
   11 CALL CELL
      IF(POW1)14,14,12
   12 IF(MAXIA-MAXI)500,14,14
C
C     AXIAL ONLY
C
   13 CALL AXIAL
C
C     SOURCE GUESS FOR NEXT ITERATION
C
   14 J=350+406*N7
      DO 15I=1,N
      J=J+1
   15 A(J)=SOUP(I)
      J=451+406*N7
      DO 16I=1,M
      J=J+1
   16 A(J)=SOPP(I)
C
  500 RETURN
      END

*     LIST
*     FORTRAN
*     LABEL
      SUBROUTINE CELL
      DIMENSION
```

```
      COMMON
      EQUIVALENCE
      MRIN=MRIN
      MAXIA=MAXIA
      IF(POW1)1,1,3
C
C     ZERO POWER CALCULATION CELL
C
    1 DO 2J=2,MAXI
      TRANSA(J,1,2)=TRANSA(2,1,2)
      DO 2K=1,NOG
      VUSIGA(J,K)=VUSIGA(2,K)
      VUA(J,K)=VUA(2,K)
      SIGAA(J,K)=SIGAA(2,K)
      DIFA(J,K)=DIFA(2,K)
      DO 2I=1,MRI
    2 DIFCH(I,J,K)=DIFCH(1,2,K)
      FO TO 500
C
C     POLYNOMIAL FIT FOR HEAT GENERATION RATE ACROSS THE FUEL TUBE
C
    3 LB1=LB(2)
      LB2=LB(3)
      DO 5I=1,5
      SUM1=0.0
      SUM2=0.0
      J=0
      DO 4K=LB1,LB2
      J=J+1
      SUM1=SUM1+PHI(K,1)*U(I,J)
    4 SUM2=SUM2+PHI(K,2)*U(I,J)
    5 AMAT(I,6)=SUM1*VUSIG(3,1)/VU(3,1)+SUM2*VUSIG(3,2)/VU(3,2)
      DO 8I=1,5
      AMAT(I,6)=AMAT(I,6)/AMAT(I,I)
      K=1
    6 IF(K-I)7,8,8
    7 AMAT(I,6)=AMAT(I,6)-AMAT(I,K)*AMAT(K,6)/AMAT(I,I)
      K=K+1
      GO TO 6
    8 CONTINUE
      DO 11I=1,5
      J=6-I
      K=J+1
      BMAT(MRIN,MAXIA,J)=AMAT(J,6)
    9 IF(K-6)10,11,11
   10 BMAT(MRIN,MAXIA,J)=BMAT(MRIN,MAXIA,J)-AMAT(J,K)*BMAT(MRIN,MAXIA,K)
      K=K+1
      GO TO 9
   11 CONTINUE
      DO 12I=1,4
   12 TERM(MRIN,MAXIA,I)=0.0
```

```
      LB2=1+LB(3)-LB(2)
      DO 13K=1,5
      SUM3=K+1
      SUM1=BMAT(MRIN,MAXIA,K)*U(K+2,LB2)/SUM3
      SUM2=BMAT(MRIN,MAXIA,K)*U(K+2,1)/SUM3
      TERM(MRIN,MAXIA,1)=TERM(MRIN,MAXIA,1)+SUM1
      TERM(MRIN,MAXIA,2)=TERM(MRIN,MAXIA,2)+SUM2
      TERM(MRIN,MAXIA,3)=TERM(MRIN,MAXIA,3)+SUM1/SUM3
   13 TERM(MRIN,MAXIA,4)=TERM(MRIN,MAXIA,4)+SUM2/SUM3
      SUM1=PIM*(TERM(MRIN,MAXIA,1)-TERM(MRIN,MAXIA,2))
      DO 14K=1,4
   14 TERM(MRIN,MAXIA,K)=TERM(MRIN,MAXIA,K)/SUM1
      DO 15K=1,5
   15 BMAT(MRIN,MAXIA,K)=BMAT(MRIN,MAXIA,K)/SUM1
      IF(ITA3)16,16,500
   16 IF(ITER-1)17,17,500
C
C     FIRST ITERATION - CELL WITH POWER
C
   17 DO 20I=1,MRI
      DO 18K=1,4
   18 TERM(I,MAXIA,K)=TERM(1,MAXIA,K)
      DO 19K=1,5
   19 BMAT(I,MAXIA,K)=BMAT(1,MAXIA,5)
      DO 20J=1,NOG
   20 DIFCH(I,MAXIA,J)=DIFCH(1,MAXIA,J)
C
  500 RETURN
      END

*     LIST
*     FORTRAN
*     LABEL
      SUBROUTINE AXIAL
      DIMENSION
      COMMON
      EQUIVALENCE
C
      MAXIAL=MAXIAL
      ICENT=(1+MAXIAL)/2
      M=M
      MRIN=MRIN
      MAXI=MAXI
      IF(ITER-1)1,1,5
    1 IF(ITA3)2,2,5
C
C     INITIAL SET UP
C
    2 H=RINT(MAXIAL,2)
      BUCK2R(1,1)=(3.14159265/H)**2
      DO 3J=1,N
```

```
    3 APOWP(1,J)=0.0
      DO 4I=1,M
    4 APOWR(1,I)=0.0
      H=RINT(MAXI,2)-RINT(1,2)
C
C     STORAGE FOR RADIAL CALCULATION AND GROUP 2 BUCKLING
C
    5 C1=SQRTF(DIF(1,2)*SIGA(1,2))
      C2=SQRTF(DIF(M,2)*SIGA(M,2))
      C3=DIF(ICENT,2)*((1.0/C1)+(1.0/C2))
      BUCK2R(MRIN,2)=(3.14159265/(H+C3))**2
      TRANSR(MRIN,1,2)=TRANS(ICENT,1,2)
      DO 6K=1,NOG
      VUSIGR(MRIN,K)=VUSIG(ICENT,K)
      VUR(MRIN,K)=VU(ICENT,K)
      SIGAR(MRIN,K)=SIGA(ICENT,K)
    6 DIFR(MRIN,K)=DIF(ICENT,K)
C
C     NORMALIZATION, POWER, AND FLUX*DIFFUSION
C
      DO 10K=1,NOG
      SUM2=0.0
      DO 8I=2,MAXI
      SUM1=0.0
      LB1=LB(I-1)
      LB2=LB(I)-2
      DO 7J=LB1,LB2,2
    7 SUM1=SUM1+PHI(J,K)+4.0*PHI(J+1,K)*PHI(J+2,K)
      SUM1=SUM1*DELR(I)
      AC3(I,K)=SUM1
    8 SUM2=SUM2+SUM1
      DO 9I=2,MAXI
    9 AC3(I,K)=AC3(I,K)/SUM2
   10 SOU(K)=SUM2
      SOU(2)=SOU(2)/SOU(1)
      SOU(1)=1.0
      SUM1=0.0
      DO 12I=2,MAXI
      POWER(MRIN,I)=0.0
      DO 11K=1,NOG
      POWER(MRIN,I)=POWER(MRIN,I)+AC3(I,K)*VU(I,K)*SOU(K)
   11 DIFCH(MRIN,I,K)=AC3(I,K)*DIF(I,K)
   12 SUM1=SUM1+POWER(MRIN,I)
      SUM2=SUM1/3.0
      LB1=1
      DO 14I=1,MAXIAL
      LB2=LB(I)
      SUM3=VU(I,1)/SUM2
      SUM4=VU(I,2)/SUM2
      POWER(MRIN,I)=POWER(MRIN,I)/SUM1
      DO 13J=LB1,LB2
```

```
   13 APOWP(MRIN,J)=PHI(J,1)*SUM3+PHI(J,2)*SUM4
      APOWR(MRIN,I)=APOWP(MRIN,LB2)
   14 LB1=LB2
      IF(ITER-1)15,15,500
   15 IF(NPO(2))16,16,500
   16 IF(MRI-2)500,17,17
C
C     FIRST ITERATION
C
   17 DO 18I=2,MRI
      TRANSR(I,1,2)=TRANSR(1,1,2)
      DO 18K=1,NOG
      VUSIGR(I,K)=VUSIGR(1,K)
      VUR(I,K)=VUR(1,K)
      SIGAR(I,K)=SIGAR(1,K)
      DIFR(I,K)=DIFR(1,K)
      BUCK2R(I,K)=BUCK2R(1,K)
      DO 18J=2,MAXI
   18 DIFCH(I,J,K)=DIFCH(1,J,K)
      DO 21I=2,MRI
      DO 19J=1,N
   19 APOWP(I,J)=APOWP(1,J)
      DO 20J=1,M
   20 APOWR(I,J)=APOWR(1,J)
   21 CONTINUE
      DO 22J=2,MAXI
      DO 22I=2,MRI
   22 POWER(I,J)=POWER(1,J)
C
  500 RETURN
      END

*     LIST
*     FORTRAN
*     LABEL
      SUBROUTINE ANPRAX
      DIMENSION
      COMMON
      EQUIVALENCE
    1 FORMAT (16H0    RADIAL ZONEI2)
    2 FORMAT (16H3    RADIAL ZONEI2)
    3 FORMAT (60H            FRACTION OF REACTOR POWER GENERATED IN THIS Z
     1ONE =F7.4/50H          AVERAGE FUEL ROD POWER GENERATION RATE =1PE
     211.4,7H BTU/HR///69H           NORMALIZED COEFFICIENTS OF FOURTH
     3ORDER POLYNOMIAL FIT OF/62H                       RADIAL HEAT GENERATI
     4ON ACROSS THE FUEL TUBE/70H     EXPONENT     0              1
     5    2            3            4/10H      AXIAL/9H      ZONE)
    4 FORMAT (1H I7,1PE15.4,4E13.4)
    5 FORMAT (63H+                         AXIAL THERMODYNAMIC/HEAT TRANSFER
     1 RESULTS/73H      AXIAL   INLET
     2                OUTLET/72H     ZONE    SIDE
```

```
     3                                 SIDE)
     6 FORMAT (2H0 1PE19.4,30H            FLOW RATE (LB/HR)E24.4)
     7 FORMAT (2H0 I6,F11.1,31H               PRESSURE (PSIA)F23.1)
     8 FORMAT (1H F18.1,32H                 ENTHALPY (BTU/LB)F22.1)
     9 FORMAT (1H F18.1,37H            COOLANT TEMPERATURE (DEG F)F17.1)
    10 FORMAT (1H 1PE20.4,34H           HEAT TRANSFER COEFFICIENTE20.4/54H
     1                                  (BTU/HR/FT**2/(DEG F)))
    11 FORMAT (1H 1PE20.4,34H            CRITICAL HEAT FLUX RATIOE20.4)
    12 FORMAT (1H F18.1,38H            CLADDING TEMPERATURE (DEG F)F16.1)
    13 FORMAT (1H 1PE20.4,34H            HEAT FLUX (BTU/HR/FT**2)E20.4)
    14 FORMAT (53H                    MAXIMUM MID-ZONE FUEL TEMPERATURE =F8
     1.1,6H DEG F)
   141 FORMAT (53H                    AVERAGE MID-ZONE FUEL TEMPERATURE =F8
     1.1,6H DEG F)
    15 FORMAT (42H                          AXIAL ZONE POWER =1PE11.4,7H BT
     1U/HR)
    16 FORMAT (56H1                     POINTWISE AXIAL HEAT GENERATION RAT
     1E)
    17 FORMAT (63H0           DISTANCE FROM                             POWER
     1 DENSITY/62H0            ENTRANCE (FT)                           (BT
     2U/HR/FT))
    18 FORMAT (1H )
    19 FORMAT (1H 0PF20.5,1PE41.4)
       MRIN=MRIN
       MAXIAL=MAXIAL
       IF(MRIN-1)20,20,32
C
C      FIRST TIME THROUGH THE SUBROUTINE
C
    20 LB1=1
       DO 22I=1,MAXIAL
       LB2=LBA(I)
       DO 21J=LB1,LB2
    21 RI(J)=(3.2808E-2)*RA(J)
       RI(LB2)=-RI(LB2)
    22 LB1=LB2+1
C
C      HEAT TRANSFER COEFFICIENTS
C
       LB2=3-NPO(3)
       DO 27K=1,2
       C(K)=PIM*RHTR(K)
       DO 26I=1,MRI
       IF(NPO(4)-I)24,23,24
    23 IF(K-LB2)24,26,24
    24 DO 25J=2,MAXI
    25 HTR(I,J,K)=TCFU/(RHTR(K)*(HTR(I,J,K)-HT(K)))
    26 CONTINUE
    27 CONTINUE
       IF(NPO(1))30,30,28
    28 DO 29J=2,MAXI
```

CHAIN LINK (2,B2) - Continued.

```
      DO 29I=1,MRI
   29 FRAC(I,J)=1.0-FRAC(I,J)
   30 ICT=4
      IF(MAXIAL-4)31,31,32
   31 ICT=5
C
C     PRINTOUT OF AXIAL RESULTS
C
   32 DO 33I=2,MAXI
      AC3(I,1)=(1.0-FRAC(MRIN,I))*POWER(MRIN,I)/C(1)
      AC3(I,2)=FRAC(MRIN,I)*POWER(MRIN,I)/C(2)
   33 AC1(I)=DZ(I)*POWER(MRIN,I)
      WRITE OUTPUT TAPE ITAO,1,MRIN
      WRITE OUTPUT TAPE ITAO,3,POWER(MRIN,1),POWER(MRIN,MAXIAL)
      WRITE OUTPUT TAPE ITAO,4(J,(BMAT(MRIN,J,I),I=1,5),J=2,MAXI)
      WRITE OUTPUT TAPE ITAO,1,MRIN
      WRITE OUTPUT TAPE ITAO,5
      WRITE OUTPUT TAPE ITAO,6,(FLOW(MRIN,I),I=1,2)
      DO 38J=1,MAXIAL
      IF(J-ICT)35,34,35
   34 WRITE OUTPUT TAPE ITAO,2,MRIN
      WRITE OUTPUT TAPE ITAO,5
   35 WRITE OUTPUT TAPE ITAO,7,J,(PRES(MRIN,J,I),I=1,2)
      WRITE OUTPUT TAPE ITAO,8,(ENTH(MRIN,J,I),I=1,2)
      WRITE OUTPUT TAPE ITAO,9,(TEMC(MRIN,J,I),I=1,2)
      WRITE OUTPUT TAPE ITAO,11,(DNB(MRIN,J,I),I=1,2)
      IF(J-1)38,38,36
   36 IF(J-MAXIAL)37,38,38
   37 WRITE OUTPUT TAPE ITAO,10,(HTR(MRIN,J,I),I=1,2)
      WRITE OUTPUT TAPE ITAO,12,(TEMW(MRIN,J,I),I=1,2)
      WRITE OUTPUT TAPE ITAO,13,(AC3(J,I),I=1,2)
      WRITE OUTPUT TAPE ITAO,14,TFMX(MRIN,J)
      WRITE OUTPUT TAPE ITAO,141,TFBAR(MRIN,J)
      WRITE OUTPUT TAPE ITAO,15,AC1(J)
   38 CONTINUE
      C1=POWER(MRIN,MAXIAL)
      DO 39I=1,NAXIAL
   39 APOWP(MRIN,I)=APOWP(MRIN,I)*C1
      DO 40I=1,MAXIAL
   40 APOWR(MRIN,I)=APOWR(MRIN,I)*C1
      WRITE OUTPUT TAPE ITAO,16
      WRITE OUTPUT TAPE ITAO,1,MRIN
      WRITE OUTPUT TAPE ITAO,17
      LB1=1
      DO 41I=1,MAXIAL
      LB3=IBA(I)-1
      WRITE OUTPUT TAPE ITAO,18
      WRITE OUTPUT TAPE ITAO,19,(RI(J),APOWP(MRIN,J),J=LB1,LB3)
      LB1=IBA(I)
      WRITE OUTPUT TAPE ITAO,19,RI(LB1),APOWR(MRIN,I)
```

CHAIN LINK (2,B2) - Continued.

```
  41 CONTINUE
 500 RETURN
     END
```

APPENDIX H

INSTRUCTIONS FOR USING THE PROGRAM

H.1 General

Fixed point data is read into the machine by using a dummy one-dimensional matrix referred to as the L-matrix. Fixed point data specifies such information as the number of space points in the calculations, the number of reactor subdivisions, and other options available to the programmer.

Certain limitations are imposed on the fixed point input which are built into the program and which the programmer cannot change. The maximum number of regions is 7, the maximum number of space points is 101, the number of energy groups is 2, and the number of downscattering groups is 1. Also, certain specifications are preset as regards the flux geometry and boundary conditions. These specifications are:

Type of Calculation	Geometry	Boundary Conditions Origin	Edge
Cell	Cylindrical	Zero Current	Zero Current
Axial	Plane	Zero Flux	Zero Flux
Radial	Cylindrical	Zero Current	Zero Flux

The L-matrix is initially set equal to zero except for certain addresses. Where these non-zero numbers occur is noted in the section "Fixed Point Addresses".

Floating point data is read into the machine by using a dummy one-dimensional matrix known as the A-matrix. Floating point data specifies such information as the geometrical dimensions, nuclear properties, and heat transfer and power parameters. The IBM 7090 stores information in column fashion such that when a two-dimensional matrix is specified by

the indices (I,J), the index to the left is the most rapidly varying. For example, if one considers a two-dimensional matrix B(I,J) and assumes that the point B(1,1) is located in the A-matrix at A(345), then the point B(2,1) is located at A(346), B(3,1) at A(347), etc.

As pointed out, the maximum number of regions is 7 and the number of groups is 2. Where the indices (I,J) refer to a nuclear property, the first index (i) denotes the regional position and (J) the group. number. For the B-matrix considered above, the address for the point B(1,2) falls at A(352) and B(7,2) at A(358). If the number of regions to be used is less than 7, the address for the point B(1,2) must always fall at address A(352), regardless of how many regions are specified. The difference between Group 1 and Group 2 addresses is always equal to 7, regardless of how many regions are used.

To point out how this information is used, consider the diffusion coefficient for cell properties, which is denoted by the symbol $D^c(I,J)$ in the section "Floating Point Addresses". In this section the address for $D^c(1,1)$ is A(508). The addresses for each of the cell diffusion properties is shown below.

$D^c(1,1)$	=	A(508)	$D^c(1,2)$	=	A(515)
(2,1)	=	(509)	(2,2)		(516)
(3,1)	=	(510)	(3,2)		(517)
(4,1)	=	(511)	(4,2)		(518)
(5,1)	=	(512)	(5,2)		(519)
(6,1)	=	(513)	(6,2)		(520)
(7,1)	=	(514)	(7,2)		(521)

The A-matrix is initially set equal to zero except for certain addresses. Where these non-zero numbers occur is noted in the section "Floating Point Addresses".

H.2 Data Input

There are five card types necessary to solve a problem. For problems other than the first on the same run, only one each of the cards indicated below is necessary. The data from one problem is stored and not changed within the machine, except as noted for L(55) and L(121). This greatly reduces the input time for data and cuts down on the number of cards that must be punched. These cards must appear in the order indicated below.

1. Program Control Card and Steam Table Data.

   a. First Problem in a Run. The first card following the "* DATA" card must contain a non-zero digit punched in Column 2 and a decimal point in column 3. This causes the program to enter a subroutine which sets up the computer and reads in 529 cards containing the steam properties necessary for problem solution. The card, which follows the steam table data, contains the maximum allowable DNB-ratio and the nozzle efficiency. The steam table data cards should not be changed unless the person making the change has thoroughly studied subroutine THERMO in the program. To specify the DNB-ratio or nozzle efficiency, the information is placed in the computer in the following manner:

DNB-Ratio		Nozzle Efficiency	
Column		Column	
1	Blank	13	Blank
2	0	14	0
3	Decimal Point	15	Decimal Point
:	Any Digits	:	Any Digits
12		24	

b. Problems in a Run other than the First. Unless it is desired to change either the DNB-ratio or nozzle efficiency, this card is blank. If changes in either of these quantities is to be made, the procedure for the first problem in a run must be followed and the complete steam table data must be read in again.

2. Alphanumeric Data.

Punch the digit 1 in column 1. In the remaining 79 columns on the card, punch any desired alphanumeric information. The information punched on this card will head the print-out of the data that is supplied to the program.

3. Fixed Point (L-Matrix) Data.

The punches on this card must follow the format given below. If this form is not followed, an error signal will be printed and the problem will be terminated.

Column	Information
1	Number of pieces of L-matrix data on the card
2	Left blank unless it is the last card of fixed point data, in which case the number 1 is punched in this column
3-12	Relative address of the first piece of data on the card. All data following the first piece of data must be stored consecutively. For instance, if L(152) is the first piece of data, then the digit 1 is punched in column 10, the digit 5 in column 11, and the digit 2 in column 12. The last digit of the address must appear in column 12.

Column	Information
13-24) 25-36) 37-48) 49-60) 61-72)	Fixed point L-matrix data with between 1 and 5 pieces of data on the dard, according to the contents of column 1 on the card, with the address of the contents of columns 13-24 determined by column 3-12. As was the case for columns 3-12, the last digit for each of the numbers punched in the different fields must lie in the last column of the field.

4. Floating Point (A-Matrix) Data.

The punches on this card must follow the format given below. If this form is not followed, an error signal will be printed and the problem will be terminated.

Column	Information
1	Number of pieces of A-matrix data on the card.
2	Left blank unless it is the last card of floating point data, in which case the number 1 is punched in this column
3-12	Relative address of the first piece of data on the card. The same restrictions apply for the columns as were pertinent to column 3-12 for L-matrix data
13-24) 25-36) 37-48) 49-60) 61-72)	Floating point A-matrix data with between 1 and 5 pieces of data on the card, according to the contents of column 1, with the address of columns 13-24 determined by the contents of columns 3-12. As an example of how floating point data is fed into the machine, assume that the number 0.0034567 is to

read into columns 13-24. In the usual representation, this can also be written as $3.4567 \times 10^{-3} = 0.34567 \times 10^{-2}$. In the E-type format used, the number would be punched on the card as follows:

Column	Digit	Column	Digit
13	Blank	19	6
14	0	20	7
15	.	21	E
16	3	22	-
17	4	23	0
18	5	24	2

5. Alphanumeric Data.

Punch the digit 1 in column 1. In the remaining 79 columns on the card, punch any desired alphanumeric information. The information punched on this card will head the print-out of the problem solution. This card can be a duplicate of card type 2.

H.3 Fixed Point Addresses L(XXX) for Card Type 3

XXX	Quantity
47	Number of cell regions; must be set equal to 7
48	Interface numbers of cell boundaries; must be old and in ascending order; maximum number of points in region 3 is 21; miniumum number of points/region (in any region) = 7; number of interface numbers indicated must equal 7 to agree with L(47); last interface number cannot exceed 101, the maximum number of space points allowed.

XXX	Quantity
55	Number of control regions for homogeneous poison search if search is made on cell calculations; if L(55) = 0, program interprets poison as being in all cell regions and sets L(55) = L(47) and puts poison section of region 1 into all cell positions.
56	Control region numbers for cell search; if L(55) is non-zero, number of control regions must agree with L(55); control region numbers must be in ascending order; number of highest control region cannot exceed L(47)
65	Convergence testing method for solution of flux difference equations in cell calculations; if L(65) = 1, test is made on the integrated value of k_{eff} between two successive iterations; if L(65) = 2, test is made on the variation of the pointwise source terms between two successive iterations; L(65) = 2 is the more stringent testing method; program sets L(65) = 1 initially
80	Number of axial regions; minimum number is 3; maximum number is 7
81	Interface numbers of axial boundaries; odd and in ascending order; minimum number of points/region = 7; number of interfaces must agree with L(80); last interface number cannot be greater than 101
98	Convergence testing method for flux iterations for axial calculations; see L(65)
113	Number of radial regions; minimum number is 2, maximum number is 7
114	Interface numbers of radial boundaries; odd and in ascending order; minimum number of points/region = 7; number of interfaces must agree with L(113); last interface number cannot be greater than 101

XXX	Quantity
121	Number of control regions for homogeneous search if search is made in radial regions; same restrictions as for L(55) except they are applied to L(113)
122	Control region numbers for radial search; same restrictions as for L(56) except as they apply to L(113) and L(121)
129	Maximum number of iterations allowed for flux convergence; program sets this number to 50 initially
130	Maximum number of iterations allowed for criticality convergence; program sets this number to 15 initially
131	Convergence testing method for flux iterations for radial calculations; see L(65)
132	Criticality master search control number; if L(132) = 1, search is made on cell calculations; if L(132) = 3, search is made on radial calculations; L(132) must be specified for the problem.
133	Maximum number of iterations allowed for thermodynamic/heat transfer calculations; program sets this to 25 initially
134	Intermediate printout control; if L(134) = 0, no printout of intermediate results as the calculation proceeds; L(134) = 1 gives intermediate printout of results; program sets L(134) = 1 initially
152	Inlet flow side designation; if L(152) = 0, flow enters inside the fuel tube; if L(152) = 1, flow enters outside the fuel tube; program sets L (152) = 0 initially
153	Blocked flow control number; if L(153) = 1, a coolant channel is blocked for flow; if L(153) = 0, this option is not used; program sets L(153) = 0 initially

XXX Quantity

154 Flow path which is blocked; if L(154) = 1, inlet flow is blocked; if L(154) = 2, outlet flow is blocked; if flow is blocked; L(153) must be non-zero, program sets L(154) = 0 initially

155 Radial region in which flow is blocked; L(155) must be less than L(113); if flow is blocked, L(153) and L(154) must also be non-zero; program sets L(155) = 0 initially

162 Maximum number of radial power sweeps; for a zero-power calculation, this number should be about 10; for a calculation with power, the program will be in group 8 when 5 minutes of computer time has elapsed; convergence appears to be relatively fast to the final steady state power distribution but it is not achieved within 5 minutes; to obtain more results than those given by setting L(134) = 1, set L(162) = 5 or 6 to get an answer printout, which will also include a signal to indicate that final convergence has not yet been achieved; program initially sets L(162) = 5

H.4 Floating Point Addresses A(XXX) for Card Type 4

XXXX Quantity

445 $\chi(I,J)$ - fission spectrum; program sets fission spectrum equal to 1.0 for energy group 1 and 0.0 for energy group 2 for all 7 values of I; if this preset condition does not satisfy the programmer's requirements, change the values such that there is no regional variation for either energy group.

Nuclear Macroscopic Cell Properties (Superscript c)

459 $\nu\Sigma_f^c$ (I,J) in cm^{-1}; region 3 contains the fuel so addresses A(461) and A(468) must be non-zero

XXXX	Quantity
473	ν^c (I,J); region 3 contains the fuel so addresses A(475) and A(482) must be non-zero
487	Σ_s^c (I) in cm^{-1}; downscattering cross section for each region from group 1 to group 2; no information is necessary for regions 1 or 5 since these are coolant regions and properties are generated from nuclear microscopic coolant input
494	Σ_a^c (I,J) in cm^{-1}; absorption cross section which does not include removal by downscattering for group 1; see A(487)
508	D^c (I,J) in cm; see A(487)
522	Σ_p^c (I) in cm^{-1}; thermal poison cross section (group 2) for each of the regions
529	T_p^c (J); ratio of poison cross section in group J to poison cross section in group 2; independent of region

Nuclear Macroscopic Radial Reactor Properties (Superscript r)

The properties of the radial reflector must be specified. Dimensions used correspond to those used for corresponding cell properties. If, for example, the number in L (113) is 6, corresponding to 5 radial core subdivisions, plus a radial reflector, the addresses for the radial reflector absorption cross section are A (1311) for group 1 and A (1318) for group 2. Group 2 addresses always are 7 greater than group 1 addresses for the same property, regardless of how many radial regions are specified in L (113).

1299	Σ_s^r (I)
1306	Σ_a^r (I,J)
1320	D^r (I,J)
1334	Σ_p^r (I)
1341	T_p^r (J)
1343	k_{eff}; program sets this number to 1.0 initially

Nuclear Microscopic Water Properties (Superscript w)

Cross sections for all coolant properties are specified in ba[illegible]/molecule. The program then internally generates macroscopic properties for the inlet and mixing plenums plus cell regions 1 and 5. Index J denotes group number, of which there are two.

1719 $^{w}_{s}$; downscattering cross section from group 1 to group 2

1720 $^{w}_{a}(J)$; absorption cross section

1721 $^{w}_{tr}(j)$; transport cross section

Convergence Testing and Extrapolation

Satisfying convergence criteria for criticality and power distribution calculations is basically dependent on the result of flux calculations. To make physical sense, the convergence limit for flux calculations should be smaller than for either criticality or power distribution. Inasmuch as the same convergence criterion is used for heat transfer and power calculations and that the values of viscosity, thermal conductivity and surface tension of water are calculated internally from the results of a polynomial fitting of their respective properties, a convergence limit of less than 0.01 for the power distribution increases the running time for the program without any resulting increase in accuracy.

1724 Convergence limit for flux calculations

1725 Convergence limit for criticality calculations

1726 Convergence limit for power/heat transfer calculations

1727 Extrapolation factor for flux calculations; program sets this value to 0.8 initially, a value which seems to work quite satisfactorily

Geometrical Inputs (All dimensions are in cm)

1740 Distance from the origin of cylindrical interfaces for cell calculations; seven increasing values must be specified

1747 Distance from the bottom of the inlet plenum of interfaces which subdivide the reactor into axial regions; distances must be specified in increasing value and the number of values given must agree with the contents of L (80); the last value given is the reactor height

1754 Distance from the origin of cylindrical interfaces which subdivide the reactor into radial regions; distances must be specified in increasing value and the number of values given must agree with the contents of L (113); the last value given is the reactor radius

Power/Thermodynamic/Heat Transfer Inputs (Units of Btu,hr,ft,lb,^{o}F)

If a zero-power calculation is to be done, only the contents of A(1736) and A(1737) have to be specified. For a zero power calculation that is to be used to estimate the maximum obtainable value of k_{eff} for a given reactor size and composition, the calculation is greatly speeded by setting L(130) = 0, L(132) = 3, L(134) = 1, and A(1334) to some small positive value greater than 10^{-38}.

1728 Reactor power

1729 Total flow through the second pass channels in the core

1730 Nozzle/orifice area contraction ratio at second pass entrance; ratio = throat area/second pass channel flux area; value must lie between 0 and 1.0.

1731 Thermal conductivity of inner cladding (cell region 2)

1732 Thermal conductivity of fuel material (cell region 3)

1733 Thermal conductivity of outer cladding (cell region 4)

1734 Interface heat transfer coefficient between fuel and cladding

1735 Maximum allowable fuel temperature

1736 Pressure in the inlet plenum (psia)

1737 Enthalpy of water in the inlet plenum

1738 Density of core, excluding coolant flow area

1739 Density of radial reflector

1765 Nozzle/orifice area contraction ratio at first pass entrance; ratio = throat area/first pass channel flow area; the value must lie between 0 and 1.0

H.5 Steam Table Data

The subroutine THERMO utilizes a set of punched cards which summarize the data in the steam tables. This group of cards is logically broken up into two sets, the first containing data for the saturated state, the second the superheated state, which are read into the computer in that order.

The one hundred and twenty-three cards that summarize the saturated state span the range from 100°F to the critical temperature. The first 122 cards are spaced at 5° temperature intervals, i.e., the first card is for a saturation temperature of 100°F, the second for 105°F, and card number 122 for 705°F. The last card is for 705.4°F. The eight pieces of data that appear on each card are:

Columns	Data
1 - 10	Temperature ($^{\circ}$F)
11 - 20	Pressure (psia)
21 - 30	Specific volume of saturated liquid (ft^3/lb)
31 - 40	Specific volume of saturated vapor (ft^3/lb)
41 - 50	Enthalpy of saturated liquid (Btu/lb)
51 - 60	Enthalpy of saturated vapor (Btu/lb)
61 - 70	Entropy of saturated liquid (Btu/lb/$^{\circ}$F)
71 - 80	Entropy of saturated vapor (Btu/lb/$^{\circ}$F)

The placement of the saturated data within each of the 10-column fields is arbitrary. The only requirement is that the decimal point be punched in each of the fields at its appropriate position in the data number. It is suggested that the first column of each of the fields be left blank.

For the superheated data, the 14 temperature points selected are arbitrary but must be arranged in order of increasing value. The program specifically uses the fact that the 29 pressure points start with a value of 100 psia and increase by 50 psi increments, ending with a top pressure of 1500 psia. There are thus a total of (14 x 29 =) 406 cards for the superheated state. The information given on each of the cards is arranged as follows:

Columns	Data
1 - 10	Temperature ($^{\circ}$F)
11 - 20	Pressure (psia)
21 - 30	Specific volume (ft^3/lb)
31 - 40	Enthalpy (Btu/lb)

Note that the program does not use entropy values for the superheated state. The same comments made concerning saturated data placement within each of the 10-column fields is applicable to the superheated data.

The arrangement of the superheated data cards is accomplished by dividing the cards into 14 groups (based upon temperature) and for each temperature value arranging each of the sub-groups in increasing order of pressure values from 100 to 1500 psia. Thus, assuming it was desired to span the temperature range from 500°F to 2000°F, the cards would be arranged as follows:

Superheat Card No.	Temperature (^{o}F)	Pressure (psia)
1	500.0	100.0
2	500.0	150.0
.	.	.
.	.	.
.	.	.
406	2000.0	1500.0

In this example, the saturation pressure for $500^{0}F$ is 680.8 psia. For cards one through twelve, specific volume and enthalpy values would be obtained from the superheated steam tables. Card number 13 corresponds to a pressure of 700 psia, which is greater than the saturation pressure at $500^{o}F$, so superheated data is not applicable. For this case, cards 13 through 29 would only have temperature and pressure values punched in columns 1 - 20 and the remainder of the card would be blank.

APPENDIX I

LIST OF REFERENCES

Chapter 1

1. "Power Reactors the World Around", NUCLEONICS, Volume 2, Number 8, August, 1963

2. "Reactors on the Line, Nuclear Ship SAVANNAH", NUCLEONICS, Volume 20, Number 7, July, 1962

3. MAC MILLAN, D.C. and M.L. Ireland, Jr., "Economic Selection of Steam Conditions for Merchant Ships", Transactions Society of Naval Architects and Marine Engineers, Volume 56, 1948

4. CHENG, H.M. and C.E. Dart, "Cycle and Economic Studies for a 25,000-Maximum SHP Steam Power Plant for Single Screw Tanker Installation", Transactions Society of Naval Architects and Marine Engineers, Volume 66, 1958

5. NICHOLS, W.O., M.L. Rubin and R.V. Davidson, "Some Aspects of Large Tanker Design", Transaction Society of Naval Architects and Marine Engineers, Volume 68, 1960

6. MAC MILLAN, D.C. and E.C. Rhode, "Improved Steam Propulsion Plant to Reduce Building and Operating Costs", Transactions Society of Naval Architects and Marine Engineers, Volume 70, 1962

7. "630A Maritime Nuclear Steam Generator Scoping Study", GEMP-108, Office of Technical Services, U.S. Department of Commerce, Washington, 1962

8. "Recommended Practices for Preparing Marine Steam Power Plant Heat Balances", Technical and Research Bulletin No. 3-11, Society of Naval Architects and Marine Engineers, New York, 1961

9. GIBLON, R.P. and C.W. Stott, "Effect of Steam Conditions and Cycle Arrangement on Marine Power Plant Performance as Determined by the Electronic Computer", Transactions Society of Naval Architects and Marine Engineers, Volume 69, 1961

10. WHITE, A.O. and W.C. Smith, Jr., "An Analysis of Steam Propulsion Plants for Minimum Weight", Paper presented at Meeting of the Philadelphia Section, Society of Naval Architects and Marine Engineers, November 29, 1956

11. POWELL, S.C., "Estimation of Machinery Weights", Transactions Society of Naval Architects and Marine Engineers, Volume 66, 1958

Chapter 5

1. "Safety Considerations Affecting the Design and Installation of Water-Cooled and Water-Moderated Reactors on Merchant Ships", Technical and Research Bulletin No. 3-6, Society of Naval Architects and Marine Engineers, New York

2. UNTERMEYER, S., "Direct Steam Generation for Power", NUCLEONICS, Volume 12, Number 7, 1954

3. TAYLOR, L.S., "Radiation Protection Standards", NUCLEONICS, Volume 21, Number 3, 1963

4. ROCKWELL, T., III, "Reactor Shielding Design Manual", TID-7004, Office of Technical Services, Department of Commerce, Washington, 1956

5. MAC MILLAN D.C., "Some Developments in the Economic Application of Nuclear Power to Merchant Ships", TID-7563, Office of Technical Services, Department of Commerce, Washington, 1958

6. LANDIS, J.W., "The Power Plant for the First Nuclear Merchant Ship (NS SAVANNAH)", TID-7563, Office of Technical Services, Department of Commerce, Washington, 1958

Chapter 6

1. "Reactors on the Line, Nuclear Ship SAVANNAH", NUCLEONICS, Volume 20, Number 7, July, 1962

2. "630A Maritime Nuclear Steam Generator Scoping Study", GEMP-108, Office of Technical Services, Department of Commerce, Washington, 1962

3. RICE, R.B., J.I. Owens, W.M. Gaines, R.C. Larsen and R.J. Noorda, "Automatic Control of T7 Tanker Boiling Water Reactor Propulsion System Preliminary Design and Economic Evaluation", GEAP-3528 (Rev 1), Office of Technical Services, Department of Commerce, Washington, 1960

Appendix A

1. WEINBERG, A.M. and E.P. Wigner, "The Physical Theory of Neutron Chain Reactors", University of Chicago Press, 1958

2. SOKOLNIKOFF, I.S. and R.M. Redheffer, "Mathematics of Physics and Modern Engineering", McGraw-Hill Book Company, Inc., New York, 1958

3. HILDEBRAND, F.B., "Methods of Applied Mathematics", Prentice-Hall, Inc,, Englewood Cliffs, N.J., 1952

4. MARLOWE, O. and E.M. Gelbard, "WANDA - A One-Dimensional Few Group Diffusion Equation Code for the IBM704", WAPD-TM-28, Office of Technical Services, Department of Commerce, Washington, 1957

5. FERZIGER, S.H., G.S.C. Wang and P.F. Zweifel, "Diffusion Lengths in Heterogeneous Media", Nuclear Science and Engineering, Volume 10, 1961

6. GLASSTONE, S. and M.C. Edlund, "The Elements of Nuclear Reactor Theory", D. Van Nostrand Company, Inc., Princeton, 1952

7. JOANOU, G.D. and J.S. Dudek, "GAM-I: A Consistent P_1 Multigroup Code for the Calculation of Fast Neutron Spectra and Multigroup Constants", GA-1850, 1961

8. HUGHES, D.J. and J.A. Harvey, "Neutron Cross Sections", BNL-325, Government Printing Office, Washington, 1955

9. FLATT, H.P., D.C. Baller and E.R. Cohen, "AIM-5: A Multigroup, One-Dimensional Diffusion Equation Code", NAA-SR-4694, Office of Technical Services, Department of Commerce, Washington, 1960

Appendix B

1. MC ADAMS, W.H., "Heat Transmission", Second Edition, McGraw-Hill Book Company, Inc., New York, 1942

2. HILDEBRAND, F.B., "Methods of Applied Mathematics", Prentice-Hall, Inc., Englewood Cliffs, N.J., 1952

Appendix C

1. KEENAN, J.H. and F.G. Keyes, "Thermodynamic Properties of Steam", John Wiley and Sons, New York, 1936

2. GAMBILL W.R., "Physical Properties of Water", Chemical Engineering, Volume 66, 1959

3. PERRY, J.H., "Chemical Engineers' Handbook", Third Edition, McGraw-Hill Book Company, Inc., New York, 1950

4. STEIN, R.P. and W. Begell, Department of Chemical Engineering, Columbia University, New York, 1955

5. HEINEMAN, J.B., "An Experimental Investigation of Heat Transfer to Superheated Steam in Round and Rectangular Channels", ANL-6213, Office of Technical Services, Department of Commerce, Washington, 1960

6. MC ADAMS, W.H. et al., Industrial Engineering Chemistry, Volume 41, 1949

7. BUCHBERG, H. et. al., Proceedings of the Heat Transfer and Fluids Mechanics Institute, Stanford University, 1951

8. MRAVCA, E.A., Nuclear Superheat Meeting No. 3., TID-7609, Office of Technical Services, Department of Commerce, Washington, 1960

9. CLARK J.A. and W.M. Rosenhow, Transactions American Society of Mechanical Engineers, Volume 76, 1954

10. JENS, W.H. and P.A. Lottes, ANL-4915, Office of Technical Services, Department of Commerce, Washington, 1952

11. ISBIN, H.S., A. Kvamne, Y. Yamazaki, I. Garcia, Jr., and C.M. Stendahl, "Heat Transfer to Steam-Water Flows", Proceedings of the 1961 Heat Transfer and Fluid Mechanics Institute, Stanford University, 1961

12. COLLIER, J.G., "A Review of Two-Phase Heat Transfer (1935 - 1957)", AERE CE/R 2496

13. POLOMIK, E.E., S. Levy and S.G. Sawacha, "Heat Transfer Coefficients with Annular Flow During Once-Through Boiling of Water to 100% Quality at 800, 1100 and 1400 PSI", GEAP-3703, Office of Technical Services, Department of Commerce, Washington, 1961

14. LEVY, S., "General Correlation of Boiling Heat Transfer", American Society of Mechanical Engineers, ASME Paper No. 58-HT-8, 1958

15. PARKER, J.D. and R.J. Grosh, "Heat Transfer to a Mist Flow", ANL-6291, Office of Technical Services, Department of Commerce, Washington, 1961

16. DE BORTOLI, R.A., S.J. Green, B.W. Le Tourneau, M. Troy, and A. Weiss, "Forced Convention Heat Transfer Studies for Water in Rectangular Channels and Round Tubes at Pressures Above 500 PSIA", WAPD-188, Office of Technical Services, Department of Commerce, Washington, 1958

17. VISCARDI, J.E., Editor, "Reactor Heat Transfer Conference of 1956", TID-7519 (PT. 1), Book 2, Office of Technical Services, Department of Commerce, Washington, 1957

18. BELL, D.W., "Correlation of Burnout Heat Flux Data at 2000 PSIA", Nuclear Science and Engineering, Volume 7, 1960

19. TONG, L.S., H.B. Currin and A.G. Thorp, II, "New Correlations Predict DNB Conditions", NUCLEONICS, Volume 21, 1963

20. MARTINELLI, R.C. and D.B. Nelson, "Prediction of Pressure Drop During Forced Circulation Boiling of Water", Transactions of the American Society of Mechanical Engineers, Volume 70, 1948

21. ARMAND, A.A., "The Resistance During the Movement of a Two Phase System in Horizontal Pipes", AERE-TRANS-808, 1959

22. SHROCK and Grossman, "Local Heat Transfer Coefficients and Pressure Drop in Forced Convection Boiling", University of California, Institute of Engineering Research, Series No. 73308-UCX 2159, 1957

Appendix D

1. KEENAN, J.H., "Thermodynamics", John Wiley and Sons, New York, 1941

Appendix F

1. GARDNER, M.F. and J.L. Barnes, "Transients in Linear Systems", Volume I, John Wiley and Sons, New York, 1942

Uncited References

1. BENJAMIN, M.W. and J.G. Miller, "The Flow of Saturated Water Through Throttling Orifices", Transactions of the American Society of Mechanical Engineers, Volume 63, 1941

2. BERKOWITZ, L., S. Bertoletti, J. Lesage, G. Peterlonge, G. Soldaini and R. Zavaltarelli, "Results of Wet Steam Cooling; Pressure Drop, Heat Transfer and Burnout Measurements with Round Tubes", TID-12092, Office of Technical Services, Department of Commerce, Washington

3. BOTTOMLEY, W.T., "Flow of Boiling Water Through Orifices and Pipes", Transactions of the North East Coast Institution of Engineers and Shipbuilders, Volume 53, 1936-1937

4. BROWN, R.A., "Flashing Expansion of Water Through a Converging-Diverging Nozzle", UCRL-6665T, Office of Technical Services, Department of Commerce, Washington, 1961

5. BURNELL, J.G., "Flow of Boiling Water Through Nozzles, Orifices and Pipes", ENGINEERING, Volume 164, 1947

6. CHANG, Y-P., "Final Report - Section 1. An Analysis of the Critical Conditions and Burnout in Boiling Heat Transfer, Part I. Critical Conditions. Part II. Critical Heat Fluxes. Section 2. A Correlation of Boiling Heat Transfer from the Nucleation Theory - Including Effects of System Acceleration and Forced Convection", TID-14004, Office of Technical Services, Department of Commerce, Washington, 1961

7. DEISSLER, R.G., "Analysis of Turbulent Heat Transfer, Mass Transfer and Friction in Smooth Tubes at High Prandtl and Schmidt Numbers", NACA-TN3145, 1954

8. DUKLER, A.E. and O.P. Bergelin, "Characteristics of Flow in Falling Liquid Films", CHEMICAL ENGINEERING PROGRESS, Volume 48, 1952

9. DUKLER, A.E., "Dynamics of Vertical Falling Films", CHEMICAL ENGINEERING PROGRESS, Volume 55, 1959

10. ELROD, H.G., Jr., "Tentative Calculation Procedure for Pressure Drop and Volumetric Density in Two Phase Flow", NDA-2132-7, Office of Technical Services, Department of Commerce, Washington, 1960

11. FIEDLER, R.A., "Shock Location During Two-Phase Flow in an Overexpanded Nozzle", UCRL-6676, Office of Technical Services, Department of Commerce, Washington, 1961

12. GIMERA, R.J., "Interim Progress on the Study of the Application of an Organic Moderated Reactor for Propulsion of a 50,000 Ton Marine Tanker", NAA-SR-Memo-1783, Office of Technical Services, Department of Commerce, Washington, 1958

13. HEWITT, G.F., "Analysis of Annular Two Phase Flow: Application of the Dukler Analysis to Vertical Upward Flow in a Pipe", AERE-R3680, 1961

14. HODKINSON, B., "The Flow of Hot Water Through a Nozzle", ENGINEERING, Volume 143, 1937

15. ISBIN, H.S. and H. Fauske, "Critical Two Phase Steam Water Flows", TID-11061, Office of Technical Services, Department of Commerce, Washington, 1960

16. JONES, A.B., "Hydrodynamic Stability of a Boiling Channel", KAPL-2170, Office of Technical Services, Department of Commerce, Washington, 1961

17. LOTTES, P.A., "Nuclear Reactor Heat Transfer", ANL-6469, Office of Technical Services, Department of Commerce, Washington

18. LOVE, W.J., "Critical Pressure Ratio for a Nozzle with Two Phase Fog Flow", HW-64269, Office of Technical Services, Department of Commerce, Washington, 1960

19. MANEELY, O.J., "A Study of the Expansion Process of Low Quality Steam Through a De Laval Nozzle", UCRL-6230, Office of Technical Services, Department of Commerce, Washington, 1962

20. MASSENA, W.A., "Steam Water Pressure Drop and Critical Discharge Flow - A Digital Computer Program", HW-65706, Office of Technical Services, Department of Commerce, Washington, 1960

21. MAURER, G.W., "Bibliography on Two-Phase Heat Transfer", WAPD-TM-249, Office of Technical Services, Department of Commerce, Washington, 1960

22. MUMM, J.F., "Heat Transfer to Boiling Water Forced Through a Uniformly Heated Tube," ANL-5276, Office of Technical Services, Department of Commerce, Washington, 1954

23. NEUSEN, K.F., "Optimizing of Flow Parameters for the Expansion of Very Low Quality Steam", UCRL-6152, Office of Technical Services, Department of Commerce, Washington, 1962

24. OWENS, W.L. Jr., "Two Phase Pressure Gradient", International Developments in Heat Transfer, Part II, American Society of Mechanical Engineers, 1961

25. PIGFORD, T.H. and E.A. Mason, "Preliminary Comparison of Uranium and Thorium Fueling for BeO Reactor", GAMD-1207, Office of Technical Services, Department of Commerce, Washington, 1960

26. SCHMIDT, R.L. and L.F. Fidrych, "Boiling Water Reactor for Merchant Ship Propulsion", Proceedings of the 1958 Nuclear Merchant Ship Symposium, TID-7563, Office of Technical Services, Department of Commerce, Washington, 1958

27. STEAMER, A.G. and H.D. Ongman, "Free Surface Separation of Steam and Water for Application in a Marine Reactor at 1000 psig", GEAP-3489, Office of Technical Services, Department of Commerce, Washington, 1960

28. VON KARMAN, Th., "The Analogy between Fluid Friction and Heat Transfer", Transactions of the American Society of Mechanical Engineers, Volume 61, 1939

29. WEBER, H.E. and L.R. Glicksman, "A Study of the Effects of Ship's Motion on Free-Surface Steam-Water Separation", GEAP-3492, Office of Technical Services, Department of Commerce, Washington, 1960

30. WEISS, D.H., "Pressure Drop in Two-Phase Flow", ANL-4916, Office of Technical Services, Department of Commerce, Washington, 1952